Technical Transactions

Czasopismo Techniczne

Volume 6

Year 2017 (114)

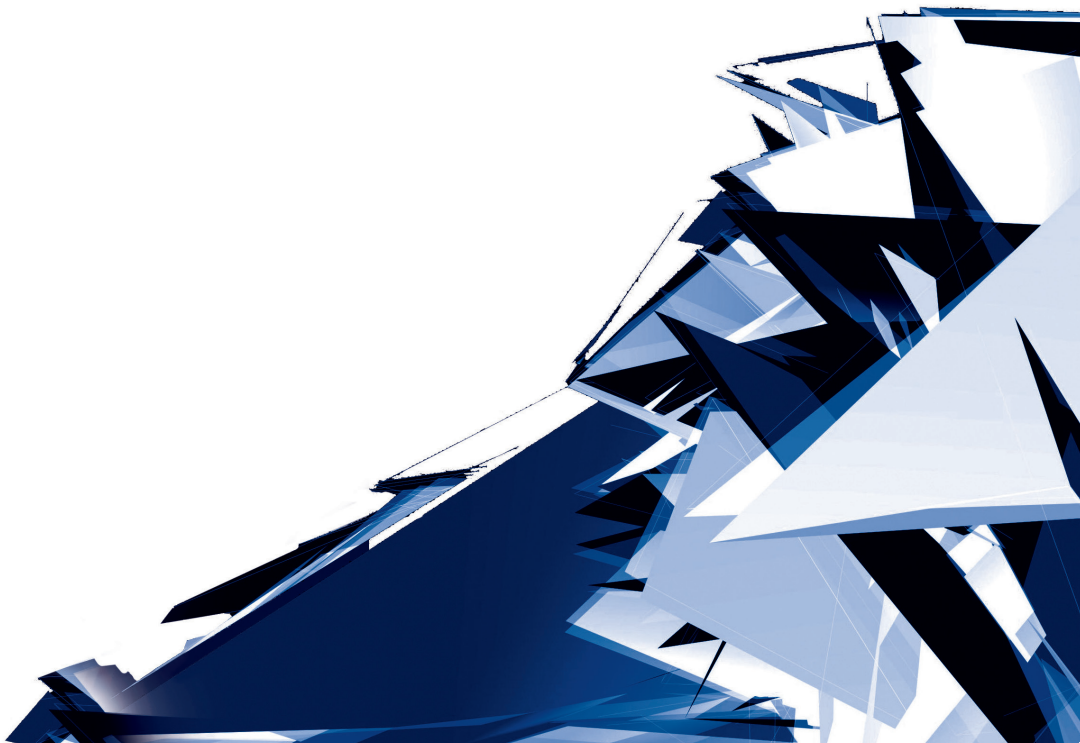

Chairman of the Cracow University of Technology Press Editorial Board
Przewodniczący Kolegium Redakcyjnego Wydawnictwa Politechniki Krakowskiej

Tadeusz Tatara

Editor-in-chief
Redaktor naczelny

Józef Gawlik
(jgawlik@mech.pk.edu.pl)

Scientific Council
Rada Naukowa

Jan Błachut – University of Liverpool (UK)
Wojciech Bonenberg – Poznan University of Technology (Poland)
Tadeusz Burczyński – Silesian University of Technology (Poland)
Massimo Corcione – Sapienza University of Rome (Italy)
Leszek Demkowicz – The University of Texas at Austin (USA)
Joseph El Hayek – University of Applied Sciences (Switzerland)
Ameen Farooq – Technical University of Atlanta (USA)
Zbigniew Florjańczyk – Warsaw University of Technology (Poland)
Marian Giżejowski – Warsaw University of Technology (Poland)
Sławomir Gzell – Warsaw University of Technology (Poland)
Allan N. Hayhurst – University of Cambridge (UK)
Maria Kušnierova – Slovak Academy of Sciences (Slovakia)
Krzysztof Magnucki – Poznan University of Technology (Poland)
Herbert Mang – Vienna University of Technology (Austria)
Arthur E. McGarity – Swarthmore College (USA)
Antonio Monestiroli – Polytechnic of Milan (Italy)
Ivor Samuels – University of Birmingham (UK)
Mirosław J. Skibniewski – University of Maryland (USA)
Günter Wozny – Technical University in Berlin (Germany)
Roman Zarzycki – Lodz University of Technology (Poland)

Native Speakers
Weryfikacja językowa

Robin Gill
Justin Nnorom

Series Editors
Redaktorzy Serii

ARCHITECTURE AND URBAN PLANNING
Mateusz Gyurkovich
(mgyurkovich@pk.edu.pl)

CHEMISTRY
Radomir Jasiński
(radomir@chemia.pk.edu.pl)

CIVIL ENGINEERING
Marek Piekarczyk
(mpiekar@pk.edu.pl)

ELECTRICAL ENGINEERING
Piotr Drozdowski
(pdrozdow@usk.pk.edu.pl)

ENVIRONMENTAL ENGINERING
Michał Zielina
(mziel@vistula.wis.pk.edu.pl)

PHYSICS, MATHEMATICS AND COMPUTER SCIENCES
Włodzimierz Wójcik
(puwojcik@cyf-kr.edu.pl)

MECHANICS
Andrzej Sobczyk
(andrzej.sobczyk@mech.pk.edu.pl)

Section Editor
Sekretarz Sekcji

Dorota Sapek
(dsapek@wydawnictwo.pk.edu.pl)

Editorial Compilation
Opracowanie redakcyjne

Aleksandra Urzędowska
(aurzedowska@pk.edu.pl)

Typesetting
Skład i łamanie

Anna Basista

Design
Projekt graficzny

Michał Graffstein

www.ejournals.eu/Czasopismo-Techniczne
www.technicaltransactions.com
www.czasopismotechniczne.pl

© 2017 Cracow University of Technology
ISSN 0011-4561

Basic version of each Technical Transactions magazine is its online version
Pierwotną wersją każdego zeszytu Czasopisma Technicznego jest jego wersja online

Contents

MECHANICS

PHYSICS

TECHNICAL TRANSACTIONS 6/2017
CZASOPISMO TECHNICZNE 6/2017
ARCHITECTURE AND URBAN PLANNING
DOI: 10.4467/2353737XCT.17.099.6575

Krzysztof Kosała (kosala@agh.edu.pl)
Department of Mechanics and Vibroacoustics, Faculty of Mechanical Engineering and Robotics, AGH University of Science and Technology

A COMPARATIVE ANALYSIS OF THE INDEX ASSESSMENT OF CHURCH ACOUSTICS USING RASTI AND STI

ANALIZA PORÓWNAWCZA WSKAŹNIKOWEJ OCENY AKUSTYCZNEJ KOŚCIOŁÓW Z UŻYCIEM RASTI I STI

Abstract

The article presents modified global assessment indices, developed in previous studies, for measuring the acoustic quality of Roman Catholic churches: the four-parameter Gap index and the Gi index based on five acoustic parameters. The replacement of *RASTI*, previously used in the acoustic assessment of churches, with *STI* has broadened the scope of church assessment and contributed to an improvement in the accuracy of the proposed method. Verification of new calculation procedures was performed on the 12 churches included in the calculation model and, additionally, on another church.

Keywords: church acoustics, index method, acoustic quality

Streszczenie

W artykule przedstawiono zmodyfikowane, opracowane w ramach wcześniejszych badań, wzory na wskaźniki globalne oceny jakości akustycznej kościołów rzymsko-katolickich: 4 parametrowy Gap oraz bazujący na 5 parametrach akustycznych wskaźnik Gi. Zamiana dotychczas używanego w akustycznej ocenie wskaźnikowej kościołów *RASTI* na *STI* poszerzyła zakres możliwości oceny kościołów oraz przyczyniła się do poprawy dokładności zaproponowanej metody. Weryfikację nowych procedur obliczeniowych przeprowadzono na 12 kościołach wchodzących w skład modelu obliczeniowego oraz dodatkowo na przykładzie jednego kościoła.

Słowa kluczowe: akustyka kościołów, metoda wskaźnikowa, jakość akustyczna

1. Introduction

Studies into the acoustic properties of worship spaces have been conducted by many researchers [4, 5, 7, 9, 15–17, 21]. Various acoustic parameters associated with the transmission of speech [4, 5] or activities outside the liturgy, such as the concert function of those interiors, have been investigated [16]. For rating the speech and music in churches, a method based on the use of two separate indices of acoustic assessment was proposed by Berardi [2]. A similar approach was shown by Álvarez-Morales *et al.* [1], where indices separately evaluating speech and music were developed for large-sized churches.

A large part of the author's research has concerned the development of a uniform method to comprehensively evaluate the acoustic properties of churches with a wide range of sound production. The proposed index method [7, 8, 13], modified in later years, is based on the global index of assessment, which is a function of several partial indices, providing more accurate information concerning reverberation, speech intelligibility, music sound quality, external noise and sound strength in the investigated churches.

Until now, the proposed version of the index method for assessing the acoustic quality of Roman Catholic churches in terms of speech intelligibility has used *RASTI*. Due to the current computing capabilities that allow the calculation of *STI* practically at the same time as *RASTI*, it is proposed to use a more accurate index (*STI*) in the index method. Therefore, it is necessary to develop new formulas for the existing GAP and GI single number global indices, as shown in the article.

2. *STI* and *RASTI* speech transmission indices

Providing a fairly good intelligibility of transmitted speech is essential in many facilities for public use, especially in places of worship. Next to the subjective methods used to assess the acoustics of interiors in terms of speech intelligibility, objective methods stand out, including *RASTI* (Rapid Speech Transmission Index) and *STI* (Speech Transmission Index) [3]. The *RASTI* method is derived from the *STI* method and is its shortened version.

Both methods, proposed by Houtgast and Steeneken [19], determine speech intelligibility by identifying and assessing the impact of the room, i.e. its internal conditions prevailing on the sound signal received by the audience [18]. Determination of the speech intelligibility is carried out by calculating the *RASTI* or *STI* ratios from the modulation transfer function (MTF), which is associated with the subjective scale of speech intelligibility [19,3].

In 1981, Schroeder showed that the MTF can be determined by the Fourier transform of the impulse response [20]:

$$m(f_m) = \int_0^\infty p^2(t) e^{-j\omega t} dt \Big/ \int_0^\infty p^2(t) dt \tag{1}$$

where:

$p(t)$ – impulse response function.

To determine the *STI*, it is necessary to calculate the MTF for seven octave frequency bands from the 125–8000 Hz range, while the *RASTI* requires two octave frequency bands of 500 Hz and 2000 Hz [22]. *RASTI* values can be determined using a Brüel & Kjaer 3361 measuring set: Rapid speech transmission index meter [19]. Currently, by using a computer and software (e.g. Dirac Room Acoustics Software from Brüel & Kjaer), *STI* and *RASTI* can be obtained from the impulse response registered in the studied interior. In most applications in room acoustics, *RASTI*, using a simplified set of modulation transfer functions, gives results similar to those obtained by using *STI*. However, due to the fact that the current technical capabilities, using fast computer calculations, allow *STI* to be obtained almost immediately, it is preferable, due to the greater accuracy of the result set, to use just *STI* instead of *RASTI*.

3. GAP and GI single number indices in acoustics assessment of churches, the index method

Based on years of research into the uniform assessment of the acoustic quality of churches, preceded by acoustic measurements of many such interiors, in 2013, in the paper [14], the GAP (Global Acoustic Properties) single number global index for assessing the acoustic properties of Roman Catholic churches was proposed. The value of this index was calculated on the basis of acoustic parameters obtained from measurements inside the church, such as reverberation time T_{30}, clarity of music C_{80}, speech intelligibility *RASTI* and disturbing noise level L_{Aeq}. On the basis of these parameters and developed calculation procedures, shown in [14], the partial indices were determined respectively: reverberation *R*, music sound *M*, speech intelligibility S and external disturbance *D*. By using these indices, it is possible to obtain information about the extent to which acoustic parameters are consistent with their preferred values, on a scale of 1 (parameter corresponds to its preferred value) to 0 (parameter deviates significantly from a preferred value).

The development of mathematical formalism for the overall GAP single number index was possible after obtaining the acoustic parameters of a group of objects (8 churches) and required the use of appropriate analytical tools. In order to avoid the duplication of some information in the synthetic single value of overall assessment, due to the fact that certain parameters (and thus the partial indices) are correlated to each other, it is proposed to group the indices which are correlated (*R*, *M* and *S*) and uncorrelated (*D*). From correlated indices, using the SVD technique (Singular Value Decomposition) and an 8´3 matrix (8 churches, 3 partial indices) obtained a vector of values reduced to RMS single number indices. Thereafter, using Comparative Multivariate Analysis (CMA), the calculated weight of two uncorrelated variables – the RMS and D vectors, containing the values of indices of the 8 churches, is obtained.

Finally, the overall GAP single number index is presented as a weighted sum [14]:

$$GAP = 0.6RMS + 0.4D \tag{2}$$

where:

RMS – the reduced partial single number index of assessment of selected acoustic properties of the church: reverberation, the sound of music and speech intelligibility (based on *RASTI*),

D – the partial index of external disturbance.

Using the GAP single number index, the acoustic quality of 8 churches (on the basis of which the calculation model was designed) was evaluated [14]. The GAP index can assess any acoustic Roman Catholic church, as shown in [10]. Using simulation studies, the acoustic parameters of the 3D model of the church assessed with the GAP index may be carried out while taking the presence of the audience into account [12].

The approach developed in [14] for index assessing the acoustic quality of churches in 2014 proposed the extension for assessing with one uncorrelated partial index S_T as a function of the sound strength G [11]. Studies have shown that it is possible to evaluate the acoustic properties of churches using a single number based on 5 acoustic parameters (T_{30}, C_{80}, *RASTI*, L_{Aeq} and G). Based on the analysis of acoustic parameters and related partial indices, it was determined that, for a group of 12 churches, the mathematical formalism for the GI (Global Index) global single number index is given by the formula [11]:

$$GI = 0.5RMS + 0.3S_T + 0.2D \tag{3}$$

where:

S_T – the partial index of sound strength.

A uniform assessment of the acoustic quality of 12 analysed church interiors, as shown in Fig. 1 and carried out with the use of GI, more fully reflects the acoustic conditions prevailing in them. The GI global index, developed on a 12-element calculation model constituting a pattern, is applicable to the assessment of any church [10].

The two developed computational models – the GAP and GI indices used *RASTI* (S = *RASTI*) to evaluate speech intelligibility. It is possible to increase the accuracy of the index assessing the acoustic quality of the churches in terms of speech intelligibility, as signalled in [12], by using a more accurate index, which is the *STI*, the subject of this article. Inclusion of the *STI* in the global assessment requires the introduction of new weights of the partial indices, and thus the development of new formulas for the existing global indices.

12 Roman Catholic churches were studied including historical (in that number some wooden: SE, AA, JO) and modern buildings, of a cubic capacity from 1102 to 41378 m^3, with differing floor shapes and interior furnishing appropriately to the architectural style in which they were built. Different geometrical parameters were given in Table 1. The surveyed churches are built on various ground plans, among others, such as: rectangular – NS and JC, oval – PA and BM, triangular – PK or Greek cross – AP (Fig. 2). The surveyed interiors have several common features. These are wooden pews, floors made of marble or ceramic tiles, stained glass windows, and organs located on the gallery over the church main entrance (Fig. 1). Apart from three historical wooden churches, the wall finishing in churches is cement-lime plaster coated with emulsion paint. Most of these churches are described in more detail in [7].

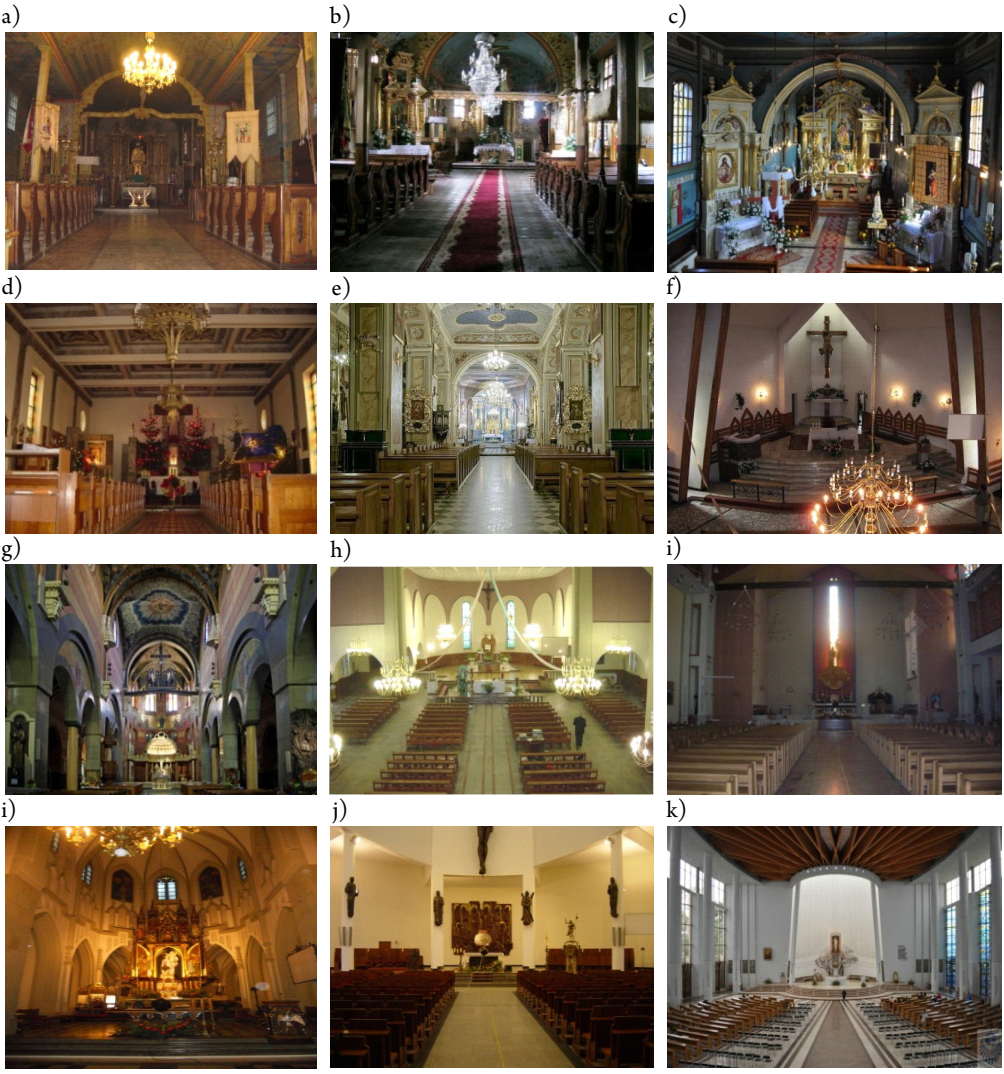

Fig. 1. Tested churches: a) St. Sebastian's Church in Strzelce Wielkie (SE), b) St. Andrew's Apostle Church in Gilowice (AA), c) St. Joachim's Church in Krzyżanowice (JO), d) The Holiest Sacred Heart's Church in Cracow (NS), e) St. Clemens Church in Wieliczka (KL), f) The Holy Cross Increase Church in Psary (PK), g) The Jesuits Fathers Church in Cracow (JE), h) St. Peter and Paul Apostles' Church in Trzebinia (AP), i) St. John the Baptist Church in Cracow (JC), j) St. Joseph's Church in Cracow (JF), k) St. Paul Apostle Church in Bochnia (PA), l) Sanctuary of the Divine Mercy in Cracow (BM)

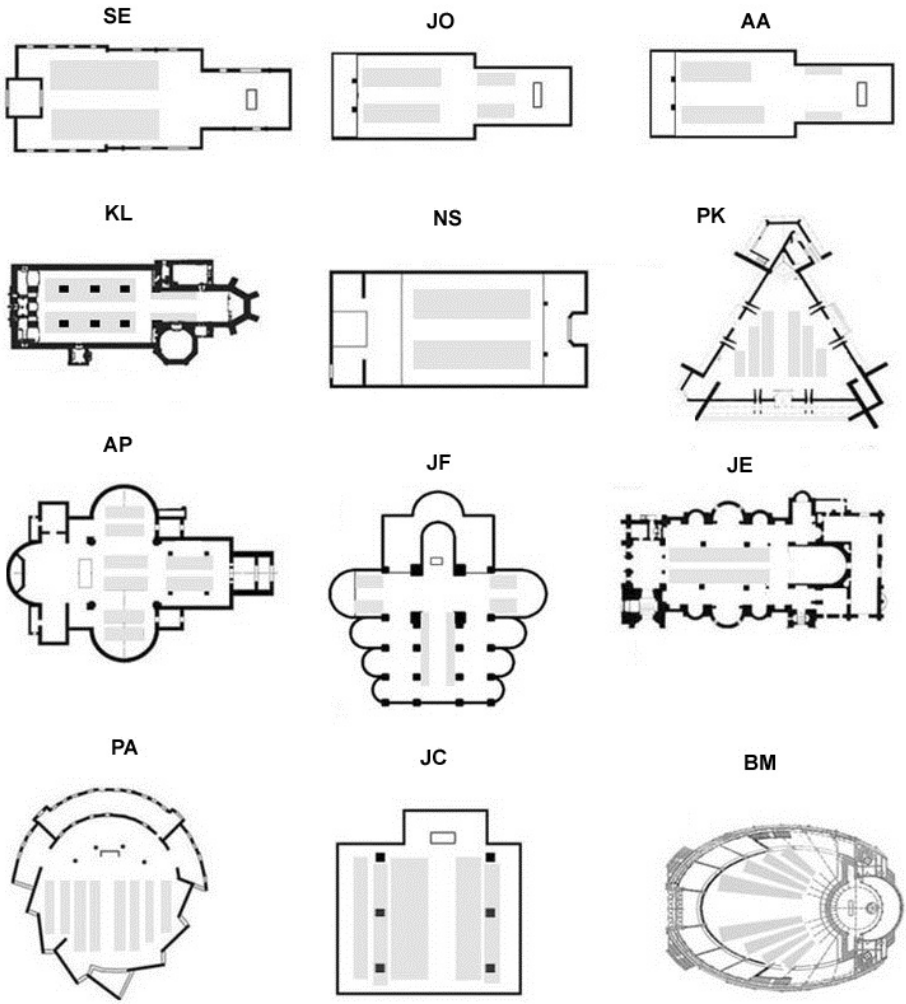

Fig. 2. Ground plan with pew zone (shaded area) for the 12 churches surveyed

Table 1. Geometric data of the 12 churches surveyed

Church ID	Style/year of build	Volume [m³]	Floor area [m²]	Length [m]	Height [m]
SE	Neoclassical/1785	1102	121	16.5	7.4
JO	Neoclassical/1794	1770	230	17.4	7.7
AA	Neoclassical/unknown	1215	188	23	7.3
KL	Neoclassical/1806	6380	712	55	13
NS	Modern/1928	2750	275	25	10
PK	Modern/1986	6800	589	31	12.6

AP	Modern/1927	12000	1187	55	10.2
JF	Neo-gothic/1909	16962	1223	44	22
JE	Modern/1921	9120	550	52	19
PA	Modern/1985	14000	812	35	25
JC	Modern/1989	14360	977	33	22
BM	Modern/2002	41378	1973	65	24

4. Speech intelligibility in churches, index *s*

To determine speech intelligibility in churches, both *RASTI* and *STI* are used. Evaluation of speech intelligibility in Catholic churches using *RASTI* has been the subject of many studies conducted by Carvalho [4, 5] and Lencastre [5]. Research showed the extent to which sound amplification systems improve speech intelligibility. The results of acoustic research conducted by Desarnaulds *et al.* [6] in 6 churches showed that the audience increases the speech intelligibility of *STI* = 0.050 when the sound amplification system is on and the *STI* = 0.035 when the sound amplification system is off.

In [14], the values of *RASTI* were shown versus the distance between the receiver and sound source for the 8 surveyed, unoccupied churches. In 7 churches, not taking into account the receivers placed nearest to the sound source, the speech intelligibility was bad and poor. Only one church, a historic wooden one, SE, had good or fair speech intelligibility.

In the current version of the index method assessment of the acoustic quality of Roman Catholic churches [14, 11], the partial index of speech intelligibility S corresponding to *RASTI* adopts the values of the same range, at each of the evaluation indices (partial and global), in line with the assumptions of the proposed method [8], i.e. from 0 to 1. According to these assumptions, all acoustic parameters, including *RASTI*, are calculated without taking into account the sound amplification system in the tested church interiors and in the conditions of unoccupied churches.

As part of further research into the improvement of the index method, proposed modifications concerned the new partial index of speech intelligibility $s = STI$, instead of the previously used $S = RASTI$, meaning that the assessment using the index method is more accurate.

Fig. 3 shows the averaged, from the measuring points, values of *RASTI* and *STI* obtained from the impulse responses recorded during the *in-situ* measurements in 12 churches.

The values of *RASTI* in the investigated churches are from 0.17 to 0.53, while the *STI* values range from 0.27 to 0.57 (Fig. 3). In all churches, the *STI* values are from 2 to 10% greater than *RASTI*. Only three historic wooden churches (SE, JO, AA), have sufficient speech intelligibility, in which the values of *STI* (or *RASTI*) of 0.5–0.6 in the interiors without sound amplification systems are considered as satisfactory conditions.

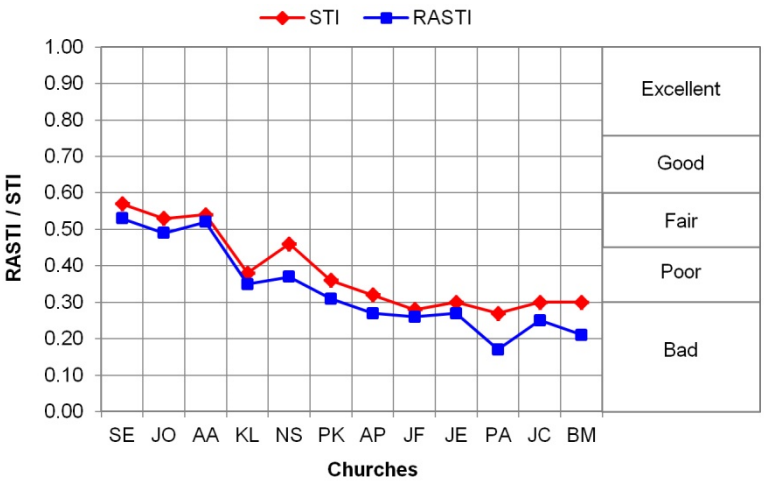

Fig. 3. Speech intelligibility, *RASTI* and *STI* in 12 investigated churches

5. The proposal of the new Gap and Gi single number indices of assessment

The introduction of *STI* instead of *RASTI* in the index calculation procedures entails the need to develop new formulas for the GAP and GI global indices, which will be replaced respectively by Gap and Gi.

Table 2 shows the acoustic parameters and partial indices, calculated for the 12 analysed churches.

Table 2. Acoustic parameters and partial indicies calculated for 12 churches

Church ID	Acoustic parameters					Partial indices of assessment					
	T_{30} [s]	C_{80} [dB]	STI	L_{Aeq} [dB]	G_{mid} [dB]	*R*	*M*	*s*	*D*	RMs	S_T
SE	1.4	2.5	0.57	27.3	5.2	1.00	1.00	0.57	1.00	1.00	1.00
JO	1.6	0.8	0.53	22.9	2.4	1.00	1.00	0.53	1.00	0.95	0.53
AA	1.6	1.3	0.54	35.1	3.8	0.97	1.00	0.54	0.37	0.95	0.85
KL	2.8	–2.7	0.38	32.2	2.8	0.78	0.73	0.38	0.58	0.56	0.62
NS	2.6	–1.9	0.46	34.6	5.8	0.78	0.81	0.46	0.39	0.70	0.97
PK	4.1	–4.0	0.36	33.4	4.3	0.51	0.60	0.36	0.47	0.39	0.96
AP	5.5	–6.6	0.32	39.6	0.3	0.23	0.40	0.32	0.24	0.15	0.07
JF	6.1	–8.8	0.28	29.6	1.0	0.12	0.27	0.28	1.00	0.00	0.22
JE	6.0	–4.3	0.30	32.3	9.3	0.10	0.57	0.30	0.57	0.17	0.63
PA	8.1	–6.5	0.27	26.3	4.9	0.00	0.41	0.27	1.00	0.02	1.00
JC	7.4	–6.8	0.30	32.1	2.3	0.00	0.39	0.30	0.59	0.05	0.51
BM	7.6	–6.5	0.30	28.8	–0.5	0.00	0.41	0.30	1.00	0.06	0.00

The calculation model based on the Gap single number index was determined on the basis of the procedure described in [14]. Based on research conducted in 12 churches, the index observation matrix **A1**:12×3 was developed. In MATLAB (Fig. 4), the matrix **A1** containing the correlated indices R, M and, based on *STI*, the new index s (Tab. 1) was decomposed of Singular Values (by using SVD) to generate a vector with reduced partial single number indices of assessment for selected acoustic properties of the church RMs, analogously as described in [14]. The RMs index is strongly correlated with the partial indices *R*, *M* and *s*. The coefficients of linear correlation *r* are equal to 0.98, 0.99 and 0.99, respectively (Fig. 4).

Uncorrelated with each other, the indices RMs and D ($r = 0.07$) are constituents of the weighted sum, which is the Gap single number global index. Weights assigned to the two indices were calculated according to the procedure shown in [14], using Comparative Multivariate Analysis (CMA).

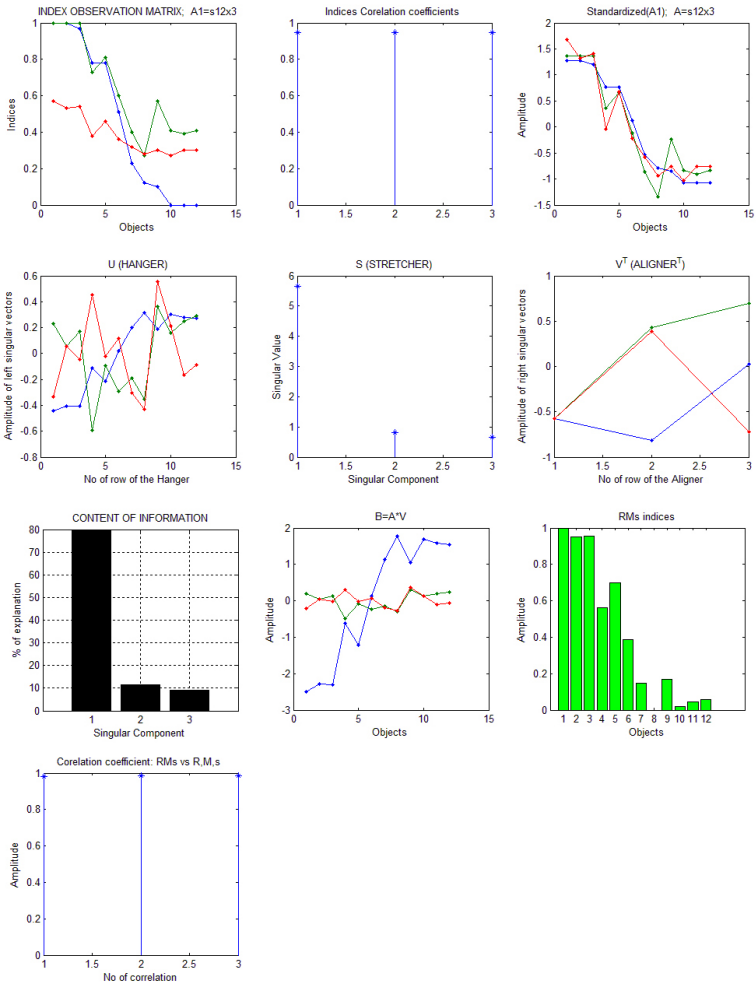

Fig. 4. Reduced indices RMs of 12 investigated churches

Modified Gap global index of the acoustic properties of Roman Catholic churches expressed by the formula:

$$Gap = 0.68RMs + 0.32D \tag{4}$$

where:

RMs – the reduced partial single number index of assessment of selected acoustic properties of the church: reverberation, the sound of music and speech intelligibility (based on *STI*).

In a similar way, also using CMA, weights were obtained for the three uncorrelated indices RMs, *D* and S_T (r < RMs, S_T > = 0.51; r < *D*, S_T > = – 0.09) needed to obtain the formula for the Gi global index.

The modified *Gi* global index of acoustic quality of Roman Catholic churches was defined as:

$$Gi = 0.48RMs + 0.3S_T + 0.22D \tag{5}$$

6. Application of modified global indices in assessment of surveyed churches

Fig. 5 shows the comparison lists of 12 surveyed churches using global acoustic assessment of traditional (GAP) and modified (Gap) indices, based on 4 acoustic parameters and Fig. 6. – the global assessment of traditional (GI) and modified (Gi) indices, based on 5 acoustic parameters.

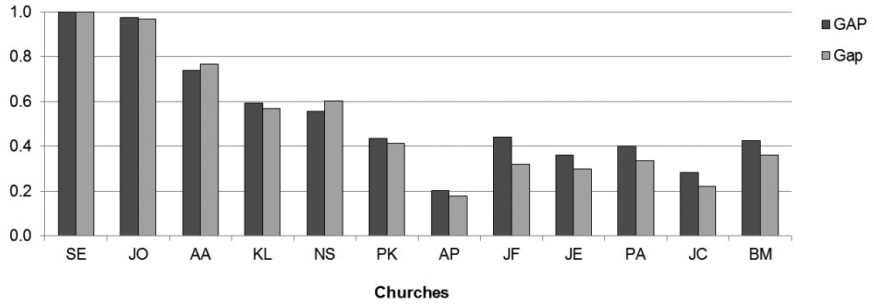

Fig. 5. Global assessment of 12 churches using GAP and Gap indices

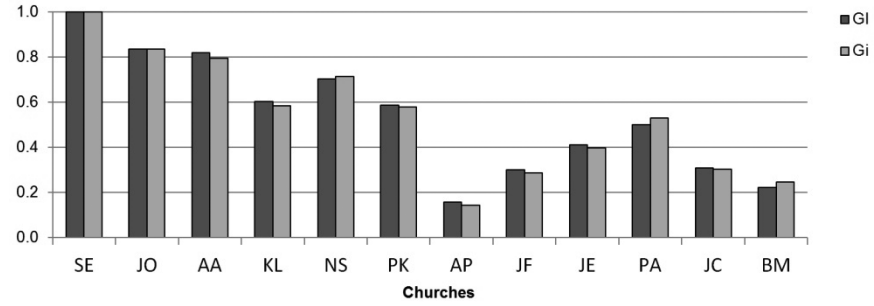

Fig. 6. Global assessment of 12 churches using GI and Gi indices

From the graphs shown in Fig. 5 and 6, it can be seen that modification of the formulas of the global indices, resulting from the replacement of *RASTI* by the more accurate *STI*, contributed to the values of global indices to a greater extent on the assessments of 4 parameters (Fig. 5) than on the assessments of 5 parameters (Fig. 6).

Fig. 7 shows a comparison of global assessments of 12 churches by modified Gi and Gap global indices. Assessments of these indices are based on *STI*.

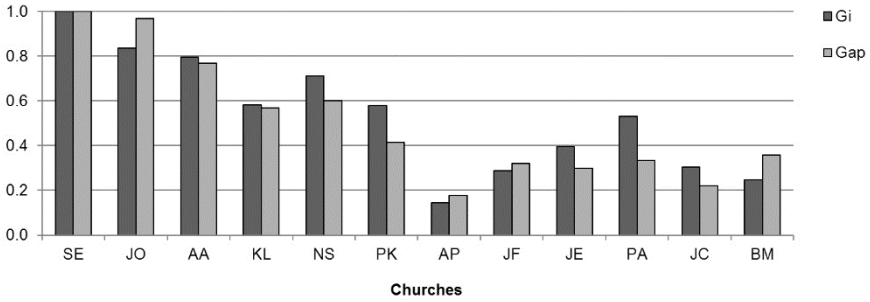

Fig. 7. Global assessment of 12 churches using Gi and Gap indices

The proposed new Gi and Gap global indices take a wide range of values from close to 0 (poor acoustic quality of the church) Gi = 0.15, Gap = 0.18, to equal the value of 1 (very good acoustic quality of the church).

Table 3 shows a comparison of the coefficients of linear correlation between global indices (traditional and modified) and acoustic parameters as well as partial indices. Modified global indices are more strongly correlated with the new partial index of speech intelligibility s (*STI*) than traditional global indices with the old index S (*RASTI*).

Table 3. Coefficients of a linear correlation between global indices, acoustic parameters and partial indices

	T_{30} [s]	C_{80} [dB]	RASTI (STI)	L_{Aeq} [dB]	G_{mid} [dB]	*R*	*M*	*S* (s)	RMS (RMs)	*D*	S_T
GAP	–0.81	0.88	0.88	–0.55	–	0.85	0.88	0.88	0.89	0.38	–
Gap	–0.87	0.93	(0.94)	–0.46	–	0.91	0.93	(0.94)	(0.94)	0.27	–
GI	–0.85	0.93	0.87	–0.35	0.44	0.89	0.93	0.87	0.91	0.12	0.75
Gi	–0.82	0.92	(0.89)	–0.39	0.43	0.87	0.92	(0.89)	(0.91)	0.15	0.75

Index assessment can be conducted for any of the Roman Catholic churches, as shown in the example of St. Elizabeth of Hungary Church in Jaworzno Szczakowa [10], where the GAP and GI indices and GAP_{occ}, taking into account the presence of the audience, were used. The assessment of acoustic conditions in the occupied church was possible after a testing simulation on the developed acoustic model of the church (Fig. 8).

The use of the modified global index to assess this church is shown. Table 4 shows the acoustic parameters of the church derived from the acoustic measurements, taking into account the presence of the audience using simulation tests.

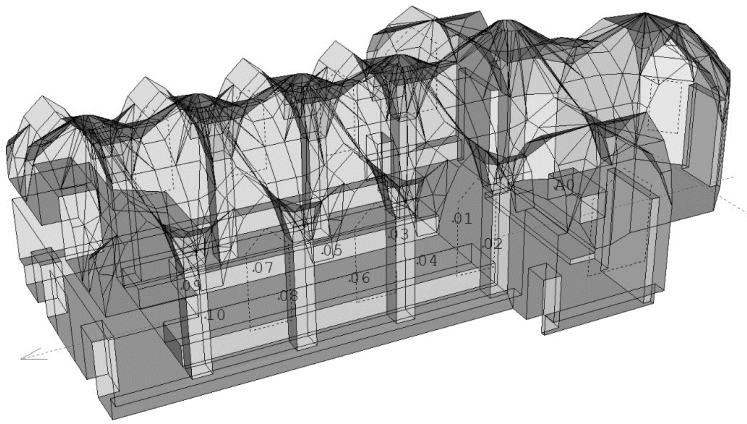

Fig. 8. Acoustic model of St. Elizabeth of Hungary Church in Jaworzno Szczakowa

Table 4. Acoustic parameters of the unoccupied and occupied St. Elizabeth of Hungary Church

Church	Acoustic parameters				
	T_{30} [s]	C_{80} [dB]	RASTI (STI)	L_{Aeq} [dB]	G_{mid} [dB]
unoccupied	3.3	–4.33	0.33 (0.37)	31.4	5.29
occupied	2.05	–0.65	0.46 (0.47)	31.4	–

Based on the acoustic parameters, the partial as well as the global indices of acoustic properties of the church were determined, as shown in Table 5. Global assessment for the church using the modified Gap and Gi global indices, based on *STI*, practically does not differ from the values of the traditional GAP and GI indices, based on *RASTI*.

Table 5. Partial and global indices of assessment of acoustic properties of St. Elizabeth of Hungary Church

Church	Partial indices						Global indices			
	R	*M*	*S* (s)	RMS (RMs)	*D*	S_T	GAP	GI	Gap	Gi
unoccupied	0.63	0.57	0.33 (0.37)	0.45 (0.42)	0.68	1	0.54	0.66	0.5	0.65
occupied	0.90	0.93	0.46 (0.47)	0.86 (0.81)	0.68	–	0.79	–	0.77	–

Comparison of the acoustic properties of the unoccupied and occupied St. Elizabeth of Hungary Church using the modified index method with the Gap and Gap_{occ} indices shown in Fig. 9.

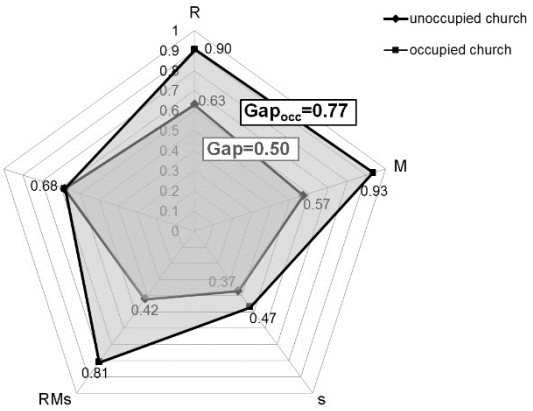

Fig. 9. Assessment of acoustic properties of the unoccupied and occupied the St. Elizabeth of Hungary Church using the modified index method with the Gap and Gap_{occ} indices

Assessment of the acoustic properties of St. Elizabeth of Hungary Church using the modified index method with the Gi index shown in Fig. 10.

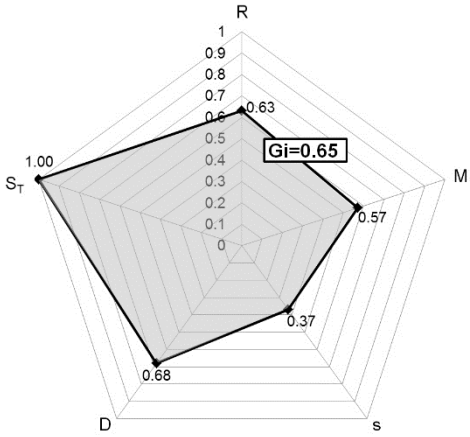

Fig. 10. Assessment of the acoustic properties of the unoccupied St. Elizabeth of Hungary Church using modified index method with Gi index

7. Conclusions

Analysis of the acoustic parameters of the data set consisting of 12 Roman Catholic churches, with a capacity from about 1100 to 41000 m^3, of different interior designs and different geometries, enabled the development of computational models as global assessment indices of the acoustic quality of churches. After the acoustic measurements in churches by using global indices, which were general measures and functions of *RASTI*, it was possible to make the assessment based on 4 acoustic parameters (GAP) and a more accurate one, based on 5 acoustic parameters (GI). Re-using the model with the data structure – acoustic

parameters of 12 churches but containing acoustic measurement values of *STI* in these churches – has enabled the development of new formulas for the global indices: Gap, as a function of acoustic parameters, such as: T_{30}, C_{80}, *STI* and L_{Aeq}, and Gi, which is a function of T_{30}, C_{80}, *STI*, L_{Aeq} and *G*.

New formulas for the global indices have widened the scope of the proposed index method of objects, in which, instead of *RASTI, STI* is measured. Currently, *STI* can be calculated from the impulse response registered in the church interior as quickly as *RASTI*. Assessments of the acoustic quality of the churches made using the new global indices, which are functions of the *STI*, can be considered as more accurate in comparison with traditional global indices, based on *RASTI*.

The new global indices may be applied for the assessment of any Roman Catholic church, not only to the 12 objects in the index observation matrix. Verification of new indices were shown to assess St. Elizabeth of Hungary Church, where the acoustic model, developed in earlier studies, also allowed the audience presence to be taken into account.

This paper has been executed within the project No. 11.11.130.955.

References

[1] Álvarez-Morales L., Girón S., Galindo M., Zamarreño T., *Acoustic environment of Andalusian cathedrals*, Building and Environment, 103, 2016, 182–192.

[2] Berardi U., *A double synthetic index to evaluate the acoustics of churches*, Archives of Acoustics, Vol. 37(4), 2012, 521–528.

[3] Brachmański S., *Exmerimental comparison between speech transmission index (STI) and mean opinion scores (MOS) in rooms*, Archives of Acoustics, Vol. 31(4), 2006, 171–176.

[4] Calvalho A.P.O., *Relations between rapid speech transmission index (RASTI) and other acoustical and architectural measures in churches*, Applied Acoustics, Vol. 58(1), 1999, 33–49.

[5] Carvalho A.P.O., Lencastre M.M.F, *Catholic Churches, Sound- Reinforcement Systems and RASTI.* International Journal of Acoustics and Vibration, 2000, Vol. 5(1), 7–14.

[6] Desarnaulds V., Carvalho A., Monay G., *Church acoustic and the infuence of occupancy*, Building Acoustics, Vol. 9(1), 2002, 29–47.

[7] Engel Z., Engel J., Kosała K., Sadowski J., *Podstawy akustyki obiektów sakralnych*, ITE, Kraków–Radom 2007.

[8] Engel Z., Kosała K., *Index method of the acoustic quality assessment of sacral buildings*, Archives of Acoustics, Vol. 32(3), 2007, 455–474.

[9] Kamisiński T., Kinasz R., Rubacha J., Kulowski A., *Badania doświadczalne i modelowe parametrów akustycznych wnętrza kościoła pw. Marii Magdaleny we Lwowie*, Materiały XII Polskiej Konferencji Naukowo-Technicznej: Fizyka budowli w teorii i praktyce, Politechnika Łódzka, Łódź 2009.

[10] Kosała K., *Calculation models for acoustic analysis of St. Elizabeth of Hungary Church in Jaworzno Szczakowa*, Archives of Acoustics, Vol. 41(3), 2016, 485–498.
[11] Kosała K., *The comparative analysis of acoustic properties of Roman Catholic churches using the index method*, Acta Physica Polonica A, 125, 2014, 99–102.
[12] Kosała K., *Wskaźnikowa ocena wpływu publiczności na jakość akustyczną wybranych kościołów*, [in:] *Postępy akustyki*, M. Meissner (ed.), Seminarium OSA 2016, Warszawa–Białowieża, 12–16 September 2016, 401–412.
[13] Kosała K., *Zagadnienia akustyczne w obiektach sakralnych*, Ph.D. dissertation, AGH, Kraków 2004.
[14] Kosała K., Engel Z.W., *Assessing the acoustic properties of Roman Catholic churches: A new approach*, Applied Acoustics, Vol. 74, 2013, 1144–1152.
[15] Kosała K., Kamisiński T., *Akustyka wielofunkcyjnych wnętrz sakralnych*, Technical Transactions, Vol. 11-A/2011, 115–122.
[16] Kulowski A., Kamisiński T., Kinasz R., *Koncertowa funkcja kościoła pod wezwaniem św. Marii Magdaleny we Lwowie*, Materiały Międzynarodowego Seminarium: Odnowa struktur miejskich w świetle zrównoważonego rozwoju, Politechnika Gdańska, Gdańsk 2005, 81–86.
[17] Meyer J., *Kirchenakustik*, Frankfurt am Main, Verlag Erwin Bochinsky, 2003.
[18] *Podstawy sterowania dźwiękiem w pomieszczeniach*, A. Gołaś (ed.), AGH, Kraków, 2000.
[19] RASTI *Technical Review*, No. 3, Brüel&Kjaer Naerum, 1995.
[20] Schroeder M.R., *Modulation transfer functions: definition and measurement*, Acustica, 49, 1981, 179–182.
[21] Wróblewska D., Kulowski A., *Czynnik akustyki w architektonicznym projektowaniu kościołów*, Wydawnictwo Politechniki Gdańskiej, Gdańsk, 2007.
[22] http://www.ymec.com/manual/esa/appendix.htm (access: 30.12.2016).

TECHNICAL TRANSACTIONS 6/2017
CZASOPISMO TECHNICZNE 6/2017
ARCHITECTURE AND URBAN PLANNING
DOI: 10.4467/2353737XCT.17.084.6560

Katarzyna Słuchocka (katarzyna.sluchocka@put.poznan.pl)
Chair of Drawing, Painting, Sculpture and Visual Arts, Faculty of Architecture, Poznan University of Technology

Representation of architectural idea and interpretation as part of the protection of cultural heritage

Zapis idei oraz interpretacji architektonicznej jako elementy ochrony dziedzictwa kulturowego

Abstract

Architecture and urban planning, classified as technical disciplines of science, in their records of creative works, also maintain representations of architectural ideas in the form of drawings, sketches or paintings. Ancillary to national heritage collections, they are an extensive source of information, which links the autonomous vision of the creator with the form outline, thus, creating an external context of such a form. Original architectural notations are part of the documentation of designs that were later executed and those that failed to be executed at all; furthermore, they confirm the high quality of expertise and the individual approach typical of leading professionals in the field across the world. The inspiration drawn from the 20th and 21st century facilities, translated into the language of artistic expression, proves the interdisciplinarity of the architectural profession and its communicative and educational assets shall be subject to particular protection and shall be displayed in order to elevate the rank of their meaning in the design process as well as in the collection of national, cultural heritage.

Keywords: representation – document, artistic value, cognitive value

Streszczenie

Architektura i urbanistyka, zaliczana do dziedziny nauk technicznych, w swoim rejestrze kreacji twórczych zawiera także zapis idei architektonicznych przedstawianych w postaci rysunków, szkiców, malarstwa. Jako dopełnienie zbiorów dziedzictwa kultury i sztuki stanowią one bogate źródło informacji, scalające autonomiczną myśl twórcy z zarysem formy, budującej kontekst zewnętrzny. Autorskie notacje architektoniczne są częścią dokumentacji zrealizowanych i niezrealizowanych projektów, także potwierdzeniem wysokiej jakości warsztatu zawodowego oraz indywidualnych postaw reprezentujących czołówkę światowego środowiska twórczego. Inspiracje czerpane z obiektów XX i XXI wieku, przekładane na język wypowiedzi plastycznej, dowodzą interdyscyplinarności specyfiki zawodu architekta, a ich komunikatywne oraz edukacyjne wartości powinny być w szczególny sposób chronione i eksponowane, podnosząc tym samym rangę znaczenia zarówno w procesie projektowym, jak i w zbiorach narodowego dziedzictwa kultury.

Słowa kluczowe: zapis – dokument, wartość artystyczna, wartość poznawcza

1. Introduction

The pure form of dialogue between a gesture and mind is one of the fundamental elements of the creation process. It reflects the image of an inner world, enabling the sensual verification based on the examination of the representative vision of reality, consequently contributing to the progress of design work. Representing the parts of space with the use of drawing, painting and graphic notation is a key factor in the cognitive process and the development of the ability to use information contained in other, finished sketches and drawings simplifies and speeds up the process of creating new forms. Noticing shortcomings has a direct impact on judgement and decision making, problem solving and, finally, on the success of one's design actions. "The first sketches – representation of the architect's ideas, are (...) transformations of the final architectural form and the initial design of the creation to be executed later, as well as images that allow the viewer to better understand the thing" [1]. At this stage of creation, the creator themselves is the viewer. The original output is multidisciplinarily compared with short-term memory sensual information on a given idea [2, p. 246–250]. The set of previously adopted signals describing the phenomenon being developed is a kind of a buffer stock of sensual, pictorial information, including visual data from iconic memory, short-term memory images and many traces of the long-term memory visual code . Cognitive attention in combination with selective function are close-coupled with motivational tensity – in this case – related to the design task. The process takes place in the individualisation area, which is responsible for past experiences and the ability to use the privileged signals that are relevant for the purposeful action, which is planned or being implemented, whereas the exploration of imagination shall lead to a profiled change of the form shape. Here, we can say that a representation – a sketch, drawing or painting – performs a confrontational function. A record, like a mirror, helps us to make conscious auto-corrections, which translates into increased aesthetic value of a piece of work and into the optimization of the entire process of designing [3, p. 43–49].

2. sketch ↔ auto-correction ↔ optimization

One of the basic tools in the architect's work – a hand-made record – is at the same time his individual business card, thus, elevating the technical nature of the profession to the rank of pure art. Both, pure art and the art of designing, enclose their main expression in the final form of an artefact. Such an artefact is then assessed with respect to the values contributing to its standard, quality, degree of innovation, proper match to the context; whereas the initial phase of conceptual ideas in the form of conceptual sketches, sketches of ideas or the hand-made visualisations – watercolour paintings, acrylic painting or pencil drawings – become of lesser importance. Hidden in drawers or briefcases, complementing the design visions as unique "side effects" of the creative process, they have exceptional value of autonomous pieces of art, and quite often, prove to be the only set of drawing or painting notes, which, for us, can become a source of invaluable information about the facilities, which no longer exist or which have never been erected. Combined with the existing photographic documentation of erected facilities,

they make up archive footage comprising unique information on the epoch and architectural and urban planning legacy. Furthermore, the artistic value combined with the cognitive value of the hand-made spatial notations, in the context of entire output of the author, complement the image of an architect as an interdisciplinary creator. Specific features repeatedly found in drawing representations are attributed to the sets of works and these identify the originator, reflecting upon their quality of artistic work, which, from the conception of space, is transformed into the existing reality, and with inherent sensitivity affects the shape of form and its functions, diligently constructing another 3D division. Works complementing the design visions, penetrating the cul-de-sacs of imagination, depicting the codes of creative thinking, the ones uncompleted because of intersecting decision dilemmas and – the completed ones – ready to be hung on the walls of prestigious galleries. Architecture being an embodiment of perfection, far from illusory portrayal of reality, full of realism of creative projection, assigned to respective components of space, founded on the disciplines related to an architect's work, which at the same time is an inspiring example of popularisation of the art of architecture, aspiring to be an independent artistic accomplishment, whose output needs to be protected by a conservator.

3. creative autograph ↔ document

With a specific line, gesture or tool, the architectural drawing is considered a mark of creative identity, an autograph "negligently" signed on some random piece of a medium, the autograph of spatial sensitivity as well as an important document in this dynamic process of shaping the external environment of man.

The sensational reception of the "side effects" of design processes complemented with technical content contributes to the positive feedback on the necessity of using drawing and drawing-related media in the context of the growing potential of electronic recording, to a large extent deprived of any identity and previous duality of vision creating imagination and reality being its context. Its unique nature, and communicative (architect – investor) and educational function contribute to the phenomenal character of architectural drawing or painting representation [4, p. 259–262]. It increases the awareness of both theoretical and practical professional issues, at the same time introducing some fresh element originating from individual traits of the creator wandering along the planes that are relevant in search of the implementation solutions for their architectural visions. They also link, often independent, motivational areas and scientific fields, proving the interdisciplinarity of the architectural profession, creating a specific space like engineers, combined with the message complementing the city or urban texture, mindfully, with full responsibility for the decisions taken, taking advantage of all the qualities of the context, meaning to continue well the job of the former "constructors". Architecture – part of human culture – requires a properly developed module of consciousness, also stimulated with the output of designers comprising drawing, painting or graphic notations.

Bringing to light the niche output of architects, ancillary to their creations, shall also stimulate the activity in the field of expression of one's original observations, emotions or associations through oil or acrylic painting.

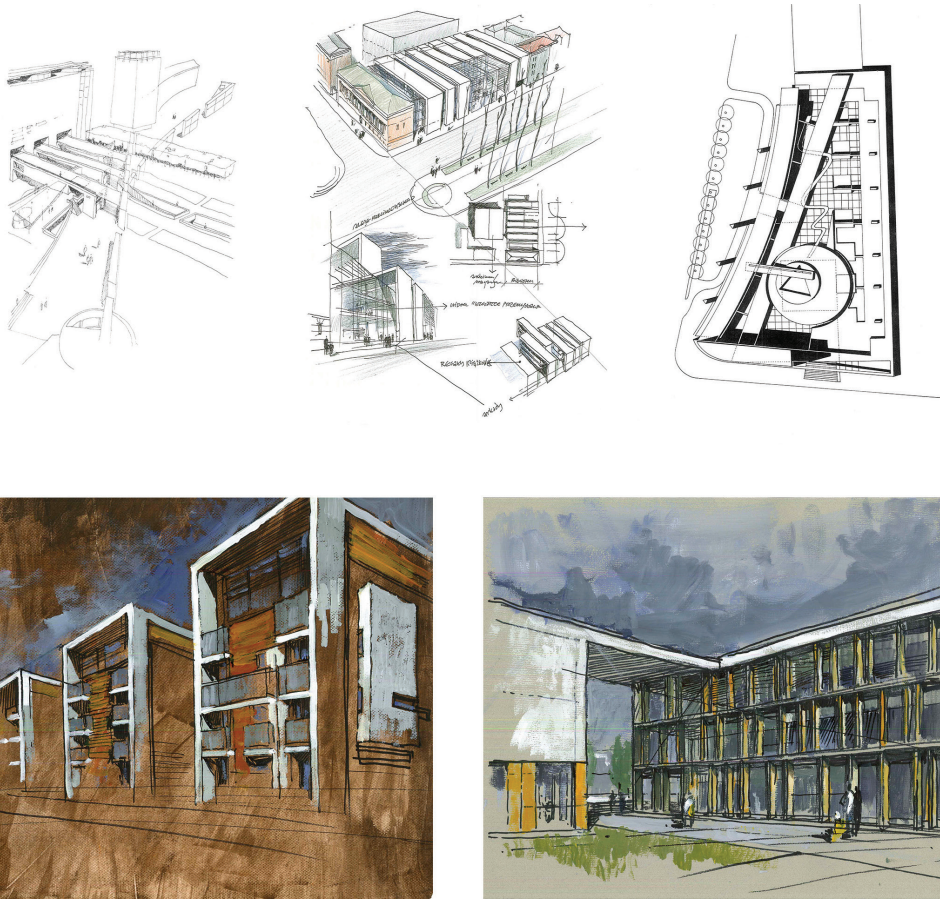

Fig. 1–3. Initial sketches depicting creator's visions during the designing process; the represented ideas document particular stages of an architectural project, at the same time being a standalone work of artistic value: Fig. 1. Rafał Lisiak, initial sketches, drawing ink, coloured pencil, paper, handmade visualisations, acrylic, paper

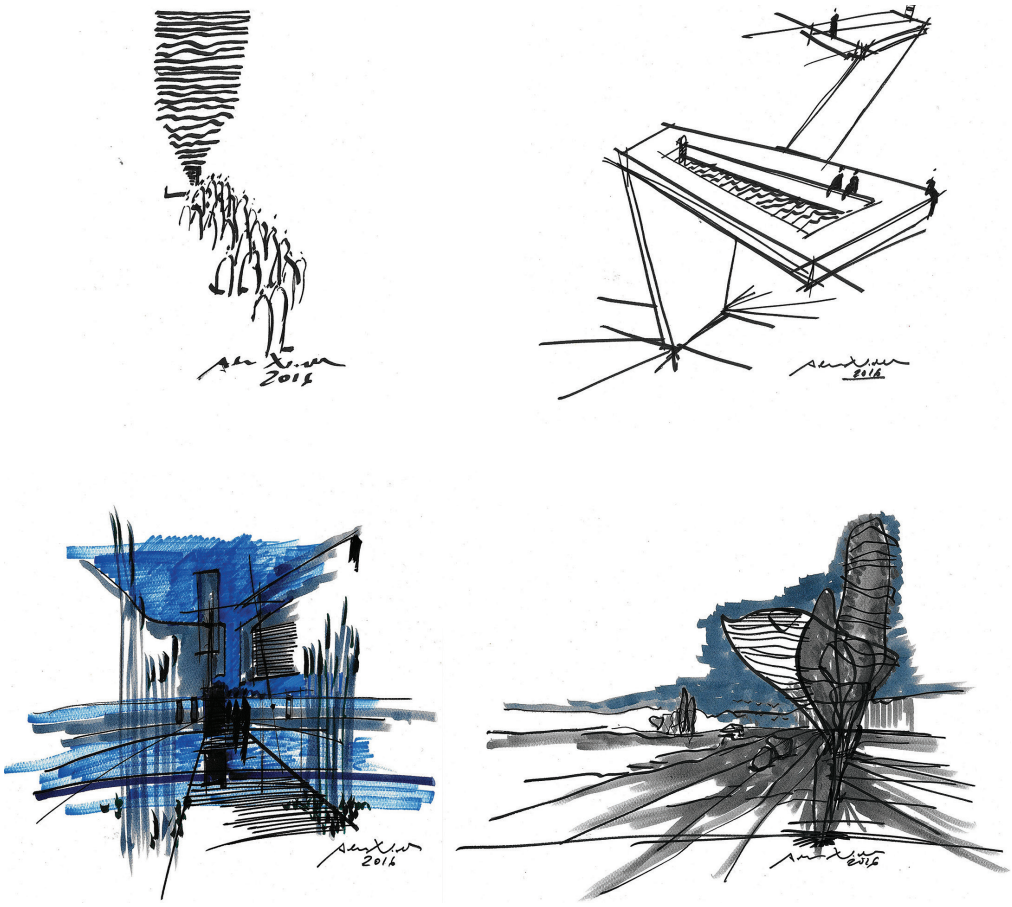

Fig. 1–3. Initial sketches depicting creator's visions during the designing process; the represented ideas document particular stages of an architectural project, at the same time being a standalone work of artistic value: Fig. 2. Adam Nadolny, initial sketches, drawing ink, promarker, paper

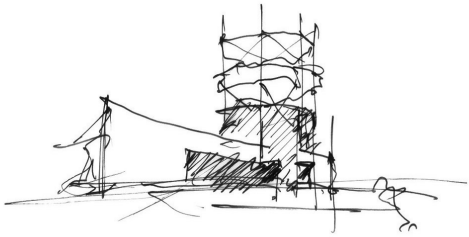

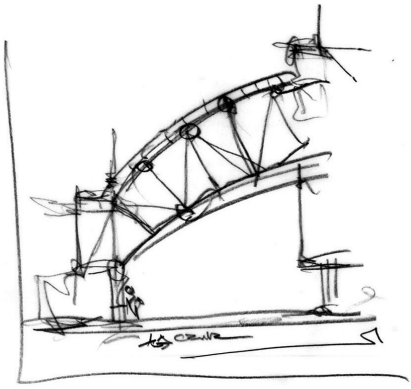

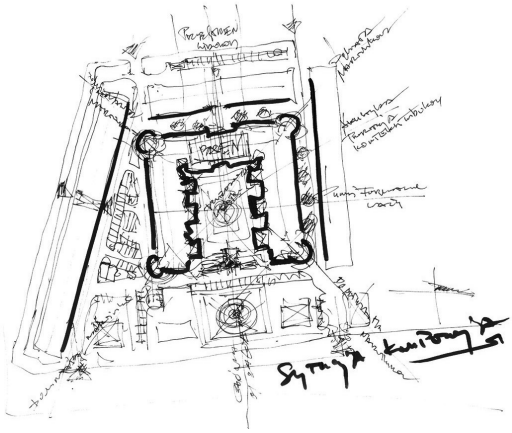

Fig. 1–3. Initial sketches depicting creator's visions during the designing process; the represented ideas document particular stages of an architectural project, at the same time being a standalone work of artistic value: Fig. 3. Sławomir Rosolski, initial sketches, drawing ink, paper, carbon paper

4. architecture ↔ comments ↔ image

Collections of conceptual sketches, sketches viewed substantively as the foundation for the key phase of the design, both black and white and colour confrontational drawings, are in majority the ready-made conceptions of the image. Fascination with architecture is a popular theme in arts, yet, interpreting the form created by a given architect, we will have to deal with the multi-functional role of its message. Architecture grasped in images – a comment on projections, cross-sections and façades of particular buildings, perceived in 2D or 3D perspective, is part of the creation process and confirmation of inter-dependencies between the quality of the design structure and the quality of artistic visual expression. Impression and intention. Form, function – image. An architectural composition, based on proportions, modules, numbers of external layer shapes, being a piece of sculpture, completed with important functional content, is linked together by dualism. Interpretation – author's graphical representation of a technical notation of the engineering thought is a stimulant for further searches for definitions of the said space within the individualisation area. It underlines the indefiniteness of opportunities for the popularisation of architectural ideas and the importance of the impact of an image upon imagination of the viewer, and activates and provokes those involved to further dialogue, at the same time creating new quality. New quality serves here as a specific agent hired to lead the viewer to a desired mental state, with particular focus on the emotions, cognitive processes and identity [5, p. 55–66]. The specific nature of this quality originates from perception of architecture as a narrowly-specialised field, constituting the grounds for creative activities. This specific nature derives from strong anchorage of the architect in the area of designing, which preconditions their perception of the facilities and space we encounter on a daily basis. Codes used by an architect – a system of norms, numbers, line connected shapes – presented as a painter's message, can be transposed to the inter-relations between craftsmanship and pure art.

Searches for an original name to be coined for the relationship between architecture and emotions expressed in paintings dismiss redundant qualities, focusing on concise options. Perceiving architecture via the prism of the construction of form and its functions in a 2D picture or drawing format enables us to better focus on the most significant content parts, based on the synthesis of illusory tricks, quotations from projections of respective buildings and on the emotional message. Conceptuality of presentation is expressed via selection of means of expression, which becomes legible in the orderly layout of the format – such as the results of the analysis and synthesis of a spatial form, and artistic expressions representing selected, architectural interiors and exteriors, may, in effect, introduce certain rules for their division accounting for the impact such a space may exert upon the quality and lifestyle of man.

The role of an architect is to shape space in a manner underlying the cannons of beauty, harmonious with our historical and cultural heritage and guaranteeing functional and mental comfort to the viewers. Any activity in the sphere of pure art shall be based on an assumption of analysis and artistic risk or otherwise an architect, as an artist, and finally as a human being, will not be able to properly interpret and express their opinions. Such an activity

Fig. 4–5. Painterly commentary on existing architecture as authors' artistic projections based on the example of selected Poznań architects' work; combining fascination for two worlds – numbers, standards, structures and compositions expressed in painting – resulting in a new value of content message transferring:
Fig. 4. Rafał Lisiak, from series entitled Miasta (Cities), acrylic painting
Fig. 5. Katarzyna Słuchocka, from series entitled Interpretacje (Interpretations), acrylic painting inspired by the technical drawings of an architectural object, acrylic

shall always involve tackling the problem and coming up with new solutions suitable to the observations and conclusions thereof, derived from the nature of architecture. The scope of an architect's interest in the pursuit of artistic activity should not be the production of the so-called pieces of art, but rather the way, in which art can contribute to the understanding of our surroundings and the benefits thereof. An artefact created on the basis of other artefacts implies a continuation of such creations, thus expanding the range of stimulants of space perception and making the viewers more sensitive to its quality and rank. Such a process can furthermore become a topic of constructive, social polemics.

5. image ↔ emotions ↔ cognitive process

Projections grasped in the form of an image are subject to assessment of their composition, expression, selection of colours and gesture. These components, as parts of a sentence, provide translation for the language of designing, reflecting upon the author thereof and indicating the hypothetical direction of further development. Designed space, not some incidental space, implies featuring a well-composed picture. "Aggressive space, depressing space, light, comfortable or ergonomic space", like in a mirror, is reflected in the painting or drawing, which as a carrier of the messages, is able to reach a wide range of viewers and to provoke them to pursue the cognitive process in the context of the images they know from daily life, but which they hardly perceive as an interpretative message in the attire of artistic contents.

Creative activity of an architect, so far seen as the 'side effect' and as so described herein, should not be marginalised in their output. Such important iconographic material needs to be perceived as work equivalent to the designed and constructed building, urban layout or any other spatial form. An analytical approach to artistic expression, founded on design awareness, knowledge of the principles of construction, will definitely render a message of pure art enriched with substantive contents. Such form of the picture-document must gain recognition within the holistic approach advocated by various scientific and artistic societies in modern organisation of science aimed at progress in scientific knowledge, at proposals of new scientific theses and expansion of the existing state of research. Interdisciplinarity of architectural profession, which finds and combines answers to questions arising at different stages of designing in the field of technology, history, psychology, ecology or geography and which strongly voices its opinions in the field of arts or fine arts, thus, confirms the high quality of artistry of the authors, who, except for an archaic today rapidograph and omnipresent computer software, can skilfully use a brush, a pencil, a crayon and ink ....

As Immanuel Kant maintained – space is a condition of the possibility of experiences. Often deemed as having no share in sensual activity, in the Euclidean concept, it was and shall always be a context for cognition and, at the same time, a main board displaying the process of constructing the representation of our surroundings. Architecture plays a significant role in shaping the global exterior, which is then objectively and subjectively perceived by man. The macro and micro scale of overlapping zones of inter-relations makes up our living space. According to Edward Twitchell Hall, space as a specific product of culture [6, p. 9–11], shall

be perceived depending on anthropological conditions via the physical and cultural sense. Sensing space in the context of omnipresent architecture – a crucial part of cultural heritage, via synergic, secondary perception based on the spatial form and its interpretations of the original drawing, painting or graphical notations, makes the communities more aware of and more sensitive to the context of their surroundings and develops a sense of their identity.

References

[1] Młodkowski J., *Aktywność wizualna człowieka (Visual acvitiy of man)*, Wydawnictwo Naukowe PWN, Warszawa–Łódź 1998.

[2] Maluga L., *Autonomiczne rysunki architektoniczne (Autonomous architectural drawings)*, Oficyna Wydawnicza Politechniki Wrocławskiej, Wrocław 2006.

[3] Gzell S., *O Architekturze, Szkice pisane i rysowane (About architecture, written and drawn sketches)*, Wydawnnictwo Blue Bird, Warszawa 2014.

[4] Hall E.T., *Ukryty wymiar (Hidden dimension)*, Warszawskie Wydawnictwo Literackie MUZA SA., Warszawa 1997.

[5] *Defining architectural space*, thesis No., 2 of XIII Edition of International Scientific Conference of Institute of Architectural Design WAPK.

[6] Słuchocka K., *Rysunek – autograf wrażliwości przestrzennej (Drawing – autograph of spatial sensitivity)*, Technical Transactions, 4-A/2015, 43–49.

TECHNICAL TRANSACTIONS 6/2017
CZASOPISMO TECHNICZNE 6/2017
CHEMISTRY
DOI: 10.4467/2353737XCT.17.085.6561

Magdalena Mazur
Tomasz Janda
Electricity de France, Cracow Division, Poland
Witold Żukowski (witold.zukowski@pk.edu.pl)
Faculty of Chemical Engineering and Technology, Cracow University of Technology

Chemical and thermal methods for removing ammonia from fly ashes

Chemiczne i termiczne metody usuwania amoniaku z popiołów lotnych

Abstract

The presence of ammonia in ashes (i.e. ammonia slip) is a direct consequence of the methods used for denitrification – selective catalytic and non-catalytic reduction (SCR, SNCR). The excess unreacted ammonia used in both of these methods passes as a constituent to ash, impairing its properties, and thus affects the quality of the commercial product. The summary of the available methods for removing NH_3 from fly ashes is presented. Both chemical and thermal methods of removing NH_3 are described. The results of the chemical methods depend on the kind of additional reagents used and composition of fly ashes. Thermal methods seem to be simpler and easier to use, but they are used mainly on the smaller scale.

Keywords: flyash, deammonisation

Streszczenie

Obecność amoniaku w popiele (tzw. poślizg amoniaku) jest bezpośrednią konsekwencją stosowanych metod odazotowania spalin – katalitycznej i niekatalitycznej selektywnej redukcji (SCR, SNCR). Stosowany w obu tych metodach nadmiar amoniaku przechodzi w formie nieprzereagowanej do popiołu, pogarszając jego właściwości użytkowe i tym samym wpływając na jego jakość jako produktu komercyjnego. Prezentujemy przegląd dostępnych metod usuwania NH_3 z popiołu, chemicznych a także termicznych.Efektywność metod chemicznych zależy od rodzaju zastosowanego substratu i składu popiołu lotnego. Metody termiczne wydają się prostsze i łatwiejsze w zastosowaniu, ale są używane głównie w instalacjach o mniejszej skali.

Słowa kluczowe: popiół lotny, deamonizacja

1. Introduction

The adaptation of energy production facilities to meet the new and more demanding standards for emissions of nitrogen oxides (NOx), which came into effect on 1 January 2016, involves many aspects. A direct consequence of the methods of denitrification –both catalytic and non-catalytic selective reduction (SCR, SNCR) is the presence of ammonia in ashes (i.e. ammonia slip). Both methods create excess of unreacted ammonia, passing to the flue gases, bonded to particles of fly ash in the free form or as a part of ammonia salts, and degrading its properties, and thereby affecting the quality of commercial solid products [1–4].

Ammonia is widely used in industrial processes, in large quantities. It is a combustible gas, toxic, corrosive, and irritantto the human mucous membranes. These properties mean that ammonia is fraught with danger for human health and life. When bound with fly ash it may be released as a result of the operation during storage or during processing of materials, which in its composition contain fly ash[4].

The report made by the Electric Power Research Institute (EPRI) shows that the problems related to the ammonia content in fly ash have become a problem for coal plants in recent years, due to the increased use of ammonia in the process of the denitrification of flue gases. The study was conducted on the basis of samples from Conectiv's BL England station, Georgia Power's Plant Yates and the Orlando Utilities Commission (Table 1) [5].

Table 1. Examples of fly ashesand its ammonia concentration [5]

Sample name	Source unit	Unit type	Coal type	Ammonia source	Nominal ammonia concentration
Yates	Georgia Power, Plant Yates, Unit #5	CE, T-fired	Eastern Bituminous, High-VolatileA, 1.2% Sulfur	FlueGas Conditioning	150 ppmw
Stanton	Orlando Utilities Commission, Stanton, Unit #2	B&W, Wall-fired	Eastern Bituminous, High-Volatile A, 1.1% Sulfur	SCR	100 ppmw
BL England	Conectiv, BL England, Units #1 and #2	B&W, Cyclone-fired	Eastern Bituminous, 2 % Sulfur	SNCR	700 ppmw

Based on the study on the release of ammonia from the ash, it has been shown that for objects that will be dealing with sales of ammonia containing ash, the chemical composition of the ash can be significant. From this point of view, there is the possibility of the release of ammonia during the subsequent use of fly ash as an additive to, for example, concrete. It seems that particular ash processing will force secretion of ammonia regardless of the ash characteristics. Therefore the total amount of ammonia present dictates the height of the release of ammonia, and whether it will be released or not [5].

While an analysis of the ammonia injection to electrostatic precipitators has shown that this may result in an increase in the ammonia content in the ash up to 2000–2500 ppm, resulting in ash

that is not suitable as a concrete additive. Moreover, it was shown that ammonia slip at the level of 2 ppm may result in increased ammonia content in the fly ash above 100ppm and thus prevents the sale of such a non-market ash [6]. Fly ash as a cement additive must meet appropriate criteria in terms of physical and chemical properties. A higher ammonia content leads to more intense and unpleasant odour generated during processing. Despite the fulfilment of the basic parameters of ash, an unpleasant smell is not acceptable, thus based on industrial practice it was concluded that the ashes should contain up to 100 ppm of ammonia. On the other hand, power generation plants can generate fly ash ammonia contents of 200 to 2500 ppm [7].

In such cases it is necessary to modernize the ash processing plant to implement the chosen method of removing excess ammonia, occurring mainly in the form of ammonium sulphate [6]. It should be mentioned that no Polish and EU regulations on permissible level of NH_3 in fly ash have been developedthus far. Such regulations have been developed in particular countries due to the possibility of further utilization of fly ash.

2. The origin of NH_3 in by-products of combustion – mechanism of ammonia transfer to ash

Ammonia is a polar, colourless, toxic, irritating the mucous membranes, gaseous compound with a characteristic odour. It condenses into a colourless liquid at a boiling point of –34°C (239.74 K), with a high heat of vaporization (1.3 g/kJ). It is most often used in refrigeration. It is soluble in water, where it is present in the form of ammonium ion (reaction 1), due to its interaction with water molecules and generation of hydrogen bonds.

$$NH_{3(g)} + H_2O \leftrightarrow NH_4^+ + OH^- \quad (1)$$

Due to its high solubility (1 volume of water dissolves 1176 volumes of $NH_{3(g)}$ at. 0°C) in aqueous solutions it occurs in the undissociated form, and to a certain degree it dissociates (in a solution of conc. 0.1 mol/dm^3 only 1% ammonia molecules are present in the form of ions NH_4^+). Consequently, aqueous ammonia solutions behave like a weak base. Solubility decreases with increasing temperature and increases with the increase of $NH_{3(g)}$ partial pressure (equation 2 and 3) [8, 9].

$$k_H = \frac{NH_{3(aq)}}{p_{NH3(g)}} \quad (2)$$

$$nk_H = \frac{4092}{T - 9.70} \quad (3)$$

wherein:

k_H – Henry's constant;
$NH_{3(aq)}$ – the concentration of ammonia in aqueous solution;
$p_{NH3\,(aq)}$ – partial pressure of ammonia.

Ammonia in aqueous solution is present in two chemical forms which differ significantly in their toxicity: unionized, toxic NH_3 and ammonium NH_4^+ (with low toxicity). A state of equilibrium between the two forms is represented by the equation (4) [8, 9].

$$NH_3 \cdot nH_2O_{(aq)} \leftrightarrow NH_4^+ + OH^- + (n\text{-}1)H_2O_{(l)} \quad (4)$$

The ratio of both forms of ammonia is mainly dependent on the pH of the solution and, to a lesser extent, on temperature. The increase in the pH causes shift of the equilibrium to unionized form of NH_3. At pH = 9.2 there is a balance between the concentration of both forms. As temperature rises, the equilibrium moving towards lower pH values [9].

Ammonia bonds to ash directly as unreacted substrate used in flue gas denitrification systems. Depending on the method used for denitrification, its sources are [8, 9]:

- SCR (selective catalytic reduction) Installation – due to addition of 24% solution of NH_3, in stoichiometric excess: 1.02–1.1 with respect to NO_x.
- SNCR (selective non-catalytic reduction) Installation – addition of 40% urea solution $CO(NH_2)_2$, in stoichiometric excess: 2.0–3.1.

Excess of ammonia reacts with other gaseous components of flue gas to form ammonium salts (sulphates, carbonates, chlorides), which can be in solid or liquid form, depending on the temperature. The latter can eventually evaporate and leads to the formation of solids. This process is promoted by a steam and increased temperature. In the largest amount (approx. 75%) ammonium hydrogen sulphates and sulphites are formed (Equation 5–7). Sulphites have a strong hygroscopic character and are therefore trapped in electrostatic precipitators – no significance for the process [9]. The SO_3 presence in the exhaust gas is the main factor leading to the formation of sulphate and bisulphates [9, 10].

$$NH_3 + SO_3 + H_2O \rightarrow NH_4HSO_4 \quad (5)$$

$$NH_3 + H_2SO_4 \rightarrow NH_4HSO_4 \quad (6)$$

NH

(7)

$$NH_3 + NH_4HSO_4 \rightarrow$$

To simplify the process of passing ammonia to ashes, two steps are proposed [8, 9]:

a) Intrinsic ammonia adsorption: NH_3 occurs as molecules adsorbed on the surface of the ash particle creating chemical bonds, an important role in the mechanism of the process is played by active acid sites on the surface of the ashes particles; the process is reversible;
b) Ammonia deposition: NH_3 is present as an ammonium salt (mainly sulphates and bisulphates), which adhere to the grain ash.

Ammonium bisulphate, is a solid compound with the chemical formula $(NH_4)HSO_4$, a decomposition temperature of 147°C and a very high solubility in water (for the pure $(NH_4)HSO_4$ has a solubility of 1000 g/dm^3). It is soluble in some organic solvents (e.g. methanol) and insoluble in acetone. It is a product of incomplete neutralization of sulphuric acid (VI) with ammonia, or may result from thermal decomposition of ammonium sulphate (reaction 8):

$$(NH_4)_2SO_4 \rightarrow NH_4HSO_4 + NH_3 \quad (8)$$

It has a strong hygroscopic character, a high viscosity (in liquid form) and therefore also causes corrosion and slag formation. In contrast, secondary component–ammonium sulphate is a dry, non-sticky powder having a particle diameter of ≤10 μm and unlikely to undergo deposition, but is carried along with the flue gas to electrostatic precipitators, where is not trapped and is considered to participate in PM10 emissions [9, 10].

In a solution of ammonia salts, when pH increases above 7 it can cause the transition of ammonia into the gas phase. It is precisely this phenomenon which is the most significant in the context of ammonia release from the ashes. For example, if the ash is wet, basic compounds can react with water, pH may be high and NH_3 is released in gaseous form. This phenomenon occurs because of the neutralization of acidic groups of solids, which previously bonded the NH_3. This reaction is often seen in the processing of ash in cement production plants [10].

The literature [5, 11–15] indicates a close relation between ammonia adsorption and qualitative composition of the ash and the conditions of its formation. With increasing amounts of unburnt carbon, the possibility of NH_3 adsorption increases –ashes with a higher content of silicates and aluminosilicates have a lower affinity for ammonia. It was confirmed that the oxides present on the surface of the carbon adsorb ammonia. This is explained by the fact that the acidic functional groups are combined with oxides and act as a Bronsted acid with respect to ammonia as a base. As a result of acid-base interaction proton transfer can occur to produce an ammonium ion NH_4^+, which then interacts with an acidic or amide side causing formation of imides [11]. In other words, the existence of the ash surface acidic groups facilitates attachment of ammonia –by creating a kind of "active site" which attracts NH_3 molecules. The increase of the acid groups is observed mainly for ash from lower quality coal. Conditions conducive to the adsorption of ammonia are a reducing atmosphere and a rapid lowering of temperature, causing a glassier phase in the ashes [11].

3. Chemical methods of removing ammonia from fly ash

3.1. STI Technology

STI a patented technology which involves the addition of a small amount of water and alkali to the ashes in order to release ammonia, and then its catalytic reduction, or uptake during processing in wet absorbers. The process reduces the total ammonia concentration to less than 100 ppm by weight of the dry fly ash. This value eliminatesa detectable ammonia

odour in the product during use, and thereby does not impair other properties of the product. Key features of the STI process are [6, 7, 16]:

- The addition of water: thisis efficient alone, but more efficient when combined with other methods.
- The addition of alkalis: accelerates the reaction the release of NH_3, but too much addition causes the ashes to be useless.

The main parameters, which were given and claimed in the patent granted:

- addition of 5% H_2O (< 20%),
- addition of 5% alkali (< 10%),
- addition of 0.25–1% CaO, $Ca(OH)_2$
- process temperature 15–65.5°C
- process time 15 min (below 30min).

The principle of the method is displacement of a weaker base (NH_4^+) in the salt ($(NH_4)_2SO_4$) by a stronger ion (Ca^{2+}) according to Reaction 9. The chemical reaction takes place in a thin surface film of the aqueous phase surrounding the ash particles which is formed as a result of the addition of water while vigorous stirring. A larger contact area and the process of diffusion in the liquid phase accelerate the reaction rate. Steps which can limit the speed of the process are: the hydration reaction of quicklime (reaction 10), the migration of calcium ions and hydroxyl to the solution, dissociation of $Ca(OH)_2$ which increases the pH of the mixture (reaction 11), which are accompanied by precipitation of the solid (reaction 12). Ammonium salt existing in the mixture is soluble in water, goes into the ionic form (reaction 13). Followed by reaction with hydroxyl ions goes into gaseous ammonia (reaction 14) [6, 7, 16].

The overall reaction is as follows:

$$(NH_4)_2SO_{4(s)} + CaO_{(s)} \rightarrow 2NH_{3(g)} + CaSO_{4(s)} + H_2O_{(g)} \quad (9)$$

Detailed reactions:

$$CaO_{(s)} + H_2O \rightarrow Ca(OH)_{2(s)} \quad (10)$$

$$Ca(OH)_{2(s)} \leftrightarrow Ca^{2+} + 2OH^- \quad (11)$$

$$Ca^{2+} + SO_4^{2-} \rightarrow CaSO_{4(s)} \quad (12)$$

$$(NH_4)_2SO_{4(s)} \leftrightarrow 2NH_4^+ + SO_4^{2-} \quad (13)$$

$$NH_{3(g)} + H_2O \leftrightarrow NH_4^+ + OH^- \quad (14)$$

The reaction of ammonium salts with lime is highly privileged because of a chemical imbalance. A key feature of the STI is the limited quantity of water (1 to 4%, typically 2 wt.%) and small amounts of alkali (< 2%). A larger amount of water is detrimental to the process – it causes dilution of the reaction system, and thus slows down the release of ammonia, at the same time it increases the moisture content of the ash, which must be subsequently removed from the

solid product. The pH of the resulting mixture of ash-lime-water should be higher than 10. Small amounts of alkali are added to provide this pH value, depending on the natural acidity of the ash. Therefore, this method is most suitable when the pH of the ash is high, the displacement of the equilibrium of the reaction is the easiest and requires minimal costs of raw materials[6, 7, 16]].

In subsequent publications, authors show the maximum efficiency of ammonia removal in the reaction of quicklime in the presence of 1–4% water at pH > 10 [9–11].Table 2 shows the dependence of efficient response time with respect to the amounts of substrates used under an unacceptable concentration of NH_3 to 100 ppm [6, 7, 16].

The usage of an equivalent amount of $Ca(OH)_2$ instead of CaO improves response time by eliminating the limiting step (Reaction 10), but on the other hand the reaction (10) is strongly exothermic and produces heat affecting the rate of the reaction and the phase transitions of water in the gaseous state. The usage of an equivalent amount of NaOH against $Ca(OH)_2$ decreases the efficiency of the reaction because of the extremely high values of pH > 14 and leads to ashagglomeration [6, 7, 16].

Use of an equivalent amount of $Ca(OH)_2$ instead of CaO improves response time by eliminating the limiting step (Reaction 10), but on the other hand the reaction (10) is strongly exothermic and provides heat affecting the rate of the reaction and the phase transitions of water in the gaseous state. Use of equivalent amount of NaOH relative to $Ca(OH)_2$ decreases the efficiency of the reaction because of the extremely high values of pH > 14 and ashagglomeration [6, 7, 16].

Table 2. Dependence of the reaction time on the content of the substrates, pH = 8.8 [7]

Alkali content	Water content	Reaction time [min]
0.25% CaO	4%	>> 15
0.5% CaO	4%	10
0.5% CaO	2%	> 15
1% CaO	2%	8
1% CaO	1%	>> 15
0.36% NaOH	4%	> 15
0.33% $Ca(OH)_2$	4%	> 15
0.66% $Ca(OH)_2$	2%	8
0.66% $Ca(OH)_2$	4%	4

In the process mentioned above, there are two stages in which ash is mixed with lime and water. The successively deammonized ash is transported to the dryers where, at approx. 65°C, evaporation of water from the ash takes place. Then the gaseous ammonia can be converted to nitrogen, or captured in water absorbers [7].

There are disadvantages of STI technology:

- It is necessary to build an ammonia – ash separation plant.
- Additional costs arising from the use of alkalis;
- The decrease in production efficiency associated with the need to remove moisture from the ash;

- The by-product, in the case of non-catalytic methods will be NH_3. Then it is necessary to use e.g. acid scrubbers. This is an additional element that causes an increase in capital expenditures.

The advantages of the installation of STI[6,7,16]:

- The high efficiency of the process – the reduction of ammonia from 87% at the end of the ammonia content of 100 mg/kg;
- The byproduct of the process of enrichment of ash is molecular nitrogen (N_2), which is an inert gas and does not increase the negative impact on the environment, in the case of the use of catalytic methods;
- Possibility of use N_2 for other purposes (e.g. explosion and fire protection, reducing the microbial degradation of biomass stored in a silo);
- The process occurs at ambient temperatures, drying the ash need only raise the temperature to 65°C;
- The final product is a high quality ash, which can be used as an additive for concrete production;
- The process of removing ammonia can be installed as a separate system in existing plants;
- The process has been implemented industrially since 1997;
- The ability to use fly ash from fluidized-bed boilers and dust;
- No restrictions on the DeNOx method(work with both SCR and with SNCR).

In Florida, two installations have been built: in Tampa and in Jacksonville. Both systems include the patented process, which reduces the content of ammonia in fly ash levels greater than 2000 ppm to < 75 ppm. The first plant capacity is 350.000 t/y. The installation includes three separators. On the other hand, the installation in Jacksonville contains two separators and the process of ammonia removal is 300.000 t/y. By 2013, 12 such installations have been implemented, i.a.: North America, Europe and Canada [17].

3.2. ASMTechnology

This technology involves treating the fly ash with calcium hypochlorite, $Ca(ClO)_2$, as a strong oxidizing agent[18]. The ammonia contained in the ash is oxidized to nitrogen with 95%efficiency, and also chloride ions are released. Under conditions of equimolar mixture of hypochlorite to ammonia, N2 is the product, but too large an excess of reagents in the relation 2:1 (Cl:N) results in the oxidation of NH_3 to nitrates. In practice the additive is applied in 1.0 to 1.5 molar excess relative to ammonia. A larger excess of reagents is used if the ash has higher carbon content or lower than the optimum pH value. Reaction proceeds according to the equation:

$$2NH_3 + 3ClO^- \rightarrow N_2 + 3Cl^- + 3H_2O \quad (15)$$

Table 3 shows the experimental results obtained. Calcium hypochlorite has been preliminarily dissolved in water and sprayed in the form of a mist to ash and then mixed.

Table 3. Oxidation efficiency and ammonia removal data [18]

Proportion of reagents (Cl:N)	Addition of calcium hypochlorite [kg/t]	Moisture content(%)	Final NH_3 content (ppm)	Reaction efficiencyNH_3(%)
0.0:1.0	0	0	500	0
0.5:1.0	1.81	1	300	40
1.0:1.0	3.62	2	30	94
1.5:1.0	5.44	3	20	96
2.0:1.0	7.26	4	15	97

The ammonia removal depends on: the pH of the ash, the process temperature, the process time, the amount of reagent, and the amount of reducers (in the ash) which can slow down the reaction [18]. It is proposed to use two methods depending on the moisture of ash: dry mixing (dry ash) – the reagent is activated by the addition of water and then in its active form reacts with ammonia or wet mixing (wet ash) –occurs more rapidly, a good mixing of the components is necessary. In practice, systems in the United States process ash containing of NH_3 at the 75–300 ppm level, using 1–1.4 kg of calcium hypochlorite per 1 ton of ash. Technologies are adapted to operate in the range of 0–2.7 kg of calcium hypochlorite per 1 ton of ash, depending on its quality. The reported costs of running the installation with a capacity of 150 ton/h is less than $500 000, and the building time of the installation is 6 to 9 months (according to data for 2005) [18].

The advantages of the ASM technology:

- the small amount of reagent used,
- the small investment and low maintenance costs,
- two variants of the process: dry or wet, depending on the destination of ash,
- the cost of the reagent can be minimized by using technology equipped with the "on demand" option. Then the ash is cleaned when necessary.

The disadvantages of ASM technology:

- license fee,
- the addition of excess calcium hypochlorite can cause difficulties with the ashes,
- usage if dry calcium hypochlorite because of its strong oxidizing properties (constituent of explosive mixtures) carries the obligation to comply with stricter safety standards and regulations,
- usage of wet method generates additional energy and costs,
- it is not specified how to prevent corrosion caused by calcium hypochlorite and its impact on the life of the installation, which does not preclude the need for additional corrosion protection.

3.3. Catalytic methods of conversion of ammonia to nitrogen

Selective catalytic oxidation (SCO) of ammonia to nitrogen based on reaction (17) [19, 20]:

$$4\,NH_3 + 3O_2 \rightarrow 2N_2 + 6\,H_2O \qquad (17)$$

For the catalytic activity in this process, we can use e.g.: CuO, Fe_2O_3, Co_3O_4, MnO_2, MoO_3, V_2O_5, CuO/La_2O_3, CuO/RuO_2. The main problem is to obtain good selectivity with respect to nitrogen. More recently, catalyst systems have been proposed were oxides of Mg-Cu-Fe are formed from the precursor, a hydrotalcite $(Mg_6Al_2(CO_3)(OH)_{16}.4(H_2O))$ [20, 21]. The best obtained results are: 60% conversion rate of the ammonia to N_2 with a selectivity of over 90% at 450°C for the composition of the inlet gas: 0.5% ammonia, 2.5% oxygen, 97% of inert gas [20, 21]. The publication indicates that the catalyst is resistant to water vapour, however, it doesn't show the information about the sensitivity to SO_2.The SCO process using these catalysts can be carried out in the temperature range of 300–450°C. At a laboratory scale, with gas flow of 40 ml/min and the amount of catalyst 100mg no significant decrease in the conversion extent to GHSV 61600h-1 catalyst loading was observed. There are two reaction paths within the SCO. The first two-step reaction "in situ" (18, 19) [19, 20]:

$$4NH_3 + (3+2x)O_2 \rightarrow 4NO_x + 6H_2O \quad (18)$$

$$3NO_x + 2xNH_3 \rightarrow (x+1.5)N_2 + 3xH_2O \quad (19)$$

The second is based on $\cdot NH_2$ radical formation, with the intermediate stage comprising hydrazine formation (20–23) [19,20]:

$$NH_{3(g)} \rightarrow NH_{3(ads)} \quad (20)$$

$$NH_{3(ads)} \rightarrow \cdot NH_{2(ads)} + H^+ + e^- \quad (21)$$

$$2\cdot NH_{2(ads)} \rightarrow N_2H_{4(ads)} \quad (22)$$

$$N_2H_{4(ads)} \rightarrow N_2 + 4H^+ + 4e^- \quad (23)$$

The advantage of selective oxidation of ammonia is the ability to eliminate it, prior to separation of the ash from the exhaust gas, while the necessity of the catalysis is the disadvantage. Then the problem might be catalyst poisoning in the presence of components such as SO_2 or some of the heavy metals present in the ash, such as As, Hg, Pb. However, no detailed information has been found about thelifespan of catalysts used in the process. The license fee for the implementation of the technology will increase investment costs [19, 20].

In addition, a copper/titanium dioxide catalystis proposed, which works well at lower temperatures (95% conversion rate of the ammonia at a temperature of 250°C with a oad of catalyst GHSV = 50 000h^{-1}. The reaction selectivity to nitrogen is above 93% at temperatures up to 350°C [19, 20]. The problem concerning the catalytic process is the leaching of the catalyst bed with the flue gas contaminated with ash. A scheme for the mechanism of selective oxidation of ammonia to nitrogen over a Cu/TiO_2 is shown in Figure 1 [19, 20].

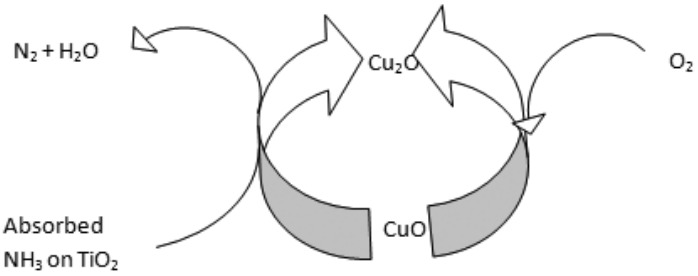

Fig. 1. Illustration of the mechanism of selective oxidation of ammonia to nitrogen over a Cu/TiO_2 [19, 20]

On the other hand, another catalyst system is described by the authors of publication [21]. The study involved Cu–SSZ-13 (a new, more robust and active small-pore Cu-exchanged chabazite (CHA; SSZ-13 and SAPO-34) zeolites have been recently commercialized, in this paperwe explore the effect of using Cu–SSZ-13 as the SCR component of the ASC) and Pt/Al_2O_3 in several variants. Reactions on catalysts are describedby the reaction equations (18, 19). The catalysts were tested in: pure form, dual-layer catalysts, where dual-layer catalysts comprised a Cu–SSZ-13 top layer and a Pt/Al_2O_3 base layer and mixed layer. In each embodiment, the catalyst has the form of monoliths with a cell density of 400 cpsi and dimensions of 1 in. diameter and 3 in. length. These were cut into 2 or 0.5 cm long, ~0.8 cm diameter samples, and were coated by dipping the monolith.Tested catalysts are shown in Table 4.

Table 4. etailed description on monolith catalysts used [21]

Samplename	**Pt loading (g/ft^3 monolith)**	**Pt/Al_2O_3 loading (g/in^3 monolith)**	**Cu–SSZ-13 loading (g/in^3 monolith)**
Pt(3)	2.7	1.4	0
Cu–SSZ(1.5)	0	0	1.5
CuZ(0.85)Pt(3)	2.8	1.4	0.85
CuZ(1.5)Pt(3) - a	2.6	1.3	1.5
CuZ(1.5)Pt(3)_high - b	2.5	1.3	1.5
CuZ(3)Pt(3)	2.8	1.4	3
Hybrid - c	2.7	1.4	2.2

a – Dual layer and mixed catalysts.
b – Cu wt% in Cu–SSZ-13 used ~5.71.
c – 0.7 g/in^3 of Cu–SSZ-13 coated on top of mixed CuZ(1.5)Pt(3).

The prepared catalyst was placed in a tubular reactor and subsequently treated using three differentgas mixtures. First; Cu-SSZ-13, 500 ppm NH_3, 375 ppm NO, 125 ppm NO_2, 5% O_2, 2.5% H_2O, 2% CO_2, bal. Ar. GHSV= 66k h^{-1}; second; Cu-SSZ-13, 500 ppm NH_3, 375 ppm NO, 125 ppm NO_2, 5% O_2, 2.5% H_2O, 2% CO_2, bal. Ar. GHSV= 265k h^{-1};Third; Cu-SSZ-13, 500 ppm NH_3, 500 ppm NO, 5% O_2, 2.5% H_2O, 2% CO_2, bal. Ar. GHSV= 265k h^{-1}.Figures 2,3and 4 show the results obtained for the Cu-SSZ-13 [21].

For the first test the maximum NH_3 conversion was 94% at 300°C. For the second and third test while increasing the volume flow rate, the degree of conversion decreased, as seen in Figures 2 and 3 [21].

Figure 5 (a, b, c, d) shows the results of the tests of the catalysts described in Table 4. The highest selectivity of 90% relative to the $N_2$is given by catalyst CuZ(1.5)Pt(3) and CuZ(3)Pt(3)_high at 375°C. The authors also describe the effect of the content of individual elements on the catalytic activity of the catalysts used [21].

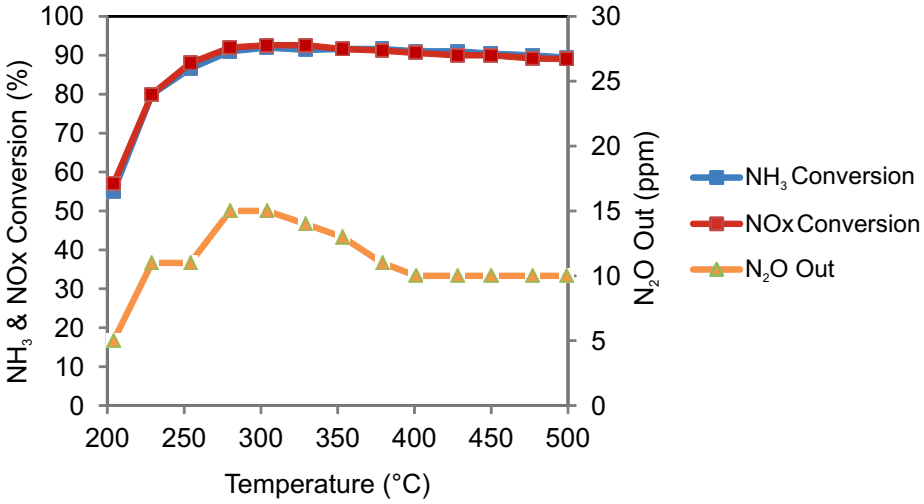

Fig. 2. Catalyst: Cu-SSZ-13, 500 ppm NH_3, 375 ppm NO, 125 ppm NO_2, 5% O_2, 2.5% H_2O, 2% CO_2, bal. Ar. GHSV= 66k h^{-1}[21]

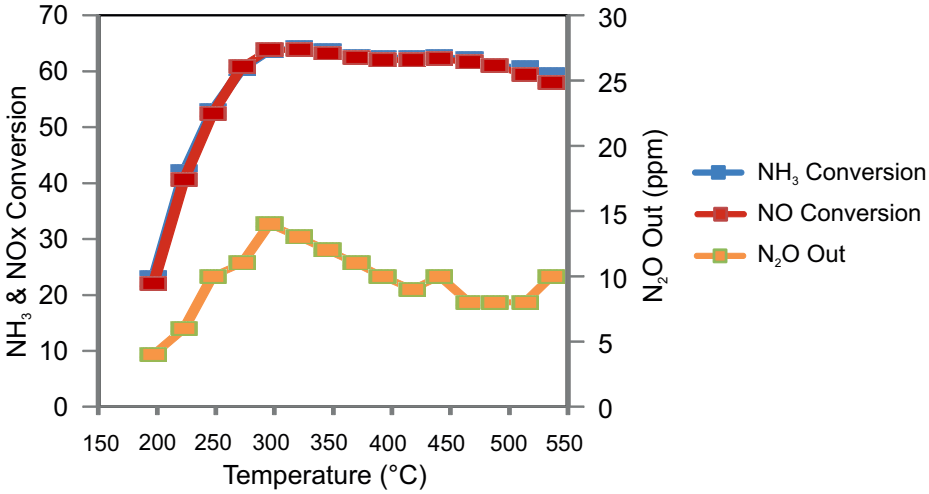

Fig. 3. Catalyst: Cu-SSZ-13, 500 ppm NH_3, 375 ppm NO, 125 ppm NO_2, 5% O_2, 2.5% H_2O, 2% CO_2, bal. Ar. GHSV= 265k h^{-1}[21]

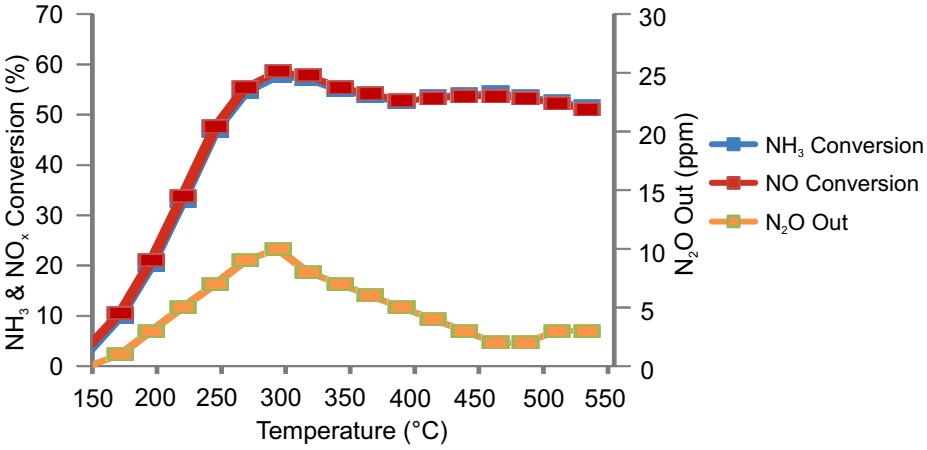

Fig. 4. Catalyst: Cu-SSZ-13, 500 ppm NH_3, 500 ppm NO, 5% O_2, 2.5% H_2O, 2% CO_2, bal. Ar. GHSV= 265k h^{-1}[21]

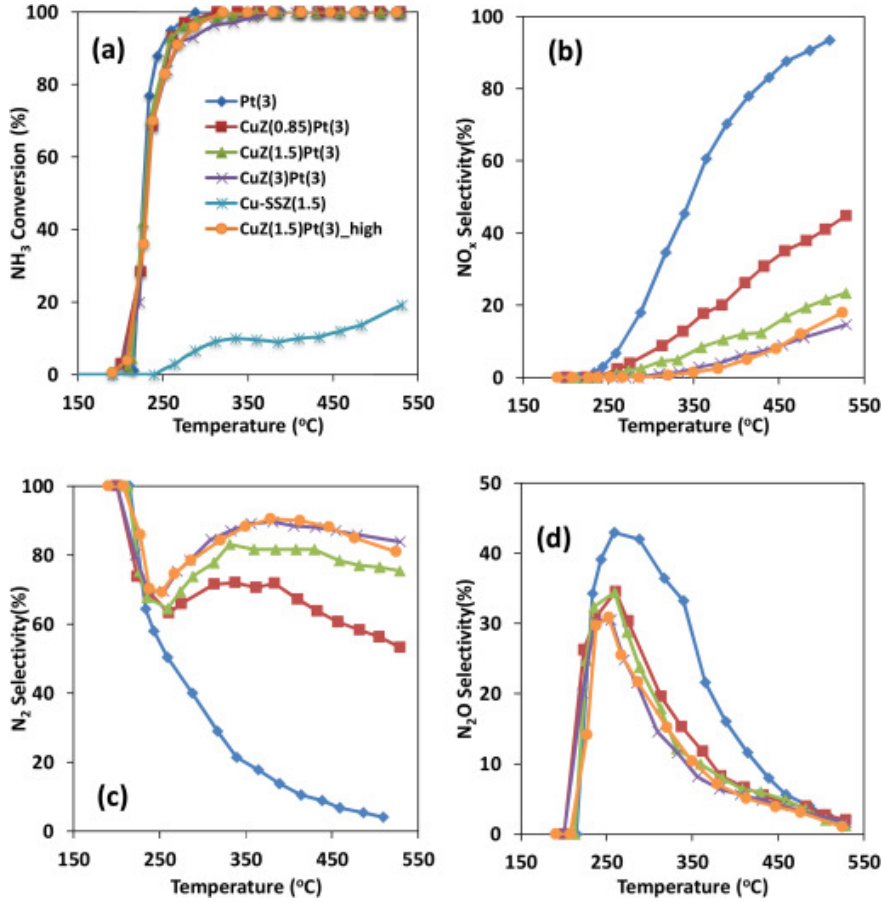

Fig. 5. Research of catalysts (a) NH_3 conversion, (b)NO_x selectivity, (c) N_2 selectivity (d) N_2O selectivity; 500 ppm NH_3, 5% O_2, 2.5% H_2O, 2% CO_2 and GHSV=66 k h^{-1}[21]

3.4. Ash ozonation

According to the literature [21] fly ash can act catalytically on the process of oxidation of ammonia with ozone atroom temperature (23^0C). Tests were carried out using a fixed bed reactor. The aim of the research was to investigate the catalytic properties of fly ash with a constant ammonia content ($11ppm_v$) This led to efficiency between 35–60% of ammonia conversion at a starting concentration about 11ppm by volume, and the ozone concentration in the range of 62 to 866 ppm by volume. The catalytic activity of the ash slightly depends on their origin. The best results obtained by the authors are:

- 45% degree of conversion of ammonia, the ammonia content of the initial 11 ppmvol; residence time 0.34s; an ozone concentration of 62 ppmv.; amount of ash in the bed 5 g;
- The content of formed nitrogen dioxide does not exceed 3%.

The potential reaction mechanism is as follows (reactions 24–29):

$$\begin{gathered} 3 \\ 3 \\ + \rightarrow HO_3 \rightarrow OH \\ - + H \\ - \rightarrow HO^{-+O_3 \rightarrow O^{-+O}} \cdot O \\ O_3 + OH \end{gathered} \tag{24}$$

$$O_{3(g)} + \text{charcoalormetaloxide} \rightarrow \ldots \rightarrow OH_{(ads)}\ ph > 9 \tag{25}$$

$$OH_{(ads)} + NH_{3(g)} \rightarrow NH_{2(ads)} + H_2O_{(g)} \tag{26}$$

$$OH_{(g)} + NH_{2(ads)} \rightarrow N_{(ads)} + H_2O_{(g)} \tag{27}$$

$$NH_{(ads)} + OH_{(g)} \rightarrow N_{(ads)} + H_2O_{(g)} \tag{28}$$

$$2N_{(ads)} \rightarrow N_{2(g)} \uparrow \tag{29}$$

All phases could initiate adsorption/reaction with ozone. In the use of char the authors speculate that it is primarily carbon that interacts with O_3 - meanwhile metals could also be present on the char surface, due to the presence of ash in the original biomass. The general consensus in the literature is that ozone dissociatively adsorbs onto metal oxides (Mn, Co, Cu, Fe, Ni) forming active oxygen species (O, ·OH). Additionally was observed that gas humidification favours the process [21].

The authors of the patent [22] provide experimental data of ammonia oxidation by ozone. The process was conducted by applying water to the ash in the form of a mist or warm humid air, constituting 1–5 wt-% moisture in the solid ash. Under these conditions, in the so-called water fog method was implemented using a mixture of ozone, air with ozone, oxygen with

ozone, and oxygen with 30% hydrogen peroxide as a co-oxidizing agent (co-oxidant), as a source of fog. All the results of the methods which used ozone with dry or semi-dry ash (1–5% water) are shown in Table 5. In all variants of the process, pH should be increased (pH > 10) by using an addition of $Ca(OH)_2$ [22].

Table 5. Resultsof ozonation by O_2 or O_3 [22]

Oxidizing agent	Final content of NH_3 (ppm)*
O_2 (150°C)	1200
O_3 4000 ppm (20°C)	850
O_3 4000 ppm (150 °C)	500
O_3 2 % obj. (150°C)	400

* initial concentration NH_3 at 1200 ppm.

Ozone reduces the ammonia content in all the conditions used, and the best results were obtained for an ozone concentration at a level of 2% by volume and process temperatures of 150°C [22].

3.5. Methods of wet and semi-dry ammonia leaching

3.5.1. Ammonia absorption with the modified turbulent scrubber usage

Studies were performed using an exhaust gas scrubber containing fly ash and operating in batch mode. Exhaust gases are introduced into the water by a thin gap, and then through the use of multiple baffles a highly turbulent flow of the gas-liquid mixture was obtained. This approach allows single step removal of fly ash to a hydraulic diameter to 0.5 microns) and a water-soluble gases such as ammonia [23–25].

Key features of the resulting solutions are:

- Maximum efficiency of removal of ammonia (79%) was obtained with a gas initially containing 45 ppm by volume of ammonia at a flow rate of 3.5 m^3/min; the water level in the apparatus was 60 cm;
- Maximum efficiency of removal of fly ash (62.48%) is achieved for particles having a diameter of 0.25 microns with a mass flow rate of the exhaust gas ratio of 140 mg/min; volumetric flow rate of the exhaust gas 3.5m^3/min, the water level in the apparatus 58 cm,
- The maximum recorded pressure drops in the flow (150 mm H_2O) was obtained for volumetric flow rate 4.5m^3/min and the water level in the apparatus 60 cm.

In the cited publication there were no design guidelines for increasing the scale of operations. Tests were carried out at room temperature. In the case of continuous mode of operation, a second apparatus –a filtration device – would be required. Other problems will be wastewater containing traces of heavy metal and vibrations generated during operation (due to the strongly turbulent flow) [23–25].

3.5.2. Humid air in a stationary or fluidized bed

There is also a process proposed in which the fly ash is in contact with a humid air in a stationary or fluidized bed. Parameters used at lab scale[23–25]:

- Gas distributor: porous glass 0.15–0.18 mm,
- Reactor diameter of 25 mm,
- Flow of moist air of 0.9–0.8 l/min,
- The amount of ash 10 g.

However, the required time contact (on the order of several hours) precludes usage. In the cited work the use of so-called atomized mist in form of suspended micro droplets of water has also been proposed. The dispersion of water in the air was obtained using an ultrasound device. In this case, at a contact time of five minutes the ammonia content was reduced from 950 ppm to about 250 ppm. Measurements were carried out in batch mode in which each phase of wetting or drying the ash lasts about 10 minutes. A disadvantage of the system may be that more moisture will cause ash particle agglomeration which leads to an increase in flow resistance in the fluidized bed. Furthermore, hydrogen peroxide has been proposed as the oxidizing agent [23–25].

3.6. The release of ammonia to the water from fly ash

Studies show that ammonium sulphate and ammonium interact strongly enough with the surface of the ash to make the release of ammonium ion much slower than the expected rate of dissolution in the water. Despite this, after a period of about 10 minutes, about 85% of ammonia was released from the ash into the water [23–25].

4. Thermalmethods

It is known from thermogravimetry studies that the temperature profile of ammonia release depends on the composition of the fly ash, which also indicates that ammonia is not present in the pure form of sulphate and bisulphate [32]. Typically, the release of ammonia from the ash takes place at a higher temperature than the thermal decomposition of pure ammonium sulphate (in the cited studies ammonia release temperature was 390°C for ash and 210°C for pure ammonium sulphate). It is also known that ammonia can be adsorbed on the active centres of acidic aluminium silicate in the ash. There are temperature profiles of ammonia release from the ashes available, obtained from the SCR and SNCR processes. In the case of SNCR release of ammonia was observed in the temperature range 200–400°C, in the case of SCR in the range of 320–480°C [28–35].

4.1. Carbon Burn-Out technology

Burning of carbon residue and thermal decomposition of ammonium sulphate and ammonium bisulphate has been proposed. The process is conducted in a fluidized bed reactor at a temperature of about 700°C with a residence time of 45 minutes. As a result of

this process ash content of less than 5 ppm ammonia is obtained. In addition, the ash has higher pozzolan activity and improved performance (lower TOC). The inventor of the ash technology is Progress Materials Inc., with the support of members of EPRI. Commercial installations of CBO™ include the Wateree Station of South Carolina Electric and Gas (1999, two units, process 180,000 tons per year of ash with an average of 12.5% LOI) and Winyah Station of Santee Cooper (2002; 200,000 tons of fly ash peryear) [26, 27].

4.2. ERC Technology (Energy Research Center)

It proposes a process in which the fly ash from the silo is introduced into the fluidized bed and fluidized by heated air. The release of ammonia begins at 150°C. The process is carried out with a continuous flow through the bed ash. Agglomerates of fine-grained fraction are broken down by the application of acoustic waves generated by speakers emitting sound waves of high intensity. Studies were conducted in terms of the ammonia content of 500 to 1000 ppm. It is also possible to modify the system by installing an additional electric heater (submerged in the bed). When using this method it is also necessary to install additional ash coolers –heat exchangers – at the end of the bed. The use of sound waves requires an analysis of the mechanical energy transfer efficiency as well as the transmission of vibrations of selected frequency to other parts of the apparatus in the vicinity of the installation [33, 34].

Advantages of ERC [33]:

- no need for additional resources,
- relatively easy scaling of installations operating in a continuous mode,
- no energy inputs for subsequent drying of ash,
- no investment in additional equipment (dryers, filtration, trays of raw materials),
- relatively low process temperature 343–398°C,
- the ability to remove up to 90% of ammonia absorbed in the ashes.

Disadvantages of ERC [33]:

- technology dedicated to BFB fluidized bed boilers, in which the waste gases must be above the bed as long as possible,
- technology developed at laboratory scale, lack of experience in production scale,
- need to ensure a constant flow of exhaust gas stream,
- needof fluidized bed equipped with a sound system preventing agglomeration of the bed.

4.3. Other thermal methods

Compared to other options, the advantage of processes based on thermal desorption at 300–450°C is mainly the small investment cost. In this case, it is necessary to provide thermogravimetric analysis to determine the conditions of the process. The ERC method has so far only been used for ashes with a high ammonia content (> 500 ppm) and no data are available on its effectiveness for ashes with lower ammonia content (but exceeding the maximum allowed level)[28–35].

5. Conclusions

Analysis of the cases associated with the presence of ammonia in ashes indicates that this is a direct consequence of the denitrification –catalytic and non-catalytic selective reduction (SCR, SNCR) of flue gases. The excess of ammonia used in these methods passes in unreacted form to the fly ash impairing its properties and thus affecting the quality of the final solid product. This bounding occurs due to the presence of acidic functional groups on ash particles surface which increase ammonia attachment. Ash neutralization with a base cause immediate emission of NH_3 to the environment. The optimal process that can be applied should be able to reduce the total ammonia content to less than 100 ppm in the dry ash.

Despite the variety of methods presented, it is difficult to choose a method that could be implemented in the energy market without additional modifications. For all methods, the imperfections of the applied technologies may bring investment and operational costs that should be taken into account. Additional costs are also generated by licenses for a patent covering the technology. When choosing the right technology it is necessary to consider economic aspects, production capacity and chemical composition of processed raw material as well as final product application.

References

[1] Zamorowski K., *Aspekty dostosowania energetyki krajowej do standardów emisyjnych tlenków azotu – wpływ zastosowanych technologii na pracę kotła oraz koszty realizacji odazotowania spalin*, „Energetyka" nr 6/2013,

[2] Wadrak P., *Proces inwestycyjny oraz Metody Redukcji NOx, SOx na przykładzie wybranych polskich obiektów energetycznych, Nowoczesna Energetyka Europy Środkowo-Wschodniej*, 2015.

[3] Directive 2010/75/EU of 24 November 2010 on industrial emissions (IED), The Minister of Environment of 22 April 2011. On emission standards from installations, OJ No. 95, item. 558.

[4] Brendel G.F., Bonetti J.E. et al., *Investigation of Ammonia Adsorption on Fly Ash Due to the Installation of Selective Catalytic Reduction Systems*, Technical Report.,West Virginia University Research Corp., 2000

[5] O'Connor, D., Behavior of Ammoniated Fly Ash: Effects of Ammonia on Fly Ash Handling, Disposal, and End-Use, EPRI, Palo Alto, CA: 2002, Technical report no. 1003981

[6] Gąsiorowski S.A., Bittner J., Hrach F., *Removing from Fly Ash, Separation Technologies*, LLC 101 Hampton Avenue, Needham, Massachusetts, USA, 2015.

[7] Gąsiorowski S.A., Hrach F.J., Method for Removing Ammonia from Ammonia Contaminated Fly Ash, Patent US6077494, 2000.

[8] Szponder D., *Badania wybranych właściwości popiołów lotnych z zastosowaniem analizy obrazu*, PhD thesis, AGH, 2012.

[9] Sikora T., Nowak P., *Raport z inwentaryzacji popiołów lotnych*, DBAA/13-901/3370, Research & Development Division, EDF Poland, September 2015[internal publication of EDF Polska].
[10] O'Connor D., *Ammonia Removal from Fly Ash: Process Review – Separation Technologies LLC (ST) – Ammonia Removal Process*, EPRI, Palo Alto, CA: 2007: 1012697, www.epri.com (access: 28.06.2015).
[11] Kulaots I., Gao Y-M., Hurt R.H., Suuberg E.M., *Adsorption of Ammonia on Coal Fly Ash*, International Ash Utilization Symposium, Center For Applied Energy Research, University of Kentucky, 2001.
[12] Czekaj M., Czupryński P., *Podsumowanie wiedzy w Grupie EDF Polska i EDF Polska R&D w zakresie zjawiska „poślizgu amoniaku" po instalacjach deNOx*, DBAA/10-911/3301, Research & Development Division, EDF Poland, May 2014 [internal publication of EDF Polska].
[13] Zhao Y-l., Yang W., Zhou J., et.al., *Experimental study on ammonia adsorption by coal ashes*, "Journal of Fuel Chemistry and Technology", Vol. 43(3), 266–272.
[14] Ma Z.B., Bai Z.Q., Bai Jet.al., E*volution of coal ashwith high Si/Al ratio under reducing atmosphere at hightemperature*, "Journal of Fuel Chemistry andTechnology", 40(3), 2012, 279–285.
[15] Gao Y.M., Külaots I., Chen X., et.al., *The effect of solid fuel type and combustion conditions onresidual carbon properties and fly ash quality*, Proceedings of the Combustion Institute, 29(1), 2002, 475–483.
[16] Gąsiorowski S.A., Bittner J., Hrach F., *Removing from Fly Ash, International Ash Utilization Symposium*, Center For Applied Energy Research, University of Kentucky, 2001.
[17] Ziegler, SD., Bittner, J, *Fly Ash Carbon Separation and Ammonia Removal in Florida*, IEEE-IAS/PCA Cement Industry Technical Conference (CIC), 2013.
[18] Ammonia Removal from Fly Ash: Process Review, Headwaters Ammonia Slip Mitigation (ASM™) Technology (www.epri.com), EPRI Project Manager D. O'Connor, Technical Update, 2005.
[19] Shilong He, ChangbinZhang, Min Yang, YuZhang, WenqingXu, Nan Cao, Hong He, "Separation and Purification Technology" 58, 2007, 173–178.
[20] Chmielarz L., Węgrzyn A.,Wojciechowska M., Witkowski S., Michalik M., *Selective Catalytic Oxidation (SCO) of Ammonia to Nitrogen over Hydrotalcite Originated Mg–Cu–Fe Mixed Metal Oxides*, Catalysis Letters, 141(9), 09/2011, 1345–1354.
[21] Shresthaa S., Harolda M.P., Kamasamudramb K., Kumarb A, Olssonc L., Leistnerc K., *Selective oxidation of ammonia to nitrogen on bi-functional Cu–SSZ-13 and Pt/Al2O3 monolith catalyst*, "Catalysis Today" 267, 2016, 130–144.
[22] Kastner R.J., *Catalytic ozonation of ammonia using biomass char and wood fly ash*, "Chemosphere" 75, 2009, 739–744.
[23] Mehta A.K., Hurt R.H., Gao Y., Chen X., Suuberg E.M., *Dry and Semi-dry methods for removal of ammonia from fly ash*, Patent US6746654 B2, 2004
[24] Wang H., Ban H., Golden D., Ladwig K., *Ammonia release characteristic from coal combustion fly ash*, "Fuel Chemistry Division Preprints", 47(2), 2002, 810.

[25] Cardone C., Kim A., Schroeder K., *Release of ammonia from SCR/SNCR fly ashes*, World of Coal Ash (WOCA), April 11–15, 2005.
[26] Keppeler J.G., Carbon Burn-Out, *Commercialization and Experience Update*, http://www.pmiash.com/cbo/acaa01paper.html, 2009 (access: 30.06.2016).
[27] Kirkconnell S.F., P.E. and J.G. Keppeler, P.E., *Carbon Burn-Out™ – A State of the Art in Commercial Ash Beneficiation*, PMI Ash Technologies SVP named new American Coal Ash Association Chair, May 2007.
[28] Czekaj M., Kulesz E., Jura K., *Zawartość amoniaku w popiele – analiza ryzyka związanego z zastosowaniem popiołów oraz wskazanie możliwości modyfikacji instalacji odpopielania*, Report DBAA/10-911/3002, Research & Development Division, EDF Poland, October 2012 [internal publication of EDF Polska].
[29] Górecka T., *Określanie kinetyki uwalniania się amoniaku z popiołów lotnych po uruchomieniu instalacji odazotowania*, Report no 271/703/12, ZWP Emitor, July-September, 2012.
[30] Rubel A.M., *Forms of ammonia on SCR, SNCR and FGC combustion ashes*, "Fuel Chemistry Division Preprints", 47(2), 834, 2002.
[31] Y.M. Gao, X. Chen, G. Fujisaki, A. Mehta, E.M. Suuberg and R.H. Hurt, *Dry and Semi-Dry Methods for Removal of Ammonia from Pulverized Fuel Combustion Fly Ash*,"Energy and Fuels" 16, 2002, 1398–1404.
[32] Rubel A.M., Rathbone R.F., Stencel J.M., T*hermal Characteristics of Ammonia Release from Combustion Ash*, International Ash Utilization Symposium, Center for Applied Energy Research, University of Kentucky, 2001.
[33] Conn R., Sarubac N., Levy E., *Removing ammonia from fly ash*, "Lehigh energy update", Vol. 19(2), June 2001, http://www.lehigh.edu/~inenr/leu/leu_28.pdf%5D. (access: 10.09.2015).
[34] Lawton K.B, *Ammonia removal from fly ash using a continuously operating acoustically assisted fluidized bed*, Theses and Dissertations, Lehigh University, 2002, 733.
[35] Lawton K.B., *ERC Completes development of technique for removing ammonia fr om fly ash, Lehigh energy update*, Vol. 20(1), 2002, http://www.lehigh.edu/energy/leu/leu_32.pdf (access: 10.09.2015).

TECHNICAL TRANSACTIONS 6/2017
CZASOPISMO TECHNICZNE 6/2017
CIVIL ENGINEERING
DOI: 10.4467/2353737XCT.17.086.6562

Hubert Anysz (h.anysz@il.pw.edu.pl)
Nabi Ibadov
The Team of Production Engineering and Construction Management, Civil Engineering Department, Warsaw University of Technology

Neuro-fuzzy predictions of construction site completion dates

Neuro-rozmyte prognozowanie terminów zakończenia przedsięwzięć budowlanych

Abstract

The results from two types of multi-layer perceptron artificial neural networks (Matlab R2015a was used) were compared. The first one, with only one neuron in an output layer having the value of delay in completion date of building site. The output layer of the second artificial neural network is created by three neurons. These three values represent the same delay, but in a form of three values of membership functions to fuzzy sets. In order to evaluate the accuracy of predictions, the mean squared error was used. It was necessary to find the best method of defuzzyfication predicted delays to compare the results from these two, aforementioned artificial neural networks. The level of prediction accuracy measured by mean squared error was discussed, too.

Keywords: MLP artificial neural networks, fuzzy sets, delays in completion dates

Streszczenie

W artykule porównano wyniki prognoz uzyskane wielowarstwowymi sztucznymi sieciami neuronowymi (obliczenia wykonano pakietem Matlab R2015a). Pierwsza z nich miała jeden neuron w warstwie wyjściowej, któremu przypisano wartość opóźnienia w terminie zakończenia danej budowy. Warstwę wyjściową drugiej sieci stanowiły trzy neurony, zawierające wartości funkcji przynależności tego samego opóźnienia do trzech zborów rozmytych. Do porównania dokładności prognoz uzyskanych z dwóch ww. sztucznych sieci neuronowych zastosowano średni błąd kwadratowy. Wymagało to znalezienia najlepszej metody defuzzyfikacji prognoz otrzymanych w postaci liczb rozmytych. Dokładność prognoz została porównana i przedyskutowana.

Słowa kluczowe: sztuczne sieci neuronowe MLP, zbiory rozmyte, opóźnienia terminu zakończenia budowy

1. Introduction

The delays in completion dates of construction sites have a negative impact on operations' efficiency of contractors as well as the clients. Moreover, taking into account public building investments like roads, hospitals, schools, the public suffers from the aforementioned delays.

Before the completion date of building works is set in the agreement between the client and the contractor, it is a subject of the client's analysis: what is the nearest possible, reasonable time of finishing an already designed building object. Officers can rely on knowledge obtained from past investments. They can analyze the scope of works necessary to complete already erected building objects, in order to estimate the time needed to build a new one. The other approach proposed in this paper is to verify planned time by predicting possible delays of the completion date.

Predicted values of the completion dates or delays can vary due to different capabilities of bidders. This is an opportunity to utilize delays of completion date predictions as one of the factors for multi-criteria evaluations of bidders. According to Tadeusiewicz [1], artificial neural networks (ANN) can be successfully applied for complex problems, where we suspect the existence of rules between input factors and the final effect of the process, but we are not able to fully recognize them. The complexity of public building investment is undisputed. The moment of prediction, i.e. before any building works started, makes liaison between parameters describing bidders, planned building object, and delay in completion date very weak. It was decided to check if Zadeh's theory of fuzzy sets [2, 3], applied for number of days as a unit of delay of a building site completion date, can improve the prediction accuracy of ANN.

2. ANN trained with the set of real numbers as an output, representing delays

The predictions of delays in completion dates of building sites were limited to the construction of express roads and highways completed in 2009-2013. The following data were chosen as an input:

- the value of construction works (taken as the best offer),
- the length of the section of highway to be built,
- the scope of works ("build" or "design and build"),
- the type of works (building a new road or modernization, upgrading),
- the total number of employees at the disposal of the bidder,
- the planned time of work execution (number of days) up to completion.

The delays in completion date represented by number of days were chosen as an output. The accuracy of predictions was measured by Mean Squared Error (MSE) [4].

$$MSE = \frac{\sum_{i=1}^{N} (c_i - r_i)^2}{N} \tag{1}$$

where:

c_i – the delay calculated by ANN for i set of test input data,
r_i – the real value of delay observed for i building site belonging to test set,
N – the number of test data set.

The total number of 156 sections of highways and express roads in Poland completed between 2009 and 2013 was limited to 119 data sets for calculations. This was caused by the necessity of using complete input data (number of employees mainly was not available). The building sites with extremely high delays in completion dates (exceeding 370 days) were excluded from the data set. Extremely high delays in completion dates were usually caused by very unusual reasons (e.g. protests of ecologists). It was assumed that completing the section of highway before the planned date causes delay equal to zero. The linear-maximum method [10] of the data standardization method was applied for input and output of ANN.

$$a_i = \frac{a_{0i}}{\max a_{0i}} \tag{2}$$

where:

a_i – the value of type a of input set, from i set of input data after standardization,
a_{01} – the value of type of input observed in process (before standardization),
i – consecutive number of the process being observed.

Multi-Layer Perceptron (MLP) type of ANN was used, as it was found that MLP networks have higher abilities to generalize input-output relations than ANN of Radial Basis Function (RBF) [5, 6]. It was checked empirically that for this case, i.e. predicting delays of completion dates, basing on the aforementioned inputs and [9], having 119 cases of input datasets, the following ANN gives the lowest MSE of predictions:

- 8 input neurons (two input parameters had to be represented by vectors [0, 1] or [1, 0], so it has risen the number inputs from 6 to 8),
- one hidden layer with 14 neurons,
- single output neuron – the delay in completion date,
- activation function in the hidden layer – linear with limits <–1, 1> (called *satlins* in Matlab),
- activation function in the output layer – logistic (called *logsig* in Matlab),
- teaching algorithm – conjugate gradient backpropagation (the order *trainscg* in Matlab).

It was set that first 79 cases create a teaching set of data. The rest, i.e. 40 sets, were kept for testing purposes (34%). Then, the complete set of data was randomized and calculations were proceeded. As the result of ANN calculation, a set of 40 predictions of delays was obtained (for every set of data from test data). Then, the predictions could be compared to the real values, by calculating MSE. The lowest MSE achieved (for test data) was 11 709.

3. ANN trained with the set of delays expressed by the values of membership functions to three fuzzy sets as an output

The delays in completion dates of building sites can be described by values of membership functions to fuzzy sets [8]. Three fuzzy sets were created for short, medium and long delays of completion dates. Membership function to the fuzzy set "short delays" μ_S was described by following formula:

$$(x)=\begin{cases} 1 \text{ or } x=0 \\ \dfrac{185-x}{185-0} \text{ for } 0\le x\le 185 \\ 0 \text{ for } x\ge 185 \end{cases} \tag{3}$$

where:

x – value of delay in days.

The membership function μ_M to the fuzzy set "medium delays" was defined as:

$$\mu_M(x)=\begin{cases} 0 \text{ for } x=0 \text{ or } x\ge 370 \\ \dfrac{x}{185} \text{ for } 0\le x\le 185 \\ \dfrac{370-x}{370-185} \text{ for } 185\le x\le 370 \end{cases} \tag{4}$$

where:

x – value of delay in days.

The membership function μ_L to the fuzzy set "long delays" was created too as:

$$\mu_L(x)=\begin{cases} 0 \text{ for } x\le 185 \\ \dfrac{x-185}{370-185} \text{ for } 185\le x\le 370 \\ 1 \text{ for } x\ge 370 \end{cases} \tag{5}$$

where:

x – value of delay in days.

All three fuzzy sets (short, medium sized and long) can be shown graphically in Fig. 1.

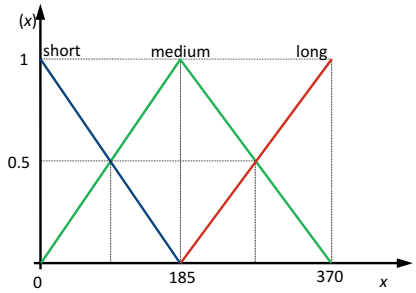

Fig. 1. Membership functions for short, medium and long delays fuzzy sets

The names of the fuzzy sets described above are partly inconsistent with their literal meaning. Nobody would say that the delay in completion date is short, when it is equal to half a year, even when the planned duration of work execution was three years. However, for the machine learning, it does not have any meaning. Much more important for the calculation is that proposed three membership functions provide that:

- for each *x* from 0 to 370 there is only one fuzzy set with the membership value not lower than 0.5,
- there is no *x* for which every membership value is lower than 0.5,
- every delay expressed in days (from 0 to 370 days) can be expressed by three membership values μ_S, μ_M, μ_S to the three fuzzy sets; one equal to 0, one higher than 0.5 and one smaller than 0.5 or one equal to 1 and the rest equal to 0.

Some examples of the fuzzyfication process concerning the set of 119 observed delays are shown in Tab. 1.

Table 1. Examples of delays shown as real numbers and values of membership functions to fuzzy sets

Real numbers	**Values of membership functions to fuzzy sets**		
Delay in days	μ_S	μ_M	μ_L
0	1	0	0
46	0.7514	0.2486	0
102	0.4486	0.5514	0
144	0.2216	0.7784	0
185	0	1	0
242	0	0.6919	0.3081
280	0	0.4865	0.5135
314	0	0.3027	0.6973
370	0	0	1

In order to apply the fuzzy sets theory to an output layer, the topology of artificial neural network had to be modified. Now output (the delay) is represented by three values of membership functions to three fuzzy sets, so the number of neurons in the output layer was increased to 3. All the other parameters remained the same (as described in chapter 2). As the values of membership functions are from 0 to 1, there was no need to standardize them. The result of calculations produced by ANN was a set of 40 predictions of delays (for test data). Each one was expressed by three predicted values of membership functions to the three fuzzy sets. MSE was not calculated for these predicted "fuzzy delays" (for each membership function value separately or as a sum of MSE), because it could not be compared to MSE calculated for predictions of delays given in days. Therefore, the defuzzyfication of the calculated predictions was required.

That is the main reason of applying the fuzzy set theory to an output of artificial neural network: by choosing the defuzzyfication method, the researcher can adjust the predictions coming with them closer to the original (not fuzzyficated) values from test data. As a result of this process, MSE can be lowered, which means that predictions will be more accurate.

In order to obtain real, crisp numbers of predicted delays (for test data), the following four methods of defuzzyfication were applied:

- the center of gravity method [7] (labeled as A):

$$x^* = \frac{\int x\mu(x)dx}{\int \mu(x)dx} \tag{6}$$

where:

x^* – real (crisp) number,
x – the value of the output variable,
$\mu(x)$ – the membership function of the output variable,

- the weighted average method [11] (labeled as B);

$$x^* = \frac{\sum_{i=1}^{n} \mu(x_i)x_i}{\sum_{i=1}^{n} \mu(x_i)} \tag{7}$$

x^* – real (crisp) number,
x_i – the value of the output variable for i fuzzy set,
$\mu(x_i)$ – the membership function of the output variable for i fuzzy set,
i – number of fuzzy set of n fuzzy sets,

- the maximum of membership function method [11] (labeled as C):

$$x^* = \max_{i=1}^{n}\left(\mu(x_i)\right) \tag{8}$$

x^* – real (crisp) number,
x_i – the value of the output variable for i fuzzy set,
$\mu(x_i)$ – the membership function of the output variable for i fuzzy set,
i – number of fuzzy set of n fuzzy sets,

- the weighted average method modified (labeled as D) where only two fuzzy sets were taken into account: medium always, and the other set with higher predicted μ (μ_S or μ_L), then formula (7) is applied.

Table 2. MSE values calculated after different methods of defuzzyfication

defuzzyfication method	MSE value
A	22 623
B	**9526**
C	10 534
D	28 699

The modification of method B was based on the fact that delays calculated for teaching ANN set of data are represented by three numbers (as shown in tab. 1) and at least one is equal to zero. Two of the three values of membership functions are equal to zero only for

0 days of delay, 185 and 370 days. Moreover, for all domains of medium delays (except 0 and 370 days), membership function μ_M has different than zero values.

All A, B, C and D methods of defuzzyfication were applied to 40 predictions received from ANN and predicted delays (in days) for the test data could be calculated. By comparing them to original delays from test data, MSE could be calculated for each method of defuzzyfication. The results are shown in Tab. 2. The lowest MSE is for the weighted average method of defuzzyfication, and it is equal to 9526.

4. Comparing the obtained results and conclusions

As it was suspected, the application of fuzzy sets theory as the output of artificial neural network (instead of one crisp number) and then searching for the best method of defuzzyfication, has brought a lower mean squared error for predictions. The obtained results are shown in Tab. 3.

Table 3. MSE calculated for ANN predictions with different outputs

Type of ANN output	MSE value
delay in days – one neuron in the output layer	11 709
delay as three values of membership function to fuzzy sets – three neurons in the output layer	9526

Applying ANN with different outputs (real, crisp value of delay – one neuron in the output layer or three values of membership functions for the same delay – three neurons in output layer) with the other parameters of ANN topology unchanged, allows one to state that the net with fuzzy set theory applied to output layer has given MSE lower by 18,6% then the net with real, crisp output.

This kind of result was expected. The fuzzyfication of delay in the completion date of a construction site, in a fact, adds some more information to the single number of delays. Moreover, the defuzzyfication of achieved predictions for test data set is a kind of post-process, made on rough predictions. Analyzing which method of defuzzyfication makes MSE the lowest resulted in it lowering, even below MSE calculated by ANN with a single, real number in an output layer. For the net with a single, real number as an output, the predictions were not post-processed. MSE equal to 9526 makes square root from it (RMSE) equal to 97 days of possible error in predicting delay in the completion date of a given construction site. It is not a precise prediction. However, taking into account the fact that the prediction can be done before any work starts on the building site, the meaning of 97 days of RMSE changes. On the other hand, it has to be emphasized that post-processing is independent from the input data, which means that the application of both tools (artificial neural networks and fuzzy sets block) can be worked out separately in order to achieve lower prediction errors.

Accurate predictions of delays in completion dates of construction sites can help in choosing the contractor providing the highest probability of completing works on time. When there

is no such contractor, it may mean that the planned time for work execution was assumed too short. The usefulness of this kind of predictions is also a subject of their accuracy. In order to achieve it, the fuzzy sets theory was applied to the output layer of MLP artificial neural networks. The block of defuzzyfication gives the chance to refine predictions, resulting in lowering the prediction error. It was proved in analysed case that post-processing of results received from ANN – when the fuzzy sets theory is applied for an output layer – can significantly lower the mean squared error of predictions.

References

[1] Tadeusiewicz R., Nałęcz M., *Biocybernetyka i inżynieria medyczna 2000. T. 6 Sieci Neuronowe*, Akademicka Oficyna Wydawnicza EXIT, Warsaw 2000.Zadeh L.A., *Fuzzy Sets*, Information and Control, 8, 1965, 338–353.

[2] Zadeh L.A., *Knowledge representation in Fuzzy Logic,* IEEE Transaction on Knowledge and Data Engineering, Vol. 1, No. 1, March 1989.

[3] Bartkiewicz J. (red. Zieliński J.S.), *Inteligentne systemy w zarządzaniu*, PWN, Warszawa 2000.

[4] Osowski S., *Sieci neuronowe w ujęciu algorytmicznym*, WNT, Warszawa 1996.

[5] Statsoft Polska Sp. z o.o., *Wprowadzenie do sieci neuronowych*, Statsoft, Kraków 2001.

[6] Ibadov N., *Determination of the Risk Factors Impact on the Construction Projects Implementation Using Fuzzy Sets Theory*, Acta Physica Polonica A, Vol. 130, No. 1, 2016, p. 107–111, DOI: 10.12693/APhysPolA.130.107.

[7] Ibadov N., *Fuzzy estimation of activities duration in construction projects*, Archives of Civil Engineering, Vol. 61, Issue 2, 2015), 23–34. DOI: 10.1515/ace-2015-0012.

[8] Anysz H. *Porównanie trafności prognoz sztucznych sieci neuronowych MLP z jedną i dwoma warstwami ukrytymi na przykładzie prognoz wyników finansowych przedsiębiorstw budowlanych*, Logistyka 3/2014, 87–94.

[9] Anysz H., Zbiciak A., Ibadov N., *The influence of input data standardization method on prediction accuracy of artificial neural networks*, Procedia Engineering 153, 2016, 66–70, DOI: 10.1016/j.proeng.2016.08.081.

[10] Rutkowski L., *Metody i techniki sztucznej inteligencji*, PWN, Warszawa 2012.

TECHNICAL TRANSACTIONS 6/2017
CZASOPISMO TECHNICZNE 6/2017
CIVIL ENGINEERING
DOI: 10.4467/2353737XCT.17.087.6563

Stanisław Belniak
Damian Wieczorek (dwieczorek@izwbit.wil.pk. edu.pl)
Institute Construction and Transportation Engineering and Management,
Faculty of Civil Engineering, Cracow University of Technology

Property valuation using hedonic price method – procedure and its Application

Wycena nieruchomości metodą cen hedonicznych – procedura i zastosowanie

Abstract

This paper discusses one of the property valuation methods, i.e. property valuation using the hedonic price method, which makes use of a classical linear regression model. The study characterises the calculation procedure of the selected method and indicates the fields of application of the hedonic approach in the construction sector. The operation of the hedonic price method is presented based on a valuation of flats in Lublin.

Keywords: property, property valuation, hedonic price method, classical linear regression model, hedonic regression

Streszczenie

Niniejszy artykuł traktuje o jednej z metod wyceny nieruchomości, tj. hedonicznej metodzie wyceny nieruchomości, która wykorzystuje klasyczny model regresji liniowej. W pracy scharakteryzowano procedurę obliczeniową wybranej metody oraz wskazano obszary stosowania podejścia hedonicznego w budownictwie. Działanie metody hedonicznej wyceny przedstawiono na przykładzie wyceny lokali mieszkalnych w Lublinie.

Słowa kluczowe: nieruchomość, wycena nieruchomości, metoda cen hedonicznych, klasyczny model regresji liniowej, regresja hedoniczna

1. Introduction

The property is defined as a controlled asset constituting a specific and defined space of the land together with its natural and anthropogenic (created by man) elements [1].

In the academic literature, property is considered in three main aspects as:

- a technical object analysed in terms of its components that comprise land and building structures together with equipment subject to wear and tear, which in turn determine the need to take actions related to maintenance of their technical efficiency and usability, their safety of use and investment with a reconstruction and development character [2],
- economic assets regarded as the subject of capital allocation, capital asset, utility asset and market asset [1–3],
- a legal object that constitutes a basis for classification of the property in legal terms, as well as for transfer of rights and property management [2].

Due to the above-mentioned economic aspect and conditioning inherent to scientific research work, the authors of the hereby publication focused their attention on the aspects related to the generation of economic benefits obtained by an investor in the form of the market value of the property.

The main purpose of this paper is to present one of the property valuation methods, i.e. property valuation using hedonic price method, which makes use of the classical linear regression model. In their study, the authors characterise the calculation procedure of the method and indicate its fields of application in the construction sector. The operation of this method is illustrated on the basis of an exemplary valuation of flats.

2. Hedonic method of property valuation

2.1. General characteristics of the hedonic method of property valuation

Methods for valuation of assets are divided into direct ones as well as indirect ones. The hedonic price method, also called the hedonic regression method, is a kind of indirect valuation method. It belongs to the family of methods based on surrogate or replacements markets [4]. The property is valuated by means of evaluation of its specific features and attributes with regards to the whole market. Analysing the regularities statistically, and more specifically, the relationship between the price and features of the property, a model is made based on that relationship, on the basis of which it is possible to estimate the price of the given property.

The purpose of using the hedonic price method is to specify the influence of the features of the property on its value. Hedonic regression is a method, thanks to which we may define the impact of the specific features of the property on its value [5]. Based on the regression method, a function determining the relation of its features to the price is created.

Table 1 presents the advantages and disadvantages of the hedonic approach to valuation.

Table 1. Advantages and disadvantages of the hedonic approach

Advantages	Disadvantages
Freedom of model creation based on available features (at the stage of model creation)	Necessity to provide substantial amount of data (at the stage of model creation)
Universality and versatility (in case when the model is constructed we may valuate many properties using it)	No possibility to make allowance for external factors, i.e. interest rate or political situation
Possibility of model updating and making corrections (the originally developed equation may be theoretically still valid)	No possibility to make allowance for the features identified as unit features or features of unique nature
Ease of use	Necessity to possess knowledge within the field of mathematical statistics to be able to build and verify the model, as well as to interpret the results

Source: own study based on [5–7].

As results from the literature, the hedonic approach (although not without some disadvantages) may be treated by economists as more reliable, since it is based on valuations disclosed on the real market.

2.2. Definition and calculation procedure of the hedonic valuation model

The relationship between the price of the asset (property) P_i and the set of its features (characteristics) [8, 9] is called a hedonic model or hedonic regression. In general, this relationship may be described with the use of the following function:

$$P_i = f\left(X_i, \alpha_i, \varepsilon_i\right) \tag{1}$$

where:

X_i – vector of asset attributes,
α_i – vector of model parameters,
ε_i – random variable.

In the hedonic price method, the valuation process consists in decomposition of the price of the asset into combinations of the specific characteristics, which reflect the importance when it comes to pricing. In fact, only the specific features of the asset are valuated, and not the asset itself.

The assumptions of the hedonic price method are similar to the assumptions known from the comparative approach, but in this case, they are more general. It results from the fact that, in the case of the hedonic approach, the importance of the specific features is shaped in relation to the total sample. It also means that the constructed model corresponds to all the observations and is universal.

The hedonic approach to property valuation is versatile, which means that, for example, we may encounter one model for property valuation within the precincts of one city or several models that have been constructed making a distinction for the specific districts. At the same time, the model composed of many models is much more detailed and gives a result, which is better adjusted to the data.

The calculation procedure of the hedonic price method may be divided into two basic stages, during which the following take place:

1) collection of data on transactions regarding the given assets (in this case property),
2) statistical estimation of the linear function that will describe the relationship between the value of the property (response variable) and the specific features having a potential impact on price (explanatory variables).

In order to make it possible to estimate the price of any property using the created function, we must note that the data on transitions regarding the property should include information both concerning the sales prices, location, as well as other significant measurable and immeasurable properties connected with the property (e.g. size, number of rooms, characteristics of the neighbouring areas, standard of finish, crime rate, environmental aspects, distance from shopping centres, etc.). Therefore, as early as at the stage of data collection, it is very important to properly process the collected data in terms of consistency, coherency and completeness of information [8].

2.3. The fields of application of the hedonic approach in the construction sector

Hedonic methods are used in the construction sector inter alia for:

- property valuation in case of which it is possible to estimate the price of the specific properties based on the constructed models,
- valuation of the specific elements (attributes), e.g. balcony in the given flat or the fact of using advanced technologies in the building,
- valuation of the qualitative aspects, e.g. through examination of changes between the values of the specific features that are not binominal variables [10],
- valuation of environmental losses or benefits on the degraded areas that may be subject to recultivation measures [9],
- research of market preferences to determine the importance and the level of their importance during the course of shaping the prices of properties [8],
- valuation of the potential health risks accompanying dangerous professions that consists in specifying the amount of additional pay for a worker for bearing additional health or life-threatening risks during work [6].

3. Characteristics of a single-equation classical linear regression model

3.1. Definition of a linear regression model

The basic model describing the relationship between the phenomena (variables) is a single-equation linear model, also called descriptive econometric model, the form of which is as follows [11]:

$$y_i = \alpha_0 X_0 + \alpha_1 X_1 + ... + \alpha_k X_k + \varepsilon_j \qquad (2)$$

where:

y_i – endogenous variable (response variable),
$X_0, X_1, \ldots, X_k$ – exogenous variables (explanatory),
$\alpha_0, \alpha_1, \ldots, \alpha_k$ – structural parameters,
ε_j – random variable.

The above-mentioned equation for a response variable is composed of a sum of two components, i.e. certain linear combination of explanatory variables ($X_0, X_1, \ldots, X_k$) and a random variable ε_j. The explanatory variables have a significant influence on shaping y_i, whereas the random variable ε_j (random disturbances) makes allowance for the total impact of other factors (excluded after analysis), not present in the model, which have an impact on shaping the response variable y_i, however, of a random (secondary) nature. The ε_j coefficient also provides for any possible, non-systematic, random errors of measurement of variables, as well as any deviations from the adopted analytical form of the model from the actual relationship between them [12].

3.2. Model estimation

The $\alpha_0, \alpha_1, \ldots, \alpha_k$ coefficients that are present in the equation (2) as the so-called structural parameters are not known in the linear regression model. Their task is to make a quantitative description of the impact of the explanatory variables (next to which they are located) on the response variable. Most frequently, one of the exogenous variables (usually the first one) is defined to be identified as $X_0 \equiv 1$. Thus, α_0 is called an absolute term of the model or regression constant [12]. Hence estimation (determination) of structural parameters α_j ($j = 0, 1, \ldots, k$) based on observation of the variables $y_i, X_1, \ldots, X_k$ becomes the main task in the construction of a linear regression model.

Due to the available n-element observation sequence for all the variables or in other words vector sequence ($y_t, x_{t1}, \ldots, x_{tk}$) ($t = 1, \ldots, n$), every realization y_t of the response variable y_i may be presented (pursuant to the assumed model) as a sum of a linear combination $\alpha_0 + \alpha_1 x_{t1} + \ldots + \alpha_k x_{tk}$ of the adequate realization of explanatory variables and unobservable realization ε_t of a random component ε_i [11, 12]. Hence we obtain the following arrangement constituting a starting point for estimation of model parameters:

$$y_i = \begin{bmatrix} y_1 \\ y_2 \\ \vdots \\ y_n \end{bmatrix}, \; X_i = \begin{bmatrix} 1 & x_{11} & \cdots & x_{1k} \\ 1 & x_{21} & \cdots & x_{2k} \\ \vdots & \vdots & \ddots & \vdots \\ 1 & x_{n1} & \cdots & x_{nk} \end{bmatrix}, \; \alpha_j = \begin{bmatrix} \alpha_0 \\ \alpha_1 \\ \vdots \\ \alpha_k \end{bmatrix}, \; \varepsilon_j = \begin{bmatrix} \varepsilon_0 \\ \varepsilon_1 \\ \vdots \\ \varepsilon_k \end{bmatrix} \tag{3}$$

The determination of model parameters takes place on the basis of a structural and statistical form of the model that is presented in the arrangement (3). Except that, the probability conditions must be met, so that estimation of parameters makes sense.

The assumptions for the linear model are as follows [11, 12]:

1) $y_i = X_i\alpha_j + \varepsilon_j$, i.e. every observation y_t is a linear function of x_{tj} observation and the random component ε_t,
2) X_i is a non-random matrix, thus the explanatory variables are non-random variables and their values are derived from observations for $t = 1, 2, \ldots, n$,
3) $r(X_i) = k + 1 \leq n$, which means that the observation matrix X_i has got a full column rank, namely the observation matrix vectors X_i (columns) are linearly independent and no collinearity of the explanatory variables occurs, and moreover the number of the explanatory variables together with the absolute term α_0 is lower than the number of observations,
4) $E(\varepsilon_j) = 0$, i.e. the value expected from the random component equals 0, which means that the multidirectional disturbances are reduced,
5) $D^2(\varepsilon_j) = \sigma^2$, i.e. the variance of random components is constant for the entire sample, whereas random components of the observation are not correlated with each other and $\sigma^2 < +\infty$,
6) $\varepsilon_j \sim N_n$, which means that the random component ε_j is characterised by an n-dimensional normal distribution.

The above-mentioned assumptions form the so-called classical model of a normal linear regression, which is most often based on the so-called classical least squares method. In order to be able to use this method for estimation of the structural parameters α_j $(j = 0, 1, \ldots, k)$ on the basis of observation of variables y_i, X_i, all the six assumptions described above must be absolutely fulfilled [11, 12].

3.3. Model verification

Model verification consists in assessment of adaptation of the model to empirical data and the quality of the estimations of structural parameters [11, 12].

The quality of calculation, namely the fact how well the regression line reflects the reality (to what extent it corresponds to the observations), may be verified inter alia by means of R^2 determination factor. The value of the factor specifies what part of variation of the response variable y has been explained by the variation of all the explanatory variables $x_1 + x_2 + \ldots + x_n$ [12].

We should note that the R^2 determination factor assumes values within the range $< 0; 1 >$. It means that if $R^2 = 1$, then the linear regression function explains in 100% the variation of the response variable y. If $R^2 = 0$, we should assume that the linear regression equation doesn't describe or explain the variation of the endogenous variable.

Other measurement methods, thanks to which we may find out how well the regression line corresponds to empirical observations include:

- residual variance that is based on examination of residual component variance [13],
- standard deviation of residuals that reflects the mean difference between the observed values of the described variable and the theoretical values [14],
- significance tests are conducted to determine, whether the given parameter assigned to the factor has got a real impact on the examined response variable [11, 13].

4. An example of application of the classical linear regression model in the hedonic method for valuation of flats

4.1. Data and assumptions adopted for the model

Functioning of the hedonic regression model will be presented based on the example of theoretical prices for 1 m^2 of usable area of a flat in Lublin.

Based on data collected from an expert (property valuer) an initial, 12-element set of features has been prepared, which constitute a set of analysed variables. The set referred to above is presented in Table 2.

Table 2. Initial set of analysed variables

No.	Name of feature	Description
1	date of transaction	an exact date of entering into agreement on the transfer of ownership (from the 1st quarter of 2009 to the second quarter of 2013)
2	area, district	one of four districts of Lublin, for which the data have been collected (Czuby, LSM, Rury, Śródmieście)
3	type of right acquired	a binominal feature referring to the right to the property (0 – cooperative ownership right, 1 – ownership)
4	floor	a feature divided into 6 floors (0 – ground floor, 1–1st floor, …, 4–4th floor, 5 – over 4th floor)
5	usable area	a measurable feature informing on the usable area of the flat
6	total flat price	a measurable feature informing on the transaction price for the flat together with belonging premises (if any)
7	price for 1 m^2 of usable area	a feature that has been created based on combination of features related to the price and floor area (as a result of dividing the first one though the second one)
8	storey	directly connected with the floor feature
9	number of overground floors	a feature characterising type of building (one-storey, multi-storey), related to the floor feature
10	year of construction	a feature described by a number of time intervals (0–50-ties and 60-ties, 1–70-ties, …, 5 – years from 2010 to 2019)
11	seller	a feature characterising the market, described binominally (0 – developer, primary market, 1 – private person, secondary market)
12	belonging premises	a binominal feature informing, whether a basement belongs to the flat (0 – no, 1 – yes)

Source: own study.

As a result of the analysis of variables, one response variable y_i has been selected, i.e. the price of 1 m^2 of usable area of a flat and six explanatory variables, i.e. area (district), type of a right

acquired, floor, year of construction, belonging premises and seller. The date of transaction has been arbitrarily deemed to be insignificant because the information about date of entering into agreement on the transfer of ownership was included in the short four years' time interval for all observations. The following has also been excluded from the final set of features adopted for the model:

- usable area and total flat price, since both these features are included the response variable y_i (price for 1 m^2 of usable area of a flat),
- storey and number of overground floors, since both these features are directly related to the explanatory variable for the floor.

The following assumptions have been adopted to construct a model:

3) the created model is based on 1211 observations that have been properly prepared and processed,
4) all the qualitative variables have been expressed in qualitative terms,
5) it has been verified for each observation, whether the random component has got a normal distribution with a mean equal to 0 and a standard deviation σ, and whether it is independent from the random components related to all other observations,
6) it has been verified for each observation, whether the random component (error) is independent from other random errors (fulfilment of this limitation is not significant from the point of view of model construction, but enables to use *t* and *F* tests at the stage of verification of model operation),
7) *y* response variable has been expressed as logarithm data to normalise the distribution of residuals, which is a condition for use of a least squares method as an estimator,
8) to calculate the price for 1 m^2 of usable area of a flat exponential function has been used, i.e. $exp(y)$.

4.2. Estimation and verification of a hedonic regression model

The least squares method was used to determine all the structural parameters α_j $(j = 0, 1, \ldots, 8)$ based on observations of $y_1, X_1, \ldots, X_8$ variables.

Due to strong collinearity, one of the variables related to the Śródmieście area has been omitted at the very beginning. Collinearity means that explanatory variables are strongly correlated with each other. It turned out in the constructed model that the Śródmieście variable was so strongly correlated with other variable that it allowed for its exclusion from the model because it provided no additional information on y_i variable [13].

Table 3 presents the results of estimation of structural parameters of the model for the following variables: Czuby, LSM, Rury, type of right acquired, floor, year of construction, belonging premises and seller. GRETL statistical package has been used in calculations.

The test for the normality of distribution of the residuals has confirmed that the random component is characterised by normal distribution. The value of the test *chi*-square $\chi^2 = 381.906$ has been obtained, with the value of test probability $p = 1.1755e\text{-}083$. The R^2 determination factor has amounted to 0.2395666, which at the assessment of model adaptation means that, the y_i variable has been explained by the factors included in the model

only in ca. 24%. The standard deviation of residuals, illustrating the mean difference between the observed values of the response variable and the theoretical values, has amounted to $s = 0.172223$. The quotient of standard deviation and the arithmetic mean of the dependent variable has resulted in the value of the factor of the random variation of the residuals $V_\varepsilon = 0.02$, which is tantamount with the fact that the random component decides about the price for 1 m^2 of usable area of a flat calculated with the used of the model only in 2%.

Table 3. The results of estimation of parameters for the dependent variable $ln(Price)$

Explanatory variable		Structural parameter		Standard error		t-student	Value p
X_0	$\equiv 1$	α_0	8.13521	ε_0	0.0337872	240.7776	< 0.00001
X_1	Czuby	α_1	–0.138665	ε_1	0.0249623	–5.5550	< 0.00001
X_2	LSM	α_2	–0.139852	ε_2	0.0323819	–4.3188	0.00002
X_3	Rury	α_3	0.0474448	ε_3	0.0193003	2.4582	0.01410
X_4	type of right acquired	α_4	–0.0638818	ε_4	0.0202477	–3.1550	0.00164
X_5	floor	α_5	–0.00238505	ε_5	0.00320693	–0.7437	0.45719
X_6	year of construction	α_6	0.0645932	ε_6	0.00381751	16.9203	< 0.00001
X_7	belonging premises	α_7	–0.0685445	ε_7	0.0138514	–4.9486	< 0.00001
X_8	seller	α_8	0.277866	ε_8	0.0173859	15.9822	< 0.00001
arithmetic mean on the dependent variable			8.430903	standard deviation of the dependent variable			0.196843
sum of the squared residuals			35.65216	standard error of the residuals			0.172223
R^2 determination factor			0.239566	R^2 corrected			0.234505
result of F statistical test			47.33458	p-value probability for the F test			1.68e-66
logarithm of likelihood			416.2902	Akaike information criterion			–814.5804
Schwarz Bayesian criterion			–768.6876	Hanna-Quinn criterion			–797.3007

Source: own study.

The performed statistical analysis has indicated that all the variables are significant, apart from the X_5 variable (floor), for which $\alpha_5 = -0.00238505$. Taking into consideration that the standard error amounts to 0.00320693 for the given variable, and that the absolute value of the testing statistic barely 0.7437 (no grounds for rejecting the null hypothesis that means no significant impact of this factor on the response variable), hence we can exclude this variable from the constructed model.

The final form of the hedonic regression model is as follows:

$$\ln(y_t) = 8.13521 - 0.138665 \cdot X_1 - 0.139852 \cdot X_2 + 0.0474448 \cdot X_3 + \\ -0.0638818 \cdot X_4 + 0.0645932 \cdot X_6 - 0.0685445 \cdot X_7 + 0.277866 \cdot X_8 \quad (4)$$

4.3. Assessment of the quality of the model based on property valuation

15 properties located in Lublin have been valued by means of the model. The formula (4) and the collected input data on properties have been used for that purpose, connected with transaction prices for 1 m^2 of usable area of a flat, location and information on the type of right acquired, year of construction, belonging premises and seller. The obtained results have been presented in Table 4.

Table 4. Comparison of transaction and theoretical prices obtained based on the model

No.	District	P_{TRANS}^{*} (PLN/m^2)	ln(P_{THR})	P_{THR}^{**} (PLN/m^2)	AB. DIFF.*** (PLN)	DIFF.**** (%)
1	Czuby	4.809.29	8.2556292	3.849.23	960.06	19.96
2	Rury	4.336.75	8.3731945	4.329.44	7.31	0.17
3	Rury	5.035.55	8.5897072	5.376.04	340.49	6.76
4	Rury	4.601.23	8.3926877	4.414.67	186.56	4.05
5	Śródmieście	3.808.07	8.2806497	3.946.76	138.69	3.64
6	Rury	4.523.03	8.4612322	4.727.88	204.85	4.53
7	Śródmieście	5.297.23	8.3491942	4.226.77	1070.46	20.21
8	Śródmieście	4.161.46	8.3491942	4.226.77	65.31	1.57
9	Rury	5.839.42	8.5864673	5.358.65	480.77	8.23
10	Czuby	3.877.89	8.4035974	4.463.09	585.20	15.09
11	Czuby	4.256.14	8.3397156	4.186.90	69.24	1.63
12	Czuby	5.064.83	8.4681906	4.760.89	303.94	6.00
13	LSM	4.409.94	8.4024104	4.457.80	47.86	1.09
14	LSM	5.232.20	8.5315968	5.072.54	159.66	3.05
15	LSM	4.441.04	8.4024104	4.457.80	16.76	0.38
MEAN		4,646.27	–	4.523.68	309.14	–
where: * transaction price, ** theoretical price, *** absolute difference, **** difference						

Source: own study.

Table 4 presents predictive and real values resulting from observations. On such a basis, it is possible to assess the quality of the hedonic model for property valuation. As can be seen, 6 among 15 estimations (40%) differ from transaction prices by more than 5%, which in case of process of flats is very significant. Moreover, in case of 3 estimations the error has exceeded 15% of the difference, which is unacceptable. The mean for the absolute difference amounts to PLN 309.14 m, which is a deviation amounting to ca. 6.65% from the mean transaction price. The fact that 5 properties have been values with accuracy below 2% should be deemed to be a positive aspect.

While considering the set of properties presented in table 4 through comparison of mean values from the both price groups (mean transaction price PLN 4.646.27 and theoretical price PLN 4.523.68), the difference between them is absolutely 2.64% (PLN 122.59), which constitutes a value nearly below half the statistical error (to 5%).

5. Conclusions

The constructed model, despite the acceptable value of standard deviation of residuals, coefficient of residual variation and statistical significance of nearly all the variables, is not satisfactory. The low value of the determination factor ($R^2 = 0.239566$) initially proves poor representation of reality by the model (insufficient description of the relationships between the prices and property features), as a result, of which the values estimated with the use of the model may be substantially different from the transaction prices.

It should be noted that the constructed model does not take into account features, such as impact of the standard of interior finish of particular properties and the neighbourhood conditions. The direct reason for this is the high level of diversity that has been observed for the districts, which could have a very significant effect on the results of the calculations (especially for two districts Śródmieście and Czuby).

In practice, it was found that the statistical error (up to 5%) resulting from maladjustment of the model is moderate, and in 60% of the performed valuations, the model has performed well. However, it is not sufficient for the determination of property prices due to their substantial value. A few percent differences between the theoretical and transaction prices would translate into differences of several – dozen thousand PLN and this will be very important in the case of drawing up estimated operates in the economy.

References

[1] Konowalczuk J., *Wycena nieruchomości przedsiębiorstw*, Wydawnictwo CH Beck, Warszawa 2009.

[2] Śmietana K., Ramian T., *Analiza ekonomiczna nieruchomości inwestycyjnych*, Wydawnictwo Uniwersytetu Ekonomicznego w Katowicach, Katowice 2014.

[3] Quigley J.M., *Real estate prices and economic cycles*, Berkeley Program on Housing and Urban Policy, 2002.

[4] Hidan N., *The economic valuation of the environment and public policy: a hedonic approach*, Edward Elgar Publishing Ltd, Cheltenham, UK, 2002.

[5] Trojanek R., *Porównanie metod prostych oraz metody regresji hedonicznej do konstruowania indeksów cen mieszkań*, Studia i Materiały Towarzystwa Naukowego Nieruchomości, Vol. 18(1), 2010, 119–132.

[6] Gundimeda H., *Hedonic price method – a concept note*, Madras School of Economics, Chennai, 2007.

[7] von der Lippe P., *Some conservative comments on hedonic methods*, Quarterly Journal of Economics, Vol. 110, 1995, 229–244.
[8] Baranzini A., Ramirez J., Schaerer C., Thalmann P., *Hedonic methods in housing markets: Pricing environmental amenities and segregation*, Springer Science & Business Media, Geneva 2008.
[9] Janik A., *Wielokryterialna metoda wyceny wartości terenów zdegradowanych*, Zeszyty Naukowe Politechniki Śląskiej, Organizacja i Zarządzanie, No. 62, 2012.
[10] Widłak M., *Metody wyznaczania hedonicznych indeksów cen jako sposób kontroli zmian jakości dóbr*, Wiadomości Statystyczne, Warszawa 2010, 1–26.
[11] Nowak E., *Zarys metod ekonometrii: zbiór zadań*, PWN, Warszawa 2002.
[12] Goryl A., Jędrzejczyk Z., Kukuła K., Osiewalski J., Walkosz A., *Wprowadzenie do ekonometrii w przykładach i zadaniach*, PWN, Warszawa 2009.
[13] Aczel A.D., *Statystyka w zarządzaniu: pełny wykład*, PWN, Warszawa 2006.
[14] Zeliaś A., Pawełek B., Wanat S., *Prognozowanie ekonomiczne: teoria, przykłady, zadania*, PWN, Warszawa 2013.

TECHNICAL TRANSACTIONS 6/2017
CZASOPISMO TECHNICZNE 6/2017
CIVIL ENGINEERING
DOI: 10.4467/2353737XCT.17.088.6564

Paweł Boroń (pboron@pk.edu.pl)
Joanna Dulińska
Institute of Structural Mechanics, Faculty of Civil Engineering, Cracow University of Technology

Dynamic response of a steel pipeline with bolted connections to a mining shock obtained with the submodeling technique

Odpowiedź dynamiczna gazociągu z doczołowymi połączeniami śrubowymi na wstrząs górniczy z wykorzystaniem techniki submodelingu

Abstract

In this paper, the dynamic response of an overground steel pipeline to a real mining shock is presented. The submodeling method was used in the calculation. Firstly, time history analysis of a simplified beam model of the pipeline (a global model) was conducted. Secondly, the 3D model of a part of the structure over the support was created (a submodel). The submodeling analysis allowed obtaining stress distribution in the bolted connection of the pipeline segments.

Keywords: pipeline, dynamic response, mining shock, submodeling

Streszczenie

W artykule przedstawiona została analiza odpowiedzi dynamicznej naziemnego gazociągu na rzeczywisty wstrząs górniczy. W obliczeniach zastosowano technikę submodelingu. W pierwszym etapie przeprowadzono obliczenia uproszczonego, belkowego modelu całego gazociągu (model globalny). W drugim etapie zastosowano model 3D fragmentu konstrukcji, obejmujący odcinek gazociągu nad podporą (submodel). Analiza z zastosowaniem techniki submodelingu pozwoliła na dokładne rozeznanie pracy złącza gazociągu oraz na określenie rozkładu naprężeń w kołnierzu i śrubach złącza.

Słowa kluczowe: gazociąg, odpowiedź dynamiczna, wstrząs górniczy, submodeling

1. Introduction

The finite element method allows to solve problems connected with engineering objects of high structural, material and geometrical complexity. While linear analyses of regular shape structures do not result in complicated numerical models and they are not very time-consuming, non-linear problems are very demanding as far as computer efforts are concerned. In case of, for example, large displacement problems or contact as well as failure mechanics, nonlinear analyses have to be carried out. These days, commercial engineering software allows for the realization of extremely complicated numerical models and performing nonlinear analysis [4, 6]. However, time and cost of calculations of that type of structures grow rapidly with the complexity of the problem. Hence, a strong tendency towards simplifying numerical models and implementing very effective techniques and algorithms of calculations is observed. Nowadays, a submodeling method is one of these powerful techniques that shortens the time of calculations to a large degree.

In the paper, the analysis of the dynamic response of an overground steel pipeline (105 m long) to a mining shock is presented. To accelerate calculations, the submodeling method was applied. The method allowed the analysis of the dynamic response of a bolted flange connection of two sections of the pipeline to a mining tremor without creating a 3D model of the whole structure. Due to the submodeling method, it was possible to model only a part of the pipeline, including the details of the connection. Not only had it significantly reduced the time and cost of the calculations, but it also allowed avoiding difficulties with densifying FE mesh of the model [2, 7].

Two FE models of the pipeline were created to calculate the dynamic response of the structure to the mining shock with the submodeling method. Firstly, a simplified beam one-dimensional model, which covered the whole structure, was realized (a global model). Then, a 3D model including only a selected part of the structure was generated (a submodel). Both models were created with the ABAQUS software [1].

2. Basic parameters of the pipeline and the flange connection technical details

An overground steel gas pipeline was chosen for the dynamic response analysis. The pipeline consisted of 7 spans of 15 m in length. The total length of the pipeline was 105 m. Such a structure can be considered as a representation of real long structures that can be modelled with one-dimensional beam models. The pipeline was supported on concrete pillars of 45 cm in height and 50 cm in width. The shape of pillars prevented overabundant displacements and a slip of the pipeline from supports. The main pipeline envelope consisted of a single pipe with an exterior diameter of 60 cm and a wall thickness of about 1.35 cm. The steel pipe was not cover by any isolation material.

Considerable length of the analysed object produced compliance of connections between parts of the structure. The typical connections in that kind of structures are welded or bolted connections. In the analysed object, bolted connections were used. The connections were

located over the fourth support. That was the support in the middle part of the pipeline. The connections were placed on both sides of the pillar, at a distance of 55 cm from the support axis. The analysed connection is the most common joint that occurs in control valve location or switching gas station (Fig. 1).

Fig. 1. Exemplary of gas network junction [5]

The connection was built as a bolted flange connection. The joint consisted of two flanges welded to the pipeline envelope. The thickness of the flange was 5 cm. The flanges were jointed together by 24 bolts, arranged uniformly around the flange (Fig. 2). The bolts used in the connection were the M30 bolts class 5.6 (yield stress of 300 MPa, resistant stress of 500 MPa).

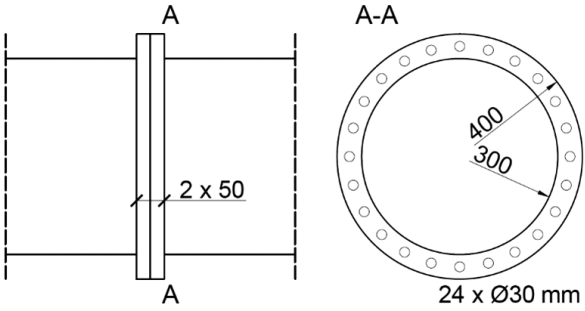

Fig. 2. Main dimensions of the pipeline segments connection

3. General concept of the submodeling technique [9, 10]

For the effective analysis of the dynamic response of pipeline to a mining shock, the submodeling technique was used [1, 7–11]. The submodeling technique is used mostly to study local parts of structures. This technique is the most useful for obtaining an accurate, detailed solution in a local region with a redefined mesh or geometry. The submodeling analysis consists of two general steps so two numerical models (a global model and a ubmodel) were needed.

The first step of the analysis is a global analysis. In this step, the calculation bases on models of whole structures (global models). The basic dimensions and the main characteristics of objects have to be modelled. Any simplifications in the global model, which do not change the dynamic response of a structure, were acceptable. The calculation conducted in this part of analysis allows to estimate the dynamic response of a structure. On the basis of the obtained results, it is possible to find zones of stress concentration. It also allows determining global displacements of a structure. During the global analysis, the results in the vicinity of the submodel boundaries are also received.

The second step is the analysis of a chosen part of a structure. This part is represented by a second model – called a submodel. In the submodel, as many details of the analysed part should be presented as possible. For example, details of connections as well as nonlinearity of geometry and material should be taking into account. That accuracy of the submodel increases the precision of results.

Both the global model and the submodel can have linear or nonlinear behaviour and can be analysed for any sequence of analysis procedures. For example, the linear dynamic response of the global model can be used to drive the nonlinear response of the submodel. The step time used in these analyses can also be different. The submodel and the global model can have different meshes. The size and type of finite elements in both models can differ.

The application of advanced (nonlinear) procedures and densified mesh leads to the obtainment of accurate results for submodels. It also makes it possible to present stress and strain distribution in small elements. Additionally, phenomena like local yield, stiffness degradation or contact behaviour can be determined for nonlinear submodel analysis only.

Using the proper boundary condition is the main problem of the submodeling technique. In the global model, boundary conditions arise from the real behaviour of structures. Supports and excitations are defined as displacements, velocities, accelerations or forces acting on structures. Boundary conditions in the submodel arise from the analysis of the global model.

The analysis of the submodel is carried out consecutively and separately from the analysis of the global model. The only link between the global model and the submodel is the transfer of the time-dependent values of variables obtained in the global analysis to the boundary nodes of the submodel.

During the global analysis, displacements of the whole structure are calculated and saved. Displacements of special sections (i.e. boundaries of the submodel) should especially be calculated. The values of those displacements are used as driven variables in the submodel [1]. The place of application of the boundary conditions (displacements and rotations) are the mesh nodes at the submodel ends. The other boundary conditions and loads are duplicated on the submodel from the global model.

4. Variants of the numerical model of the pipeline

4.1. Variant I – a beam model (global model)

In order to carry out the dynamic analysis of the pipeline with submodeling technique, two variants of a numerical model were created. Variant I of the pipeline represented the structure as a multi span continuous beam (Fig. 3). In this model, real dimensions of a cross-section and length of span were taken into account. However, the true shape of support pillars were neglected – the beam was supported at eight points only. The joint supports were applied. This type of support precluded the slip of the pipe envelope from the pillars (transverse and vertical direction were fixed).

In Variant I of the numerical model, the connection of pipe segments was neither modelled nor analysed. In the dynamic analysis, kinematic excitation was applied to the supports of the pipeline. The excitation was represented by time histories of accelerations of a real mining shock.

Beam finite elements, provided by the ABAQUS software [1], were used in Variant I of the numerical model. The mesh consisted of 3500 finite elements. The length of each element was about 3 cm. Further densification of the mesh did not introduce any noticeable changes to the results.

The beam model, which was the global simplified model of the structure, was used as the basis for further detailed analysis. The model allowed calculating stresses in the pipe envelope and also determining displacements in chosen points of the structure. The obtained displacements were used as boundary conditions in the submodel.

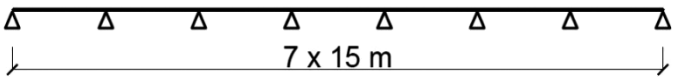

Fig. 3. Beam model of pipeline

4.2. Variant II – 3D model of the part of pipeline (submodel)

In the second part of analysis based on the submodeling technique, Variant II of the numerical model (submodel) was created. The main goal of the submodel analysis was an accurate calculation of the dynamic response of the flange connection. Especially, stresses in the bolts had to be determined. The submodel, created as a three-dimensional model, represented only a part of the pipeline located over the fourth support of structure. The length of the modeled part was 2.5 m. It was situated at 43.75–46.25 m of the total length of the pipeline. The real dimensions of the pipeline were used in a 3D model (see Fig. 2). The flange connections were modeled in detail. They were placed symmetrically, on both sides of the supports at a 1.1 m offset. The geometry of the flange and the bolt-holes as well as bolts localization were precisely reflected. The 3D submodel of the pipeline section enabled to create the real shape of the supporting pillar.

Variant II of the pipeline model was meshed using solid elements available in the ABAQUS software [1]. The applied finite elements were 8-node elements with 3 degrees of freedom in each node. The dimensions of elements in the pipe envelope were about 3 cm. That size allowed comparing the results obtained for the global analysis with the results of the submodel analysis. The submodel of the pipeline is shown in Fig. 4a. The meshing of the model is shown in Fig. 4b. Additionally, special displacement boundary conditions at both ends of the submodel were added. The values of those displacements came straight from the global analysis with the beam model.

In the dynamic analysis of both Variants of the numerical model, the kinematic excitation was applied to the structure as time histories of accelerations in three directions (longitudinal, transverse and vertical).

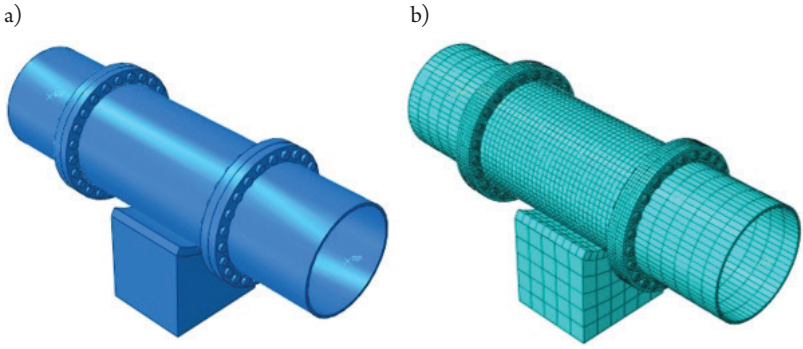

Fig. 4. 3D submodel of the pipeline (a), finite element mesh (b)

In the first step of the analysis (the global analysis with the beam model), the time histories of displacements of all nodes of the mesh were calculated and saved (three translations and three rotations). In the second step of the analysis, the displacements of chosen points, obtained during the first step, were transferred from the global beam model to the submodel. The right choice of those points in both models was an all-important issue. The points should be located at the same distance from the support in both models. In this case, the points at a distance of 1.25 m from the axis of fourth support were chosen where the ends of submodel were placed.

The appropriate transfer of the displacements from the beam model to the 3D submodel was possible due to rigid rings. The rings were hitched at the ends of the submodel. The centres of rings were located on the longitudinal axis of the pipeline. The boundary conditions (three translations and three rotations) were implemented in the centre of each ring. The use of the rigid rings allowed transferring rotations from the ring centre to the points located on the pipeline coat. Taking rotational degrees of freedom into consideration enabled to impose bending and torsional deformation of the submodel resulting from the global deformation of the whole structure, which was obtained at the first step of analysis. However, it has to be mentioned that in consequence of using rigid rings at the ends of the submodel, the circumferential deformation was neglected.

5. Data of the mining shock

The dynamic analysis of the pipeline was carried out for a strong mining shock registered near Szombierki, in the Upper Silesian Coal Basin in Poland (the main region of mining activity in Poland). The time histories of ground accelerations resulting from the tremor in three directions: horizontal – parallel to wave propagation, horizontal – perpendicular to wave propagation and vertical are presented in Fig. 5.

The registered tremor, with an energy of about $1 \cdot 10^7$ J, turned out to be one of the most severe events ever recorded in that mining area. The maximum amplitudes recorded in horizontal directions reached 0.3 m/s^2, whereas the amplitudes in the vertical direction were on the level of 0.12 m/s^2. They occurred approximately after 1.7 s of the shock. The Fourier analysis of the signals indicated that dominant frequencies were located within the range of 2–5 Hz for all directions.

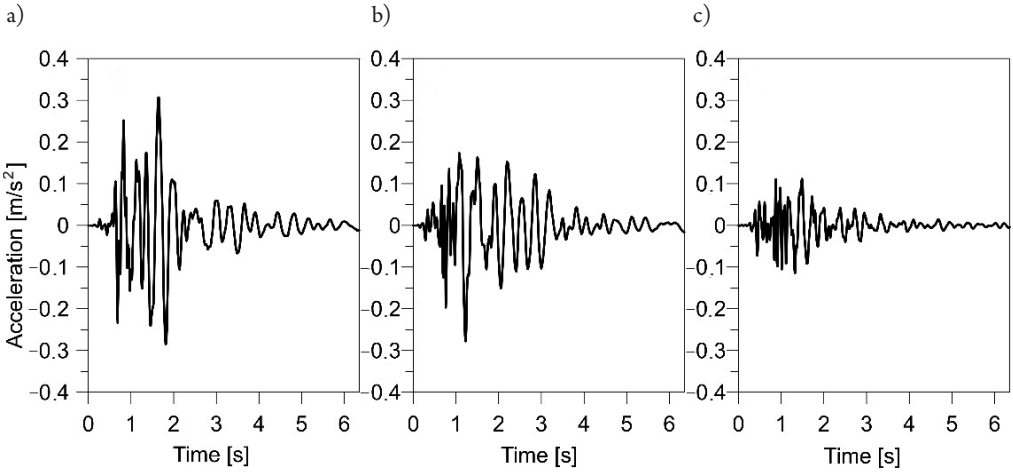

Fig. 5. Time histories of accelerations of the Szombierki mining shock in: longitudinal (a), transverse (b), vertical (c) direction

The presented time histories of accelerations were taken in the studies as the kinematic excitations of the pipeline supports. In the dynamic analysis a model of spatially varying ground motion [3, 12], which takes into consideration wave passage effect, was applied. In the model, it was assumed that subsequent points of the ground in the direction of wave propagation (along the pipeline) repeat the same motion with a certain time delay dependent on the wave velocity. This velocity depends on the stiffness of the bedrock; the stiffer the underlying bedrock is, the higher the velocity of wave propagation occurs. In this study, the wave velocity of 300 m/s, typical for clayey sands, was assumed.

6. Results of numerical analysis

6.1. Comparison of the dynamic response obtained for two Variants of the numerical model

For both Variants of the numerical model (the global beam model and the 3D submodel), the dynamic response of the pipeline to the mining shock was evaluated by the time history analysis. The Hilber-Hughes-Taylor direct integration method was used for the solution of equations of motion. The Rayleigh model of mass and stiffness proportional damping was applied. The damping coefficients $\alpha = 2.67$ and $\beta = 0.01$ were determined for damping ratios of 5% referring to the first and the second natural frequencies: $f_1 = 7.2$ Hz and $f_2 = 10.4$ Hz. In the dynamic calculations, the dead load was also taken into consideration.

The stress analysis for all nodes of the FE mesh of the steal pipeline coat was performed. In the paper, the results of the stress analysis were presented for two representative points only (Fig. 6).

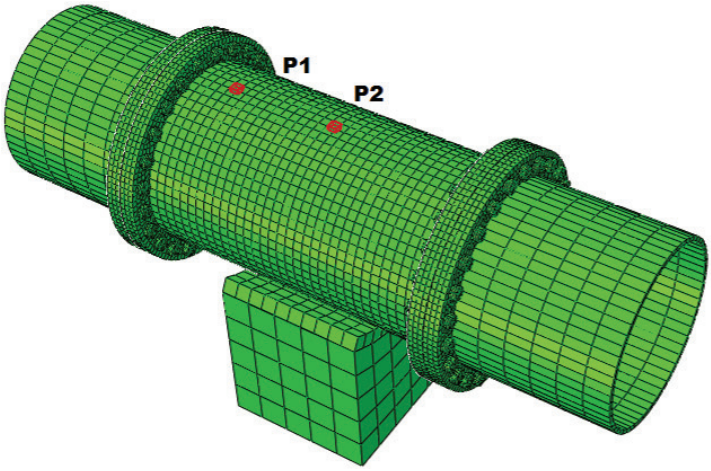

Fig. 6. Points of 3D submodel selected for the dynamic analysis

The selected points were located in the upper part of the pipe envelope. Point P1 was situated at a distance of 40 cm from the centre of the pipeline support, whereas point P2 is placed just above the centre of the support. The values of Mises stresses obtained at points P1 and P2 of the 3D submodel were compared to the values of stresses received at the corresponding points of the beam model.

The comparison of time histories of Mises stresses at point P1 that resulted from the mining shock for the beam model (dotted line) and the 3D submodel (continuous line) is presented in Fig. 7a. A similar comparison for point P2 is shown in Fig. 7b.

On the basis of Fig. 7, it can be observed that the stresses obtained for both models demonstrate the same variability in time. It is worth mentioning that the maximum values of stresses were achieved at the same moment – after 1.7 s of the shock – for both models.

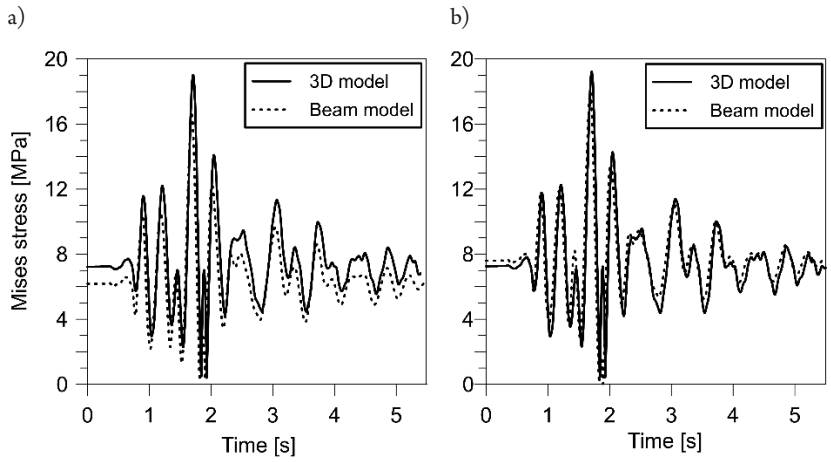

Fig. 7. Comparison of time histories of stresses for the beam model and the 3D submodel obtained at points: P1 (a), P2 (b)

The analysis of Mises stresses at point P1 (Fig. 7a) shows that the values obtained for the 3D submodel were slightly greater than those received for the beam model; however, the differences did not exceed 1.5 MPa almost the whole time. The greatest difference, which occurred for the peak values after 1.7 s, equalled 2 MPa. The peak values obtained for the 3D submodel and the beam model were 19 MPa and 17 MPa, respectively.

Additionally, it is clearly visible that the stresses resulting from the mining shock were significantly greater than the stresses originated from the dead load. The self-weight stresses achieved only 40% of the maximum stresses occurring due to the kinematic excitation.

It can also be observed that the dead load stresses at point P1 obtained for the beam and the 3D models slightly differed (Fig. 7a). The difference did not exceed 1 MPa. This difference occurred due to the modelling of the pipeline supports in both models. In the beam variant of the model, each support was idealized as a joint support connected with the pipeline coat at one point, whereas in the 3D submodel, each support was modelled with a 3D solid pillar of a width 0.5 m. In consequence, a reduction of stresses at point P1, located 40 cm from the centre of the support, was much more rapid in the case of the beam model than in case of the 3D submodel.

The results of the dynamic analysis obtained for point P2, located at the centre of the support, also indicated similarity of time histories of Mises stresses obtained for the beam model and for the 3D submodel (Fig. 7b). The maximum difference between the values of Mises stresses for both models occurred after 1.7 s of the shock. It did not exceed 1 MPa (the maximum value of the stress at this moment equalled 18.5 and 19.5 MPa for the beam model and the 3D submodel, respectively). The values of stresses at point P2, resulting from the dead load, were identical for both models due to the fact that this point is located just above the centre of the pipeline support.

The Mises stress distribution in the 3D submodel of the pipeline coat at 1.7 s of the shock is demonstrated in Fig. 8. It can be seen that the maximum values of stresses appeared in the upper part of the coat and reached 20 MPa.

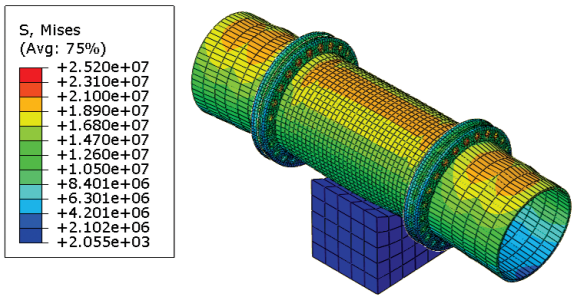

Fig. 8. Distribution of stresses in the 3D submodel (1.7 s of shock time)

6.2. Stresses in the flange connection

The main advantage of the submodeling technique is the possibility of precise stress calculation in selected parts of a structure. Due to this method, it was possible to observe the distribution of stresses on the contact surfaces of the flange connection.

The map of Mises stresses on the contact surface of connection, occurring at 1.7 s of the shock, is presented in Fig. 9. The observed stress distribution shows different values of stresses in the upper and in the lower part of the flange. It indicates that bending of the entire connection took place. The analysed map also demonstrates the concentrations of stresses around bolt-holes. The concentrations were caused by local clamping forces executed by tensioned bolts. The maximum value of stresses equalling 8.6 MPa appeared around the extreme upper bolt-hole.

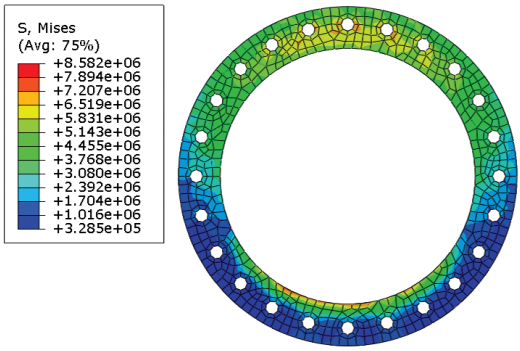

Fig. 9. Distribution of stresses on the interior flange side of the connection

In the second step of the submodel analysis, the stress distribution in the bolts was considered. The distribution of Mises stress in the bolts of the flange connection occurring at 1.7 s of the excitation was presented in Fig. 10. It can be seen that the maximum values of stresses appeared in the bolt shanks. The considerable difference in the stress levels can also be noticed for the bolts located in the upper and in the lower part of the connection. This indicates bending of the whole connection.

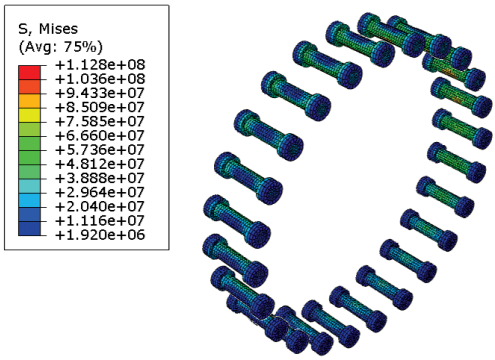

Fig. 10. Distribution of stresses in the bolts

In the next step of the analysis, the stresses in two bolt shanks were compared. The first bolt was located in the extreme upper position in the connection, whereas the second one was situated in the extreme lower part of the connection. The time histories of Mises stresses in both bolt shanks are compared in Fig. 11. The comparison shows significant differences in the dynamic response of the bolts located in the opposite parts of the connection. The stresses in the extreme upper bolt shank represented a great variability in time (Fig. 11a). During the whole shock, the values of stresses varied from 0 to 110 MPa with the peak value at 1.7 s of the shock. The stresses oscillated around the value of 40 MPa, which came from the dead load of the structure. The maximum values of stresses in the extreme lower bolt shank were much smaller and the time history looked differently (Fig. 11b). The analysis of all components of stress tensor revealed that the lower bolt is tensioned once: only one peak value of 35 MPa appeared during the whole shock, whereas the mean value resulting from the dead load was about 2 MPa.

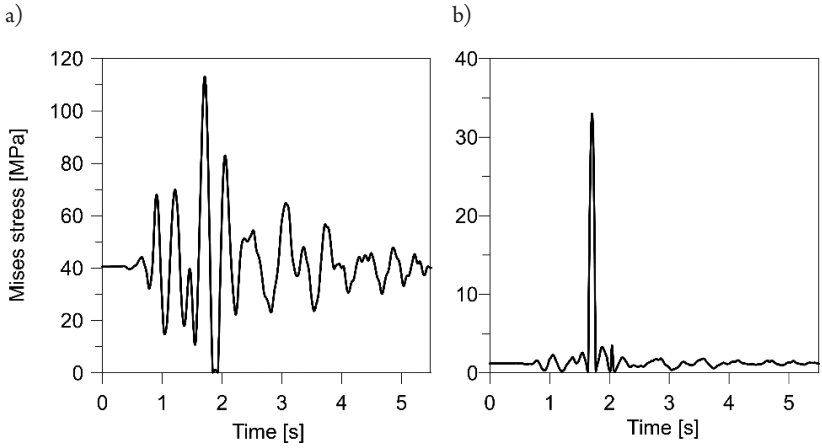

Fig. 11. Time histories of stresses in the extreme upper (a) and the extreme lower (b) bolt

Finally, the map of Mises stresses occurring in the extreme upper bolt shank at 1.7 s of the shock is demonstrated in Fig. 12. The non-uniform stress distribution of the shank indicates bending of the bolt. The greatest stress of 112 MPa appeared in the lower zone of the shank (tension), the smallest stress of 7 MPa was found in the upper part of the shank (compression).

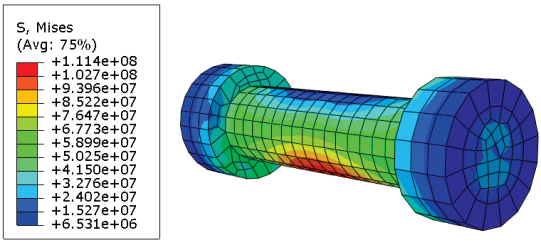

Fig. 12. Distribution of stress in upper bolt

7. Final conclusions

The analysis of the dynamic performance of the steel pipeline with bolted connections subjected to the mining shocks, obtained with the submodeling method, allowed the formulation of the following conclusions:

- The analysis of the dynamic response of the steel pipeline indicated that the strong mining shock caused a significant increase of stresses in the pipeline coat. The maximum values of stresses in the pipeline coat reached 20 MPa and they were 2.5 times greater than stresses resulting from the dead load;
- At the first stage of the dynamic analysis, the simplified beam model of the pipeline was applied. At the second stage, the three-dimensional model of a part of pipeline coat with a bolted flange connection between pipeline segments was created. The submodeling technique allowed the detailed dynamic analysis of the connection work that was impossible in the case of the global beam model;
- The observation of stress distribution in the pipeline coat indicates similarity of the results received for the global beam model and the 3D submodel;
- The stress distribution on the contact surface of flanges as well as in all bolts proved that the connection was affected with strong bending;
- The analysis revealed that the dynamic stresses, which occurred in the bolt shanks due to the shock, were significantly greater than those resulting from the dead load. The maximum values of dynamic stresses reached 110 MPa and they were almost 3 times greater than the static stresses.

References

[1] ABAQUS 2012. *User Manual* V.6.12–2, Dassault Systems Simulia Corp., Providence.

[2] Abuodha S., Burdekin F., *Finite element analysis of tubular joints in offshore structures*, "Journal of Civil Engineering" JKUAT, Vol. 6, 2001, 105–116.

[3] Dulinska J., Jasinska D., *Performance of steel pipeline with concrete coating (modeled with Concrete Damage Plasticity) under seismic wave passage*, "Applied Mechanics and Materials" Vol. 459, 2014, 608–613.

[4] Garcia-Palacios J., Samartin A., Negro V., *A nonlinear analysis of laying a floating pipeline on the seabed*, "Engineering Structures" Vol. 31, 2009, 1120–1131.

[5] Harris P., *Pipelines: The flange protection challenge. Oil & Gas technology*, 2014, http://oilandgastechnology.net (access: 14.03.2016).

[6] Horowitz B., de Sa Barreto S., *Nonlinear analysis of a prestressed steel pipeline crossing*, "Engineering Structures" Vol. 28, 2006, 390–398.

[7] Lanhao Z., Tongchun L., *An efficient finite element dynamic sub-modeling approach using the local mesh refinement technique*, "Earth & Space" 2008, 1–6.

[8] Li AQ, Wang H., *Stress analysis on steel box girders of super-longspan suspension bridges with submodel method (in Chinese)*, "Eng Mech" 24(2), 2007, 80–84.

[9] Wang, H., Li, A., Guo, T. et al., *Accurate stress analysis on rigid central buckle of long-span suspension bridges based on submodel method*, "Sci. China Ser. E-Technol. Sci." Vol. 52, 2009, 1019–1026.

[10] Wang H., Li A., Hu R., Li J., *Accurate Stress Analysis on Steel Box Girder of Long Span Suspension Bridges Based on Multi-Scale Submodeling Method*, "Advances in Structural Engineering" Vol. 13, No. 4, 2010, 727–740.

[11] Xu W, Li Z, Zhang XN., *Application of submodeling method for analysis of deck structure of diagonal cable-stayed bridge with long span (in Chinese)*, "China Civil Engineering Journal" 37(6), 2014, 30–34.

[12] Yong Y., *Response of pipeline structure subjected to ground motion excitation*, "Engineering Structure" Vol. 19, 1997, 679–684.

TECHNICAL TRANSACTIONS 6/2017
CZASOPISMO TECHNICZNE 6/2017
CIVIL ENGINEERING
DOI: 10.4467/2353737XCT.17.089.6565

Stanisław Duży (stanislaw.duzy@polsl.pl)
Grzegorz Dyduch
Wojciech Preidl
Grzegorz Stacha
Artur Czempas
Sandra Utko
Faculty of Mining and Geology, Silesian University of Technology

Evaluation of the technical condition of the "fryderyk" adit in tarnowskie góry for the purpose of eventual revitalization

Ocena stanu technicznego obudowy sztolni „fryderyk" w tarnowskich górach pod kątem jej docelowej rewitalizacji

Abstract

The "Fryderyk" adit (renamed 'Kościuszko' after World War II) is the last adit built in the area of Tarnowskie Góry, and was supposed to provide drainage for the area of exploitation of the "Fryderyk" mine. After the shutdown of the mine, the adit gained an important role in the water management of the area. The water from nearby sources flows into the river Drama through the adit. The long period of the adit's existence and the processes occurring in its area have caused a progressive process of support degradation, which increases the danger of a loss of stability and a collapse of the roof. Allowing the collapse of the adit's roof may cause surface depressions. The article presents the research results that show an evaluation of the technical condition and safety degree of the support for future failure-free usage. A range of activities that are meant to stop the natural degradation of the end section of the adit has also been suggested.

Keywords: mining monuments, support, heading stability, surface deformation

Streszczenie

Sztolnia „Fryderyk" (po II wojnie światowej „Kościuszko") jest ostatnią z wybudowanych sztolni w rejonie tarnogórskim i miała odwadniać rejony eksploatacji rud w obszarze kopalni „Fryderyk". Po zamknięciu kopalni sztolnia spełnia ważną rolę w gospodarce wodnej rejonu. Spływa nią woda z okolicznych źródeł do rzeki Dramy. Długi okres istnienia sztolni i procesy zachodzące w jej otoczeniu spowodowały postępujący proces degradacji obudowy powodujący wzrost zagrożenia utratą jej stateczności i wystąpienia zawału. Dopuszczenie do zawału sztolni może doprowadzić do powstania na powierzchni zapadlisk. W artykule przedstawiono wyniki badań obejmujących ocenę stanu technicznego i stopnia bezpieczeństwa obudowy pod kątem dalszego bezawaryjnego użytkowania wyrobiska. Zaproponowano również zakres działań mających na celu zahamowanie naturalnej degradacji końcowego jej odcinka.

Słowa kluczowe: zabytki górnicze, obudowa górnicza, stateczność wyrobisk, deformacja powierzchni

1. Introduction

Execution of the works related to the revitalization of historic underground structures requires a consideration of three mutually interlocking issues, namely:

- historical assets of the heading and taking care to minimalize the impact of corrective actions on its final state,
- state of the rock mass in the vicinity of the heading, including the possibility of discontinuous deformations on the surface,
- the condition of the support in the analyzed heading, taking into account environmental factors affecting its state.

The proposed corrective measures to counter further degradation of the heading should be the least possible impact on its historical appearance and also stop the process of natural degradation of the heading.

This problem is illustrated with the example of the "Fryderyk" adit in Tarnowskie Góry. To solve the task based on the results of research, which assessed the properties of rocks and the rock mass in the vicinity of the heading, the technical parameters of the support had to be obtained and an analysis of its stability had to be performed. The analysis of the stability of the heading is based on the probabilistic analysis of structural elements taking into account the variability of the parameters characterizing the structure and the rock mass, the variability of the cross-sectional dimensions of the heading and of its support. A classification of the conditions for maintaining the stability of the heading on each of its segments was carried out on the probability of loss of stability. The analysis was the basis to determine the necessary actions that had to be taken in order to stop the degradation of the heading, taking into account natural, technical, economic and historical conditions.

2. General characteristics of the "Fryderyk" adit

Ore mining in the region of Garb Tarnogórski was conducted since the beginning of the sixteenth century and was continued intermittently until the 1930s. Mines in the area of Tarnowskie Góry managed the water threat in two ways: either by removing water with the use of various types of treadmills and pumps or by gravity drainage of the adit tunnels by the means of drainage systems. The first tunnels in this area were drilled at the beginning of the sixteenth century.

The "Fryderyk" (Kościuszko) adit (its historical name is Tiefe Friedrich Stollen, which means "deep tunnel Frederick") is the last of eight tunnels built in the area of Tarnowskie Góry. It transported water from the following ore mining fields: Sztolniowy, Miejski, Suchogórski and Bobrownicki, which belonged originally to the mine called "Fryderyk": After World War II, the name of the adit was changed to "Kościuszko".

The outlet tunnel is located in the valley of the Drama river, east of the village of Zbrosławice. The adit spreads for about 880 m to the west, joining with river Drama. The outlet part of the underground tunnel included a classical sandstone brick gate (Fig. 1).

Fig. 1. Fryderyk" ("Kościuszko") adit inlet portal (made 02.08.2016)

The total length of all parts of the „Fryderyk" adit is approx. 4568 m, while the analysis includes 1275 m (Fig. 2).

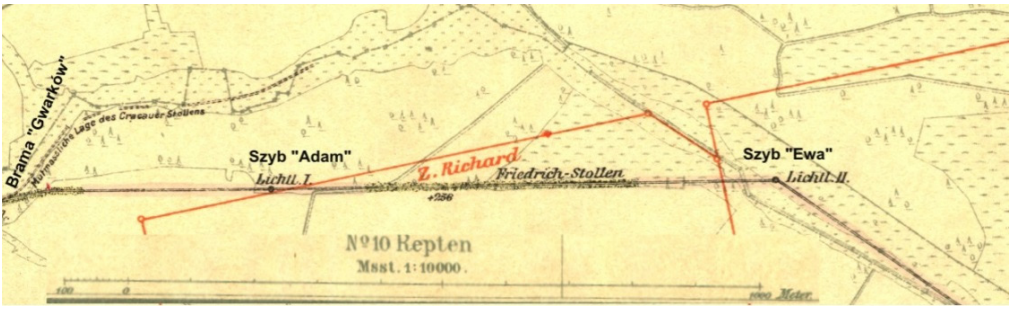

Fig. 2. The adit course, as based on the „Karte des Oberschlesischen Erzbergbaues" map from 1912 [12]

The entire length of the heading has a support made of arched, natural stone masonry (carbonate rocks). The roof with an arrow of f = 0.5 m is based on simple sidewalls with a height ranging from approx. 1.9 m to approx. 2.3 m. The thickness of the support was measured at the sidewalls, in brickwork cavities, and was approx. 0.3 m.

In places where preventive work was conducted as a result of failure, parts of the support were made from brick on concrete mortar and concrete. These enclosures were built in tunnels after 1945 and have no historical assets. The initial section of the tunnel with a length of about 110 m, azimuth 77°, is made in a masonry stone case with hewn stone on lime mortar. The section of the tunnel that collapsed in August of 2008, at a length of about 3m, does not have a concrete structure, as it was reconstructed only with the use of wooden supports. At a distance of about 4 meters from the place where the roof collapsed, a concrete support was built. In 1962, a cave-in occurred in this place and was later secured with a concrete support laid behind the shoring. There are also traces of wooden shoring planks. In that section, the dimensions of the tunnel are: width of 1.75 m and a height of 2.75 m.

3. Geological and mining characteristics in the aforementioned section of the adit

The aforementioned section of the "Fryderyk" (Kościuszko) tunnel is located in the central part of Garb Tarnogórski.

The rock mass is permeable; therefore, numerous break-ins of water and quicksand occurred during the drilling of the heading. According to the available sources, the first 60 m of the tunnel were built using the opencast method. The overburden layer in this section has a thickness of 2 to 6 meters.

Along the adit, the tunnel can be divided into sections distinguishable as being made in the quaternary sediments and limestone (Fig. 3).

Quaternary deposits are developed in the form of layers of fine yellow and brown sand, light grey silt and clay.

Limestone lies underneath the quaternary sediments, with variable strength properties and different fracturing.

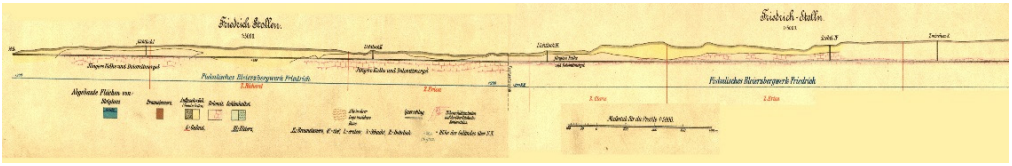

Fig. 3. The geological cross – section along "Fryderyk" adit, based on the „Karte des Oberschlesischen Erzbergbaues" [12]

4. Evaluation of the technical condition of the support in the „Fryderyk" (Kościuszko) adit

The macroscopic evaluation of the technical condition of the support showed that:

- along the entire length of the heading, the support is made of masonry vaulted natural stone. The arrow of the roof with $f = 0.5$ m is based on simple sidewalls with a height ranging from approx. 1.9 m to approx. 2.3 m. The thickness of the support measured at the sidewalls is approx. 0.3 m. Generally, the height of the support measured at the water level is approx. 1.2 m, and at the level of the heads of the sidewalls, it is approx. 1.3 m. The height of the heading grows from approx. 2.4 m in the inlet to approx. 2.8 m at a distance of approx. 1000 m. It was noted that, at short distances, the heading slightly changes its size, with the support expanding to approx. 1.75 m of height or reduces to approx. 1.9 m of height while narrowing to approx. 1.0 m,
- it was found that damages to the support vary along the adit,
- within the distance of 0–45 m from the Miners' Gate, there are losses in brickwork and mortar in the joints, loosened parts of the support and its deformation. In this section, there is a damage zone with a collapsed part of the tunnel, which was rebuilt with a wooden support (Fig. 5),

- the sections between 45–118 m, 126–143 m, 156–158 m, 632–739 m, 761–788 m, 969–979 and 1149 to 1163 meters from the Miners' Gate show earlier repairs of the support through its partial replacement with a masonry brick or monolithic concrete support. There are also a lot of biological contaminants – roots piercing the support, washing of the mortar joints by old water leaks, loosened parts of the support and washing of the sidewalls of the support (Fig. 6),
- the sections of the tunnel between 118–126 m, 143–156 m, 158–632 m, 739–761 m, 788–969 m, 979–1149 and 1163 to 1268 meters from the Miners' Gate show small losses of the support material, infiltration of salt, small flows of water, etc., which currently do not threaten the stability of the heading (Fig. 7).

In order to determine the capacity of the support, material samples were taken from the wall. Petrographic studies showed that the rock from which the sample is made has carbonate origin: limestone with clear stratification planes. The cross-sections taken during sample cutting for strength testing showed horizontal slit aperture of about 0.1 mm filled with secondary mineral association with clearly dark yellow and rusty colours. Moreover, an individual focus of about 2–5 mm quartz grains is also visible (Fig. 4).

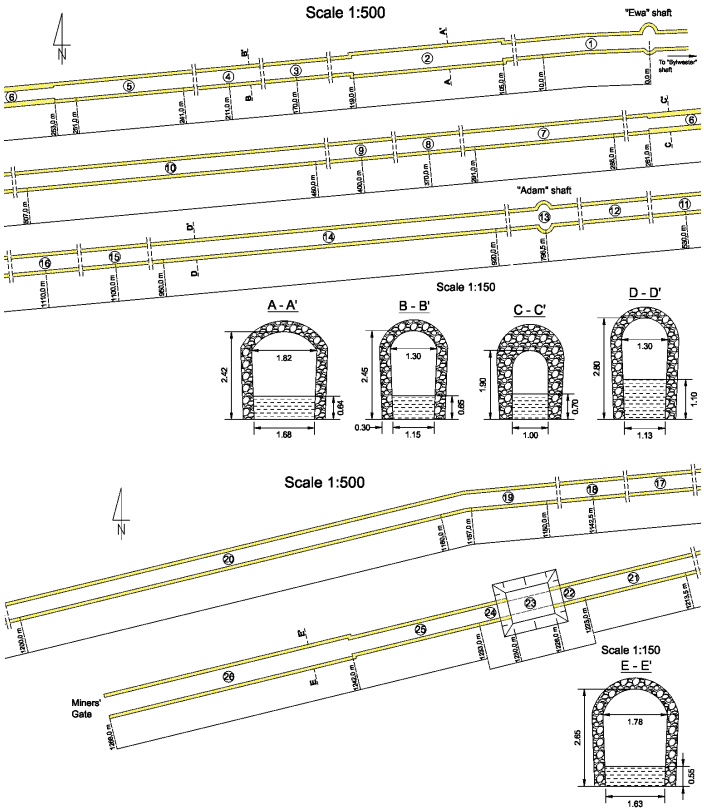

Fig. 4. The approximate location of characteristic points and damages of the support along the heading [10]

Fig. 5. View of "Fryderyk" adit in the area of point 25 on Fig. 4 [10]

Fig. 6. View of "Fryderyk" adit in the area of point 20 on Fig. 4 [10]

Fig. 7. View of "Fryderyk" adit in the area of point 9 on Fig. 4 [10]

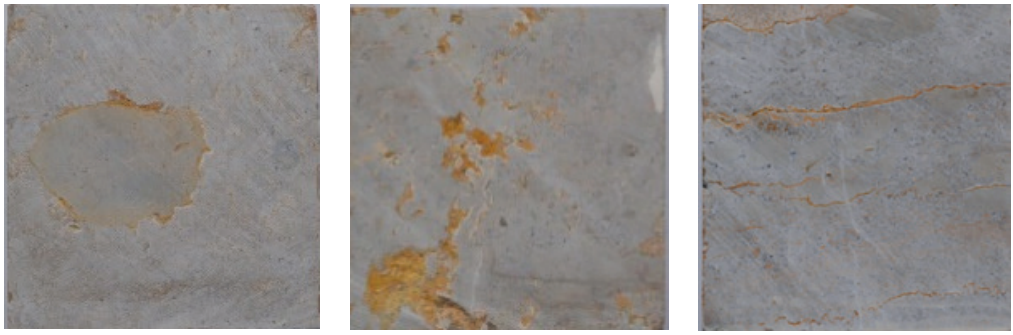

Fig. 8. Examples of sample cut surface views with visible gaps filled with a yellow-rust colored substance [10]

Limestone masonry samples taken from the support were used for strength tests. The study was conducted in accordance with PN-G-04303:1997. Test specimens were prepared in the shape of a cuboid with a square base having a side of 42 mm and a slenderness ratio equal to 1 and 2 to respect the limit of tolerance. Crosshead speed of samples was assumed to be the same as for strong rocks – equal to 1.0 MPa/s.

Figures 9 and 10 show photographs of selected samples in the testing machine, taken prior to the commencement of the tests and after the destruction of the sample.

The design value of the compressive strength and the coefficient of variation for the test material was determined according to PN-B-03020:1981. Building land. Direct foundation of the building.

In the summary of the results of research strength of the support of the heading, it was found that:

- The average design value of the compressive strength of the tested support of the heading is 3.22 MPa,

- The test proved the occurrence of local corrosion related mainly to places with water leaks behind the support; losses caused by corrosion did not usually exceed 10 mm and are not dangerous for the structure of the support,
- The excavation has numerous zones of heterogeneity within the structure of the support wall, related to losses of mortar in the joints, causing reduction of structural integrity, and thus decrease in its mechanical properties.

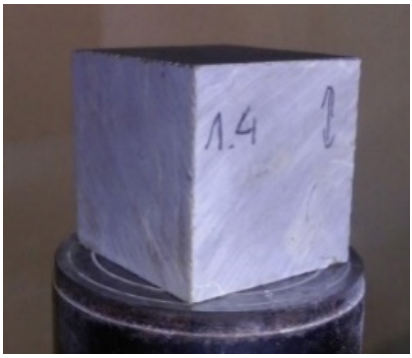

Fig. 9. View of pre-study sample in the universal testing machine [10]

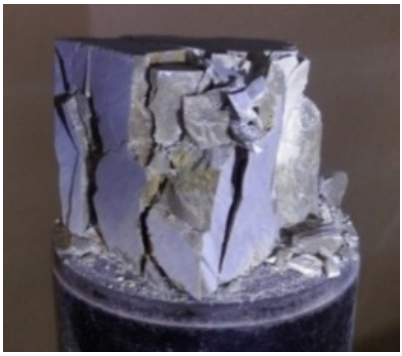

Fig. 10. View of after-study samples in the universal testing machine [10]

5. Assessment of the impact of the rock mass on the support of the heading

In case of the analyzed adit, the amount of stress in the surrounding rock mass was determined assuming a variation in its cross-sectional dimensions and changes in the strength and deformation properties of the rock mass, as well as the stress resulting from the depth of the excavation, taking into account natural and mining factors.

The impact of the rock mass on the support of the analyzed heading was assessed while having taken the following assumptions:

- due to the location, it was assumed that the excavation is located at a depth of about 24 m,
- the analyzed heading is protected with a support of variable dimensions,
- the calculations take into account the variability of stress arising from varying dimensions of the exposed roof and the conditions taking into account the stress concentration zones,
- the load of the support and the forced displacement of the heading contour were determined without taking into account the effect of mining activities, e.g. exploitation and rock mass tremors.

Taking into account the above assumptions to distinguish the models of stress and deformation forces in the rock mass in the vicinity of each of the analyzed sections of the excavation, calculations of the load were carried out at the points located along the heading, according to the rules specified by PN-G-05020:1997.

The results of the calculations are presented in Table 1.

Table 1. Examples of the results of calculations of the adit support stress (cross-sections according to Fig. 4)[10]

	C-S A-A'	C-S B-B'	C-S C-C'	C-S D-D'	C-S E-E'
q_{Nz} [kPa]	25	48	21	22	65
q_{Nx1} [kPa]	0	27	0	0	37
q_{Nx2} [kPa]	0	61	0	0	72

6. Assessment of capacity of the support structure, taking into consideration its current technical condition

While shaping models of the support structure for each section of the heading, it was assumed that:

- strength parameters of the materials of which the structure of the heading was made correspond to the results of the conducted studies,
- because of the age of the heading, it was assumed that cement and lime mortar of class M1 was used to connect the bricks of the support,
- the calculation was based on the assumption that the average thickness of the wall of the support tunnel is 0.3 m,
- strength parameters and deformation of the wall in the structure of the support correspond to the results of the conducted studies,
- the calculations were made assuming the least favorable load conditions,
- the method and the amount of the load on the analyzed segments of the support were adopted in accordance with paragraph 4.

A simplified model of the heading with a highlighted load diagram is shown in Figure 11.

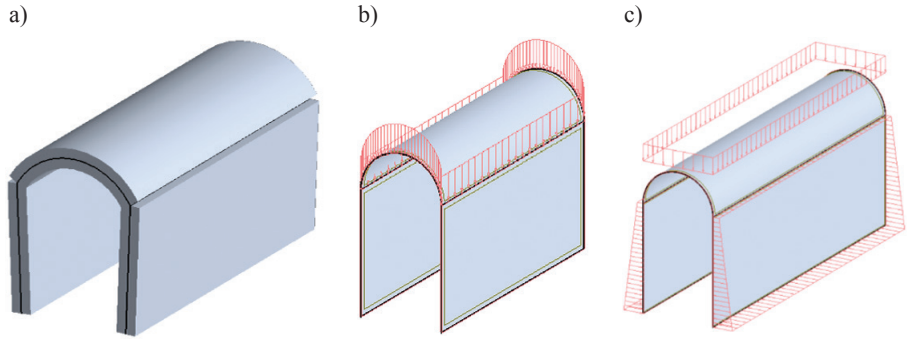

Fig. 11. A simplified heading stone support model with distinguished load schema: a) numerical projection of a fragment of the existing support on the heading section, b) schema of adopted support load in sections made in rocks, c) schema of adopted support load in sections made in quaternary sediments

Having developed those numerical models, the internal forces and the reduced stresses in the elements of the support were calculated with the use of the Autodesk Robot Structural Analysis Professional 2016 software package.

On the basis of the results of numerical modelling, the degree of security of 90 individual support segments of the analyzed heading was assessed. For this purpose, an indicator of exhaustion of structural load sections was used as expressed with a rate of exhaustion of its cross-section. The structure is considered to be safe if the ratio reaches a value of less than 1. The method of load calculation of the support used in this case and the simplified static diagram indicate that the structural elements of the support are mainly subject to compressive stress (Fig. 12 and 13).

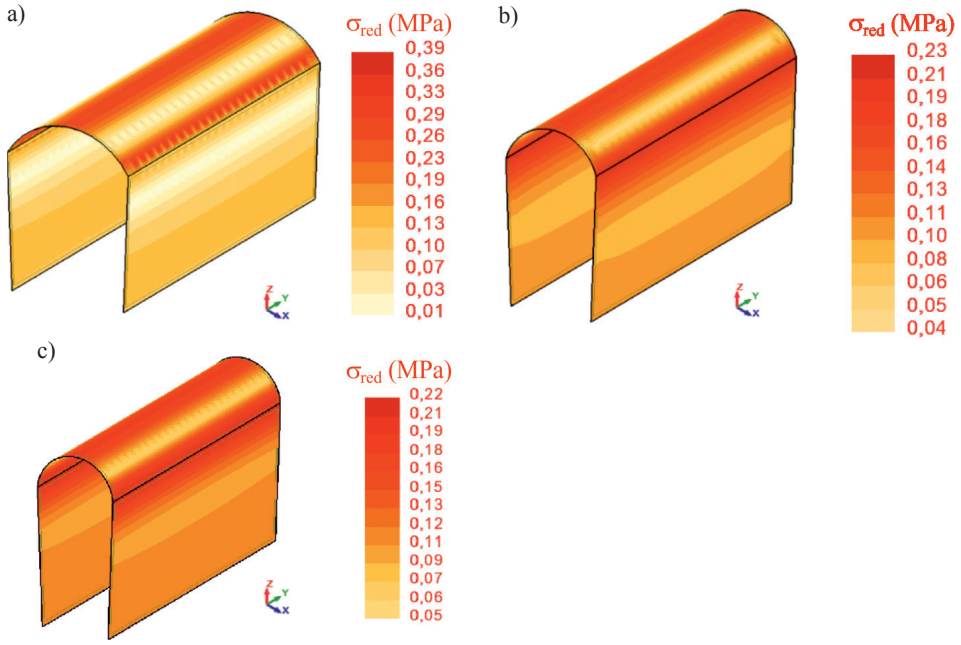

Fig. 12. Shaping of tension values reduced in support elements in heading sections made in rocks: a) in cross-section A-A' (Fig. 4), b) in cross-section B-B' (Fig. 4), c) in cross-section D-D' (Fig. 4)

On the basis of the results of numerical modeling and the analysis of the technical condition of individual support segments of the analyzed heading, it was assumed that the degree of exhaustion of the most stressed cross-section amounts to:

- in case of the sections made in hard rocks:
  - for A–A' cross-section $k = 0.12$
  - for B–B' cross-section $k = 0.07$
  - for D–D' cross-section $k = 0.07$
- in case of the sections made in quaternary sediments:
  - for B–B' cross-section $k = 0.47$
  - for E–E' cross-section $k = 0.64$

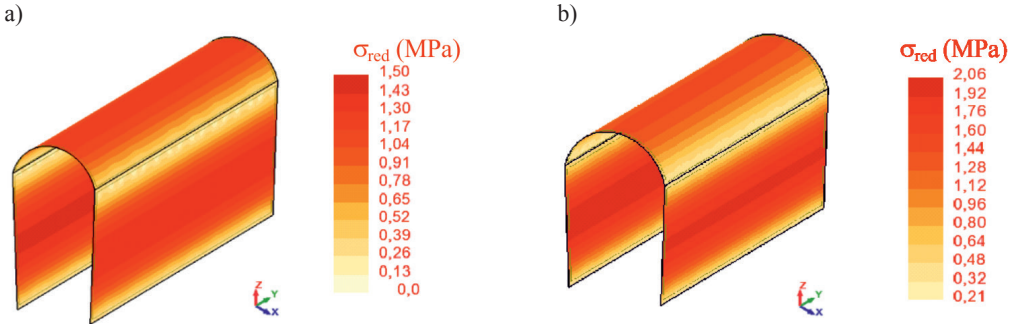

Fig. 13. Shaping of tension values reduced in support elements in heading sections made in quaternary sediments: a) in cross-section B-B' (Fig. 4.1), b) in cross-section E-E' Ffig. 4.1)

In summary, the calculation concluded that the assumptions made for the support meet the criterion of safety in view of the load-bearing capacity of the structure. The values of coefficients calculated for the sections of the heading made in the hard rocks leave a much higher safety margin than those calculated for hollow sections in the quaternary sediments.

7. Factors influencing the course of natural deterioration of the end section of the "Fryderyk" ("Kościuszko") adit

It is assumed that the static load of the support due to overburden rocks (the weight of the rocks in the zone stressing the support of the heading) and the hydrostatic pressure of water in the subsurface have the primary impact on the supports located at a small depth. In case of the analyzed "Fryderyk" (Kościuszko) adit sections in the area of the Miners' Gate, the main external factors may include:

- construction works in the area of the adit,
- changes in vegetation on the surface,
- variable water flow in the tunnel and its surroundings,
- the impact of weather conditions.

However, having assumed a shallow retention of the heading, one must reckon with the possibility of additional impacts indirectly related to the rock mass. Those interactions include:

- geostatic increase in the stress caused by water conditions in the soil layer,
- geostatic increase in the load due to other elements stressing surface directly in the vicinity of the heading,
- the occurrence of dynamic ground vibration caused by seismic activity, mining or transport.

There are no buildings along the analyzed section of the adit; the area is covered with grass, shrubs and trees. For a long time, the surface of the adit was used as a grassy meadow. In recent years, the meadow turned into a forest, which means that plants growing over the area have larger root structures that may penetrate the support (especially in the joints of the wall made of a material which is easy to chip), causing its degradation.

One of the decisive factors influencing the conditions of maintaining the stability of the adit may be construction works, for example, of a well situated virtually adjacent to the tunnel. These works led to a clear interference in the environment of the adit, through the execution of a new, vertical subsurface excavation, which had an impact on the adit – a sided unveiling of the support affecting the previously established balance in the soil. The stability of the support tunnel may also be influenced by weather conditions, especially precipitation and its impact on changes in the properties of the soil and load conditions of the support. An increased inflow of the soil as a result of precipitation and a runoff because of the drainage of the area due to the existence of the adit may also facilitate the process of suffosion, which may result in loosening of the ground. Due to the shallow depth of the location and the direct connection of the tunnel to the surface, one cannot also exclude the process of cyclic freezing and thawing of the land and of the support.

8. Assessment of risk to the surface and its infrastructure in case the support of the adit loses its stability

The fact that the heading has a shallow location in its initial section, as measured from the outlet tunnel, had a decisive influence on the increased risk of the possibility of discontinuous deformations on the surface. The possibility of such a threat was confirmed during fieldwork in a form of sinkholes. The first appeared in 1962, and the second in 2008. After a visit to the site, it was found that both sinkholes appeared as results of breakages in roof sections of the support. The sinkhole of 1962 is now partially buried and the support tunnel in this section is restored; however, the sinkhole from 2008 is only protected by wooden cabinet anchors and the area around the sinkhole is fenced and marked as a danger zone.

It can be assumed that the sinkholes generate voids located at a depth of up to 100 m. Those voids are often associated with tunnel headings that were improperly eliminated or left in its natural state [6].

For the purpose of estimating the probability of sinkholes as a result of loss of stability of the inlet section of the tunnel support, the Chudek-Olaszowski method was used [3]. The analyzed section of the tunnel runs almost horizontally at a depth of 0 to 25 m counting from the roof of the heading.

The heading was dug in the layers of sand, loam or clay, as well in the roof section of the dolomite layer, which is residual beneath the overburden. Taking into account the above information and including the depth of the heading, it should be explicitly stated that a possible collapse in the area would include the loose layer of overburden.

Thus, in the light of the Chudek-Olaszowski method, a loss of stability of the support of the heading would, beyond any doubt, result in an appearance of a sinkhole on the surface. The sinkhole would appear in the area where the loose overburden is located. Therefore, the area should be classified as D category.

9. Assessment of the safety of the support in the analyzed section of the adit

Underground headings used over a long time, especially when the access to them has been cut off for a significant time, usually have supports with a large and often very uneven degree of technical wear. In this situation, load-bearing capacity of the support can be treated as a random variable with a certain probability distribution or a certain range of variation. Similarly, the state of the rock mass in the vicinity of the heading with a long-term existence is progressive and the degradation is often very different in each section. In this case, the parameters describing the current state of the rock mass can also be treated as random variables with a certain probability distribution or range of variation. Assuming that the parameters determining the stability of the historic underground headings are random variables, it is advisable to use a probabilistic method to analyze the stability of the excavation.

In theory of reliability and security of structures based on a probabilistic analysis, the measure of reliability may be the likelihood of loss of stability. The size of the probability of impact is influenced by the so-called safety margin (the difference in the capacity of the structure and its load) and the variance of basic data to determine the stability of the heading.

The evaluation of construction safety is a solution to a two-stage probabilistic approach based on the assumption that the failure condition can be written as:

$$Z_0 = P_0 - q_0 \geq 0 \tag{9.1}$$

where:

Z_0 – safety margin,
P_0 – capacity of the support,
q_0 – load of the support.

The Cornell's reliability index (t) is assumed to be a measure of safety:

$$t = \frac{\overline{P}_0 - \overline{q}_0}{\sqrt{s_{P_0}^2 + s_{q_0}^2}}, \tag{9.2}$$

where:

s_{P0}, s_{q0} – standard deviation of capacity and load of the support.

The value of the cumulative distribution coefficient reliability $p(t)$ is the probability of the safety of the structure, while the value $[1–p\ (t)]$ is the probability of failure of the structure (loss of stability of the support).

In this method, the conditions of reliability and safety are used, such as:

$$p \leq p_a \tag{9.3}$$

where:

p – probability of the loss of stability,
p_a – accepted level of probability of the loss of stability.

One of three classes of conditions for maintaining stability of a heading can be distinguished on the basis of the relationship between the behavior of the headings and the probability of the loss of their stability, namely:

Class I – $p \leq 0.10$ – safe conditions,

Class II – $0.10 < p \leq 0.35$ – sufficient conditions (acceptable),

Class III – $p > 0.35$ – dangerous conditions (unacceptable).

In order to safely meet its technological requirements, a corridor heading should be classified as Class I. Conditionally, it is permitted to qualify for Class II, but in this case its supervisor should be ready to carry out repair works or limit the scope of its use.

Using the results of the measurements of the actual thickness of the support, the strength of its bricks and their statistical analysis, the calculations of the current capacity of the support were carried out.

Having considered the overburden of the support and its load-bearing capacity as random variables with normal Gauss distribution of probability, the probability of the loss of stability along the support tunnel was determined. The calculations were made taking into account the variability of the load and the capacity of the support along the tunnel, therefore dividing it into sections characteristic in terms of the support capacity and the size of the projected load. The results of the calculations are presented in Fig. 14.

In reference to the calculations carried out above the classification, it can be said that the following tunnel sections can be distinguished along the length of the tunnel:

Class III (dangerous conditions – unacceptable) – 0–45 m from the Miners' Gate,

Class II (sufficient conditions – acceptable) – 45–118 m; 126–143 m; 156–158 m; 632–739 m; 761–788 m; 969–979 m and 1149–1163 m from the Miners' Gate,

Class I (safe conditions) – 118–126 m; 143–156 m; 158–632 m; 739–761 m; 788–969 m; 979–1149 m and 1163–1268 m from the Miners' Gate.

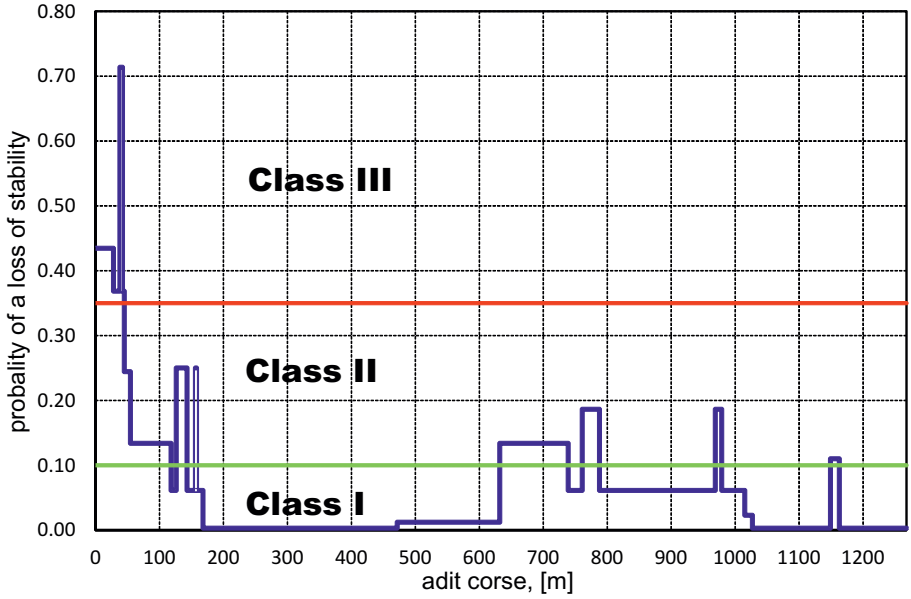

Fig. 14. Graph of the adits stability loss probability at its length

10. Summary

Summarizing the results of the study, it can be concluded that the support tunnel "Fryderyk" (Kościuszko) in its final section to the outlet in Ptakowice shows a varying degree of technical wear. The conditions affecting its state are mainly the following:

- long life of the heading,
- low quality support (mortar quality, accuracy, performance, etc.)
- the adverse impact of the environmental factors – exposure to water, vegetation and other living organisms, etc.,
- lack of maintenance and repair of the support.

On the basis on the conducted field research and performed calculations of the static strength of the support and the size of the load, while taking into account the impact of natural factors on the process of degradation of the support tunnel, the scope of necessary actions required in order to halt the natural degradation of the final section of "Fryderyk" (Kościuszko) was defined. These measures are grouped into four blocks of problems:

- practical measures needed to secure the endangered tunnel sections,
- research and technical expertise,
- design works (technical and technological projects)
- organizational activities.

Practical measures needed to secure the endangered tunnel sections:

- immediately take corrective action and protect the tunnel sections at risk of losing stability, observations of the behavior of the tunnel support and maintenance works should be carried out in the other sections,
- existing sinkholes should be secured before their further development advances.

Research and technical expertise should aim to:

- prepare updated geological documentation for the surroundings of the adit
- prepare basic geological and mining documentation,
- commence studies on the structure and properties of the rock mass,
- determine the impacts and environmental risks.

The basic design works should include:

- a utilization project for "Fryderyk" (Kościuszko) adit in terms of its further use.
- a technical design of extensive reconstruction of the final section of "Fryderyk" (Kościuszko) adit within the area of about 50 m from its inlet.
- a technological plan for the repair of the support and securing the adit.
- detailed documentation specifying the method and technology of repair of the damaged support sections.

The organizational measures should focus on:

- determination of the administrator of the adit,
- determination of the legal grounds for the functioning of the adit,
- determination of the boundaries of the area and the mining land,
- solution of the problem of land ownership.

References

[1] Chudek M., *Budownictwo podziemne cz. I. Obudowa wyrobisk korytarzowych i komorowych*, „Śląsk", Katowice 1987.

[2] Chudek M., Duży S., Kleta H., Kłeczek Z., Stoiński K., Zorychta A., *Zasady doboru i projektowania obudowy wyrobisk korytarzowych i ich połączeń w zakładach górniczych wydobywających węgiel kamienny*, KGBPiOP Pol. Śl., Gliwice–Kraków–Katowice 2000.

[3] Chudek M., Janusz W., Zych J., *Studium dotyczące rozpoznania tworzenia się i prognozowania deformacji nieciągłych pod wpływem podziemnej eksploatacji złóż*, Zeszyty Naukowe Politechniki Śląskiej, Górnictwo, No. 141, Gliwice 1988.

[4] Duży S., *Studium niezawodności konstrukcji obudowy i stateczności wyrobisk korytarzowych w kopalniach węgla kamiennego z uwzględnieniem niepewności informacji*, Zeszyty Naukowe Politechniko Śląskiej, Górnictwo, No. 277, Gliwice 2007.

[5] Kerber B., *Charakterystyka złóż w rejonie tarnogórskim. Charakterystyka rud cynku i ołowiu na obszarze śląsko-krakowskim*, Prace, Instytut Geologiczny, Wyd. Geologiczne, Warszawa 1977.

[6] Strzałkowski P., *Wpływ płytkiej eksploatacji górniczej na zagrożenie powierzchni terenu deformacjami nieciągłymi*, Zeszyty Naukowe Politechniko Śląskiej, Górnictwo, No. 246, Gliwice 2000.

[7] Duży S., *Probabilistyczna analiza stateczności budowli podziemnych*, Przegląd Górniczy, No. 4/2004.

[8] Duży S., *Ocena bezpieczeństwa konstrukcji wyrobisk korytarzowych w kopalniach węgla kamiennego z uwzględnieniem zmienności warunków naturalnych i górniczych*, Bezpieczeństwo Pracy i Ochrona Środowiska w Górnictwie, 2005, No. 6(130).

[9] Duży S., Preidl W., Bączek G., Dyduch Ł., Pawlas Ł., *Ocena niezawodności i bezpieczeństwa konstrukcji obudowy kamiennej wyrobisk Kopalni Ćwiczebnej Muzeum Miejskiego „Sztygarka" w Dąbrowie Górniczej poddanych niekorzystnemu oddziaływaniu środowiska*, Górnictwo i Geologia, 2012, 47–58.

[10] Duży S., Dyduch G., Preidl W., Stacha G., Czempas A., Utko S., *Opracowanie służące podjęciu działań dla zahamowania naturalnej degradacji końcowego odcinka historycznej sztolni „Fryderyk" („Kościuszko") w Tarnowskich Górach, z wylotem znajdującym się na terenie Ptakowic gm. Zbrosławice*, NB-189/RG-4/2016, Gliwice 2016 (not published).

[11] *Zadanie dotyczące rozpoznania możliwości i metod zabezpieczenia zapadliska przy Bramie Gwarków oraz rozpoznanie możliwości i metod zabezpieczenia wejścia do nieczynnego wyrobiska górniczego będącego miejscem wlotu nietoperzy przed osuwającymi się odłamkami skalnymi w Kamieniołomie Bobrowniki,* Praca GIG, Katowice 2015.

[12] Kraatz L., *Karte des Oberschlesischen Erzbergbaues heraus gegeben von dem Königlichen Oberbergamt zu Breslau in den Jahren 1911–1912*, Lith. Anst., Berlin 1912.

TECHNICAL TRANSACTIONS 6/2017
CZASOPISMO TECHNICZNE 6/2017
CIVIL ENGINEERING
DOI: 10.4467/2353737XCT.17.090.6566

Jarosław Konior (jaroslaw.konior@pwr.edu.pl)
Department of Construction Methods and Management, Faculty of Civil Engineering,
Wrocław University of Science and Technology

Maintenance of apartment buildings and their measurable deterioration

Utrzymanie budynków mieszkalnych a ich mierzalna degradacja

Abstract

Apartment buildings constructed prior to the First World War are important examples of Polish buildings with regard to their historical significance – the technical maintenance of such buildings remains challenging. The results of the work refer to the general population, estimated for 600 objects, that compose of about 20% of municipal downtown apartment buildings in Wrocław. The purpose of the research was to identify an influence of widely considered maintenance of apartment houses on a degree and intensity of their elements'. The goal of this research has been achieved through the analysis of symptoms reflecting the decline of the inspected elements' exploitation values, that is identification of mechanics of arising their defects. The calculated quantitative data can be used as the basis for identifying the structure of the building companies which are responsible for housing maintenance and repair.

Keywords: apartment buildings, maintenance, deterioration, technical wear

Streszczenie

Prawidłowa, tzn. systematycznie i rzetelnie przeprowadzana, ocena stanu technicznego budynków mieszkalnych stanowi podstawę do szeroko rozumianej organizacji ich obsługi technicznej, a w szczególności do organizacji prowadzenia remontów o ustalonym rodzaju, wielkości i zakresie. Ocena ta, poparta rozpoznaniem wpływu warunków utrzymania budynków mieszkalnych, jest ponadto podstawowym źródłem informacji w racjonalnym zarządzaniu zasobami mieszkaniowymi. Celem badań było rozpoznanie wpływu przebiegu procesów, utożsamianych z szeroko pojętym utrzymaniem starych kamienic czynszowych o konstrukcji tradycyjnej, na wielkość i intensywność zużycia ich elementów. Charakterystyka techniczna i typologiczne uporządkowanie ich uszkodzeń, rozumianych jako wyraz jakości utrzymania budynków mieszkalnych, umożliwiły rozpoznanie warunków eksploatacji rozważanych obiektów. W zdarzeniach losowych, gdzie próbowano opisać stany zaobserwowane (empiryczne) formułami teoretycznymi, rozważono probabilistyczną stronę zagadnienia i jej losowy charakter.

Słowa kluczowe: budynki mieszkalne, utrzymanie, degradacja, zużycie techniczne

1. Introduction

Apartment buildings constructed prior to the First World War are important examples of Polish housing style – these types of buildings account for around 10.1% of the total number of urban apartments. Furthermore, the importance of this type of building is due to the fact that they contribute to the creation of the urban environment. Maintaining the value of the urban environment requires continued effort and is a responsibility that is passed down through the generations. The effort is effective if continuity of the following process is kept: erection, maintenance, repair, maintenance, modernisation, maintenance, etc. until the demolition of the object. Due to the political and economic conditions of the twentieth century developments in many countries have been destroyed over the course of history caused by the events of war. After the Second World War, in plenty of countries in Central Europe, additional devastation factors have appeared as a consequence of a lack of houses, the migration of people and insufficient care and maintenance of buildings – a majority of them as a result of deprivation of a law of property belonged to proprietors of houses. There is currently a need to make efforts to repair and maintain such buildings. Cultural factors doubtlessly motivate such efforts. With regard to the economic and technical justification of such repair and maintenance projects, the degree of technical wear and tear of the buildings in question should be identified [1–9].

This paper is the result of technical research and analyses of old apartment buildings in Wrocław [8]. The aim of the analysis is to provide information which would assist in the planning of maintenance work for the group of the apartment houses in question. A method of scientific research for calculating the technical wear of an apartment house and the detailed results of the technical wear of twenty three considered apartment buildings elements are presented in this paper [8].

2. Research background

The analysis was performed on the apartment buildings erected before the First World War in the city centre of Wrocław [8]. These are apartment houses which were built in the nineteenth and early twentieth centuries. The buildings are situated in the part of the city which was one of very few districts that wasn't completely destroyed by the events of war. The apartment houses are three- or four-storey brick buildings, erected in longitudinal, usually three – row structural systems. With the exception of the solid basement floors, all of the other floors are examples of typical wooden floors. All the buildings are covered with wooden rafter framing, usually of purlin-collar type. The staircases are composed of wooden or steel structural elements with wooden flights of stairs.

3. Comparative analysis of technical wear

During analysis, it was repeatedly noticed that the observed technical wear Ze is greater than the theoretical one Zt during the first stage of building elements use: $Ze = f(t) > Zt = f(t)$. After exceeding some, possible to determine, age t_i the mentioned relation is inversely

proportional and works until the maximum value of building elements age: $t_{max} = 174$ years. In the considered example, the age of main walls for which the value for theoretical wear becomes higher than the value for observed wear is 87 years. The difference between theoretical and observed wear increases with the age of the building elements what indicates imperfection in calculating the technical wear according to the theoretical formulas. The mean deviation of the theoretical and the observed technical wear is –3.13. Age seems to be related to the degree to which values relating to theoretical wear and observed wear differ. This relationship seems to exist because all observed elements of the apartment houses show signs of being 'under expected life' during the first stage of building element use and 'over expected life' after exceeding the age t_i There is the only one period, approximately defined as $(t_i - T/10) < t_i < (t_i + T/10)$, where the theoretical and the observed technical wear vary by no more than 10%. The comparative analysis reveals considerable differences between the degree of technical wear calculated according to theoretical formulas and the degree of wear revealed during inspection of the apartment houses – this confirms the existing need to create a model which makes it possible to verify the reliability of the theoretical formulas. The number of gathered observations makes possible to build the model that can be applied to all particular building elements [3, 5, 9].

4. Scope of probabilistic research

The theoretical model of the deterioration of apartment buildings is a function of time t and assumed durability (expected life) T of apartment building elements. Owing to the fact that the purpose of the theoretical simulation solely establishing of a trend of the phenomenon therefore, models of a limited complexity have been chosen [7, 10, 11]. As a result of this basic level of complexity, the scope of the research has been limited to seeking the trend function among linear, power, exponential and hyperbolic dependencies (Table 1).

Table 1. Result of probabilistic research – modelling of new functions $Z_t = f(t)$ and durability T revision

SEEKING OF ALTERNATIVE FUNCTIONS Zt = *f*(*t*) BY NON-LINEAR REGRESSION METHOD										REIDUUM ANALYSIS
Z9 – STAIRS	NON-LINEAR REGRESSION				VARIANCE ANALYSIS					durability T, for which
	estimators		probability level		model		residuum		determination coef.	average deviation = 0
mathematical formulas	constant A	regression c. B	p(A)	p(B)	df	square sum	df	variance	R*R [%]	and remainder var. = min, for
LINEAR MODEL: Y = A + B X	34.4926	0.1509	0.0000	0.0126	1	1269.919	100	196.666	6.07	804
POWER MODEL: Y = AX^B	3.1387	0.1552	0.0000	0.0004	1	1.206	100	0.090	4.78	6894494
EXPONENTIAL MODEL: Y = exp (A + BX)	3.4810	0,0038	0.0000	0.0038	1	0.083	100	0.094	8.06	519
HYPERBOLIC MODEL: 1/Y = A + B X	0.0323	–0.0001	0.0000	0.0021	1	0.001	100	0.000	9.04	301
RESEARCH OF RELATION SIGNIFICANCE BETWEEN Ze and t BY RANKS OF SPEARMAN'S C.										Ross & Unger formulas
observed significance level	*p*(*S*) = 0.0264 < 0.05 – CORRELATION Ze/t SIGNIFICANT									(III class of maintenance)
ASSESSMENT OF SIGNIFICANCE DIFFERENCE BETWEEN Ze and Zt DISTRIBUTIONS										Y=X(X+T**)/2T**T**
non-parametrical tests	WU I – V	WU II	WU III	WU IV	EXPLAINATION:					T = 160 lat
"WILCOXON'S TEST"	R	R	R	R	R – distributions are significantly different					literature durability
"TEST ZNAKÓW"	R	I	R	R	I – distributions are identical					for stairs Z9: T = 120 years

The parameter values of the testing models were selected according to the non-linear regression method [7, 10, 11]. With Z as a dependent variable representing the degree of technical wear of the building element and t as its age (independent variable), a zero-hypothesis based on the rules of non-linear regression was stated. According to the hypothesis H_0, such created model does not explain a systematic alternation the variable Z to the variable *t*, described by a regression coefficient γ and enlarged by a constant random addend ξ. It appeared that the most influential factor on the random addend ξ was the condition of the considered apartment houses' maintenance. The whole of the model, equation (1), is divided into the section explained by the sought model (dependent on regression γ and the part, which is not explained by the model, defined as a remainder addend (residuum) ξ. Numerical values of parameters γ and ξ have been calculated by the method of least squares. This enabled to determine the estimators referred to the constant A (= ξ) and to the regression coefficient *B* (= γ). All of these principles are contained in the following rule:
Z – random variable (dependent = *Y*) ⇔ technical wear of building element $Z = \{z_1, z_2, ..., z_n\}$;
t – age of building element (independent variable = *X*), $t = \{t_1, t_2, ..., t_n\}$;

$$Z = \xi + f(t, \gamma) = \xi + \gamma t \tag{1}$$

where:

γ – directional coefficient of regression – part dependent on regression;

ξ – remainder addend (residuum), with values $\xi_1, \xi_2, ... \xi_k$ – not explained by model.

A variance analysis was applied to test the extent to which the theoretical model fits to the empirical data. This analysis resulted in the calculation of determination coefficient R^2. The value of coefficient R^2 provided information how big part of the observed in the sample building element's technical wear diversification was explained by its regression as to the apartment buildings age – the results of the variance analysis are shown in Table 1.

Correlation coefficients of SPEARMAN'S ranks allowed comparisons between ranks of the two variables which are present in the model – dependent variable Z and independent variable *t*. If an observed significance level $p(S)$ was lower than the assumed level of $\alpha = 0.05$, then the null hypothesis was rejected and the alternative hypothesis H_1 was accepted; therefore, the existing correlation between the technical wear and age of apartment house elements can be treated as significant (Table 1).

An assessment of the significance difference between the theoretical Zt and the observed Ze value distributions of the technical wear of building elements was undertaken through the use of two non-parametrical tests – the WILCOXON test and the 'Znaków' test. A result of the testing was the calculation of the level of probability that the sample output statistics would support the zero-hypothesis regarding the identity of variable distributions (Table 1).

The last stage of the non-linear regression method is based on a residuum analysis. It revealed a priceless piece of information about durability of the building elements considered as a posterior data [6]. The actual durability T^{**} of the apartment buildings chosen elements belongs to the period of 153–177 years and is greater than the well-known referred durability T^* – the average deviation should cross the '0' point (Fig. 1), the remainder variation should be minimum (Fig. 2).

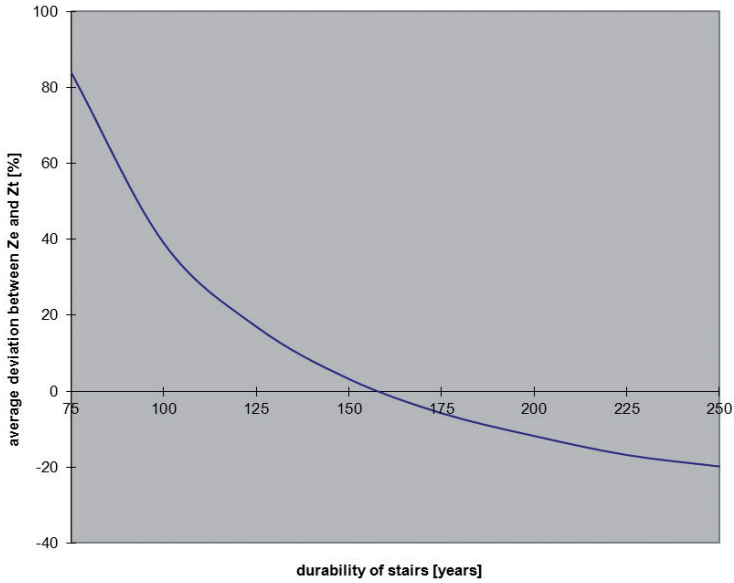

Fig. 1. Deviation between observed technical wear and estimated theoretical wear as a function of stair durability

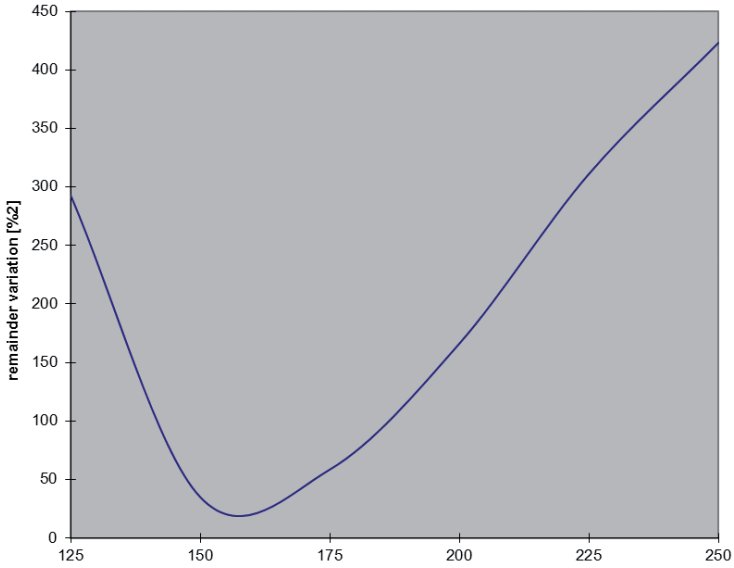

Fig. 2. Remainder variation as a function of stair durability with average maintenance of building element

Owing to the unsatisfying results of the observed states' modelling by the theoretical formulas a second attempt was made to measure the buildings deterioration. This attempt was based on looking for quantitative relationships between the defects of the elements of the apartment buildings (as an indication of state of maintenance) and the intensity of the deterioration of the considered elements [1, 2, 10, 11].

5. Conclusions drawn from research

5.1. Conclusions relating to methods of measuring the deterioration of the apartment buildings

The widely applied theoretical methods of measuring the extent of technical wear to apartment buildings and their elements insufficiently describe the state of reality. What is doubtful it is as the way of attribution these methods to maintenance conditions as the choice of too general mathematical formulas with the only two variables: t and T.

Theoretical formulas for determining the technical wear of building elements take into account their age t and durability T as the only parameters and do not include the influence of the state of the apartment buildings maintenance. The assessment of the measurable difference between the theoretical and the observed values of the technical wear of the building elements conducted using the Wilcoxon and 'Znaków' tests shows significant differences between these distributions in the majority of cases.

None of parabolic functions represent the character of the determined technical wear over time (that means a very small determination coefficient R^2 and unnaturally high quantity of parametric durability T^{**}). The exponential and hyperbolic mathematical models better represent the theoretical tendency of the apartment buildings elements' deterioration.

5.2. Conclusions regarding the influence of the maintenance of apartment houses on their deterioration

Considered apartment houses are in such period of their using when the time of a proper work up to a defect shows the character of exponential trend – an average rest of their using time is at each moment unchangeable.

Less than 30% of the technical wear of the apartment house elements is explained by their age – the maximum value of the determination coefficient is $R2 = 30.89\%$.

Two types of the building element defects play a major role in the rapid deterioration of an apartment house:

- calculated as a result of probabilistic analysis the defects caused by water penetration and humidity migration; the rule is particularly relevant in the case of poorly maintained objects;
- determined as a result of the random calculation of the mechanical defects of the structure and the surface of the elements (which result in considerable frequency and cumulating effect and lead to permanent increase in the apartment buildings elements' deterioration); the regularity is characteristic for well and average maintained objects.

6. Summary

The research (the methodological assumption, the mathematical application and the conclusions) should be treated as a piece of exploratory work. Thus, it is an attempt of the recognition of the mechanism of the reasons and effects phenomena, which an engineer

expert meets while technically inspecting a building object. This assessment, however, is naturally gifted with an immeasurable aspect (partly subjective). Creating a new model of the technical inspection of apartment buildings, based on procedures and conclusions drawn from this work, would make possible to transfer the weight of technical assessment from being qualitative to quantitative in nature. The author's intention is to direct further research connected with the widely considered measurable diagnoses of technical objects in the direction described above.

References

[1] Belniak S., Leśniak A., Plebankiewicz E., Zima K., *The influence of the building shape on the cost of its construction*, Journal of Financial Management of Property and Construction, Vol. 18, No. 1, 2013.

[2] Brunarski L., *Diagnostyczne metody badań budowli*, XXXVIII Konferencja Naukowa PAN i PZITB: Współczesne problemy techniczne i ekonomiczne w budownictwie mieszkaniowym, Krynica 1992.

[3] BS 8210 *Guide to building maintenance management*, British Standard, 1986.

[4] Kajfasz S., *Utrzymanie obiektów budowlanych – pojęcia, wsparcie naukowe*, XXXVIII Konferencja Naukowa PAN i PZITB: Współczesne problemy techniczne i ekonomiczne w budownictwie mieszkaniowym, Krynica 1992.

[5] Konior J., *Intensity of defects in residential buildings and their technical wear,* Technical Transactions, Kraków 2014.

[6] Morrison D.F., *Multivariate Statistical Methods*, McGraw – Hill Book Company, New York 1990.

[7] Multi-Author Work, *Assessment of Wrocław downtown apartment houses' technical conditions. Reports series "U" of Building Engineering Institute at Wrocław University of Technology*, Wrocław 1984–90.

[8] Marcinkowska E., *Problemy decyzyjne w projektowaniu obiektów i procesów budowlanych*, Monografie PWr, Wrocław 1986.

[9] Multi-Author Work, *Research models and methods in construction projects engineering*, O. Kapliński (ed.), PAN, KILiW, Warszawa 2007.

[10] Thier H., *Cases of damage and their analysis*, Deutscher Verlag fuer Schweisstechnik, Duesseldorf 1985.

[11] Weil G.J., *Detecting the defects*, Civil Engineering ASCE, London 1989.

TECHNICAL TRANSACTIONS 6/2017
CZASOPISMO TECHNICZNE 6/2017
CIVIL ENGINEERING
DOI: 10.4467/2353737XCT.17.091.6567

Lucyna Korona
Technical Department, Kujawy and Pomorze, University in Bydgoszcz

Janusz Tadeusz Barski (barski@uwm.edu.pl)
Institute of Building Engineering, Faculty of Geodesy, Geospatial and Civil Engineering, University of Warmia and Mazury in Olsztyn

Analysis of type of construction projects in tender formula "design and build"

Analiza struktury rodzajowej przedsięwzięć budowlanych w formule przetargowej "zaprojektuj i wybuduj"

Abstract

The construction undertakings are being realized within two basic formulas:

- Design and separately execution of works – ("P") + ("B"),
- Design and built – ("P+B") otherwise called as "design and execution of works" („Z i W").

The project realization procedure depends on the kind of undertaking and resources of the contracting authority. The choice of formula has an influence on the undertaking preparation as well as on the choice of executor and project realization. The article shows the results of research and defines the percent participation of the individual type of construction undertakings in "design and execution of work" formula that were realized in Poland in the years 2010–2016. "Design and execution of work" formula is used rarely in public procurements. The above-mentioned is confirmed by nation-wide statistic data and statistic data for the Kujawsko-Pomorskie and Warmińsko-Mazurskie provinces.

Keywords: public procurements, "design and build" formula, tendering mode, contracting authority, statistic data

Streszczenie

Przedsięwzięcia budowlane realizowane są w ramach zamówień publicznych w dwóch podstawowych formułach:

- „Projekt" i odrębnie „Budowa" – („P") + („B"),
- „Projekt wraz z Budową" – („P + B") inaczej zwaną „zaprojektuj i wybuduj" („Z i W").

Procedura realizacji projektu następuje w zależności od rodzaju przedsięwzięcia a także posiadanych zasobów przez Zamawiającego. Wybór formuły ma wpływ na przygotowanie przedsięwzięcia i tym samym wyłonienie Wykonawcy oraz realizację, czyli administrowanie projektem. W artykule przedstawiono wyniki badań dokumentacyjnych, określając procentowy udział poszczególnych rodzajów przedsięwzięć budowlanych zrealizowanych w latach 2010–2016 w formule „zaprojektuj i wybuduj" w Polsce. Formuła „zaprojektuj i wybuduj" jest rzadziej stosowana w zamówieniach publicznych, na co wskazują dane statystyczne ogólnokrajowe oraz przykładowo dla dwóch województw: kujawsko-pomorskiego i warmińsko-mazurskiego.

Słowa kluczowe: zamówienia publiczne, formuła „zaprojektuj i wybuduj", tryby przetargowe, zamawiający, dane statystyczne

1. Introduction

Works contracts in the sector of the socialized enterprises are subject to the Public Procurement Law and its relevant regulations. The law regulating auctions for works and construction services was first introduced in 1918. The regime change of 1945 and dynamically developing market economy, as well as the Polish accession to the European Union, have forced numerous and significant changes in legislation, adapting them to the current requirements.

The current system of public procurement has now been in force for twenty-three years. The first legal regulation on the award of the contract came into force in 1994. A big change in the law occurred in 2004, when Poland became a member of the European Union and had "Public Procurement Law" adapt to European standards. The obligation to use the Public Procurement Act and the announcement of auction procedures, to April 15, 2014, applied to contracts with a minimum threshold of 14 000 EURO of estimated value. From 16 pril 2014, the minimum threshold of the estimated value of the contract was increased to 30 000 EURO. A purchaser conducting the public procurement procedure must be guided by the principle of fair competition, objectivity and transparency of procedures. The Act on Public Procurement Law introduced a variety of types and forms of procurement. Hence, the problem for the investor/purchaser, especially the public, is to choose the right kind of tender, and its formula. For several years, it has been practiced in public procurement, in addition to the so-called "classic" formula using formula "design and build".

The focus of the authors of this study is a demand of purchasers to use the formula of "design and build", kind and nature of the ongoing construction projects in this formula.

In order to determine the statistical data, announcements concerning tenders granted in the period from 2010–2016 were analyzed, published in the Bulletin of Public Procurement by the Public Procurement Office on its website, as well as the report of the President on/in the office, conducted interviews with several customers and used the available literature thematic.

2. The essence and the basic assumptions adopted in public procurement carried out in the formula of "design and build"

One of the many possible tender formulas used in different countries is a system of "design and build". It was used for the first time in the US, where in recent years, the popularity of "design and build" significantly increased. This method of implementation of the investment has become one of the most significant global trends in today's construction industry.

The procedure for "design and build" assumes the implementation of the contract by the contractor, including the preparation of comprehensive design documentation. As a result of the tender procedure is showdown to determine only one subject that prepares construction design, technical projects, obtains permission or notification to build, and then performs works according to the documentation prepared. From the point of view of the customer, it is a convenient system of investment.

Model approach to the selection of contractor for the investment in Poland is different than in Western countries, as the general contractor contract is the one who has the larger share of the contract value. On the Polish construction sites general contractor, in the "design and build" formula, is usually a company that implements construction works and subcontracts the execution of the project and obtaining the necessary administrative decisions to the design firm. In Western countries, the leader is generally the design or architectural-managerial company, which prepares a draft, subcontracts and exercises supervision over the implementation of the project (Fig. 1).

The basic premise of the "design and build" is the idea that the contracts concluded in this system should allow contractors to propose their own innovative solutions, for the benefit of both the Contractor and the Employer, and be implemented faster and cheaper. They are also addressed at those applicants who do not have sufficient knowledge or experience in the implementation of the project. With projects in the formula "Z and W", there is no requirement to provide full documentation to the application for funding from the EU.

Obtaining comprehensive documentation, required permits or applications lies with the Contractor who will be selected by means of the tender procedure. The purchaser describes the subject of the contract using functional – utility object program description (PFU), including a description of the construction task, which is the object of the contract (Art. 31, paragraph. 2 and 3 of the Public Procurement Law). In the functional – utility program should be given destiny of completed construction works and the requirements imposed on them (technical, economic, architectural, material and functional). In the "design and build", often identified with the yellow FIDIC, the investor should no longer interfere in the project. The project manager should have the freedom to design, limited only to the records included in the PFU.

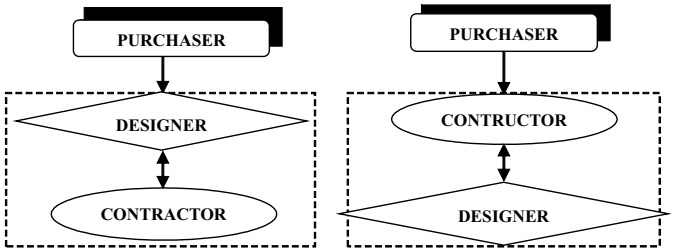

Fig. 1. Model selection of a public contract in the formula of "design and build": a) business model of Western countries, eg. German, Austrian, American, b) the prevailing model of operations in Poland, resulting from the Public Procurement Law

3. Public procurement in the years 2010–2016

The number of contracts awarded in the period 2010–2016 are presented in Table 1. It can be stated that in the years 2010–2016, there was:

- A decrease of 41.59% in the total number of public contracts awarded,
- A decrease of 47.58% in the number of contracts awarded by public works contracts,
- An increase of 329.76% in the number of all public contracts awarded in the formula Z and W,

- An increase of 368.57% in the number of contracts awarded by public works the formula "Z and W".

Despite the decline in the number of public contracts awarded, the formula of "design and build" is growing in popularity.

This is due to the fact that in the formula Z and W, the Purchaser prepares a description of the object of the contract with the functional program. It eliminates the necessity to describe the object of contract by the drafting of construction and technical execution and acceptance of construction works, which is more time consuming compared to the functional program.

The percentage participation of the "design and build" formula is shown in Fig. 2. A smaller share of formula "Z and W" in all contracts awarded in 2010–2016 shows that these orders include construction, services and supplies. The formula "Z and W" in the reporting period was mainly used in the award of a contract works, which required the development of a building design project and construction.

Table 1. The number of contracts awarded in the period 2010–2016

Year / Procurement numbers	2010	2011	2012	2013	2014	2015	2016
The total number of granted procurement	186902	177886	179250	181061	152606	118042	77734
Number of construction works contracts in procurement	57364	49442	48957	47764	46536	37316	27295
Number of contracts procurement in the formula „Z and W"	84	158	222	272	359	325	277
Number of construction works contracts in procurement works in the formula „Z and W"	70	132	186	241	325	307	258

Source: Own calculations based on Public Procurement Bulletin

The value of contracts awarded in the period 2010–2016 are presented in Table 2. After analyzing the number of contracts awarded and their values, we find:

- The average value of a contract awarded in total amounted to:
  - in 2010–0,894 mln zł,
  - in 2011–0,810 mln zł,
  - in 2012–0,740 mln zł,
  - in 2013–0,791 mln zł,
  - in 2014–0,906 mln zł,
  - in 2015–0,985 mln zł,

- the average value of a contract awarded for construction works was:
  - in 2010–1,252 mln zł,
  - in 2011–1,136 mln zł,
  - in 2012–1,220 mln zł,
  - in 2013–1,139 mln zł,
  - in 2014–1,145 mln zł,
  - in 2015–1,029 mln zł.

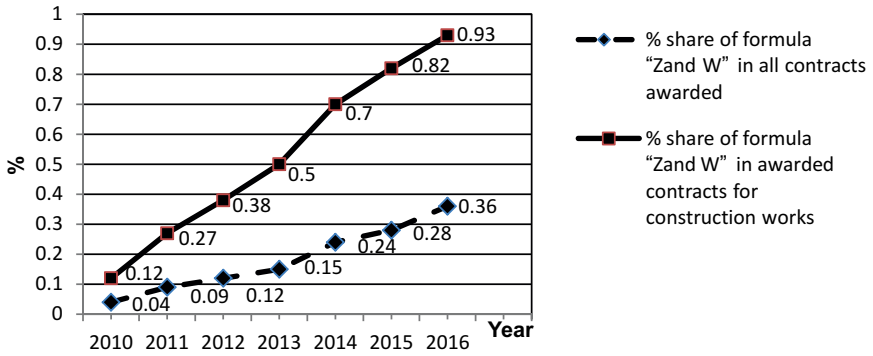

Fig. 2. Percentage participation of formula "Z and W" in the contracts awarded in the period 2010–2016

The above collation clearly shows that the construction works had an average value of one contract awarded greater than the average value of a contract awarded in total

Table 2. The value of contracts awarded in the period 2010–2016

Year / The value Of contracts	2010	2011	2012	2013	2014	2015	2016*
total orders (mld zł)	167.0	144.1	132.7	143.2	133.2	116.31	–
Orders for construction works (mld zł)	71.81	56.19	59.71	54.41	53.28	38.38	–

Source: Own calculations based on Reports Procurement Office.
* Purchaser is obliged to 1 March 2017 to submit a report.

In the analyzed period, orders were granted in different modes, as shown in Table 3. Considering the modes of public procurement is the most common procurement in general and open tender as well as the free-hand orders mode were used for construction. Award of contract in free-hand order mode usually referred to the additional and replacement works. Despite the limited tender being one of the basic procedures of public procurement in the years 2010–2016, it was used occasionally. This is possibly due to the longer term of proceedings. In the analyzed period, the procedure for awarding the concession for the service was not used because of the specifics of the contract award procedure.

Table 3. Public procurement divided in mode of granting them in the years 2010–2016

Year / Number of orders according to mode	2010	2011	2012	2013	2014	2015	2016
The total number of granted procurement including:	186 902	177 886	179 250	181 061	152 606	118 042	77 734
► Unlimited tender	142 496	144 849	149 749	1521 69	129 908	100 804	68 294
► Restricted tender,	762	564	642	609	574	393	403
► Negotiations with the announcement,	195	144	81	67	59	25	23
► Negotiated procedure without publication,	498	247	146	134	98	59	39
► Competitive dialogue	41	50	28	19	19	10	8
► Free-hand mode	35 872	26 401	23 817	23 654	18 970	14 568	7708
► Question about price,	6682	5368	4466	3988	2622	1848	1096
► Electronic bidding,	356	263	231	421	356	335	163
► Service concession.	0	0	0	0	0	0	0
Number of construction works contracts in procurement including:	57 364	49 442	48 957	47 764	46 536	37 316	27 295
► Unlimited tender	48 244	41 708	41 872	40 851	39 993	31 654	24 513
► Limited tender	470	263	273	307	249	202	221
► Negotiations with the announcement,	21	21	12	12	11	1	2
► Negotiated procedure without publication,	234	98	50	51	39	26	9
► Competitive dialogue	6	5	3	6	7	4	4
► Source procurement,	8269	7268	6643	6414	6081	5336	2473
► question about price,	14	10	9	6	12	3	5
► Electronic bidding,	106	69	95	117	114	90	68
► Service concession	0	0	0	0	0	0	0

Source: Own calculations based on Public Procurement Bulletin.

The percentage participation of modes in awarded public contracts in construction works in the formula of "design and build" is shown in Fig. 3. The growth in formula "design and build" in the contract award for construction works in 2016 was over 3-times compared to 2010. In

2010–2016 in the award of public contracts in construction works in the formula "Z and W" share of open tendering was over 90.00% and had a downward trend. The decrease share of unlimited mode in 2016 amounted to 4.02 percentage points. There was an increase in 2016 of the share of electronic bidding mode by 92.55 percentage points compared to 2012.

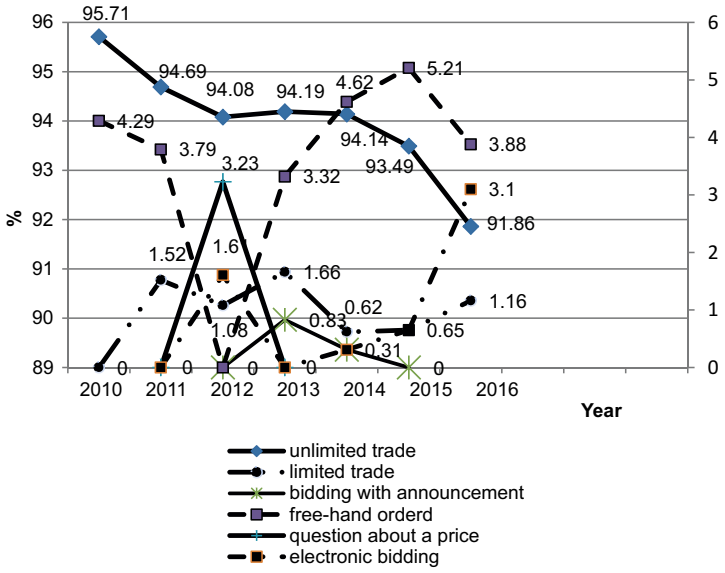

Fig. 3. Percentage participation of modes of procurement contracts in awarded public works for construction works in the formula of "design and build"

It is worth noticing that in the years 2010–2016 in the contracts awarded, public works for construction works have not been used in the contract mode: negotiations without announcement, competitive dialogue, service concession.

4. Tenders in the years 2010–2016 in two selected provinces

For comparative testing, two provinces with a similar economy were chosen. The number of contracts awarded in the Kujawsko-Pomorskie and Warmia and Mazury for the years 2010–2016 are presented in Table 4.

The data (Tab. 4) shows that in the analyzed period, more contracts and construction works contracts were awarded in the Kujawsko-Pomorskie than in the Warmia-Mazury. Despite fewer contracts awarded in the Warmia-Mazury, formula "design and build" was used more often. 23.26% more public works contracts were awarded in this formula than in the Kujawsko-Pomorskie This was caused by a greater number of factors of procurement: renovation, modernization of facilities, road infrastructure, municipal infrastructure, what is shown in Table 5.

Table 4. Public procurement in the years 2010 – 2016 in Kujawsko-Pomorskie and Warmia–Mazury*

Year / Number of orders	2010	2011	2012	2013	2014	2015	2016
Contracts awarded in the province. Kuj-pom.	8503	8633	8239	8238	7214	5721	3737
Construction works contracts awarded in the province. Kuj-pom.	2559	2369	2246	2348	2221	1876	1361
Contracts awarded in the formula „Z and W" in the province. Kuj-pom.	3	4	7	7	13	11	6
Construction works contracts awarded in the formula „Z and W" in the province. Kuj-pom.	3	4	7	6	10	9	6
Contracts awarded in the province. war.-maz	7534	7188	7320	7338	6571	4815	3081
Construction works contracts awarded in the province. war.-maz.	2398	2063	1916	1876	2002	1530	1054
Contracts awarded the formula „Z and W" in the province. war.-maz.	9	13	9	7	12	8	7
Construction works contracts awarded in the formula „Z and W" in the province. war.-maz.	4	10	7	5	12	8	7

Source: Own calculations based on Public Procurement Bulletin.
*) Not included contracts that were published in the journal of the EU.

Table 5. The number of public contracts awarded in the formula "Z and W" according to the construction of the structure of investment projects in the Kujawsko-Pomorskie and Warmia-Mazury in the years 2010–2016

Ord.	Type of works	Total public procurement in the province. Kujawsko-Pomorskie	Total public procurement in the province. Warmia-Mazury
1	Renovation, modernization, revitalization, alteration, adaptation, thermo-modernization of buildings	12	18
2	Construction of new facilities	6	3
3	Road infrastructure (including construction and reconstruction of roads, culverts, bridges, sidewalks, street lighting, investment areas)	5	11

4	Municipal infrastructure including environment (including sewage treatment plants, water and sewage networks., Landfill)	2	4
5	Municipal infrastructure including sport and tourism (including playgrounds, sports fields, marinas, bike paths)	10	6
6	Technical infrastructure (eg cranes, solar collectors, pumps, fiber optic networks, masts)	8	11
	Total	43	53

Source: Own study based on the Public Procurement Bulletin.

5. Summary

The analysis of public contracts awarded in Poland in the years 2010–2016 helped to formulate conclusions regarding tenders. In the years 2010–2016, a total of 1073481 public contracts were awarded, including 314.674 construction works contracts, which accounted for 29.31% of the total contracts awarded. The share of construction works in the total number of contracts awarded to the public tends to increase, as shown in Fig. 4.

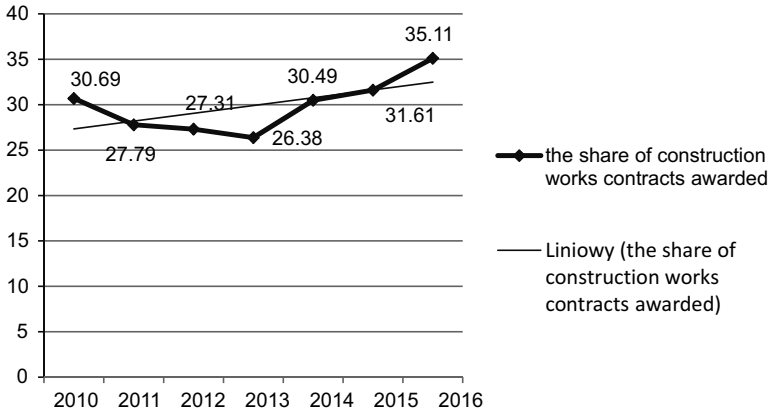

Fig. 4. Percentage of construction works in all contracts awarded in 2010–2016

The participation of formula "design and build" in the contracts awarded for construction works in the analyzed period tends to increase. In 2016, the share of formula "Z and W" increased more than seven times compared to the year 2010. It shows an increase in the amount purchasers willing to use this formula to award a public construction works contract.

The most common mode in the award of public construction works contracts was tender (more than 90.00% of the construction works contracts) and the free order.

References

[1] Kowalczyk E., *Modele udzielania zamówień o wartości poniżej 30 000 euro*, 2014, http://www.komunikaty.pl/komunikaty/ 1,79968,16271596,Modele_udzielania_zamowien_o_wartosci_ponizej_30_000.html (access: 20.12.2016).

[2] Leśniak A., Zima K., *Realizacja przedsięwzięć budowlanych w systemie zaprojektuj i wybuduj*, Przegląd budowlany No. 7–8, 2012, 67–70.

[3] Rozporządzenie w sprawie kwot wartości zamówień oraz konkursów, od których jest uzależniony obowiązek przekazywania ogłoszeń Urzędowi Publikacji Unii Europejskiej (Dz. U. z dnia 23 grudnia 2013 r. poz. 1735 oraz Dz. U. z dnia 28 grudnia 2015 r. poz. 2263, Dz. U. z dnia 22 sierpnia 2016 r., poz. 1386).

[4] Rozporządzeniem w sprawie zakresu informacji zawartych w rocznym sprawozdaniu o udzielonych zamówieniach, jego wzoru oraz sposobu przekazywania (Dz. U. z dn. 12 grudnia 2013 r., poz. 1530, Dz.U. z dn. 15 grudnia 2016 r., poz. 2038).

[5] Rozporządzenie Ministra Infrastruktury w sprawie szczegółowego zakresu i formy dokumentacji projektowej, specyfikacji technicznych wykonania i odbioru robót budowlanych oraz programu funkcjonalno-użytkowego (tj. Dz.U. z dn. 2013, poz. 1129).

[6] Tomaszewska-Pestka M., *„Zaprojektuj i zbuduj", czyli jak ominąć rafy w procesie Inwestycyjnym*, https://www.ergohestia.pl/korporacje/edukacja/odpowiedzialnosc-cywilna/%E2%80%9Ezaprojektuj-i-zbuduj%E2%80%9D--czyli-jak-ominac-rafy-w-procesie-inwestycyjnym.html&print=1 (access: 22.04.2016).

[7] Ustawa z dnia 29 stycznia 2004 r. – Prawo zamówień publicznych (tj. z 2010 r. nr 133, poz. 759, z 2013 r., poz. 907, z 2015 r., poz. 2164 z póź. zm.).

[8] Urząd Zamówień Publicznych, *Biuletyn Zamówień Publicznych*, www.uzp.gov.pl (access: 10.10.2016–12.01.2017).

[9] Urząd Zamówień Publicznych, *Sprawozdania Urzędu Zamówień Publicznych za lata 2010–2016* (access: 10.10.2016–12.01.2017).

[10] *What is Design-Build*?, [in:] „DBIA. Design-Build. Institute of America", http://www.dbia.org/about/Pages/What-is-Design-Build.aspx (access: 12.10.2017).

[10] Zdebel-Zygmunt A., Rokicki J., *System zamówień publicznych w Polsce*, Warszawa, Difin, 2014.

TECHNICAL TRANSACTIONS 6/2017
CZASOPISMO TECHNICZNE 6/2017
CIVIL ENGINEERING
DOI: 10.4467/2353737XCT.17.092.6568

Henryk Laskowski (henryk.laskowski@pk.edu.pl)
Institute of Structural Mechanics, Faculty of Civil Engineering, Cracow University of Technology

Optimal design of structural elements as a control theory problem

Optymalne kształtowanie elementów konstrukcyjnych jako problem optymalnego sterowania

Abstract

In the paper an application of the maximum principle to designing a cross section of a still frame under several loading schemes is presented. The optimal height of the web under minimum volume of still as a cost function is determined. In particular the implicit and explicit conditions of state variables at characteristic points of axis of symmetry under different loading schemes are presented.

Keywords: optimal control, maximum principle

Streszczenie

W artykule przedstawiono zastosowanie zasady maksimum w wymiarowaniu przekroju poprzecznego stalowej ramy poddanej wielu stanom obciążenia, polegającego na wyznaczeniu optymalnej, ze względu na minimum objętości stali, wysokości środnika. Szczegółowo przedstawiono jawne i uwikłane warunki zmiennych stanu w punktach charakterystycznych oraz w osi symetrii, a także sformułowania prowadzące do uwzględnienia kombinacji obciążeń.

Słowa kluczowe: sterowanie optymalne, zasada maksimum

1. Introduction

Optimisation of complex structural systems, which until recently remained in the domain of basic research, has now become a practical fact owing to the development of numerical methods on the one hand and computer software on the other. Optimal control theory has become an extremely valuable theory that can be used effectively as a tool for solving important problems of various scientific disciplines, including structural engineering. Some of the results obtained are presented in this paper.

Optimal control theory has been applied to the field of optimal design of structures with the use of the maximum principle. The principle is related to the onerous character (which until recently had been an unsurmountable obstacle) of the so-called multi-point boundary value problem formulated with reference to sets of ordinary differential equations. The specific nature of tasks faced by structural engineering manifests itself in the need to formulate not only the initial-boundary conditions, but also to take into account the internal point conditions.

At present, owing to effective numerical algorithms, complemented by the authors' own suggestions, particularly those referring to non-analytical objective functions and restricting the number of characteristic intervals as well as taking account of the secondary conditions of the *maximum* type listed in the Dircol-2.1 computer software, it is possible to undertake new and unconventional tasks related to optimisation – significant both from the perspective of the expansion of knowledge and the possible applications.

2. The subject of optimisation

The article presents the formulation of the problem of finding the optimal design of a steel I-frame subjected to various loads and the subsequent solution to this problem. The frame to be optimised is a load-bearing element of a hall. The static diagram of the frame (Fig. 1) results from the structure of the building and the manner of support.

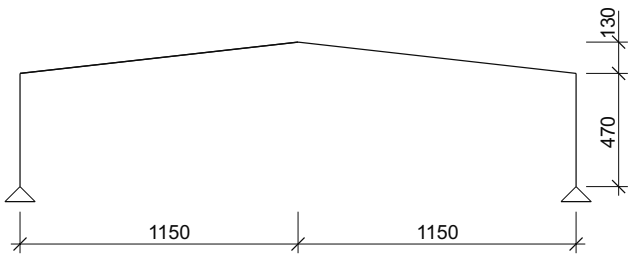

Fig. 1. The static diagram of the frame

The optimisation process will determine the course of variability of web height, whereas the dimensions of the remaining parts of the I-frame will remain constant (Fig. 2).

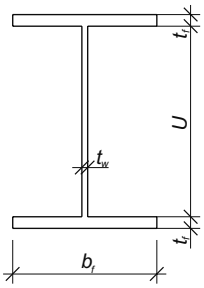

b_f = 200 mm

t_f = 16 mm

t_w = 10 mm

U – the web height (decision variable)

Fig. 2. Cross-section of the frame

3. Loads

In the process of designing a frame cross-section all the relevant computational situations that may occur during the service of the structure in which it is to be used should be taken into account. The computational situation should be understood as a specific combination of individual load systems – hereinafter called elementary loads. The number of elementary loads determines the number of state equations describing the structure and affects considerably the scope of the optimisation task. In the problem under consideration here the following elementary loads have been taken into account:

Load 1. frame dead load (maximum),
Load 2. roofing dead load (maximum),
Load 3. frame dead load (minimum),
Load 4. roofing dead load (minimum),
Load 5. snow load,
Load 6. wind load – wind from the left,
Load 7. wind load – wind from the right.

Symbols of the above elementary loads in the normal (perpendicular) and tangential direction to the frame axis have been listed in Table 1.

The static and kinematic values describing the structure are linearly dependant on the loads, which is why the corresponding values in the considered combinations may be aggregated. Unlike the number of elementary loads, the number of combinations does not affect significantly the scope of the optimisation task. This problem will be discussed further on in the paper. Twelve loads combinations have been considered, which are presented in Table 2.

Table 1. Elementary loads in the characteristic interspaces

Load		Left pillar	Left lintel	Right lintel	Right pillar
1		2	3	4	5
Load 1	q_{1t}	0	$\gamma_{\max} A \gamma_s \cos\alpha$	$\gamma_{\max} A \gamma_s \cos\alpha$	0
	q_{1n}	$-\gamma_{\max} A \gamma_s$	$-\gamma_{\max} A \gamma_s \sin\alpha$	$\gamma_{\max} A \gamma_s \cos\alpha$	$\gamma_{\max} A \gamma_s$
Load 2	q_{2t}	0	$q_{p.\max} \cos\alpha$	$q_{p.\max} \cos\alpha$	0
	q_{2n}	$-q_{p.\max}$	$-q_{p.\max} \sin\alpha$	$q_{p.\max} \sin\alpha$	$q_{p.\max}$

1		2	3	4	5
Load 3	q_{3t}	0	$\gamma_{\min} A \gamma_s \cos\alpha$	$\gamma_{\min} A \gamma_s \cos\alpha$	0
	q_{3n}	$-\gamma_{\min} A \gamma_s$	$-\gamma_{\min} A \gamma_s \sin\alpha$	$\gamma_{\min} A \gamma_s \cos\alpha$	$\gamma_{\min} A \gamma_s$
Load 4	q_{4t}	0	$q_{p.\min} \cos\alpha$	$q_{p.\min} \cos\alpha$	0
	q_{4n}	$-q_{p.\min}$	$-q_{p.\min} \sin\alpha$	$q_{p.\min} \sin\alpha$	$q_{p.\min}$
Load 5	q_{5t}	0	$q_s \cos^2\alpha$	$q_s \cos^2\alpha$	0
	q_{5n}	0	$-q_s \cos\alpha \sin\alpha$	$q_s \cos\alpha \sin\alpha$	0
Load 6	q_{6t}	$q_{w.sn}$	$-q_{w.pn}$	$-q_{w.pz}$	$-q_{w.sz}$
	q_{6n}	0	0	0	0
Load 7	q_{7t}	$-q_{w.sz}$	$-q_{w.pz}$	$-q_{w.pn}$	$q_{w.sn}$
	q_{7n}	0	0	0	0

q_{it} – load in the normal (perpendicular) direction towards the axis.
q_{in} – load in the tangential direction towards the axis.

Table 2. List of loads combinations

	C_1	C_2	C_3	C_4	C_5	C_6	C_7	C_8	C_9	C_{10}	C_{11}	C_{12}
Load 1	+	+	+	+	+	+						
Load 2	+	+	+	+	+	+						
Load 3							+	+	+	+	+	+
Load 4							+	+	+	+	+	+
Load 5		+	+	+				+	+	+		
Load 6			+		+				+		+	
Load 7				+		+				+		+

4. Formulation of the optimisation task

The essence of the optimisation task presented in this article is finding the optimal design of the frame cross-section with the variable web height. The task comprises determination of the course of variability of web height so that the serviceability and the load bearing capacity limits are not exceeded. There are an infinite number of solutions fulfilling this requirement, yet of all the possible designs only the one which is characterised by the lowest objective function value may be considered optimal. The objective function in this task is the volume of steel needed for the frame, which in the optimal solution should be possibly the smallest.

The maximum principle allows formulation of the problem which makes it possible to obtain the only solution meeting the necessary conditions of the optimisation. The selection

of the solution of all the obtained ones which is the best from the perspective of the adopted objective function does not guarantee that it is optimal because the set of obtained solutions may not include the optimal solution at all. The tasks of optimal cross-section design in structural engineering are characterised by so many constraints resulting from technical, design and standard requirements that the set of the solutions meeting the optimisation necessary conditions is not large and often contains only one solution with the lowest objective function value, i.e. optimal.

The frame to be optimised is symmetrical both in the aspect of its geometry and the loads to which it is subjected. However, experience shows – and the problem in question here is no exception – that the solutions obtained may be symmetrical or not. In this task the non-symmetrical solution proved to be "better" in terms of the objective function value than the symmetrical one. However, due to the fact that that the presented problem is of practical character and that the non-symmetrical solution is not very likely to be accepted by an investor, it has been decided that the formulation of the problem should include the condition for the solution to be symmetrical. In fact, the condition boils down to the adoption of the half-frame model with state variables in the axis of symmetry corresponding to the subsequent loads.

The formal structure of optimisation problems with the application of the maximum principle has been discussed in the cited publications on the subject. This article will only present the detailed formulations related to the problem under consideration, in compliance with the formalism of the minimum principle, which encompasses: equations of state, conjugate equations, objective function, Hamilton's function and functions of constraint.

5. Equations of state

As discussed above, it has been decided to adopt the half-frame model (Fig. 3). The independent variable x is measured from the bottom of the left pillar up to joint 2 and next horizontally to the axis of symmetry. The equations of state are formulated in two characteristic interspaces (Table 3), taking into account the state variables at the support, joint 2 and at the roof ridge (Tables 4 and 5).

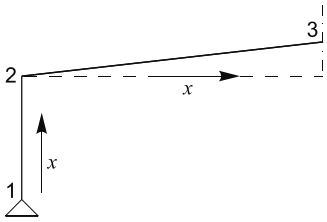

Fig. 3. The half-frame model

In the case of symmetrical loads, the conditions for static and kinematic values at the ridge (point 3) are formulated similarly to a vertically sliding fixed joint. If the elementary load is not symmetrical, as is the case of loads 6 and 7, a corresponding load of the "mirror

reflection" type is introduced. The left half of the frame bearing load 6 is a mirror reflection of the right half of the frame bearing load 7 and *vice versa*. The corresponding conditions for state variables at a point in the frame's axis of symmetry result from the above.

Table 3. Equations of state in the characteristic interspaces

State variables		Equations of state	
		Pillar	Lintel
Load i, $(i = 1 - 7)$	v_i	$v_i' = \varphi_i$	$v_i' = \varphi_i / \cos\alpha$
	φ_i	$\varphi_i' = M_i / EI$	$\varphi_i' = M_i / (EI \cos\alpha)$
	M_i	$M_i' = Q_i$	$M_i' = Q_i / \cos\alpha$
	Q_i	$Q_i' = -q_{it}$	$Q_i' = -q_{it} / \cos\alpha$
	N_i	$N_i' = -q_{in}$	$N_i' = -q_{in} / \cos\alpha$
	w_i	$w_i' = N_i / EA$	$w_i' = N_i / (EA \cos\alpha)$
V		$V' = A$	$V' = A / \cos\alpha$

v – normal displacement
φ – deflection angle
M – bending moment
Q – transverse force
N – longitudinal force
w – tangential displacement
q – load
α – the lintel inclination angle

The frame to be optimised is described by the total of 43 equations of state – 6 for each of the 7 loads plus one equation describing the volume, introduced because of the adopted objective function.

6. Boundary conditions and internal point conditions of the state variables

If the frame retains the same static diagram when subjected to several load conditions, the state variables conditions in each of these loads are the same. Therefore it is only necessary to present the state variables conditions for one symmetrical load and for two "mirror reflection" non-symmetrical loads, and they are presented below. In both cases the state variables conditions may be divided into two groups: explicit conditions and implicit conditions.

The number of the necessary state variables conditions is equal to the number of equations multiplied by the number of characteristic intervals. Thus, for one load condition described with six equations in two characteristic intervals, the number of conditions that should be formulated amounts to 12.

The explicit conditions for the symmetrical loads have been listed in Table 4, whereas the implicit conditions result from Figures 4, 5, 6 and 7.

Table 4. Explicit conditions for state variables at characteristic points for symmetrical loads

	1	2		3
		2^-	2^+	
v_i	0			
φ_i		C		0
M_i	0	C		
Q_i				
N_i				
w_i	0			
Symbols: C – condition of continuity, 0 – predefined value				

The conditions of equilibrium at joint 2:

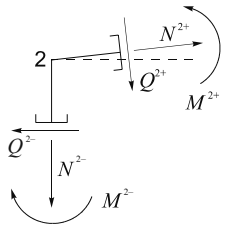

$$\sum X = 0: \qquad -Q^{2-} + Q^{2+}\sin\alpha + N^{2+}\cos\alpha = 0$$

$$\sum Y = 0: \qquad -N^{2-} - Q^{2+}\cos\alpha + N^{2+}\sin\alpha = 0$$

Fig. 4. Sectional forces at joint 2

The conditions of displacements compatibility at joint 2:

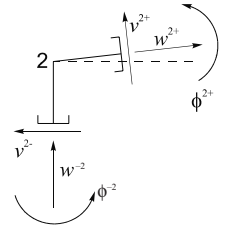

$$\delta_X^{2-} = \delta_X^{2+}: \qquad -v^{2-} = -v^{2+}\sin\alpha + w^{2+}\cos\alpha$$

$$\delta_Y^{2-} = \delta_Y^{2+}: \qquad w^{2-} = v^{2+}\cos\alpha + w^{2+}\sin\alpha$$

Fig. 5. Displacements at joint 2

The condition of forces equilibrium at joint 3:

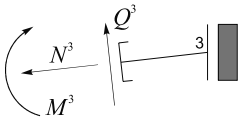

$$\sum Y = 0: \qquad Q^3\cos\alpha - N^3\sin\alpha = 0$$

Fig. 6. Sectional forces at joint 3

The condition of displacements compatibility at joint 3:

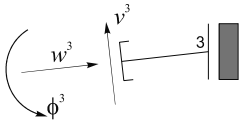

$$\delta_X^3 = 0: \qquad -v^3 \sin\alpha + w^3 \cos\alpha = 0$$

Fig. 7. Displacements at joint 3

The following conditions have been formulated for each symmetrical load:

- 6 explicit conditions (Table 4),
- 2 implicit conditions of forces equilibrium at point 2,
- 2 implicit conditions of displacements compatibility at point 2,
- 1 implicit condition of forces equilibrium at point 3,
- 1 implicit condition of displacements compatibility at point 3.

The total of 12 conditions have been formulated for each symmetrical load.

As regards the non-symmetrical loads (loads 6 and 7), the total number of 24 conditions must be formulated. The explicit conditions have been listed in Table 5. The implicit conditions at joint 2 are in this case the same as the ones related to the symmetrical loads, whereas the conditions at point 3 require discussion in greater detail.

Table 5. Explicit conditions for state variables at characteristic points for non-symmetrical loads 6 and 7

	1	2		3
		2^-	2^+	
v_6	0			
φ_6		C		
M_6	0	C		
Q_6				
N_6				
w_6	0			
v_7	0			
φ_7		C		
M_7	0	C		
Q_7				
N_7				
w_7	0			

The roof ridge joint equilibrium condition is to have the total forces and total moments acting on both sides of the joint neutralise each other to zero.
The following occurs in direction X:

$$S_{6X}^{3-} + S_{6X}^{3+} = 0$$

If we adopt the half-frame model, the component in direction X on the left side of the joint is subject to the following relations:

$$S_{6X}^{3-} = Q_{6X}^{3-} + N_{6X}^{3-} = Q_6^{3-} \sin\alpha + N_6^{3-} \cos\alpha = Q_6^3 \sin\alpha + N_6^3 \cos\alpha \,.$$

The following relations occur between sectional forces operating under load 6 and also under load 7, which is the mirror reflection of load 6 (Fig. 8):

$$S_{6X}^{3+} = Q_{6X}^{3+} + N_{6X}^{3+} = Q_6^{3+} \sin\alpha - N_6^{3+} \cos\alpha = -Q_7^3 \sin\alpha - N_7^3 \cos\alpha$$

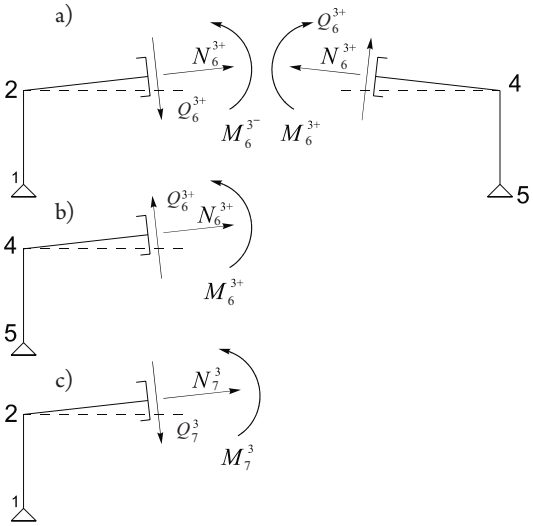

Fig. 8. Sectional forces at the roof ridge: a) in the real diagram for load 6, b) in the mirror reflection of the right part of fig. a), c) in the left part of the frame subjected to load 7, which is a mirror reflection of load 6

Hence, the relation between the transverse and longitudinal forces operating under load 6 and 7 may be written in the following form:

$$S_{6X}^{3-} + S_{6X}^{3+} = 0 \rightarrow Q_6^3 \sin\alpha + N_6^3 \cos\alpha - Q_7^3 \sin\alpha - N_7^3 \cos\alpha = 0 \,.$$

The following relations occur in the vertical direction:

$$S_{6Y}^{3-} + S_{6Y}^{3+} = 0$$
$$S_{6Y}^{3-} = Q_{6Y}^{3-} + N_{6Y}^{3-} = -Q_6^{3-} \cos\alpha + N_6^{3-} \sin\alpha = -Q_6^3 \cos\alpha + N_6^3 \sin\alpha$$
$$S_{6Y}^{3+} = Q_{6Y}^{3+} + N_{6Y}^{3+} = Q_6^{3+} \cos\alpha + N_6^{3+} \sin\alpha = -Q_7^3 \cos\alpha + N_7^3 \sin\alpha$$

Hence, the next joint equilibrium condition under load 6 and 7 takes the following form:

$$S_{6Y}^{3-} + S_{6Y}^{3+} = 0 \rightarrow -Q_6^3 \cos\alpha + N_6^3 \sin\alpha - Q_7^3 \cos\alpha + N_7^3 \sin\alpha = 0$$

From Fig. 8 also stems the condition that the moments must be equal to each other:

$$M_6^3 = M_7^3$$

The next three conditions are formulated for the kinematic values (Fig. 9).

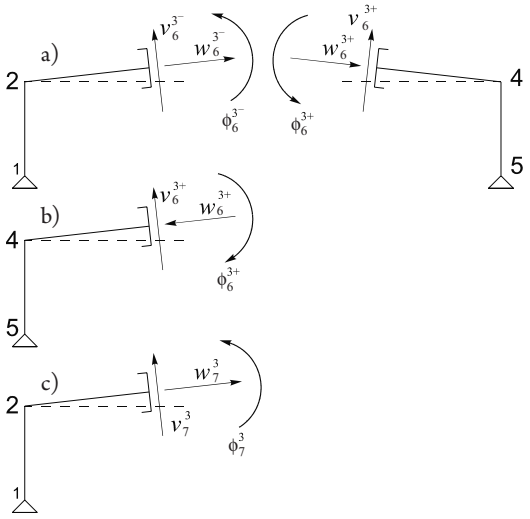

Fig. 9. Kinematic values at the roof ridge: a) in the real diagram for load 6, b) in the mirror reflection of the right part of fig. a), c) in the left part of the frame subjected to load 7, which is a mirror reflection of load 6

The conditions of displacements compatibility hold in this case (Fig. 9).
The following occurs in horizontal direction:

$$u_{6X}^{3-} = u_{6X}^{3+}$$
$$u_{6X}^{3-} = v_{6X}^{3-} + w_{6X}^{3-} = -v_6^{3-}\sin\alpha + w_6^{3-}\cos\alpha = -v_6^3\sin\alpha + w_6^3\cos\alpha$$
$$u_{6X}^{3+} = v_{6X}^{3+} + w_{6X}^{3+} = v_6^{3+}\sin\alpha + w_6^{3+}\cos\alpha = v_7^3\sin\alpha - w_7^3\cos\alpha,$$

which gives rise to the following condition:

$$u_{6X}^{3-} = u_{6X}^{3+} \rightarrow -v_6^3\sin\alpha + w_6^3\cos\alpha = v_7^3\sin\alpha - w_7^3\cos\alpha$$

The following occurs in the vertical direction:

$$u_{6Y}^{3-} = u_{6Y}^{3+}$$
$$u_{6Y}^{3-} = v_{6Y}^{3-} + w_{6Y}^{3-} = v_6^{3-}\cos\alpha + w_6^{3-}\sin\alpha = v_6^3\cos\alpha + w_6^3\sin\alpha$$
$$u_{6Y}^{3+} = v_{6Y}^{3+} + w_{6Y}^{3+} = v_6^{3+}\cos\alpha - w_6^{3+}\sin\alpha = v_7^3\cos\alpha + w_7^3\sin\alpha,$$

which gives rise to the following condition:

$$u_{6Y}^{3-} = u_{6Y}^{3+} \rightarrow v_6^3\cos\alpha + w_6^3\sin\alpha = v_7^3\cos\alpha + w_7^3\sin\alpha$$

As regards the angle of rotation, the following relations occur:

$$\varphi_6^{3-} = \varphi_6^{3+}, \qquad \varphi_6^{3-} = \varphi_6^3, \qquad \varphi_6^{3+} = -\varphi_7^3,$$

hence the condition:

$$\varphi_6^{3-} = \varphi_6^{3+} \rightarrow \varphi_6^3 = -\varphi_7^3$$

As regards loads 6 and 7, the following conditions have been formulated:

- 10 explicit conditions (Table 5),
- 4 implicit conditions of forces equilibrium at point 2,
- 4 implicit conditions of displacements compatibility at point 2,
- 3 implicit conditions of forces equilibrium at point 3,
- 3 implicit conditions of displacements compatibility at point 3.

A total of 24 conditions have been formulated as regards loads 6 and 7.

The suggested formulation of conditions in the axis of symmetry referring to the "mirror reflection" loads, with the prior adoption of the half-frame static diagrams, significantly reduces the scope of the optimal design tasks and extends the range of control theory applications in structural computations.

7. Constraints

At the stage of state variables and decision variables constraints formulation, certain dependencies specified in the technical provisions and related to the load bearing capacity and serviceability limits must be taken into account. Provided that the static diagram has been predefined and the cross-section geometric characteristics remain constant, the values which depend linearly on the load may be aggregated. The said values include static and kinematic state variables. It is therefore possible to introduce – at the stage of formulating the constraints – the combinations of stresses which were identified in the preliminary analysis, e.g. the normal stress in a given combination is the sum of the stresses exerted by the elementary loads which are components of this combination. In the problem under consideration here, the introduced constraints refer solely to normal stresses and deflections. It is a certain simplification of the constraints related to the load bearing capacity and serviceability limits as they are defined in the requirements of the standards, yet it does not obscure the problem of constraints discussed in this paper and enables a clear presentation of how the functions of the *maximum* or *minimum* type could be applied in structural optimisation for the purpose of reducing the number of constraints. It must be emphasised simultaneously that taking into account the constraints functions compliant with the requirements of the standards now in effect does not pose any problem in the optimisation process.

Normal stress in a given combination of loads may be determined on the basis of the following relations:

$$\sigma_{Ki} = \frac{\left|\sum_{j(Ki)} M_{j(Ki)} \cdot z\right|}{I} + \frac{\left|\sum_{j(Ki)} N_{j(Ki)}\right|}{A},$$

where $\sum_{j(Ki)} M_{j(Ki)}$, $\sum_{j(Ki)} N_{j(Ki)}$ are sums in the sets of axial moments and forces exerted by the elementary loads in combination K_i. For example, in combination K_3, $j(K_3) = \{1, 2, 5, 6\}$. In this way an expression has been formulated for the maximum edge stress for each of the twelve combinations. However, all of them should be lower than the highest permissible stress level. The above approach leads, without any special operations, to the formulation of 12 constraint functions, which complicates solving the optimisation problem. Application of the *maximum* function of the form: $\sigma_{\max} = \max\left(\left\{\sigma_{K1}, \ldots \sigma_{K12}\right\}\right)$ makes it possible to reduce the number of the constraints functions to one function g_1 in the form: $\sigma_{\text{perm}} - \sigma_{\max} \geq 0$. This operation, however simple it may seem, is an original achievement in the field of engineering structures optimisation with the use of optimal control theory.

Similarly, in order to accommodate the serviceability limit, another constraint function has been formulated referring to the maximum normal displacement:

$$y_{Ki} = \left| \sum_{j(Ki)} v_{j(Ki)} \right|$$

$$y_{\max} = \max\left(\left\{y_{K1}, \ldots y_{K12}\right\}\right)$$

$$g_2: \qquad y_{\text{perm}} - y_{\max} \geq 0$$

8. Formulation of the optimisation necessary conditions

The maximum principle formalism has been applied with regard to the frame to be optimised, and in particular:

1. The structure to be optimised has been described with the use of equations of state of the following type:

$$y_i' = f_i[\tilde{y}(x), U(x), x] \quad i = 1 \ \ldots \ 43 \qquad \text{(Table 3)}$$

2. State variables constraints have been formulated:

$$g_j(\tilde{y}(x), U(x)) \geq 0 \quad j = 1, 2$$

3. Hamilton's function has been formulated:

$$H = \sum_{i=1}^{43} \lambda_i \cdot f_i[\tilde{y}(x), U(x), x] + \sum_{j=1}^{2} \mu_j \cdot g_j[\tilde{y}(x), U(x)]$$

4. Hamilton's function has been used as the basis for writing the set of differential equations with conjugate variables:

$$\lambda_i' = -\frac{\partial H}{\partial y_i} \quad i = 1 \ldots 43$$

If the formal requirements specified in points 1–4 have been fulfilled, the maximum principle enables formulation of the optimisation necessary condition, namely: of all the possible solutions, which are the decision variables functions and their corresponding state variables and conjugate variables functions, the optimal solution is the maximum of Hamilton's function. The necessary condition of the optimisation, expressed in words above, may be written in the following form:

$$H[\tilde{\lambda}_{opt}(x), \tilde{\mu}_{opt}(x), \tilde{y}_{opt}(x), U_{opt}(x)] = \max_{U} H[\tilde{\lambda}(x), \tilde{\mu}(x), \tilde{y}(x), U(x)],$$

from which stems the following equation: $\frac{\partial H}{\partial U} = 0.$ allowing determination of decision variable U, provided that no constraints are active. Otherwise, the decision variable is determined from the active constraint.

9. Numerical solution

Application of the maximum principle has allowed formulation of a differential-algebraic set of equations in categories used in control theory, complete with boundary conditions and internal point conditions. The set constitutes the so-called multi-point boundary value problem, which has been solved with the use of the Dircol-2.1. computer software. Of all the values occurring in the formalism of the maximum principle, determination of the decision variable is particularly important from the point of view of the constructor, which is in this case the height of the I-frame web as well as the 43 state variables y_i, in which the frame remains within the limits of the load bearing capacity and serviceability. It has appeared that of all the possible options only the constraint resulting from the serviceability limit is active at a point (Fig. 10). Hence, it follows that, apart from the intervals in which the web height

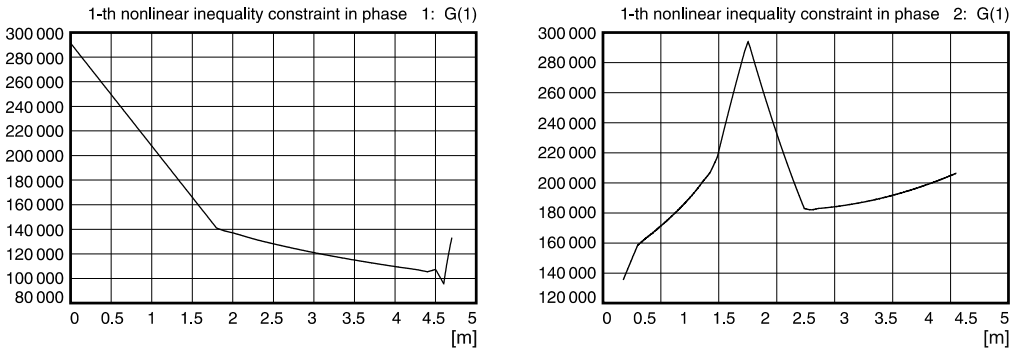

Fig. 10. The course of constraint $g1$ in characteristic interspaces [kPa]

reaches extreme values, the solution has been derived from equation $\frac{\partial H}{\partial U}=0$. The diagrams presenting constraints g_1 and g_2 (Fig. 10 and 11) are to be found below, and so are: the optimal course of the decision variable (Fig. 12), the Hamilton function (Fig. 13) and the course of state variables in the optimal solution for load 1 (Fig. 14).

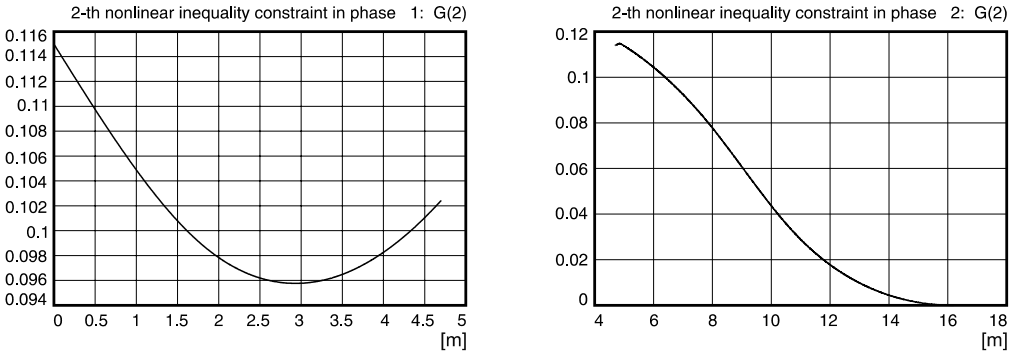

Fig. 11. The course of constraint *g*2 in characteristic interspaces [m]

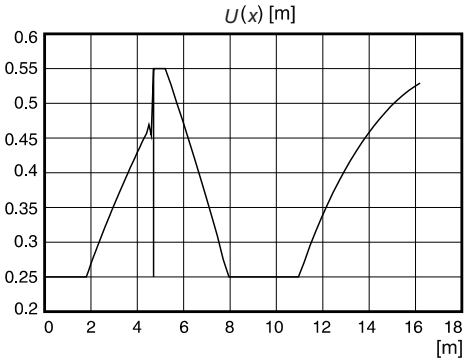

Fig. 12. Optimal course of the decision variable

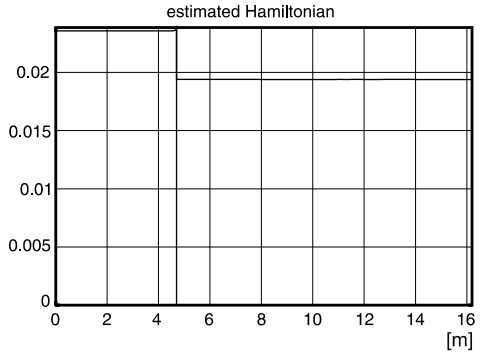

Fig. 13. The Hamilton function

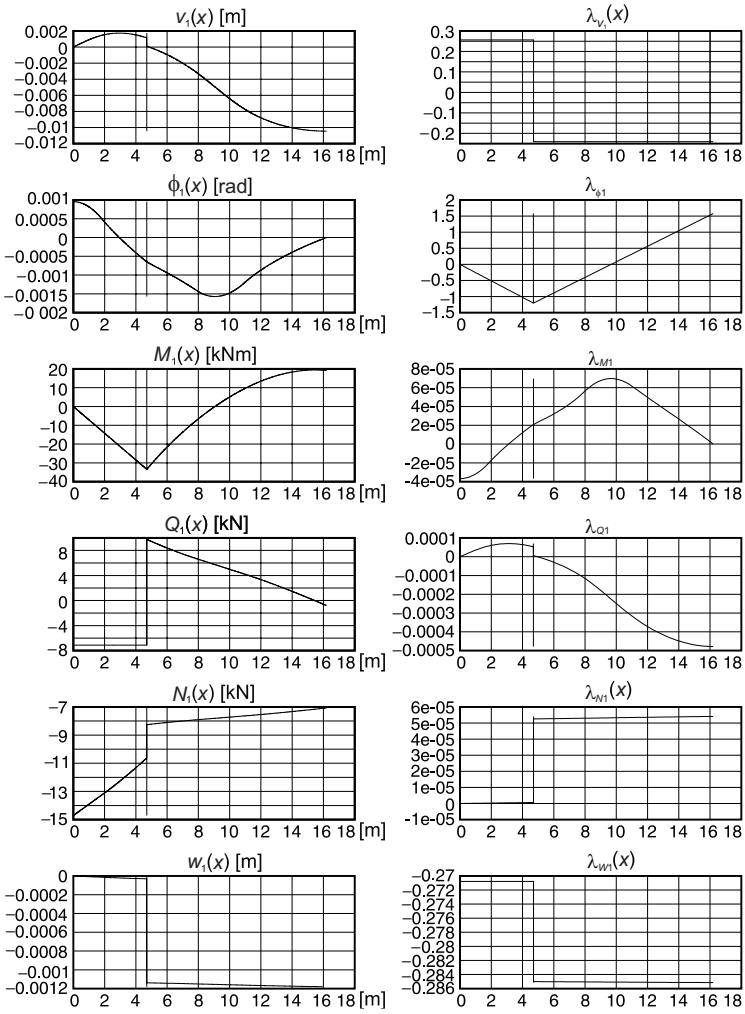

Fig. 14. State variables and conjugate variables in the situation of subjecting the frame to the first elementary load

Additionally, all the remaining values occurring in the formulated multi-point boundary value problem have also been determined.

10. Conclusions

Within the framework of the research on application of theory of optimal control based on the maximum principle in the practical design of engineering structures, a number of problems have been solved, making it possible to tackle several important design problems in the process of structure optimisation.

One of such problems is the modelling – in terms of control theory – of structures which are symmetrical in the aspects of their geometry and systems of loads yielding acceptable

in practice, symmetrical distributions of decision variables. A particular emphasis has been placed in the paper on the problem of formulating the conditions for state variables at characteristic points, including at the structure's axis of symmetry. Modelling the structure with the use of the half-frame model reduces the number of characteristic interspaces by half, which considerably facilitates, or even in certain cases enables, solving the optimisation problem, which would be difficult or impossible to solve if the real model were to be used.

Another important problem solved with the use of optimal control theory in structure optimisation is the introduction of the combination of loads into the mathematic model, which has been presented in this paper. The proposed approach, consisting in the application of the *maximum/minimum* functions, enables taking account in the mathematic model of any number of load combinations, without expanding the scope of the optimisation task.

The paper presents only those computational results which may be of interest for a constructor. Due to the character of the journal, numerous details related to very specialist problems from the field of control theory have been disregarded. For the same reason not all the results obtained in the solution of the multi-point boundary value problem formulated in the task have been presented.

References

[1] Laskowski H., Mikulski L., *Optymalne kształtowanie konstrukcji w kategoriach teorii sterowania na przykładzie belki zespolonej*, Inżynieria i Budownictwo 8/2005, 448–453.

[2] Laskowski H., *Optymalne kształtowanie stalowo-betonowych dźwigarów zespolonych w kategoriach teorii sterowania*, praca doktorska, WIL PK, 1–115, 2006, http://bc.biblos.pk.edu.pl

[3] Laskowski H., Mikulski L., *Optymalne kształtowanie stalowej ramy portalowej*, Inżynieria i Budownictwo 12/2005, 681–684.

[4] Mikulski L., Laskowski H., *Control Theory in Composite Structure Optimizing*, Pomiary, Automatyka, Kontrola 6/2009, 346–351.

[5] Mikulski L., *Optymalne kształtowanie sprężystych układów prętowych*, Monografia No. 259, Politechnika Krakowska, Kraków 1999.

[6] Mikulski L., *Teoria sterowania w problemach optymalizacji konstrukcji i systemów*, Wydawnictwo Politechniki Krakowskiej, Kraków 2007.

[7] Pesch H.J., *A practical guide to the solution of real-life optimal control problems*, Contr. Cybern., Vol. 23, No. 1–2, 1994, 7–60.

[8] von Stryk O., *User's Guide DIRCOL A Direct Collocation Method For The Numerical Solution of Optimal Control Problems*, Technische Universität Darmstadt, Fachgebiet Simulation und Systemoptimierung (SIM), Version 2.1 April 2002.

TECHNICAL TRANSACTIONS 6/2017
CZASOPISMO TECHNICZNE 6/2017
CIVIL ENGINEERING
DOI: 10.4467/2353737XCT.17.093.6569

Agnieszka Leśniak (alesniak@izwbit.pk.edu.pl)
Grzegorz Piskorz
Faculty of Civil Engineering, Cracow University of Technology

Potential reasons for works delays resulting from the provisions of the agreement

Potencjalne przyczyny opóźnień robót budowlanych wynikające z postanowień umowy

Abstract

The course of the construction process in time is shaped by a variety of factors, which, in effect, may become the reason for delays in project completion. The paper presents the outcome of research performed with Polish building works contractors. One of the aims was to try to identify the potential reasons for delays in construction works, which result from the provisions of the agreement. Early recognition and an assessment of possible risks may assist the contractor's attempts to eliminate them or to lessen the scale of delays in the project implementation.

Keywords: delays, construction works, factor identification

Streszczenie

Przebieg procesu budowlanego w czasie kształtowany jest przez wiele czynników, które w efekcie mogą stać się przyczyną nieterminowego ukończenia przedsięwzięcia. W artykule zaprezentowano wyniki badań przeprowadzonych wśród polskich wykonawców budowlanych. Jednym z zamierzeń była próba identyfikacji potencjalnych przyczyn opóźnień robót budowlanych wynikających z postanowień umowy. Wczesne rozpoznanie i ocena możliwych zagrożeń może wspomóc działania wykonawcy w celu ich eliminacji lub zmniejszenia skali opóźnień w realizacji przedsięwzięcia.

Słowa kluczowe: opóźnienia, roboty budowlane, identyfikacja czynników

1. Introduction

Despite the advanced modern technology and many tools facilitating the management of the construction process, delay of the construction implementation remains common. Early identification and the subsequent limitation or even elimination or the potential reasons for such delays may contribute to the efficient and punctual project completion.

The study in [15] revealed that the prolongation of the project completion in Poland is typically caused by the extended duration of the procedures preparing a given project for implementation.

Exceeding the time limit of works implementation specified in the agreement is a common problem in the construction industry and is significant for both the investor and the contractor. The provisions of the agreement between the investor and the contractor decide which party is going to be responsible for delays. On these grounds, the way the risks related to the implementation of construction works are distributed between the parties is established.

The paper presents the results of research dealing with building contractors designed to identify and assess the significance of factors that may generate delays in construction works. The authors proposed a classification of factors, which they predicted to be likely to be identified as early as at the stage of procedures preceding signing of the contract and which result from the provisions of the agreement.

2. Research into the reasons for construction works delay in Poland and abroad

The analysis of Polish literature reveals that a lot of the research conducted so far concerned the identification of factors that generated delays in the completion of construction works. Paper [11] presents an overview of attempts to group the factors that have been identified in the foreign literature. Publication [12] depicts groups of factors and presents the results of a preliminary survey into the delay in construction works in the opinion of various participants of the investment process. The authors of [7] focused solely on the investors' opinions. According to this group of participants, the most important reasons for the delay in construction works are the following: mistakes in project documentation, low quality of the work force and adverse weather conditions. Publications [2, 8] and [10] involve attempts made by various researchers to identify the factors influencing works delays in the opinion of contractors. Works [10] and [2] prove that, according to contractors, the most significant factors that generate delays include mistakes in project documentation, the investor's slow decision-making process and a low quality of management and supervision of the construction site. However, according to another research published in [2], the most vital factors include a large number of mistakes in project documentation, poor cooperation between the investor (the orderer) and the contractor and adverse weather conditions. Paper [8] analysed the results of research into the time risk factors presented in foreign literature, which were then compared with the results of surveys conducted among contractors in Poland. Some of the

publications also present the possibilities of applying various methods to analyse delay-causing factors: using the Dematel method [5], factor analysis [7], or the introduction of flexible strategies [14].

These works represent the increase of the interest in the problem of delays in construction works in Poland and the reasons for their occurrence. The majority concerns the identification and classification of delay-causing factors. Yet it is the possibility to predict delays that remains a vital issue for contractors and investors [1]. In publications [16, 17], the author attempted to develop a method that could predict adverse events, which could occur during the implementation of a project, either indirectly (through time delays in activities performed) or directly on the cost of the investment and the execution time.

A detailed foreign literature review is presented in [7]. It reveals that, so far, more than 100 factors influencing delays have been identified abroad, and researchers classified them in a variety of ways. One of the first studies was conducted as early as in the 70s in the USA [4]. One group of seventeen factors was established, including such elements as: weather conditions, work force availability and subcontractors' contribution. The most detailed division of factors was proposed in [13], in which ten categories were presented. Other interesting instances of categorization of factors can be found in [6] and [9].

Both the Polish and foreign publications concerning construction works delays prove that the problem is common [7]. The risk of delays during building works is high, yet the authors of the present article would like to prove that some of the factors could be identified right at the project planning stage.

3. Factors causing delays resulting from the provisions of the agreement

3.1. Methodology

The aim of this research was to show the reasons for delays in construction works according to building contractors, resulting from the provisions of the agreement. The research was performed at the beginning of 2017. Using a modern Internet platform *Profitest.pl* that allows to prepare online surveys, a questionnaire was prepared. The relevant link was sent to 462 building contractors from all over Poland. 97 correctly completed questionnaires were received back, which is 21% of the total number sent out.

The questionnaire consisted of two parts. The first one included 3 questions concerning the professional experience of the participant, the number of people employed in the company and the operating range of the business. The greatest number of the respondents (31%) were engineers with over 20-year experience. More than a half (52%) represented large companies employing over 250 people. The operating range of the respondents' businesses included both the domestic market (44%) and the international market (46%).

The second part of the questionnaire contained 20 factors found in the provisions of the agreement that can cause delays in construction works. They were arbitrarily assigned by the authors of the present paper to 6 groups, namely: 1 – Project Documentation,

2 – Administrative Decisions, 3 – Changes in Law, 4 – Construction Site, 5 – Works Planned in Winter, 6 – Social Conditions.

The respondents assessed the value of each factor by choosing a relevant number on a five-point scale: 1 – unimportant; 2 – of little importance; 3 – of average importance; 4 – important; 5 – very important. Then, for each factor, an average evaluation was calculated.

3.2. The analysis of the results in each group of factors

3.2.1. Group 1 – Project Documentation

For the contractor, project documentation is essential. It decides on the scope of the planned works and becomes the basis for the agreement. It is one of the elements that influence the shape of the tender. This group includes the following factors: 1 – lack of a complete building permit design or a detailed design; 2 – lack of a complete geology report; 3 – lack of a complete stocktaking or identification of underground networks; 4 – lack of a complete description of the order (too general, suggesting many solutions).

In the ranking created on the basis of the average assessment of the importance of the given factors, the highest evaluation was granted to the factor: lack of a complete building permit design or a detailed design (Fig. 1). Still, the difference from the remaining factors is very small. The evaluations of all the factors in this group are about 4; therefore, it can be concluded that all the factors in this group are important.

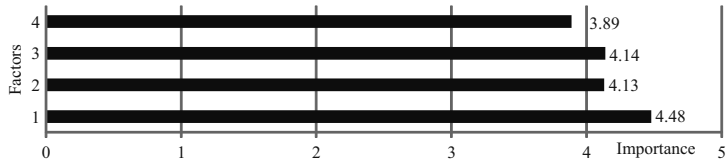

Fig. 1. Reasons for delay in the group: Project Documentation – ranked by importance (Source: own study)

In addition, the respondents proposed other factors, ones that the authors had not included in the questionnaire. These included: mistakes in project documentation, lack of reliable inter branch coordination, inconsistencies in the building permit design, the detailed design and in the technical specification.

3.2.2. Group 2 – Administrative Decisions

Before the investment receives the final building permit or the decision on permission for the implementation of a road project, it is necessary to obtain many agreements and permits, hence the next group proposed is Administrative Decisions with the following factors: 1 – not issuing within the statutory period the appropriate decision of, for example, building permit or permission for the implementation of a road project; 2 – mistakes in permits or in decisions

required for the implementation of the subject of the order; 3 – the expiry of the agreement validity, such as the permit required by Water Law Act; 4 – the risk of delays related to the limitations resulting from the provisions of the administrative decisions which the ordering party did not include in the terms of reference, such as logging and removing habitats.

In the ranking created on the basis of the average assessment of the importance of the given factors, the highest evaluation was granted to the factor: not issuing the appropriate decision within the statutory period. The remaining factors, as the ones described above, received approximately 4 points, which should be unambiguously interpreted that they are all important (Fig. 2).

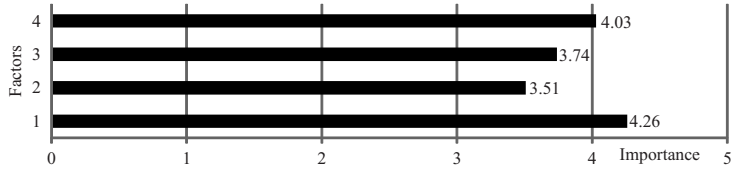

Fig. 2. Reasons for delay in the group: Administrative Decisions – ranked by importance (Source: own study)

Moreover, the respondents in this group also pointed to such additional factors as: other administrative requirements, for example, heritage conservator supervision and archaeological supervision, disregarding other necessary administrative permits by the ordering party, for instance, arrangements with local road authorities about determining the routes of trucks.

3.2.3. Group 3 – Changes in Law

The project must comply with the regulations in force at the time of the ordering party's construction works acceptance. References in the contract to the published standards are regarded as references to the issue of the current contract on the date of the tender submission, unless the contract states otherwise. In the case of the new or revised national standards coming into force after the date of tender submission (that is, during the contract implementation), the ordering party makes a decision about ensuring compliance with such standards. [3]. Therefore, a group Changes in Law has been proposed, including such factors as: 1 – changes in the regulations in the Act on Nature Conservation [22] and Water Law [21], for example, on the basis on the agreement on nature conservation, within the landscape protection area, prohibition of earthworks that permanently deform the terrain may be introduced; 2 – changes in the regulations in the Energy Law [19] specifying, among others, the rules of concluding contracts for connection to the network, or requirements for installations and networks submitted for connection, such as building connection; 3 – changes in the regulations in the Geodetic and Cartographic Law [18], which, among others, regulates the register of geodetic network utilities, especially important at the stages of investment planning; 4 – changes in the regulations in the Geological And Mining Law [23] related to, for instance, performing geological works and preparing geological and engineering

documentation necessary to construct a building object when a geology engineering report is not sufficient; 5 – changes in the regulations in the Environmental Law [20], for example, if nature protection is not possible, but the Law requires that actions must be undertaken to repair the damage, especially by environmental compensation.

The average evaluation of the factors in this group is about 3, which means that the respondents consider the problem related to changes in law as of average importance (Fig. 3). The respondents added the following factors: changes in the project due to the imprecise provisions in the permission for the implementation of a road project and changes in the tax legislation.

Fig. 3. Reasons for delay in the group: Changes in Law – ranked by importance (Source: own study)

3.2.4. Group 4 – Construction Site

A vital stage for the timely start of the project is transferring the building site within the contractually prescribed period. Failure to transfer it for reasons attributable to the ordering party or other, beyond the contractor's control, generates delays. Therefore, a group called the Construction Site was proposed, consisting of the following factors: 1 – having no right to administer the area for construction purposes on the part of the investor; 2 – lack of possibility to begin works due to the presence of places of worship at the construction site, for example, shrines; 3 – lack of access to part of the site due to undocumented environmental conditions or unregulated development areas.

The answers provided by the respondents reveal that having no right to administer the area, whole or a part of it, for construction purposes on the part of the investor is the highest-ranking factor that may cause delays (Fig. 4).

Fig. 4. Reasons for delay in the group: Construction Site – ranked by importance (Source: own study)

3.2.5. Group 5 – Works Planned in Winter

Planning construction works in winter requires taking into consideration adverse weather conditions that could influence the time of completion the subject of the order. This is the only group that consists of only one factor. Here, the respondents did not propose any other factors, yet they did pay attention to the reasons for such works planning by the ordering party. This factor received an average evaluation of 3.89, which means that it is important as a potential reason for delays.

3.2.6. Group 6 – Social Conditioning

Protests of residents or blocking entrance to the construction site by various organizations have a significant influence on the occurrence of delays in construction works. Therefore, the authors proposed a group with three basic factors: 1 – the possibility of constraints and difficulties in accessing the building site; 2 – possible protests of residents living in the area neighbouring the construction site; 3 – possible protests related to environmental protection.

The average evaluations of the factors in this group range between 3 to 4 points, therefore the problem of social conditioning was judged as important (Fig. 5).

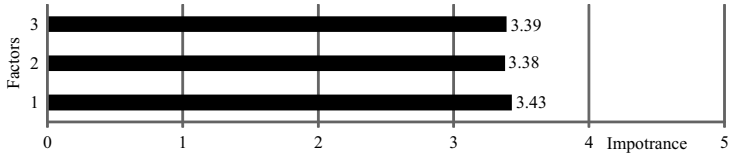

Fig. 5. Reasons for delay in the group: Social Conditioning – ranked by importance (Source: own study)

4. Conclusions

The present study involves a classification of factors that can cause delays of construction works into 6 groups. The factors proposed include only those that the authors judged as possible to identify before concluding the contract and which result from the provisions of the agreement. In total, 20 factors were indicated.

The analysis of the research results revealed that 3 groups out of 6, namely Project Documentation, Administrative Decisions and Construction Site, contain factors ranked above 4 points. The most important factors causing delays of construction works include the lack of a complete building permit design or a detailed design, not issuing the appropriate decision within the statutory period and having no right to administer the area for construction purposes on the part of the investor.

What is worth emphasizing is the strong commitment of the participants, who frequently added new factors to those proposed by the authors. Some of the additions the authors are planning to analyse further in the future research.

The results obtained show that, as early as at the planning stage, the analysis of the provisions of the agreement reveals a number of factors which can cause delays during the performance of the works. Their identification, evaluation and appropriate actions undertaken to limit or even eliminate the factors may decrease the scale of delays in construction projects.

References

[1] Anysz H., *Analiza zależności opóźnień w realizacji kontraktów na wykonanie robót budowlanych od czynników leżących poza sferą organizacji budowy i robót budowlanych*, Teoretyczne podstawy budownictwa, T. II, Procesy budowlane, 2012, 69–82.

[2] Anysz H., Zbiciak A., *Przyczyny powstawania opóźnień w realizacji kontraktów budowlanych – analiza wstępnych wyników badania ankietowego*, Autobusy: Technika, Eksploatacja, Systemy Transportowe, (3), 2013, 963–972.

[3] Akram S. et al., *Opóźnienia i zakłócenia w projektach budowlanych*, Komisja Europejska, Leonardo da Vinci – Transfer Innowacji, Warszawa, Ankara, Ascot, Mondavio 2012.

[4] Baldwin J.R., Manthei J.M., *Causes of delays in the construction industry*, ASCE Journal of the Construction Division, 97, 1971, 177–187.

[5] Dytczak M., Ginda G., Wojtkiewicz T., *Identyfikacja roli czynników opóźnień realizacji złożonych przedsięwzięć budowlanych*, Budownictwo i Inżynieria Środowiska, 2, 2011, 481–485.

[6] Faridi A.S., El-Sayegh S.M., *Significant factors causing delay in the UAE construction industry*, Construction Management and Economics, Vol. 24, Issue 11, 2006, 1167–1176.

[7] Głuszak M., Leśniak A., *Czynniki powodujące opóźnienia budowy – wielowymiarowa analiza statystyczna*, [In:] *Zastosowanie metod matematycznych w wybranych problemach zarządzania w budownictwie*, S. Belniek (ed.), Kraków 2015, 79–105.

[8] Jaśkowski P., Biruk S., *Analiza czynników ryzyka czasu realizacji przedsięwzięć budowlanych*, Czasopismo Techniczne, 1-B/2010, 2, 2010, 157–166.

[9] Kazaz A., Ulubeyli S., Tuncbilekli N.A., *Causes of delays in construction projects in Turkey*, Journal of Civil Engineering and Management, 3/2012, 426–435.

[10] Leśniak A., *Przyczyny opóźnień budowy w opiniach wykonawców*, Czasopismo Techniczne, 1-B/2012, 2, 57–68.

[11] Leśniak A., *Skąd się biorą opóźnienia?*, Builder, 1/2010, 24–25.

[12] Leśniak A., Plebankiewicz E., *Opóźnienia w robotach budowlanych*, Zeszyty naukowe WSOWL, Nr 3 (157) 2010, 332–339.

[13] Ogunlana S., Promkuntong K., *Construction delays in a fast-growing economy: comparing Thailand with other economics*, International Journal of Project Management, 14 (1), 1996, 37–45.

[14] Pasławski J., Drzewiecka J., *Analiza zakłóceń procesów budowlanych*, Budownictwo i Inżynieria Środowiska, 2/2011, 475–479.

[15] Połoński M., *Wiarygodność szacowanych kosztów planowanych inwestycji na tle barier w procesie inwestycyjnym*. Acta Scientiarum Polonorum. Architectura 2007, 6 (3), 35–41.

[16] Skorupka D., *Identification and Initial Risk Assessment of Construction Projects in Poland*, Journal of Management In Engineering", Vol. 24, No. 3, American Society of Civil Engineers, 2008, 120–127.
[17] Skorupka D. *The method identification and qualification of construction project risk*, Archives of Civil Engineering, LI, 4, Warszawa 2005, 647–662.
[18] Ustawa z dnia 17 maja 1989 r. Prawo geodezyjne i kartograficzne, Dz. U. 1989 nr 30, poz. 163.
[19] Ustawa z dnia 10 kwietnia 1997 r. Prawo energetyczne, Dz. U. 1997 nr 54, poz. 348.
[20] Ustawa z dnia 27 kwietnia 2001 r. Prawo ochrony środowiska, Dz. U. 2001 nr 62, poz. 627.
[21] Ustawa z dnia 18 lipca 2001 r. Prawo wodne, Dz. U. 2001 nr 115, poz. 1229.
[22] Ustawa z dnia 16 kwietnia 2004 r. O ochronie przyrody, Dz. U. 2004 nr 92, poz. 880.
[23] Ustawa z dnia 9 czerwca 2011r. Prawo geologiczne i górnicze, Dz. U. 2001 nr 163, poz. 981.

TECHNICAL TRANSACTIONS 6/2017
CZASOPISMO TECHNICZNE 6/2017
CIVIL ENGINEERING
DOI: 10.4467/2353737XCT.17.094.6570

Beata Nowogońska (b.nowogonska@ib.uz.zgora.pl)
Institute of Structural Engineering, University of Zielona Góra

Prediction of changes in the performance characteristics of a building

Prognoza zmian właściwości użytkowych budynku

Abstract

Over the course of their use, building structures are subject to constant destructive processes, which can take various courses. Over time, performance characteristics deteriorate, and can be partially restored as a result of repair works. The article presents a proposal for the prediction of changes in the performance characteristics of a building based on the adaptation of principles applied in predicting the operational reliability of technical objects.

Keywords: degree of wear, prediction, life distribution

Streszczenie

Obiekty budowlane podczas użytkowania podlegają ciągłym procesom destrukcyjnym o zróżnicowanym przebiegu. W miarę upływu czasu następuje obniżanie właściwości użytkowych, a częściowe ich przywrócenie następuje w wyniku napraw. W artykule przedstawiona jest propozycja prognozy zmian właściwości użytkowych budynku oparta na adaptacji zasad stosowanych w prognozowaniu niezawodności eksploatacyjnej obiektów technicznych.

Słowa kluczowe: stopień zużycia, predykcja, rozkład czasu życia

1. Introduction

In accordance with the recommendations of PN-ISO 7162:1999 standards [1], an assessment of the performance characteristics of a building should be carried out, and the changes in these characteristics should also predicted over time by developing a method simulating the predicted degradation of a good over time. The set of PN-ISO standards "Planning the Service Life of a Building" [e.g. 2, 3] provides general guidelines regarding the issues of predicting the service life of a building. These standards contain an introduction to predicting performance characteristics, though without details regarding forecasting. They highlight difficulties in indicating degradation, even in the case of similar buildings, as there are many variables influencing the service lives in practice. The variety of buildings, environments, surroundings and quality of construction works, as well as future conditions of maintenance, lead to uncertainty in forecasting service life. In one of the standards [2], there is an entry stating that the course of the service life runs in accordance with the Weibull distribution and its possible modifications.

The classification of methods for predicting the service life of buildings (Predicted Service Life Distribution of the Component – PSLDC) was given by Sobotka, Bucoń [4], and comprises deterministic, probabilistic and simulation methods. Deterministic methods based on the PN-ISO standard provide merely approximated results. Probabilistic methods, on the other hand, based on indicating variables of the service model as random values with a known probability distribution, are labour-intensive. The second group of probabilistic methods for describing the course of the destruction process are methods containing Markov chains. Markov chains are often applied for describing the destruction process of bridges and technical infrastructure. Such studies are also assumed for buildings. The service process of a building structure, as a cycle containing eight operational states, was presented by Kasprowicz [5]. Another example of applying (Bucoń, Sobotka [6]) discrete Markov chains is the description of the destruction process of a residential building described in four states.

Compromise methods for determining the service life of a building, somewhere between the not very accurate deterministic methods and probabilistic methods requiring a high quantity of data, are simulation methods (according to Sobotka, Bucoń [4]), which are based on developing a mathematical model using probability distributions for determining the individual variables of the model. Studies carried out by Olearczuk [7], connected with the loss of performance abilities of buildings, provided a result in the form of a linear function of changes in the performance ability of the building.

An assessment of performance characteristics (at a specified date of service) is the matrix method, developed by a team comprising Owczarek, Orłowski, Szklennik [8] and based on the following criteria: safety of the building, safety of ecological and ergonomic service, technical conditions of service, quality of service, operational satisfaction of the owner, and realizational and operational effectiveness.

Based on the hazard, failure and disaster analyses of buildings presented by Runkiewicz [9], it turns out that most of them occur in masonry constructions (44%)

among all building technologies, and in residential buildings (41%) among all other types of buildings. Attention is drawn to the increasing needs for renovation in residential buildings by, among others, Biliński [10], Czapliński and Marcinkowska [11], Kucharska-Stasiak [12], Linczowski [13], and Skarzyński [14]. According to the author, there is a need to develop prognoses of changes in the performance characteristics of a building for the entire time it is in service. Such prognoses will be useful when panning renovation works.

2. Prognosis of changes in the performance characteristics of building components

The problem of ensuring an adequate level of the technical condition of a building occurs over the entire period it is in service. In solving problems connected with developing a prediction of changes in performance characteristics of a residential building, it is suggested to use algorithms of determining changes in the reliability of technical devices. The prognosis of unfavourable processes will make it possible to determine the time frame in which the technical condition of a building will be unsatisfactory in the future, and thus necessitate repair works. A measure of the reliability of technical devices is the $R(t)$ function, also referred to as the survival function [e.g. 15].

For modelling situations in survival analysis, when the probability of failure changes over time, the Weibull distribution is most often applied as the distribution of the random variable of the time that a building is fit for service. This distribution has been widely applied for many years as the distribution of the time of proper operation and durability of the analysed goods [eg. 16–18]. When studying changes in the performance characteristics of a residential building, when the wear of the building along with the passing of time is treated as a significant cause of failure, formulas based on the Raleigh distribution, which is a specific case of the Weibull distribution, are apt.

The PRRD model (Prediction of Reliability according to Raleigh Distribution) of changes in the performance characteristics $R_i(t)$ of the i-th building component in time t, based on the Raleigh distribution and using durability periods of component T_{Ri} from data found in literature, is described by the relationship [19]:

$$R_i(t) = \exp\left[-(t/T_{Ri})^2\right] \tag{1}$$

3. Prognosis of changes in the performance characteristics of an entire building

Each building component serves a specific task. Elements serving structural functions have the most significant influence on the service life of a building. Other auxiliary elements influence the performance characteristics of a building to a lesser degree, with their influence resulting, above all, from the fact that damaged auxiliary elements can

lead to changes in the parameters of basic elements. The intensities of the influence of performance characteristics of the *i*-th components in the form of a scale of weights of elements A_i based on scale [20] serving to assess the quality of a building were accounted for when determining the performance characteristics of the entire building, which is a collection of n components.

Changes in the performance characteristics of building $R_A(t)$ in time t are determined by the relationship:

$$R_A(t) = \sum_{i=1}^{n} [A_i x R_i(t)] \tag{2}$$

4. Prediction of changes in performance characteristics of building undergoing repair works

The proposed method of predicting changes in the performance characteristics is to support activities aimed at avoiding an inadequate technical condition of a building. The effective service of a building ought to be based on maintaining an adequate level of performance characteristics of the building, while renovation processes are the means of realizing this task. All types of renovation works have a significant effect on the technical condition of a building over the course of its further use. Full characterization of a building undergoing repairs must account for the initial condition as well as changes in the performance characteristics after the completion of repair works.

Prediction of changes in the performance characteristics $R_A(t)$ of the building undergoing repairs.

$$R_M(t) = \sum_{i=1}^{s} [A_i x R_i(t)] + \sum_{i=1}^{p} [A_i \cdot k_n \cdot R_i(t - c_j)] \tag{3}$$

where:

$R_i(t - c_i)$ – performance characteristics of *i*-th component in the c_i repair cycle,
c_i – time building has been in service (in years) since the component was repaired.
s – number of building components which have not been repaired,
p – number of components in the building having undergone repairs in a given repair cycle, remaining symbols as above.

Changes in the performance characteristics of the $R_i(t - c_i)$ component can be indicated according to relationship (1) based on the PRRD model, under the assumption that repair works lead to an increase (or decrease) in the reliability of a component to the maximum value raised (or lowered) by the correction factor k_n.

5. Model system of building use

The following assumptions have been made in the proposed model of determining changes in the performance characteristics of a building undergoing repairs:

1) Repair work cycles for building components:
   c_1 = 55-year cycle – covering paint coatings of walls and ceilings, oil paint coatings of wooden elements,
   c_2 = 15 Gutters and downpipes, electrical fittings,
   c_3 = 30 wooden stairs, plumbing, plumbing fittings, gas pipes,
   c_4 = 60 wooden ceilings, roof trusses, ceramic tile roof cover, exterior plaster, doors and windows (frames), glass, floors and floor finishes, interior plaster, furnaces and radiators of central heating system, electrical wiring,
2) The times of carrying out repair words on building components result from the lifespan of these elements:
   $c_1 = 5$, $c_2 = 15$, $c_3 = 30$, $c_4 = 60$.

The recommendations regarding the times of carrying out planned preventive maintenance works were initially determined based on research and the lifespans of the building components. The proposed renovation works, which are aimed at maintaining the building in a good, satisfactory or average technical condition, rely on preventive measures and prevent the premature occurrence of unfavourable changes.

The obtained results of predictions of changes in the performance characteristics of a renovated building according to Rule (3) under the previously made assumptions have been presented in Figure 1. For comparative purposes, changes in the performance characteristics throughout the service life of an unrenovated building have been presented with a dashed line. The prediction was determined according to Formula (2).

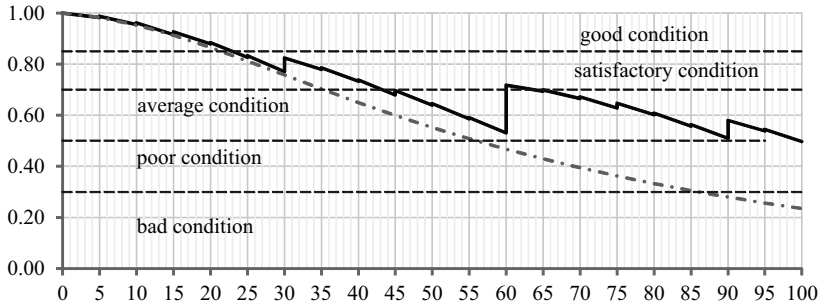

Fig. 1. Prediction of changes in the technical condition of a renovated building and unrenovated building, so-called life curve

The limits of the tolerance ranges, determined by the area of technical conditions, i.e. good, satisfactory, average and poor, have been indicated in Figure 1. The limiting values of the technical conditions were assumed in accordance with values corresponding to the degrees of technical wear.

6. Summary

The necessity to predict damage arises during all periods of the life cycle of a technical object. The prediction of the degradation of a building can be expected to be helpful in the process of reacting to damage to buildings as a result of aging. Modelling various possible scenarios of the service life of a building according to the proposed methodology will allow for the optimal planning of maintenance works.

References

[1] PN-ISO 7162:1999 Wymagania użytkowe w budownictwie. Treść i układ norm dotyczących oceny właściwości użytkowych.

[2] PN-ISO 15686-1: 2005 Budynki i budowle. Planowanie okresu użytkowania. Część 1: Zasady ogólne.

[3] PN-ISO 15686-2: 2005 Budynki i budowle. Planowanie okresu użytkowania. Część 2. Procedury związane z przewidywanym okresem użytkowania.

[4] Sobotka A., Bucoń R., *Kierunki rozwoju metod przewidywania okresu użytkowania obiektów budowlanych*, Problemy Rozwoju Miast, No. 4/2005, 58–67.

[5] Kasprowicz T., *Eksploatacja obiektów budowlanych*, Materiały konferencyjne 51 Konferencji Naukowej KILiW PAN i KN PZITB – Krynica 2005, 171–178.

[6] Bucoń R., Sobotka A., *Niezawodność eksploatacyjna obiektów budowlanych*, Prace naukowe Instytutu Budownictwa Politechniki Wrocławskiej, Wyd. Politechniki Wrocławskiej, nr 87/2006, 265–272.

[7] Olearczuk E., *Eksploatacja budynków, problemy, prawidłowości, postępowanie*, Wydawnictwo i Zakład Poligrafii Instytutu Technologii Eksploatacji, Warszawa 1999.

[8] Owczarek S., Orłowski Z., Szklennik N., *Koncepcja systemowej oceny zużycia budynków*, Prace Naukowe Instytutu Budownictwa Politechniki Wrocławskiej, Wyd. Politechnika Wrocławska 2006 No. 87, 341–346.

[9] Runkiewicz L., *Zagrożenia obiektów budowlanych a potrzeby remontów i wzmocnień*, Materiały X Konferencji „Problemy remontowe w budownictwie ogólnym i obiektach zabytkowych", Wyd. Politechniki Wrocławskiej, Wrocław 2002, 349–360.

[10] Biliński T., *Brak szans polepszenia sytuacji mieszkaniowej w Polsce*, Kwartalnik Naukowy „Problemy rozwoju budownictwa" 2/2001, 1–9.

[11] Czapliński K., Marcinkowska E., *Typologia starych budynków mieszkalnych ze względu na potrzebę ich odnowy,* Materiały konferencyjne 34 Konferencji Naukowej KILiW PAN i PZITB, Krynica 1988, 18–25.

[12] Kucharska-Stasiak E., *Ekonomiczne problemy zużycia i remontowania zasobów mieszkaniowych*, Materiały konferencyjne 38 Konf. Naukowej KILiW PAN i KN PZITB, Krynica 1992, 81–87.

[13] Linczowski Cz., *Naprawy, remonty i modernizacje budynków*, Wydawnictwo Politechniki Świętokrzyskiej, Kielce 1997.

[14] Skarzyński A., *Próba ogólnej systematyki sytuacji kryzysowych oraz wybranych towarzyszących im działań techniczno-organizacyjnych,* XI Konf. Inż. Wojskowej „Zarządzanie i organizacja działań w sytuacjach kryzysowych", Warszawa 2000, 43–52.
[15] Niziński S., *Elementy diagnostyki obiektów technicznych,* Wydawnictwo Uniwersytetu Warmińsko-Mazurskiego, Olsztyn 2001.
[16] Cordeiro, G., Ortega, M., and Lemonte, A., *The Exponential-Weibull Lifetime Distribution,* Journal of Statistical Computation and Simulation 84/2013 (12), 1–15.
[17] Walpole R.E., Myers R.H., *Probability and Statistics for Engineers and Scientists,* Macmillan Publishing Company, London 1985.
[18] Khelassi, A., Theilliol, D., Weber, P., *Reconfigurability Analysis for Reliable Fault-Tolerant Control Design,* International Journal of Applied Mathematics and Computer Science 21/2011 (3), 431–439.
[19] Nowogońska B., *Badanie ewolucji stanu technicznego budynku,* Journal of Civil Engineering, Environment and Architecture, 2016, Vol. 33, No. 63 (1/I/16), 35–42.
[20] Arendarski J., *Trwałość i niezawodność budynków mieszkalnych,* Arkady, Warszawa 1978.

TECHNICAL TRANSACTIONS 6/2017
CZASOPISMO TECHNICZNE 6/2017
CIVIL ENGINEERING
DOI: 10.4467/2353737XCT.17.095.6571

Edyta Plebankiewicz (eplebank@izwbit.pk.edu.pl)
Jarosław Malara
Insitute of Construction and Transportation Engineering & Management,
Cracow University of Technology

The algorithm for the evaluation of construction workers' labour productivity

Algorytm oceny wydajności pracy robotników budowlanych

Abstract

The paper presents an algorithm that allows to calculate the potential productivity of construction workers, including the factors that influence them. Its development involves one of the classifications of factors. In the next step, the elements of fuzzy logic were used for the parameterization of factors. Subsequently, a survey was applied to specify the gradation of individual factors with regard to their impact on productivity. The paper as a whole presents a mathematical algorithm, the practical application of which was presented too.

Keywords: algorithm, labour productivity, construction workers

Streszczenie

Artykuł przedstawia algorytm pozwalający na obliczenie potencjalnej wydajności pracy robotników budowlanych uwzględniający czynniki na nich oddziałujące. Do jego budowy wykorzystana została jedna z klasyfikacji czynników. W kolejnym etapie przedstawiono sposób wykorzystania elementów logiki rozmytej do parametryzacji czynników. Następny krok polegał na wykorzystaniu badań ankietowych do określenia gradacji poszczególnych czynników pod kątem ich stopnia wpływu na wydajność. Całość publikacji prowadzi do zaprezentowania matematycznego algorytmu, którego możliwości zastosowania w praktyce również zostały przedstawione.

Słowa kluczowe: algorytm, wydajność pracy, robotnicy budowlani

1. Work environment of the construction worker

Construction works have a dynamic character. Apart from the diversity of the works, a great significance is given to the instability of factors related to the influence of the environment. In literature [3, 4, 7], there were attempts to describe this dynamicity by means of algorithms. However, their scope of operation was related only to a mathematical relationship between the algorithm and schedule building [15, 17, 19]. The basic problem of the procedure described is the lack of a detailed analysis of the reasons for the occurrence of the differences. Apart from the technological issues, labour productivity of construction workers, depending on the influence of a variety of factors [13], is an important element. Therefore, a comprehensive approach to the subject should include information about the work environment of the construction worker. An indispensable element is the identification and evaluation of the factors that influence his work.

Previous research already concerns various classifications of factors influencing the labour productivity of construction worker [9, 14, 16]. It is worth emphasizing that they all specify which aspects should be analysed when performing an evaluation of labour productivity of a construction worker. The authors of the present paper chose publication [14] to analyse which factor, in their opinion, describes construction works in the most universal way. The factors included there are presented in Table 1. A characteristic feature of this classification is

Table 4. Classification of the factors affecting labour productivity

Factor group	Factors
Time spent outside work	► suitable length of rest ► worker's absence ► time spent with the family (WLB)
Weather conditions	► biometeorological conditions ► temperature ► humidity ► rainfall ► extreme work conditions (temp. and humidity)
Psychophysical conditions	► stress ► fatigue ► health ► age ► recovery
Organization and management of the worker	► ergonomics ► noise ► duration of work shift ► salary ► organization of work and workstations
The remaining factors	► day of the week ► experience ► adaptation to new operating conditions or a new technology

Source: [14].

the lack of relationship between individual factors with a particular construction work. This feature allows to make an attempt to develop a mathematical algorithm, including the factors that surround the worker, to describe the productivity of the work that he attains.

2. The premises of the algorithm describing labour productivity of construction workers

The classification described in the previous section serves as input data for the development of the algorithm, which makes the workers' labour productivity dependent on the factors that influence it. According to the authors, the factor itself needs to be described by at least two variables:

- influence on labour productivity – that is, a measure of the degree of positive/negative impact on labour productivity;
- degree of significance of the factor – the parameter differentiating individual factors among each other due to the strength of the impact on labour productivity,

Within the framework of the presented concept, it appeared necessary to introduce one, very important rule. The description of the factor impact should be brought to a common unit, since only in this way can the parameters presented be compared. For instance, it is difficult to use the day of the week, for example. Wednesday with a temperature of 12°C and noise of 77 dB, in one mathematical algorithm. To standardize the descriptions of factor impact on the work productivity, the basic tenets of the theory of fuzzy sets [10] were used. This mathematical method allows to define the space in which a factor fully influences labour effectiveness. Here, it is necessary to provide a definition, which states that fuzzy set A in a certain non-empty space $X = \{x\}$, written down as $A \subseteq X$, is a set of pairs [2] (1, 2):

$$A = \{(\mu_A(x), x)\}, \forall x \in X \tag{1}$$

where:

$$\mu_A : X \to [0, 1] \tag{2}$$

is a membership function of a fuzzy set [18]. The function assigns to each element $x \in X$ its degree of membership in fuzzy set A. The subsequent parts of the paper describes the scope of the positive influence of the factor on the labour productivity of construction workers, which is called the set of high efficiencies.

To define the degree of impact of the factor on labour productivity of construction workers, a survey was prepared, as described in [12, 14]. The results served to build a preliminary database of coefficients. At this stage, some of the factors identified in Table 1 were aggregated and each was assign a number. The result is presented in Table 2.

Table 1. Assignment of numbers to factors

Factor number	Factor name
c_1	Ergonomics
c_2	Noise
c_3	Duration of work shift
c_4	Salary
c_5	Organization of the workstations
c_6	Stress
c_7	Fatigue
c_8	Health
c_9	Age of the worker
c_{10}	Recovery of strength
c_{11}	Rainfall
c_{12}	Air temperature
c_{13}	Wind
c_{14}	Time spent with the family
c_{15}	Worker's absence
c_{16}	Day of the week
c_{17}	Adaptation to new operating conditions

Source: own study.

On this basis, using survey results and the Likert scale [6] individual factors were assigned to one of the four groups. The effect of the assignment is presented in Table 3.

Table 2. The division of the degree of factor influence on individual groups

Name of the group – impact on labour productivity of construction workers	Low	Average	High (Important)	Very high (very important)
Factors assigned	c_3, c_{10}, c_{14}, c_{15}	c_2, c_6, c_9, c_{11}, c_{12}, c_{13}, c_{16}, c_{17}	c_1, c_5, c_7, c_8	c_4
Weighting factor	0.25	0.5	0.75	1

Source: own study.

The authors consider the assignment in Table 3 as preliminary and allow the possibility of differentiating the weighting factors due to the nature of works. For example, in the case of external works, it is necessary to increase the importance of factors associated with weather

conditions. There exist a number of mathematical methods, which allow to calculate the value of the degree of impact coefficients.

The last element of the algorithm is the computational module. It allows to perform calculations on the basis of parameterized factors. The following formula (3) was adopted:

$$Wp = \left[\left(\frac{\sum_{i=1}^{17} \mu_A(c_i) \cdot w(c_i)}{\sum_{i=1}^{17} w(c_i)} \right) + 0.5 \right]^y \quad (3)$$

where:

- Wp – labour productivity,
- $\mu_A(c_i)$ – the value of the membership function of the set of high productivities for the i-th factor,
- $w(c_i)$ – the value of the function of the degree of the impact of the i-th factor on labour productivity,
- y – coefficient correcting the interval width of the possible occurrences of the Wp function values.

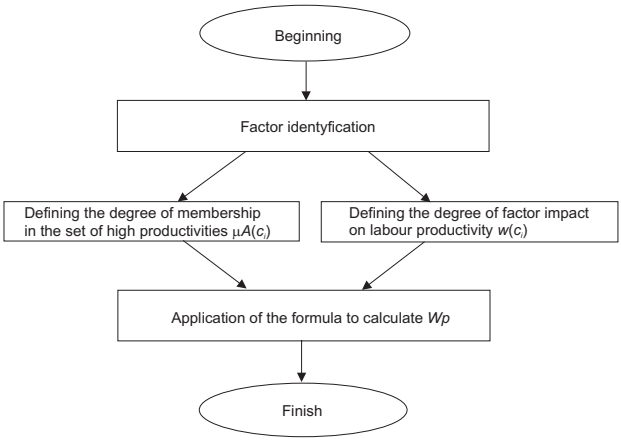

Fig. 1. Operating diagram of the algorithm – own study

The thus obtained value of labour productivity of construction workers is a non-individual value. The value $W_p = 1$ means average productivity. $W_p < 1$ below average, while $W_p > 1$ indicates a value above the norm assumed. The assumption about defining labour productivity corresponds to the way data are published by the Central Statistical Office [8]. In formula (3), the value of the quotient of the sum in each case is in the interval of <0, ..., 1>, hence the necessity to move the centre of the interval by 0.5 so that for the average quotient value, interpreted as average productivity, the result obtained equalled 1, meaning 100% of productivity, or accomplishment of the assumed norm. The exponential form of the function is related to the possibility of adjusting the width of the interval of possible results. Example intervals $<z_1, \ldots, z_2>$, depending on the value of the power of y are presented in Table 4.

Value z_1 means a minimum theoretical value of function W_p, while z_2 is the maximum. The authors analysed the sensitivity of formula (3) to the change of exponent y and, as a result of the conducted simulations, the calculated correlation coefficient was only slightly changed by +/–0.02. This proves that exponent y serves to adjust the value of function (3) with the actual results and it only takes into account the degree of sensitivity of the tested construction work on the interaction of all the factors.

To illustrate the operation of the algorithm describing labour productivity of construction workers, a block diagram was created (Fig. 1).

Table 3. Examples of interval values dependent on exponent *y*

y	0	0.25	0.5	0.75	1	2	3	4	5
z_1	1	0.84	0.71	0.59	0.5	0.25	0.13	0.06	0.03
z_2	1	1.11	1.22	1.36	1.5	2.25	3.38	5.06	7.59

Source: own study.

3. Applications of the algorithm

This section presents four basic applications of the algorithm for labour productivity of construction workers:

- prediction of the amount of labour per worker,
- assessment of the possibility to meet the deadline,
- indication of factors the correction of which may increase productivity,
- reliable assessment of the worker's individual potential.

The most intuitive way of using formula (3) is for the specification of the amount of the labour performed by the worker. In order to do so, one needs to account for the effect of the labour, which can be either retrieved from the Contractors Estimator or defined on the basis of own observation. The calculations also require the specification of the time in which the worker is to perform a given activity. Due to the variable values $\mu_A(c_i)$ the time should not exceed the duration of a single work shift. Applying the formula (3) of labour productivity of construction workers to predict the amount of the labour performed can be defined by the following formula (4):

$$V_p = W_p^{(')} N_j T_i \tag{4}$$

where:

V_p – amount of labour performed,
$Wp^{(')}$ – labour productivity on the basis of the basic formula (simplified),
N_j – individual labour effect [j.m./r-g],
T_i – duration of the labour performed [r-g].

Another potential benefit resulting from the application of the algorithm (Fig. 1) is the assessment of the possibility of meeting the deadline for the completion of the construction tasks. After evaluating the degree of membership of individual factors to the set of high

productivities $\mu_A(c_i)$ and establishing the degree of the influence of individual factors on productivity $w(c_i)$, one receives the value of function W_p, for which the value lower than one means a combination of factors that negatively influence productivity. This means that it is likely that the worker or the whole team under consideration will not perform the average amount of labour. A value greater than 1 means such combination of factors, which give the possibility of achieving a more than average amount of labour. The evaluation of the factors alone and applying formula (3) do not require any specification of the value of the base unitary effect, then the results obtained present combinations of factors beneficial and adverse for productivity. Due to such an application of the mathematical model, one can prepare a simulation of the workstation and its surroundings before the works begin to achieve the assumed target quantity of the planned work.

Another benefit of the algorithm (Fig. 1) is the ability to react to the quantitative results of the labour achieved by workers. After a couple of days, assessment with the use of the productivity model. Then, by simulating changes in work conditions and correcting the value of the degree of the impact for these factors that can be influenced (such as noise, ergonomics or salary), one is able to predict the potential productivity value.

This will allow to predict whether the change of the conditions and working environment, especially by their improvement, will boost the chances to implement a task on time with unchanged personnel resources available, and whether it will be necessary to increase employment [5]. Thus, the productivity model can be used in the process of scheduling construction works, in the selection of work teams and in the specification of the necessary minimum staffing to implement the task on time [11].

The mathematical model presented here may also become an auxiliary tool to evaluate construction workers with reference to their productivity and industriousness [1]. Taking into account the factors influencing them, one receives a more rounded picture of their work, thus the feedback provided by the analysis of work time is fuller too. For instance, out of two workers, *X* and *Y*, performing the same type of tasks on different construction sites, worker *X* achieved an example productivity $W_p = 0.92$ on his first day on the construction site. While this value is below average, the worker was exposed to unfavourable weather conditions, collaborated with incompetent staff supervision, received faulty tools and the analysis of his productivity took place on Friday. On the other hand, worker *Y*, on the 23rd work day, achieved the value of productivity of $W_p = 1.13$. This result is, theoretically, above average, yet worker *Y* performed in very good weather conditions, was supervised by a well-organized and communicative works manager, had new and fully functional tools and the productivity analysis took place on Wednesday. For the sake of simplification, the remaining factors were the same for both workers. The example shows that a comparison of the same values of the productivity function without the comparison of work conditions for individual workers is biased and should not remain the only source of information about the productivity achieved by workers.

4. Summary

The paper presented a novel approach to the issue of labour productivity of construction workers. The authors chose one of the existing classifications of factors influencing the productivity of workers, and then they used it for a further analysis of the problem. The strength of the study is its universality. In the subsequent steps of the proceedings, the issue of comparison of various factors were analysed. As a solution, the basic assumptions of the fuzzy set theory were applied. The main advantage proved to be the standardization of factors by describing them without the presence of natural entities. In this way, the development of a mathematical algorithm was enabled. The assessment of the degree of the impact of individual factors on the labour productivity of construction workers involved a survey, which became the basis of the preliminary database of coefficients. They allowed the gradation of individual factors in relation to their strength of influence on the subject of the research. In effect, a mathematical algorithm for proceedings has been constructed to calculate labour efficiency of construction workers. The paper also presented the potential applications of the solution under consideration. The possibilities of its implementation depend on the following: prediction of the amount of labour, assessment of the possibility of meeting the deadlines, identification of factors that need to be corrected and an individual assessment of labour productivity of a construction worker.

References

[1] Becker B.A., Huselid M.A., Ulrich D., *Karta wyników zarządzania zasobami ludzkimi*, Wolters Kluwer Polska Sp. z o.o, Warszawa 2012.

[2] Chan A.P.C., Wong F.K.W., Wong D.R., Lam E.W.M., Yi W., *Determining an optimal recovery time after exercising to exhaustion in controlled climatic environment: application to construction works*, Building and Environment, 56, 2012, 28–37.

[3] Chen J.. Yang L., Su M., *Comparison of som-based optimization and particle swarm optimization for minimizing the construction time of a secant pile wall*, Automation in Construction, 18, 2009, 844–848.

[4] Cooke B., Williams P., *Construction planning. programming and control*, Wiley-Blackwell, New Jersey 2009.

[5] Eaton. D., *Zarządzanie zasobami ludzkimi w budownictwie*, Poltext, Warszawa 2009.

[6] Gatignon H., *Statistical analysis of management data*, 2003.

[7] Gonzalez V., Alarcon L., Maturana S., Bustamante J., *Site management of work-in-process buffers to enhance project performance using the reliable commitment model: case study*, Journal of Construction Engineering and Management – Asce, 137, 2011, 707–715.

[8] Główny Urząd Statystyczny, Urząd Statystyczny w Katowicach, Wskaźniki Zrównoważonego Rozwoju, Moduł krajowy, Wydajność Pracy, Katowice 2016.

[9] Hoła B., Mrozowicz J., *Modelowanie procesów budowlanych o charakterze losowym*, Dolnośląskie Wydawnictwo Edukacyjne, Wrocław 2003.

[10] Ibadov N., Kulejewski J., *Rozmyte modelowanie czasów wykonania robót budowlanych w warunkach niepewności*, Czasopismo Techniczne, Budownictwo, B-1, 2010, 139–155.
[11] Kugler M., Kordi B., Franz V., *Support of the work preparation in building construction by simulation*, Bauingenieur, 87, 2012, 396–401.
[12] Malara J., *Ocena wpływu wybranych czynników na wydajność pracy w opinii robotników budowlanych*, [in:] Bzówka J., *Współczesny stan wiedzy w inżynierii lądowej*, Monografia, Wydawnictwo Politechniki Śląskiej, Gliwice 2015, 359–366.
[13] Malara. J., *Wpływ czasu pracy pracowników budowlanych na organizację robót*, [in:] J. Bzówka, *Wiedza i Eksperymenty w Budownictwie*, Monografia, Wydawnictwo Politechniki Śląskiej, Gliwice 2014.
[14] Plebankiewicz E., Juszczyk M., Malara J., *Identyfikacja i ocena czynników wpływających na wydajność pracy robotników budowlanych*, Przegląd Naukowy – Inżynieria i Kształtowanie Środowiska, 65, 2014, 271–278.
[15] Połoński M., *Harmonogramowanie realizacji przedsięwzięć budowlanych z uwzględnieniem buforów czasu wyznaczonych na podstawie analizy ryzyka*, Budownictwo i Architektura, 12, 2013, 47–52.
[16] Radziszewska-Zielina E., Sobotka A., Plebankiewicz E., Zima K., *Wstępna identyfikacja i ocena parametrów wpływających na wydajność układu operator-maszyna do robót ziemnych*, Budownictwo i Architektura, 12(1), 2013, 53–60.
[17] Russell M.M., Howell G., Hsiang S.M., Liu M., *Causes of time buffers in construction project task duration*, Journal of Construction Engineering and Management, 140, 2014, 325–336.
[18] Rutkowska D., Piliński M., Rutkowski L., *Sieci neuronowe. algorytmy genetyczne i systemy rozmyte*, PWN, Warszawa–Łódź 1997.
[19] Wambeke B.W., Hsiang S.M., Liu M., *Causes of variation in construction project task starting times and duration*, Journal of Construction Engineering and Management Asce, 9, 2011, 663–677.

TECHNICAL TRANSACTIONS 6/2017
CZASOPISMO TECHNICZNE 6/2017
CIVIL ENGINEERING
DOI: 10.4467/2353737XCT.17.096.6572

Dariusz Skorupka
Maciej Walczyński
Rafał Siczek
Magdalena Kowacka (m.kowacka@wso.wroc.pl)
Faculty of Management, the Military Academy of Land Forces

Application of unmanned aerial vehicles for revising dispersion of time of key undertakings

Wykorzystanie bezzałogowych platform latających do aktualizowania dyspersji czasu wykonania kluczowych przedsięwzięć

Abstract

The paper summarizes the concept of using unmanned aerial systems for construction work monitoring. Mobile drones can be used for determining the current stage of a given subtask in a complex construction project. Such control allows more adequate determination of the completion time of a given task, leading to more effective project schedule management.

Keywords: drones, construction works, project

Streszczenie

W pracy zostanie przedstawiona koncepcja wykorzystania bezzałogowych platform latających do monitoringu prac budowlanych. Mobilność dronów pozwala na ich wykorzystanie do wyznaczania aktualnego stanu w jakim znajduje się podzadanie złożonego projektu budowlanego. Kontrola wpłynie na dokładniejsze wyznaczenie czasu zakończenia danego zadania, a tym samym na lepsze zarządzanie harmonogramem całego projektu.

Słowa kluczowe: dron, prace budowlane, projekt

1. Construction project planning

Construction projects are connected with the development and execution of strategic and operational plans, which determine how the task goals are achieved [9]. Construction project planning-related documents include: a schedule, execution plan, budget, financing and cash flow plans, and a resource plan.

Construction work planning is often computer-aided; computer programmes eliminate most errors, e.g. when some tasks or resources overlap or are duplicated. In order to begin scheduling, one needs to gather information on the tasks required to complete a project, their duration, relations between them, resources needed for these tasks, their amount and availability.

In the literature of the subject, there are different ways of presenting the sequence of tasks implemented at various phases of scheduling. The paper describes the division into pre-launch phases (phases A1 and A2) and phase B implemented in the course of a project:

A1: Project scheduling, which ensures high chances for meeting the final deadline of a project and determination of the deadline acceptable for all project stakeholders;

A2: In the case of missing the project's planned deadline, one prepares a risk assessment, defines causes and undertakes steps to minimise the risk.

B: Verification of the planned deadline on the basis of controls undertaken in equal time intervals. Moreover, revision of chances of meeting the deadline and undertaking of certain steps to enhance meeting the project's deadline. In case of failure, revision of the deadline and presentation of all consequences of the above [11].

The aforementioned phases are the basic ones and their execution ensures constant control over both operational and strategic planning of a construction undertaking.

Delays in construction projects are often not taken into account in the schedule planning phase, mostly due to difficulties in estimating possible construction work delays and final deadlines of given processes.

Delays can be analysed by various techniques, including:

- CPM,
- PERT,
- the global impact technique where one plots all individual delays on a schedule, and when summed up, excluding their concurrence, they give a total overrun of the project's duration,
- the breakdown technique, based on the critical path method (CPM), takes into account all types of delays and the simultaneousness of their occurrence,
- the snapshot technique where one distinguishes periods of delaying events and compares them while analysing both as-planned and revised schedules,
- the time impact analysis, similar to the snapshot technique, where delaying events are focal points,
- the net impact technique, non-related to the CPM network, with the major difference that the revised schedule takes into account net effect of all delays [1].

Construction work planning is a process that requires large experience and know-how on the possibility of the occurrence of unexpected events affecting, to a large extent, the time of

completion of a construction project. According to the research team, efficiency of planning, and also of construction undertaking implementation, can be increased by application of new technologies, such as drones.

2. Unmanned aerial vehicles and time of key construction projects

Nowadays, unmanned aerial vehicles (UAVs) are one of the fastest developing technologies. They are increasingly used in various construction undertaking and large companies active in the construction industry apply drones in their specialised programmes. UAVs serve mostly as observation devices [10]. Live viewing of activities undertaken on construction fields, current tracking of equipment operation, work optimisation, and increased safety are a small fraction of what these devices offer. Drones can be easily equipped in an additional observation module, IT, or any other state-of-the art devices, which significantly increases their abilities [10].

Most of all, small flying machines can be equipped in a wide array of sensors and scanners detecting radiation or creating a map of a given area. Drones play the role of "scouts", automated cartographers, and eyes of professionals in places they sometimes cannot reach on their own. Komatsu, one of the leading producers of construction equipment, introduces drones to its research and development programmes. UAVs measure construction fields from the air and send data to the computer, which creates a 3D terrain model. This way, measurements are ready within hours, not days. Basing on the model, excavators and bulldozers can perform given construction works without operators. 3D models of which position and attachments will be remotely controlled are transmitted to smart machines by cloud computing.

Fig. 1. Quadrocopter assisting in construction works (source: komatsu.com)

In many cases, the application of unmanned aerial vehicles is much cheaper than regular methods. A drone does not need an airstrip, it is controlled from the ground and it does not consume litres of petrol. Therefore, its application is not cost intensive. Close observation of high objects does not pose a problem either.

3. Methods

As opposed to projects from other areas of economy, in construction undertakings, one should take into consideration a wide array of factors affecting the time of completion of a project. They include: design documents, a relatively long duration of construction works, weather conditions, or background conditions. From the economic point of view, the duration of an entire construction undertaking should be as short as possible, and the duration of key stages should be revised as often as possible. Therefore, there is the need for modelling of construction undertakings in such a way that it adequately reflects the course of real construction processes and precisely estimates their completion times. New technologies are of great help in such processes.

Continuous software development allows creating more and more precise models, which reflect a better investigation of problems. One should mention here, inter alia, laser scanning: terrestrial (TLS – Terrestrial Laser Scanning), airborne (ALS – Airborne Laser Scanning), and mobile (MLS – Mobile Airborne Laser Scanning), as well as photogrametry: terrestrial, mobile (MMS), and airborne. Not to forget about georadar measurements (GPR – Ground Penetrating Radar). Each of the aforementioned technologies allows developing products that are useful in designing, construction, as-built measurements, or road object monitoring.

The literature on project management and scheduling proposes numerous methods to reduce the duration of undertakings. One of them is reduction of time of given processes (time-cost trade off problem), which is directly related to an increase in costs. Depending on the type of undertaking, higher costs can arise from the introduction of shift work, extra hours, working on public holidays, or application of state-of-the-art materials or mounting system work in a given project. The relation between time and costs of processes can be modelled by linear relationship, non-linear relationship or in the discrete form [5, 7–9].

One can distinguish the following algorithms: Critical Path Method (CPM), time-cost analysis (CPM/MCX), and Program Evaluation and Review Technique (PERT), the probabilistic method of project planning and control; they are applied in network scheduling [6, 12]. As in CPM, the core of PERT is the critical path analysis. The difference between both

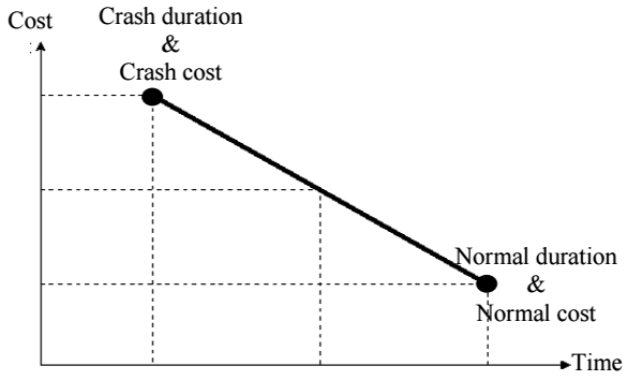

Fig. 2. Linear relationship between time and cost of execution

methods is that in CPM time is defined, whereas in PERT it is a random variable; an advantage of the latter technique. Due to such approach to time of tasks a project is composed of, statistic methods can be used to estimate risk related to completion of individual tasks, groups of tasks, and an entire project on time, and determine probability of their accomplishment in a pre-defined time.

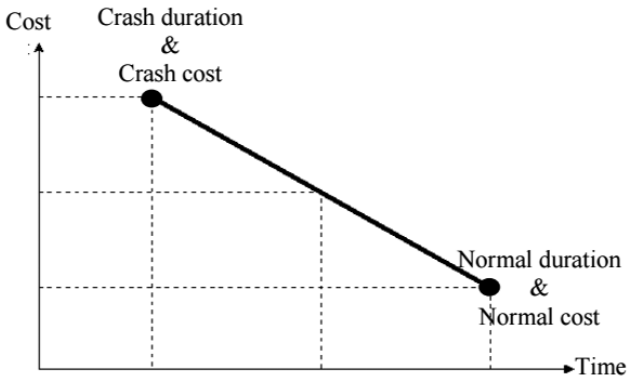

Fig. 3. Non-linear relationship between time and cost of execution

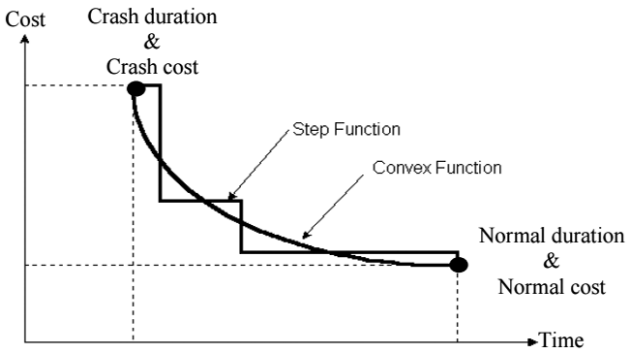

Fig. 4. Discrete relationship between time and cost of execution

PERT arbitrarily assumes that the time distribution is a beta distribution. It is the continuous density function as follows:

$$f(t) = H(t-a)^{p-1}(t-b)^{q-1} \tag{1}$$

$$\text{for } a < t < b \tag{2}$$

where:

a, b, p, q – parameters of the distribution,

H – normalisation constant depending on the parameters.

In PERT these parameters are replaced with three values, relatively easy to determine [6, 12]:

- optimistic time estimate $(a = C_o)$,
- most likely time estimate (C_p),
- pessimistic time estimate $(b = C_{pe})$.

Basing on these variables, one estimates the expected time of a given task, the basis of the critical path analysis, and the expected time variance, which determines the expected difference between the expected time and the real time of accomplishment of a given task. An estimate *t* is most often based on the weighted:

$$T_{[r} = \frac{C_o + 4C_p + C_{pe}}{6} \tag{3}$$

$$\sigma^2 = \frac{\left(C_{pe} - C_o\right)^2}{36} \tag{4}$$

One of the biggest problems in using network methods is determination of time of given tasks. However, often in case of similar projects, such linear projects (road construction), the estimation of duration of given tasks is highly probable.

4. Estimation of statistical parameters in construction undertakings by means of drones

The increased deployment of modern technologies and more advanced computerisation take place not only in the automotive industry (for example, autonomous self-driving cars by Tesla or Google), but also in the construction industry, as it was mentioned in the previous chapter. A construction investment, understood as a process, is divided into four crucial stages:

- programming,
- designing,
- execution,
- operation.

The execution phase of any construction project is of high importance due to the significant costs it generates. Cost reduction in this phase allows a significant reduction of costs of the entire investment. Cost optimisation can be introduced in this phase of an investment project, inter alia, by proper scheduling of construction works. It turns out that the old saying "time is money" applies even in the construction industry. Optimisation methods used in the industry include network methods, which were described in the previous chapter on the example of CPM and PERT. It should be noted that construction undertakings – as most of the projects undertaken in non-laboratory conditions – are subject to uncertainty. Such uncertainty may be related with various aspects of project implementation, for example ensuring financing continuity; however, the present paper is limited only to the optimisation of execution time of given construction work stages. PERT is a simple, probabilistic method based on the

assumption that statistical parameters of probability distribution for time of given project's phases (including the execution of a construction undertaking) can be estimated by means of the set of three pre-defined parameters:

- optimistic time estimate,
- most likely time estimate,
- pessimistic time estimate.

The aforementioned CPM is a specific, deterministic example of the PERT method where the pre-defined values of the estimates are equal.

It is assumed that the use of unmanned aerial vehicles (constructed as the so-called flying wings, or multicopters), equipped in the set of sensor, allows mass (and as a consequence) cheap control of construction field in complex construction projects. UAV's can be used in planning part of a project to collect data about the conditions of work implementation. Moreover, UAV's can be used in the execution stage of the project for the identification of the state of works execution. Data accumulated in this way will be used for development of a wide database with times of subsequent phases of a large number of construction investments. Such database could contribute to a reduction of uncertainty with respect to time of subsequent planned actions. Basing on PERT:

- estimated time of subsequent phases can be determined with larger precision (due to a wide data base with objective data),
- pessimistic and optimistic times can be subject to decreased dispersion in relation to the estimated time of execution due to more precise estimation of variability in time (dynamics).

Determining statistical parameters by means of previously conducted research will limit uncertainty with reference to dispersion of time parameters describing the time probability distribution for the execution of a given construction project phase. However, it may turn out that construction works will be subject to an array of abnormal random events (permanent and long-term precipitation, strong winds, frequent construction equipment failures, etc.). In such a case, the time of the investigated undertaking will go far beyond the typical confidence interval. Early detection of an anomaly in the course of a given undertaking will be also possible by means of permanent monitoring with unmanned aerial vehicles. Such application of drones will allow an immediate introduction of changes in scheduling of projects, which turned out to be difficult to model due to the occurrence of rare random events. Task scheduling with uncertain statistical parameters of time distribution for subsequent phases, as random parameters of the Erlang distribution or normal distribution, is more broadly investigated by Bożejko, Rajba, and Wodecki [2, 3], as well as Hejducki and Rogalska [4].

5. Summary

The paper proposes and describes the concept of using unmanned aerial vehicles for developing databases with times of execution of subsequent phases in construction projects. Such database will offer more precise planning and execution of complex construction

undertakings due to better understanding of the parameters describing the probability distributions of the time of subsequent phases of a construction undertaking. The authors plan to conduct research using drones to verify their assumptions.

References

[1] Alkass S., Mazerolle M., Harris F., *Construction delay analysis techniques, Construction Management and Economics*, Vol. 14, 1996, 375–394.

[2] Bożejko W., Rajba P., Wodecki M., *Stochastyczny problem przepływowy z terminami zakończenia operacji, Innowacje w Zarządzaniu i Inżynierii Produkcji*, R. Knosala (ed.), Oficyna Wydawnicza Polskiego Towarzystwa Zarządzania Produkcją, Vol. II, Opole 2015, 633–644.

[3] Bożejko W., Rajba P., Wodecki M., *Stable scheduling with random processing times,* [in:] *Advanced Methods and Applications in Computational Intelligence* (R. Klempous, J. Nikodem, Z. Chaczko (eds.), Topics in Intelligent Engineering and Informatics series Vol. 6 (2014), ISBN 978-3-319-01435-7, Springer, 61–77.

[4] Bożejko W., Hejducki Z., Rogalska M., Rajba P., Wodecki M., *Harmonogramowanie robót budowlanych w systemie potokowym z niepewnymi danymi*, Zeszyty Naukowe Wyższa Szkoła Oficerska Wojsk Lądowych im. gen. Tadeusza Kościuszki, No. 4 (166) 2012, 80–95.

[5] Brucker P., Drexl A., Mohring R., Neumann K., Pesch E., *Resource-constrained project scheduling: Notation, classification, models, and methods*, European Journal Operational Research 1999, Vol. 112, No. 1, 3–41.

[6] Brandenburg H., *Zarządzanie Projektami*, Wydawnictwo Akademii Ekonomicznej w Katowicach, Katowice 2002.

[7] Jaśkowski P., Politechnika Lubelska, Sobotka A., Kraków – *Modelowanie problemu redukcji czasu realizacji przedsięwzięcia budowlanego*, Przegląd budowlany 9/2008.

[8] Jaśkowski P., Sobotka A., *Multicriteria construction project scheduling method using evolutionary algorithm*, Operational Research – An International Journal 2006, Vol. 6, No. 3, 283–397.

[9] Kasprowicz T., *Inżynieria przedsięwzięć budowlanych*, Wydawnictwo i Zakład Poligrafii Instytutu Technologii Eksploatacji, Radom–Warszawa 2002.

[10] [Skorupka D., Siczek R., Walczyński M., Kowacka M. *Wykorzystanie mobilnych platform latających w badaniach termowizyjnych*, Materiały Budowlane 2016, No. 6, 139–140.

[11] Skorupka D., Kuchta D., Górski M., *Zarządzanie ryzykiem w projekcie*, WSOWL, Wrocław 2012.

[12] Trocki M., Grucza B., Ogonek K., *Zarządzanie Projektami*, PWE, Warszawa 2003.

TECHNICAL TRANSACTIONS 6/2017
CZASOPISMO TECHNICZNE /2017
CIVIL ENGINEERING
DOI: 10.4467/2353737XCT.17.097.6573

Elżbieta Szafranko (elasz@uwm.edu.pl)
Faculty of Geodesy, Geospatial and Civil Engineering, University of Warmia and Mazury in Olsztyn

The idea of graphic profiles for supporting a choice of material and technological solution

Idea profili graficznych przy wyborze wariantu rozwiązań technologiczno materiałowych

Abstract

When constructing buildings and building structures, we must often solve dilemmas regarding the implementation of specific technologies and materials. Depending on the planned use of a building, its functions and the expectations of its future users, some solutions may be superior to others. Because of a high number of factors that weigh on the final decision, it is necessary to employ efficient decision-support tools. Having analysed such a cases, the author has developed her own approach based on a graphic template of an investment project, which is compared to the profiles of assessed variants. The article presents the approach using an example of constructing a production floor building, where the ambient conditions will be harsh due to the planned production profile. The analysis included construction variants with a roof supported by one of the three types of girders: wooden, steel and prestressed concrete ones.

Keywords: building materials, investment project variants, multi-criteria methods, graphic method

Streszczenie

Realizując obiekty budowlane, niejednokrotnie musimy rozstrzygnąć dylematy dotyczące zastosowania konkretnych technologii i materiałów. W zależności od przeznaczenia obiektu, jego funkcji i oczekiwań przyszłych użytkowników różne rozwiązania mogą okazać się lepsze. Ze względu na dużą ilość czynników wpływających na ostateczny wybór konieczne jest zastosowanie sprawnych narzędzi wspomagających proces decyzyjny. Autorka, analizując podobne przypadki, wypracowała własną metodę postępowania opartą na graficznym szablonie inwestycji obrazującym oceny ważności kryteriów i porównaniu go z profilami ocenianych wariantów. W artykule przedstawiono sposób postępowania na przykładzie realizacji konstrukcji hali produkcyjnej, w której panują trudne warunki związane z planowaną produkcją. Analizie poddano warianty realizacji przekrycia opartego na dźwigarach, drewnianym, stalowym i żelbetowym sprężonym.

Słowa kluczowe: materiały budowlane, warianty inwestycji, metody wielokryterialne, metoda graficzna

1. Introduction

The preparation for the execution of a building project typically involves an elaboration of a few solution variants. The variants are submitted to analysis in the context of technical and technological characteristics, economic aspects, working conditions during the construction process and other specific parameters. When preparing a design of a new construction, it is mandatory to comply with relevant standards and directives, technical regulations binding in the construction industry, work safety and hygiene regulations, fire protection regulations as well as many other standards and regulations, and to secure technical approvals, provide construction technical specifications and obtain administrative decisions. The costs of a construction project arise from site-specific characteristics, transportation and the need to employ qualified workers and hire specialist equipment [1]. The costs of using a raised construction can be affected, for example, by the required maintenance works. Thus, making any decision regarding a planned construction project in such a complex environment requires an efficient decision support method, which will allow us to take into consideration all significant aspects and, on the other hand, will enable us to identify a variant, which can satisfy these requirements to the highest possible degree. Because of a multitude of available methods and techniques used for analysis of variants, it is often difficult to decide which method should be chosen so as to achieve the desired effect. While selecting the most appropriate approach, it is advisable to consider such aspects as readability, quality and verifiability of achieved results and the applied mathematical apparatus [2, 11].

2. Methodology of computational methods

When selecting a particular approach to the assessment of construction and building material solutions, it is crucial to check whether the methods taken into account will correspond well to the specific nature of our project. Other important characteristics of a selected assessment method include the readability and clarity of results, the applied mathematical apparatus, easy applicability of the method, and verifiability of the results. It is also worth considering the procedure involved in the preparation of input data and the subjectivity of an assessment, the latter being a consequence of using expert opinions in most of evaluation approaches. Among numerous multi-criteria assessment methods, let us mention the Multi Criterial Evaluation (MCE), Analytic Hierarchy Process (AHP) or Indicator Method (IM) [8–11].

The underlying foundation of each of these methods is the establishment of assessment criteria, their importance and degree to which they are satisfied by subsequently evaluated solutions. Each method allows the user to take into consideration many diverse criteria. The hierarchy method enables one to divide the factors into main criteria and subcriteria, while the other two approaches assign importance to all criteria on the same level of comparison. The extent to which criteria are fulfilled by an evaluated decision variant can be identified

by the degree of satisfying the main criteria and appropriately grouped partial criteria. Decomposition of a problem facilitates an assessment and is actually the essence of the hierarchy method. The literature provides calculation methods for all the three approaches mentioned above [8–11].

3. An example of the application of an analytical method

To illustrate an analysis of variants, fragments of calculations for three alternative solutions of a roof girder are presented [3–7,12]. Five groups of criteria have been established, and they will serve for evaluating the alternatives in the further analytical stage:

A. Construction work criteria
   - A1. Ease of transportation and construction,
   - A2. Heavy load bearing capacity,
   - A3. Easy and quick assembly,
   - A4. Light weight of the construction,

B. Economic criteria
   - B1. Costs of manufacturing the element,
   - B2. Costs of transport,
   - B3. Costs of assembly and construction,

C. Environmental criteria
   - C1. Resistance of the construction to changeable moisture,
   - C2. Resistance to low temperatures,
   - C3. Resistance to biological corrosive factors,
   - C4. Fire resistance,
   - C5. Recyclability,

D. Maintenance criteria
   - D1. Resistance to blows,
   - D2. Easy repair and strengthening,
   - D3. Frequency of repairs and maintenance works,
   - D4. Works done to protect the construction from external factors,

E. Others
   - E1. Production floor accessible to large vehicles,
   - E2. Production process possible at low temperatures,
   - E3. Response to vibrations.

The importance of the main criteria and subcriteria was assessed. Their value is comprised in the 0–1 interval. The fulfilment of individual criteria by the analysed solutions was evaluated on a 0–6 scale, where 0 means the lack of fulfilment of a given criterion, while 6 denotes the maximum fulfilment of this criterion. The calculations are set in table 1. Because the building for which the roof structure is to be designed will serve production purposes, high importance has been attributed to the environmental conditions in which the construction elements will work and to the maintenance conditions.

Table 1. Specification of the weights of the main criteria and subcriteria

Criteria	Subcriteria	Main weights	Sub-weights	Weights
	a1	0.12	0.07	0.008
A	a2	0.12	0.18	0.022
	a3	0.12	0.35	0.042
	a4	0.12	0.40	0.048
	b1	0.14	0.22	0.031
B	b2	0.14	0.36	0.050
	b3	0.14	0.42	0.059
	c1	0.29	0.14	0.041
C	c2	0.29	0.15	0.044
	c3	0.29	0.17	0.049
	c4	0.29	0.24	0.070
	c5	0.29	0.30	0.087
	d1	0.4	0.11	0.044
D	d2	0.4	0.27	**0.108**
	d3	0.4	0.29	**0.116**
	d4	0.4	0.33	**0.132**
	e1	0.05	0.26	0.013
E	e2	0.05	0.32	0.016
	e3	0.05	0.42	0.021

The results of our calculations suggest that the major subcriteria, which can decide upon the choice of girder structure, are the ones that identify the need for repairs and for the protection against the environmental factors that will affect adversely the roof-supporting structure (d2, d3, d4). Table 2 contains results of our assessment of the fulfilment of these criteria by the evaluated variant solutions (v1, v2, v3).

The analysis performed as described above shows that the highest total score was achieved by the timber girder structure – w1. However, this result may not be in complete agreement with the investor's expectations because the final assessment value is affected by the points scored for the fulfilment of other, less significant criteria. For example, subcriterion 3d is satisfied to the highest degree by variant 2, which scored the lowest total number of points. Moreover, analysis of the results may be laborious and difficult due to a high number of data generated by the calculations. The complicated mathematical apparatus and, occasionally, the vagueness of calculation results may discourage investors from such analyses. During her research, the author has developed an alternative approach, based on graphic evaluation of variants supported by profiles.

Table 2. Assessment of the evaluated variants

Subcriteria	Weights	v1	Assessment of v1	v2	Assessment of v2	v3	Assessment of v3
a1	0.008	2	0.016	0.5	0.004	3	0.024
a2	0.022	2.5	0.055	0.7	0.015	3.5	0.077
a3	0.042	3	0.126	1	0.042	4	0.168
a4	0.048	3	0.144	2	0.096	4.5	0.216
b1	0.031	1	0.031	1	0.031	3	0.093
b2	0.050	3	0.150	2	0.100	4.5	0.225
b3	0.059	4	0.236	2.5	0.147	5	0.295
c1	0.041	3	0.123	1.5	0.061	1	0.041
c2	0.044	3	0.132	1.5	0.066	1	0.044
c3	0.049	4	0.196	2	0.098	1.5	0.073
c4	0.070	5	0.350	2.5	0.175	2	0.140
c5	0.087	5	**0.435**	3	0.261	3	0.261
d1	0.044	2	0.088	2	0.088	1.5	0.066
d2	0.108	3	**0.324**	3	**0.324**	2.5	0.270
d3	0.116	3	**0.348**	4.5	**0.522**	3	**0.348**
d4	0.132	5	0.660	4.5	0.594	3	**0.396**
e1	0.013	1	0.013	0.5	0.007	1	0.013
e2	0.016	2	0.032	1	0.016	1.5	0.024
e3	0.021	3	0.063	1.5	0.032	1.5	0.032
			3.522		2.679		2.806

4. Analysis according to the graphic method

As mentioned above, time- and labour-consuming calculations frequently discourage investors and designers from certain analytical methods. Moreover, the implied necessity to analyse results in the form of a series of numbers leads to some problems while implementing the discussed assessment methods in practice. Therefore, while analyzing variants of different building material solutions in the field of civil engineering, the author has developed a new methodology based on the comparison of graphic profiles of available variants with a template of criteria for a given solution.

A template is produced by arranging main criteria in the order of increasing value of weights in groups of main criteria. The subcriteria are ordered according to the same principle.

In the case discussed in this paper, the order was determined in accordance to the assigned weights: A – 0.12, B – 0.14, C – 0.29 and D – 0.4, followed by other criteria specific for the circumstances surrounding each specific design. Table 3 shows the subcriteria arranged according to the same principle, while fig. 1 illustrates the achieved template of criteria.

The next step is to evaluate variant solutions and to construct profiles for each analysed variant. The data should be arranged according to the order assumed for the template. In our case, we are expected to evaluate three possible solutions for building roof girders: timber, prestressed concrete and steel structures. The assessment of these variants is presented in table 4, while the templates and profiles are illustrated in Fig. 1, 2, 3 and 4.

Table 3. Data for elaboration of a template of criteria

Criteria	Subcriteria	Weights
	a1	0.008
a	a2	0.022
	a3	0.042
	a4	0.048
	b1	0.031
b	b2	0.050
	b3	0.059
	c1	0.041
c	c2	0.044
	c3	0.049
	c4	0.070
	c5	0.087
	d1	0.044
d	d2	0.108
	d3	0.116
	d4	0.132
	e1	0.013
e	e2	0.016
	e3	0.021

Table 4. Assessment of the variants

Subcriteria	v1	v2	v3
a1	0.016	0.004	0.024
a2	0.055	0.015	0.077
a3	0.126	0.042	0.168
a4	0.144	0.096	0.216
b1	0.031	0.031	0.093
b2	0.150	0.100	0.225
b3	0.236	0.148	0.295
c1	0.123	0.062	0.041
c2	0.132	0.066	0.044
c3	0.196	0.098	0.073
c4	0.350	0.175	0.140
c5	0.435	0.261	0.261
d1	0.088	0.088	0.066
d2	0.324	0.324	0.270
d3	0.348	0.522	0.348
d4	0.660	0.594	0.396
e1	0.013	0.006	0.013
e2	0.032	0.016	0.024
e3	0.063	0.031	0.032

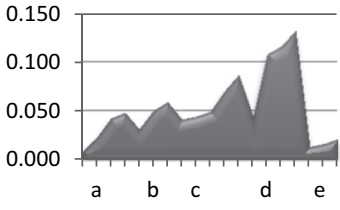

Fig. 1. Template of criterion

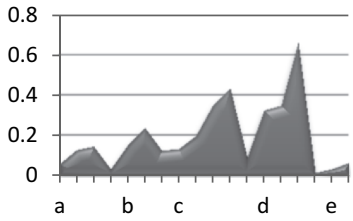

Fig. 2. Profile of variant 1

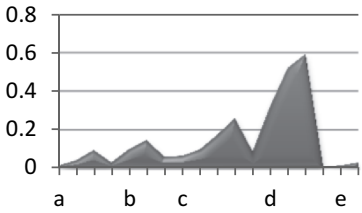

Fig. 3. Fig. 3. Profile of variant 2

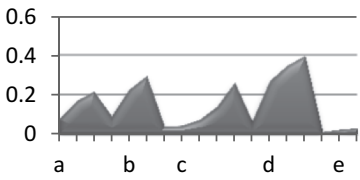

Fig. 4. Profile of variant 3

Once the shapes of the profiles are compared, we can deduce that the profile of variant 1 is in the best agreement with the template of the criteria. This conclusion confirms the result achieved by the calculation method presented earlier. In addition, it lets us take into account the specific features of the solution and, following the comparison of the profiles, it enables us to evaluate the most important characteristics of the variants. Analysis of the graphic profiles of solutions is simpler, more user-friendly and generates more trustworthy results. Moreover, comparative analysis of the graphic similarity of profiles can be performed with software that can calculate probability percentages.

5. Summary and analysis of the results

In the process of preparing oneself for the construction of building structures, it is extremely important to analyse various variants of an investment project. One of the problems that a designer faces is to select structural and building material solutions. Analysis of available technologies should involve a decision-support method.

The model approach presented above shows a possible application of the graphic method, based on multi-criteria assessment methodology, for the evaluation of several alternative variants. The graphic method, prepared in the form of profiles for all variants subsequently compared with a template of criteria, is the most user-friendly approach to the interpretation of results obtained through a multi-criteria analysis. Ready-made profiles, which can be used by architects, designers and investors, are met with a warm reception in the world of engineers.

References

[1] Dziadosz A., Kończak A., *Review of selected methods of supporting decision-making process in the construction industry*, "Archives of Civil Engineering" 62(1), 2016, 111–126.

[2] Foley CM., Schinler D., *Automated design of steel frames using advanced analysis and object-oriented evolutionary computation*, "Journal of Structural Engineering" 129(5), 2003, 648–660.

[3] Frühwald E., Serrano E., Toratti T., Emilsson A., Thelandersson S., *Design of safe timber structures-how can we learn from structural failures in concrete, steel and timber*? Report TVBK-3053, Lund 2007.
[4] Gencturk B., Hossain K., Kapadia A., Labib E., Mo Y., *Use of digital image correlation technique in full-scale testing of prestressed concrete structures*, "Measurement" (47), 2014, 505–515.
[5] Haughian CP., *Improvement in composite metallic girders*, U.S. Patent No. 183,(160), 10 Oct. 1876.
[6] Konczak A., Paslawski J., *Decision Support in Production Planning of Precast Concrete Slabs Based on Simulation and Learning from Examples*, "Procedia Engineering" (122), 2015, 81–87.
[7] Libby JR., *Modern prestressed concrete: design principles and construction methods*, "Springer Science & Business Media", 2012.
[8] Szafranko E., *Methodology of the assessment of investment project variants based on multi-criteria analyses*, QUAESTI-Virtual Multidisciplinary Conference, (1), 2015.
[9] Szafranko E., *Ways to determine criteria in multi-criteria methods applied to assessment of variants of a planned building investment*, "Czasopismo Techniczne" 2-B/2014, 41–48.
[10] Szafranko E., *Application of the analytic hierarchy process (AHP) to evaluation of variants of a planned road investment project*, "Journal of International Scientific Publications: Materials, Methods & Technologies" 7(1), 2013, 152–163.
[11] Walker A.. *Project management in construction*, John Wiley & Sons, 2015.
[12] Wilby CB., *Structural Concrete: Materials; Mix Design; Plain, Reinforced and Prestressed Concrete*, Design Tables, Elsevier, 2013.

TECHNICAL TRANSACTIONS 6/2017
CZASOPISMO TECHNICZNE 6/2017
MECHANICS
DOI: 10.4467/2353737XCT.17.098.6574

Aneta Szewczyk-Nykiel (aneta.szewczyk-nykiel@mech.pk.edu.pl)
Institute of Material Engineering, Cracow University of Technology

Microstructure and properties of sintered metal matrix composites reinforced with SiC particles

Mikrostruktura i właściwości spiekanych kompozytów o osnowie metalowej umacnianych cząstkami SiC

Abstract

Based on the prealloyed and diffusion bonded powders (Distaloy SA and Distaloy SE) different metal matrix composites reinforced with SiC particles were produced by the conventional powder metallurgy technology and the effect of varied amounts of SiC particles on microstructure evaluation and selected properties were investigated. It was stated that the mass fraction of SiC has a great effect on the density, porosity, shrinkage, hardness and wear resistance of studied composites. In the case of both Distaloy SA and Distaloy SE matrix materials, the optimum SiC content is 4 wt. % due to the highest wear resistance and hardness of sintered composite.

Keywords: metal matrix composites, SiC particles, Distaloy SA, Distaloy SE, sintering, density, hardness, wear resistance, microstructure

Streszczenie

Konwencjonalną technologią metalurgii proszków otrzymano z proszków stopowanych i wyżarzanych dyfuzyjnie kompozyty o osnowie metalowej umacniane cząstkami SiC. Dokonano oceny wpływu udziału cząstek SiC na ich mikrostrukturę i wybrane właściwości. Udział masowy cząstek SiC wywiera znaczny wpływ na gęstość, skurcz, twardość, odporność na zużycie ścierne badanych kompozytów. W spiekanych kompozytach o osnowie Distaloy SA, jak i Distaloy SE optymalna zawartość SiC wynosi 4 % wag. ze względu na najwyższą odporność na zużycie ścieranie i twardość.

Słowa kluczowe: kompozyty o osnowie metalowej, cząstki SiC, Distaloy SA, Distaloy SE, spiekanie, gęstość, twardość, odporność na zużycie ścierne, mikrostruktura

1. Introduction

Ceramic particle-reinforced metal matrix composites are an attractive group of structural materials. They have found wide use in various engineering applications, especially for aerospace, automotive, wear and cutting applications [1–9]. This is due to good mechanical properties as well as the combination of special properties with ease of fabrication [1, 3, 7, 10]. These industrially important composites exhibit properties which are better in comparison to metals [11]. The most interesting of these are: higher ratio of strength-to-density as well as stiffness-to-density, greater wear resistance and fatigue resistance and better elevated temperature properties [1, 6, 8, 12].

It is worth mentioning that particulate reinforcement has some important advantages in comparison to the other types of reinforcements. Namely the production procedures are simpler and relatively cheaper, the cost of reinforcements is comparatively low, and the properties for the composite are isotropic. And finally, there is good compatibility with most practised manufacturing processes like welding, machining, deformation processing etc. [3, 9, 13, 14]. Furthermore, ceramic particles introduced into a metal matrix can greatly enhance the mechanical and tribological properties as well as the anti-corrosion behaviour of such composites [15, 16]. The most common types of particulate reinforcements are oxides (Al_2O_3), carbides (SiC, TiC, WC) and borides (TiB_2) [1, 5, 10, 12, 16, 17]. Particle-reinforced MMCs typically contain less than 25 vol. % ceramic reinforcement. The typical dimensions of the most frequently used ceramic particles are within the range between 1 and 100 μm.

Particle-reinforced MMCs can be produced by both solid state (powder metallurgy technology) [1, 2, 4, 5, 10, 11, 14, 15, 17–21] and liquid phase techniques (stir casting) [3, 8, 12, 13, 16]. It should be pointed out that powder metallurgy technology ensures some advantages, namely: lower energy consumption, higher raw material savings, near net-shape or net-shape parts fabrication, part dimensional accuracy, lower cost, simpler equipment for processing and shorter processing times and of course higher composition uniform distribution and a wide range of composition selection for the metal matrix, which is important in the case of production of MMCs [1, 17–20].

Based on a review of the literature, it can be stated that most papers relate to the lightweight metal matrix composites [4–6, 8–13, 16]. It can be noted that aluminium and aluminium alloys are the most popular matrix for particle-reinforcement MMCs. They are very attractive materials due to their low density, their capability to be strengthened by precipitation, good corrosion resistance, high thermal and electrical conductivity, and high damping capacity [8, 11–13]. For these reasons, aluminium and aluminium alloy matrix composites have been extensively investigated in terms of preparation methods as well as parameters affecting the mechanical and tribological properties, and corrosion behaviour as well as microstructure evolution [4–8, 10–12, 16]. Generally, researchers have focused on the influence of the chemical nature of ceramic reinforcements and the chemical composition of the matrix on the microstructure as well as the properties of these composites.

Nevertheless, it should be emphasized that there is a growing interest in iron-based matrix composites. In these MMCs, iron [17–19], low-alloyed steels [1, 2, 14], tool steels as well as

stainless steels [7, 15, 21–23] are used as the matrix material, while particulate reinforcement is usually Al_2O_3, TiC, TiB_2, SiC, WC or TiN. For example, iron and steel matrix composites reinforced with TiC or TiB_2 ceramic particulates have recently received considerable attention because of good hardness and wear resistance and high values of toughness [7]. Furthermore these materials are easy to fabricate and costs are not high.

Analysis of the literature [17–19] leads to the conclusion that the type and particle size of carbide as well as sintering temperature have an influence on the mechanical properties of the sintered Fe-carbide composites. In the case of sintered Fe – (5 wt. %) SiC composites, the properties such as tensile strength and hardness increased with decreasing carbide particle size (in the range of 20–32 μm) and increasing sintering temperature (in the range from 1100°C up to 1200°C) [18, 19]. Moreover the tensile strengths and hardness of these materials were higher than those of the sintered Fe-WC composites. According to [17, 19] the microstructure of sintered Fe – carbide composites strongly depends on the sintering conditions. It was observed that some SiC particles contacting with iron particles may decompose during the sintering process, and then silicon and carbon atoms can diffuse into iron particles which results in the formation of a new phase [17–19]. It was found that the sintering temperature to 1000°C assured the preservation of SiC particles, while sintering temperature to 1150°C caused the appearance of Fe_3Si, cementite or perlite. It was also reported [17–19] that some iron silicides (for example, Fe_3Si, FeSi, and $FeSi_2$) can be formed during sintering as a consequence of the reaction between iron and SiC. Moreover, the introduction of too much SiC powder (more than 8 wt. %) caused the formation of liquid during sintering [17]. The aforementioned decomposition of SiC particles caused the growth of the voids surrounding the SiC particles as well as a decrease in the SiC particle size [18, 19]. While in the case of Fe-WC, Fe-TiC, and Fe-VC composites, carbide particles were stable during heating up to 1200°C. But sintering at a temperature above 1250°C caused decomposition of carbide and reaction between iron and carbide [18, 19]. Therefore, no improvement in the mechanical properties was observed.

There are also some studies on metal matrix composites reinforced with SiC particles [1–23]. Al/Al alloy – SiC [1, 3–6, 8–13, 16], Fe – SiC [17–19] as well as steel – SiC [1, 2, 7, 14, 15, 20–23] composites should be primarily listed. It is known that silicon carbide possesses high hardness and good wear resistance, high strength, good thermal characteristics and also resistance to oxidation at high temperatures and a very attractive cost [1, 8, 15].

For instance, papers [17, 20] are related to sintered Fe – SiC and 316L steel – SiC composites. In the case of these studies, the content of SiC varied in the range of 0% up to 10%. The addition of silicon carbide particles decreased the sintered density of Fe – SiC and also 316L – SiC composites. The mechanical properties (UTS, yield strength, elongation, hardness) of the sintered 316L – SiC composites were higher than those of sintered 316L steel. Furthermore, the mechanical properties increased with increasing SiC content [20]. The sintered Fe – SiC composites exhibited an increase in UTS, yield strength, and hardness similar to sintered 316L – SiC composites [17].

Due to their properties, the low and medium alloyed steels including Distaloy and also Ancorsteel are widely used in the production of sintered components such as complex, precise,

high strength machine parts [14, 24–27]. Distaloy is a prealloyed and diffusion bonded powder. This means that the alloying elements i.e. copper, nickel and molybdenum are bonded in particulate form to the basic iron particles. This powder production process, as well as balanced nickel and copper contents, provides the minimum segregation and also contribute to dimensional stability [24]. Distaloy is today widely used in applications demanding high strength and wear resistance. It turns out that low and medium alloyed steels are also good candidates for matrix of MMCs (especially with wear properties) [14, 25, 26]. But thus far there have only been very few papers relating to these particulate-reinforced MMCs [1, 2, 14].

The microstructure and mechanical properties of sintered Distaloy DC – SiC composites were studied [2]. It was stated that the increase in SiC_p content (from 0.5 wt. % to 1 wt. %) decreased the density of sintered Distaloy DC – SiC composites but improved their hardness and wear resistance.

Articles [1, 14] deal with Distaloy SA and Distaloy AE MMCs reinforced with SiC particles in an amount of 20%. It was stated that these composites exhibited higher hardness and wear resistance, as well as mechanical properties in comparison with sintered Distaloy steels.

In this study different Distaloy matrix composites reinforced with SiC particles were produced using the conventional powder metallurgy technology. They were prepared from prealloyed and diffusion bonded Distaloy SA and Distaloy SE powders mixed with silicon carbide in the amount of 2 and 4 wt. %. The primary aim of this study was to determine the effect of the chemical composition on microstructure evaluation and selected properties of sintered Distaloy – SiC composites.

2. Materials for research

In the present studies, prealloyed and diffusion bonded powders of Distaloy SA and Distaloy SE (manufactured by Höganäs) were used. The chemical composition of these powders is shown in Table 1. Silicon carbide (product of ALDRICH Chemistry, purity of 99.8 %) was used as particulate reinforcement.

Table 1. Chemical composition of Distaloy SA and Distaloy SE powders (wt.%)

	Ni	Cu	Mo	Fe
Distaloy SA	1.75	1.50	0.50	Bal.
Distaloy SE	4.00	1.50	0.50	Bal.

The following powder mixtures were prepared:

- Distaloy SA – 2 wt.% SiC,
- Distaloy SA – 4 wt.% SiC,
- Distaloy SE – 2 wt.% SiC,
- Distaloy SE – 4 wt.% SiC.

In order to compare the results, pure Distaloy SA and Distaloy SE powders were also used in these studies.

3. Experimental procedure

The abovementioned powder mixtures were prepared by mixing in a Turbula® mixer for 5 hours. Then different compositions of mixed Distaloy – SiC powders and also Distaloy powders were uniaxially pressed in a rigid matrix at 600 MPa into cylindrical samples of size 20×5 [mm]. The sintering process was carried out in a Nabertherm furnace. All green compacts were sintered in a pure (99.9992%) and dry (dew point below –60°C) hydrogen atmosphere. The flow rate of the gas was 100 ml/min. The temperature of isothermal sintering was 1240°C. The sintering time was 60 minutes. The samples were slowly heated to the isothermal sintering temperature at a rate of 10°C/min. The cooling rate from sintering temperature to ambient temperature was also 10°C/min.

The density measurements of green compacts were carried out by the geometrical method. The density and porosity of the sintered samples were measured by the water-displacement method (according to the demands of the PN-EN ISO 2738:2001 norm).

Before and after sintering, samples were measured to estimate dimensional changes (PN-EN ISO 4492:2013-07E).

According to PN-EN ISO 4498:2010E the hardness by Vickers method was determined with the computer-aided hardness tester INNOVATEST CV-600.

Wear tests were performed by a ball-on-disc method using a T01-M tester. The various applied loads (10 and 20 N) and sliding speeds (0.12 and 0.2 m/s) and a constant sliding distance of 500 m were used. All wear tests were performed in air and without any lubricant. The wear resistance of the composites was evaluated by means of wear rate.

Metallographic cross-sections were prepared. The microstructural study of the sintered metal matrix composites was conducted with a Nikon Eclipse ME 600P Light Optical Microscope.

4. Results and discussion

In Figure 1a) the effect of SiC content on green and sintered density of Distaloy SA and Distaloy SA – SiC composites are shown. Figure 1b) presents the same dependence but for Distaloy SE and Distaloy SE – SiC composites. In these composites, the proportions of the matrix and particulate reinforcement are expressed as the weight fraction because it is appropriate to fabrication. However, the weight fraction was converted to volume fraction because it is generally used in property calculations. The rule of mixture is commonly known because it helps in approximating the property values such as the density of composites. Figures 1a) and 1b) also show the values of theoretical sintered density in comparison with the measured density values of the studied Distaloy SA-SiC and Distaloy SE-SiC composites with different weight percentage of SiC.

It can be observed that Distaloy SA has higher green and sintered density in comparison to Distaloy SE, but also Distaloy SA matrix composites reinforced with SiC particles exhibit higher values of these densities relative to Distaloy SE-SiC composites.

It can be concluded that the presence of SiC particulate reinforcement caused a reduction in density (as compared to matrix materials) after pressing as well as the sintering process. By adding SiC to Distaloy up to 4 wt. % green and sintered density decrease. The decrease in density may be attributed to the low density of the SiC particles. An addition of SiC particles impedes material densification during sintering and lower relative densities were obtained for sintered Distaloy SA – SiC and Distaloy SE – SiC composites. The effect of the increased number of SiC particles on the deterioration of sinterability was also found in the case of sintered Distaloy DC – SiC composites [2].

In the case of both Distaloy SA – SiC and Distaloy SE – SiC composites, the values of theoretical and experimental sintered density are different from each other, but the trend of density change is the same: the higher the SiC content, the lower the sintered density. It can be assumed that the SiC particles inhibit the transport mechanisms leading to densification of the matrix material during sintering.

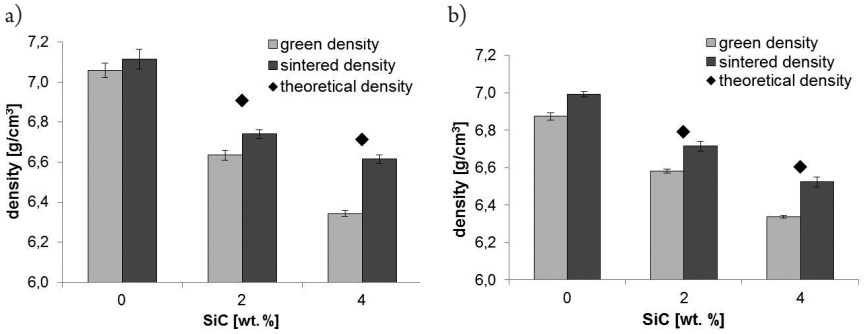

Fig. 1. Green density, theoretical and experimental sintered density:
a) Distaloy SA-SiC composites, b) Distaloy SE-SiC composites

As can be seen in Figures 2a) and 2b), Distaloy-SiC composites exhibit slightly higher open and closed porosity in comparison to sintered Distaloy and furthermore increase of SiC content up to 4 wt. % decreases values of porosity.

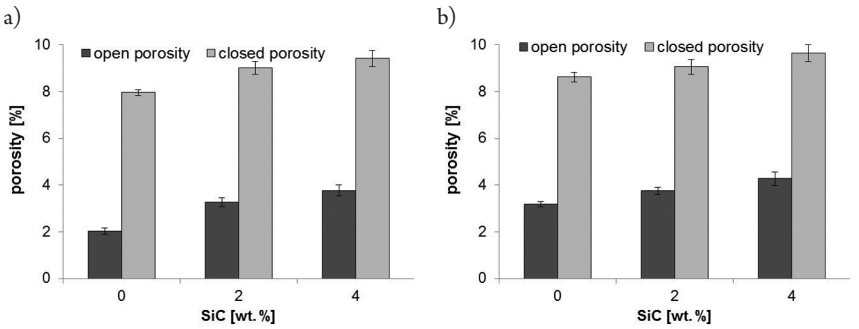

Fig. 2. Open and closed porosity:
a) Distaloy SA-SiC composites, b) Distaloy SE-SiC composites

In order to designate the dimensional change, measurement of samples heights was carried out before and after the sintering process. Figure 3 presents the results obtained. It can be observed that the samples of Distaloy as well as the composites undergo shrinkage during sintering. Distaloy SA shows a slightly higher shrinkage and better densification compared to Distaloy SE. In the case of the composites, increasing SiC content up to 4 wt. % leads to raising the shrinkage, but this increase in dimensional change does not improve densification. Higher green and sintered density and smaller dimensional shrinkage were observed in Distaloy SA and Distaloy SE.

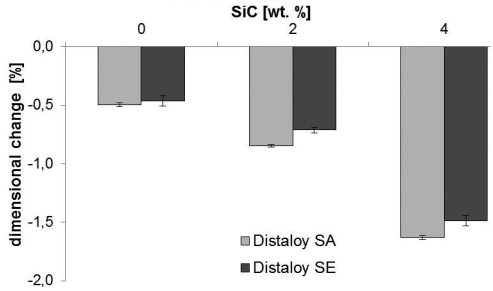

Fig. 3. Dimensional change (designated after sintering) for studied materials

The results of the hardness measurement by the Vickers method of materials studied are presented in Figure 4. It can be observed that Distaloy SA exhibits slightly higher hardness in comparison to Distaloy SE. This is explained by the lower nickel content in the chemical composition of Distaloy SA (1.75% Ni) and higher martensite fraction. The presence of particulate reinforcement effects a significant increase in the hardness of the sintered Distaloy SA – SiC as well as Distaloy SE – SiC composites. An increasing SiC content up to 4 wt. % leads to a maximum hardness in the composites studied. The increase in hardness is related to higher hardness of SiC in comparison to the matrix materials. It can be stated that this is in accordance with the mixtures rule. The introduction of reinforcement having higher hardness to a matrix material with lower hardness leads to higher hardness of composite.

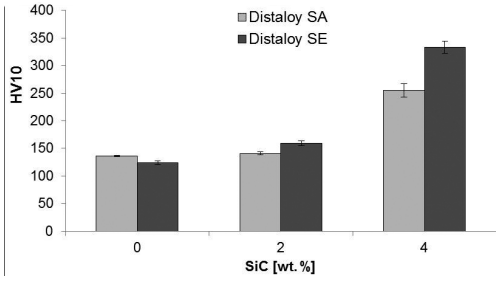

Fig. 4. The effect on SiC content on hardness of sintered Distaloy SA – SiC and Distaloy SE – SiC composites

Figure 5 shows the variation of the wear rate of the materials investigated. It can be observed that regardless of the applied loads, the wear rate of both Distaloy SA – SiC and

Distaloy SE – SiC composites is significantly lower than that of their matrix materials and furthermore it decreases with the increase SiC content. It can be seen that the wear rate of the sintered steels as well as the composites increases with applied load.

This was also observed in the relationship between the hardness and the wear rate of these composites. Namely, the higher the hardness, the lower the wear rate. It can be concluded that Distaloy matrix composites reinforced with 4 wt.% SiC reach the highest hardness and wear resistance. These results are consistent with paper [2], namely with the increase in silicon carbide particles (from 0.5 up to 1 wt. %), the micro-hardness and wear rate values of Distaloy DC matrix composites improved.

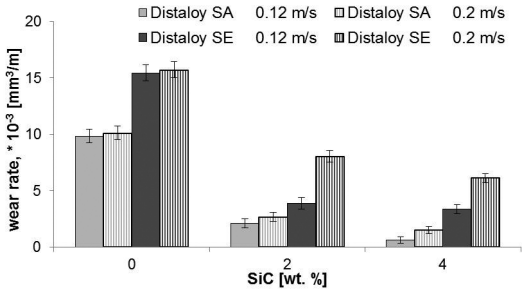

Fig. 5. The effect on SiC content on wear rate of sintered Distaloy SA – SiC and Distaloy SE – SiC composites

It was confirmed that the microstructure of sintered Distaloy SA and Distaloy SE is a mixture of different phases: ferrite, bainite/pearlite, martensite and Ni-rich austenite [28]. This is due to the chemical heterogeneity of Cu, Ni and Mo elements and their low diffusion rate at the sintering temperature. The microstructure observation leads to the following statements. A significant difference in the morphology of porosity between sintered Distaloy and Distaloy matrix composites reinforced with SiC particles was not found. The shape and size of pores are almost the same. Practically all pores are irregular in shape and partially connected to each other.

The selected microstructures of the composites studied are presented in Figures 6–10.

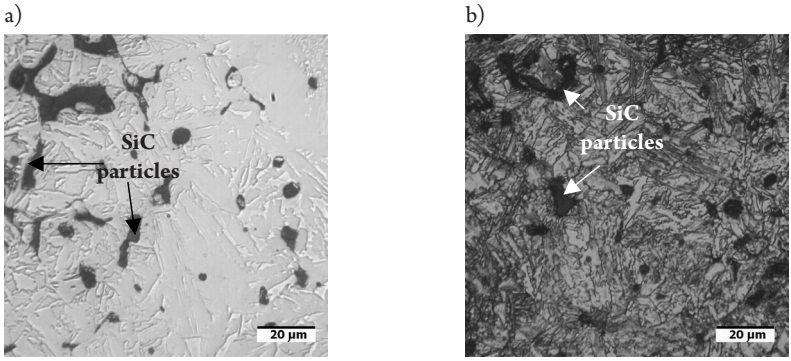

Fig. 6. Microstructure of sintered Distaloy SA – 2 wt.% SiC composites: a) unetched, b) Nital etched

The microstructure studies revealed that the microstructure of investigated materials is heterogeneous. No microstructural gradient between the surface and the centre of the sample was observed. The distribution of SiC particles is nearly homogeneous. It should be pointed out that the slight agglomeration of fine SiC particles and formation of porous structure in the areas adjacent to these particles occur in the microstructure of sintered Distaloy SA and Distaloy SE matrix composites. In the case of the composites studied, the microstructure basically consists of a mixture bainite, martensite, ferrite and, of course SiC particles on the grain boundaries.

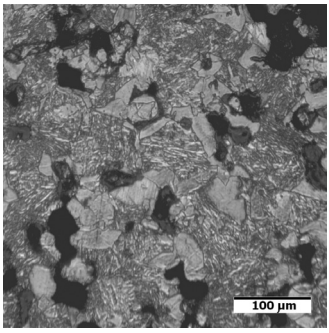

Fig. 7. Microstructure of sintered Distaloy SA – 4 wt.% SiC composites.

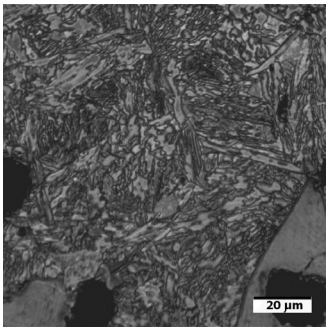

Fig. 8. Microstructure of sintered Distaloy SA – 4 wt.% SiC composites.

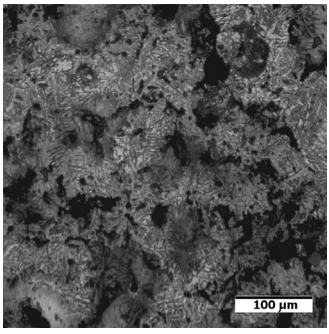

Fig. 9. Microstructure of sintered Distaloy SE – 2 wt.% SiC composites

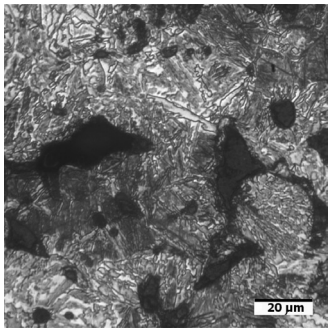

Fig. 10. Microstructure of sintered Distaloy SE – 2 wt.% SiC composites

5. Conclusion

Based on commercially available grades of prealloyed and diffusion bonded powders, metal matrix composites reinforced with SiC particles were manufactured using the conventional powder metallurgy technology. The experimental results showed that the mass fraction of SiC has an impact on properties such as the density, porosity, shrinkage, hardness and wear resistance of these composites.

The nickel content in the chemical composition is the basic difference between Distaloy SA and Distaloy SE alloys. In effect, differences in densification after pressing and sintering, as well as the hardness of these materials, can be noted.

The microstructure studies revealed that the particle distribution is nearly homogeneous. Moreover, the agglomeration of fine SiC particles was observed, as was the formation of porous structure in the areas adjacent to these particles. The latter have resulted in lower densification and higher porosity of studied composites in comparison to sintered Distaloy. The green density as well as sintered density of Distaloy SA and Distaloy matrix composites decrease by increasing the particulate reinforcement whereas the open and closed porosity increase.

The hardness of these composites increases with the increasing SiC content. The increase of hardness is related to the presence of hard SiC particles on the grain boundaries of material matrix.

The results obtained show that the constituents of microstructure and hardness are important parameters affecting the wear behaviour of sintered materials. Materials with microstructure containing basically mixture of martensite, bainite and SiC particle display a lower wear rate. The higher the hardness of the investigated materials the lower the wear rate, and thus the higher wear resistance.

It was concluded that in the case of both Distaloy SA and Distaloy SE the optimum SiC content is 4 wt. % due to the highest wear resistance and hardness of the sintered composite.

References

[1] Badoi I., Dumitru N., Bojin D., *Microstructure and Mechanical Behaviour of SiC Particles Reinforced in Aluminium and Iron Matrix Composites*, Brasov CEEX Conference, 2008, July 27–29.

[2] Öksüz K., Kumruoğlu L., Tur O., *Effect of Sic_p on the Microstructure and Mechanical Properties of Sintered Distaloy DC Composites*, "Procedia Materials Science", 11/2015, 49–54.

[3] Rawal S., *Metal-matrix composites for space applications*, "JOM", 53/2001, 14–17.

[4] Abhik R., Xaviora M., *Evaluation of Properties for Al-SiC Reinforced Metal Matrix Composite for Brake Pads*, "Procedia Engineering", 97/2014, 941–950.

[5] Venkatesh B., Harish B., *Mechanical properties of metal matrix composites (Al/SiC_p) particles produced by powder metallurgy*, "International Journal of Engineering Research and General Science", 3(1)/2015, 1277–1284.

[6] Zakaria H.M., *Microstructural and corrosion behavior of Al/SiC metal matrix composites*, "Ain Shams Engineering Journal", 5(3)/2014, 831–838.

[7] Akhtar F., *Ceramic reinforced high modulus steel composites: processing, microstructure and properties*, "Canadian Metallurgical Quarterly", 53(3)/2014, 253–263.

[8] Singla M., Dwivedi D., Singh L., Chawla V., *Development of Aluminium Based Silicon Carbide Particulate Metal Matrix Composite*, "Journal of Minerals & Materials Characterization & Engineering", 8(6)/2009, 455–467.

[9] Kumar G., Rao C., Selvaraj N., *Mechanical and Tribological Behavior of Particulate Reinforced Aluminum Metal Matrix Composites – a review*, "Journal of Minerals & Materials Characterization & Engineering", 10(1)/2011, 59–91.

[10] Leszczyńska-Madej B., *The effect of sintering temperature on microstructure and properties of Al – SiC composites*, "Archives of Metallurgy and Materials", 58(1)/2013, 43–48.
[11] Nuruzzaman D., Kamaruzaman F., *Processing and mechanical properties of aluminium-silicon carbide metal matrix composites*, "Materials Science and Engineering", 114/2016, 11–17.
[12] Suryanarayanan K., Praveen R., Raghuraman S., *Silicon Carbide Reinforced Aluminium Metal Matrix Composites for Aerospace Applications: A Literature Review*, "International Journal of Innovative Research in Science, Engineering and Technology", 2(11)/2013, 6336–6344.
[13] Baisane V. P., Sable Y.S., Dhobe M. M., Sonawane P.M., *Recent development and challenges in processing of ceramics reinforced Al matrix composite through stir casting process: A Review*, "International Journal of Engineering and Applied Sciences", 2(10)/2015, 11–16.
[14] Badoi I., Tudor A., *Development and wear characterization of metal matrix composites in systems prealloyed steel powders reinforcement with SiC and Al_2O_3 particles*, Brasov CEEX Conference, 2008, July 27–29.
[15] Carvalho O., Madeira S., Buciumeanu M., Soares D., Silva F.S., Miranda G., *Pressure and sintering temperature influence on the interface reaction of SiC_p/410L stainless steel composites*, "Journal of Composite Materials", 50(15)/2016, 2005–2015.
[16] Saravanan C., Subramanian K., Ananda V., Sankara R., *Effect of Particulate Reinforced Aluminium Metal Matrix Composite – A Review*, "Mechanics and Mechanical Engineering", 19(1)/2015, 23–30.
[17] Yodkaew T., Morakotjinda M., Tosangthum N., Coovattanachai O., Krataitong R., Siriphol P., Vetayanugul B., Chakthin S., Poolthong N., Tongsri R., *Sintered Fe-Al_2O_3 and Fe-SiC*, "Composites Journal of Metals, Materials and Minerals", 18(1)/2008, 57–61.
[18] Chakthin S., Poolthong N., Thavarungkul N., Tongsri R., *Iron-Carbide Composites Prepared by P/M*, "Processing Materials for Properties", 2009, 577–584.
[19] Chakthin S., Morakotjinda M., Yodkaew T., Torsangtum N., Krataithong R., Siriphol P., Coovattanachai O., Vetayanugul B., Thavarungkul N., Poolthong N., Tongsri R., *Influence of Carbides on Properties of Sintered Fe-Base Composites*, "Journal of Metals, Materials and Minerals", 18(2)/2008, 67–70.
[20] Mima S., Yotkaew T., Morakotjinda M., Tosangthum N., Daraphan A., Krataitong R., Coovattanachai O., Vetayanugul B., Tongsri, *Carbide-Reinforced 316L Composite*, The Fourth Thailand Materials Science and Technology Conference, Pathum Thani, Thailand, 31 March –1 April 2006.
[21] Coovattanachai O., Mima S., Yodkaew T., Krataitong R., Morkotjinda M., Daraphan A., Tosangthum N., Vetayanugul B., Panumas A., Poolthong N., Tongsri R., *Effect of admixed ceramic particles on properties of sintered 316L stainless steel*, "Advances in Powder Metallurgy and Particulate Materials", 7/2006, 161–171.
[22] Carvalho O., Soares D., Silva F.S., *Optimization of sintering temperature and compaction pressure of stainless steel/SiC composites*, 8º Congresso Nacional de Mecânica Experimental Guimarães, April 21–23, 2010.

[23] Ertugrul O., Park H.S., Onel K., Willert-Porada M., *Structure and properties of SiC and emery powder reinforced PM 316L matrix composites produced by microwave and conventional sintering*, "Powder Metallurgy", 58(1)/2015, 41–50.
[24] Lindskog P., *The history of Distaloy*, "Powder Metallurgy", 56(5)/2013, 351–361.
[25] Karwan-Baczewska J., *Processing and properties of Distaloy SA sintered alloys with boron and carbon*, "Archives of metallurgy and materials", 60(1)/2015, 41–45.
[26] Zarebski K., Putyra P., *Iron powder-based graded products sintered by conventional method and by SPS*, "Advanced Powder Technology", 26/2015, 401–408.
[27] Öksüz K.E., Gün T., Şimşir M., *The microstructure and wear behaviour of sintered Astaloy 85Mo*, "Transactions on Engineering Sciences", 137/2014, 545–552.
[28] *Metallography, Höganäs Handbook for Sintered Components*, eds. Höganäs AB, 2015.

TECHNICAL TRANSACTIONS 6/2017
CZASOPISMO TECHNICZNE 6/2017
MECHANICS
DOI: 10.4467/2353737XCT.17.100.6576

Ryszard Wójtowicz (rwojtowi@pk.edu.pl)
Institute of Thermal and Process Engineering, Faculty of Mechanical Engineering, Cracow University of Technology, Cracow, Poland

Andrey A. Lipin
Aleksandr G. Lipin
Faculty of Chemical Engineering and Cybernetics, Ivanovo State University of Chemistry and Technology

The performance of the Rushton turbine eccentrically positioned in a mixing vessel. Part I: the qualitative CFD analysis

Charakterystyka pracy mieszadła turbinowego Rushtona usytuowanego ekscentrycznie w mieszalniku. Część I: analiza jakościowa CFD

Abstract

A qualitative analysis of a liquid flow generated by a *Rushton* turbine eccentrically located in an unbaffled mixing vessel is presented in this paper. On the basis of *CFD* simulations the influence of the impeller position in the vessel on the flow pattern, velocity distributions and turbulence parameters are examined. Data are presented in visualisations and distribution maps created with various flow visualisation criterions. The results of this work can be used for the design and optimisation of mixing equipment applied in the industry.

Keywords: mixing, Rushton turbine, impeller eccentricity, flow circulation, CFD simulations

Streszczenie

Przeprowadzono jakościową analizę przepływu cieczy generowanego przez mieszadło turbinowe tarczowe Rushtona, usytułowane ekscentrycznie w mieszalniku bez przegród. Na podstawie symulacji numerycznych CFD określano wpływ położenia mieszadła w zbiorniku na wybrane parametry przepływu, tj. model przepływu, rozkłady prędkości cieczy czy też parametry burzliwości. Dane symulacyjne opracowano w postaci grafik wizualizacyjnych oraz wektorowych i konturowych map rozkładu, tworzonych w oparciu o różne kryteria wizualizacji przepływu. Uzyskane wyniki mogą być wykorzystane podczas konstruowania i optymalizacji aparatów z mieszadłami stosowanych w warunkach przemysłowych.

Słowa kluczowe: mieszanie, mieszadło turbinowe Rushtona, niecentryczność mieszadła, przepływ cieczy, symulacje CFD

1. Introduction

The *Rushton* turbine is one of the most popular impellers used in mechanically agitated vessels [1]. It is characterised by universality in use for various multiphase systems (gas-liquid, liquid-liquid or solid-liquid systems) and mixing effectiveness [2]. The primary issue for the description of the *Rushton* turbine's performance is the investigation and analysis of the quantities and parameters in a generated flow. They determine the efficiency of the mixing processes, e.g. breakup of drops, bubbles or suspension of solid particles. There are numerous papers focused on investigations/measurements of flow generated by the *Rushton* turbine in the literature [3–5]. In their experiments, the authors used different, usually advanced research techniques, e.g. *CFD* modelling [3], *Particle Image Velocimetry (PIV)* [4] or *Laser Doppler Anemometry (LDA)* [5]. However, most of these experiments were conducted in standard mixing vessels equipped with baffles of a standard design and geometry.

An interesting alternative to standard, baffled mixing vessels are unbaffled ones with eccentrically (not in accordance with the tank axis located) impeller [1]. The impeller displacement causes a change in the flow pattern in the vessel. Distinct, asymmetric circulation loops are induced in the apparatus. For identification of liquid flow generated by an eccentrically positioned *Rushton* turbine, numerical modelling and *CFD* simulations were applied. This study is a continuation of the research described in [6].

2. Computational model

The stirred vessel analysed in the numerical investigations is shown in Figure 1. It consists of an unbaffled cylindrical tank *1* (internal diameter $D = 0.286$ m) with a flat bottom. Inside the tank a single, standard *Rushton* turbine *2* was located (Fig. 1b). The impeller has the diameter $d = D/3$ and the impeller off-bottom clearance was set at $h = d$. The impeller rotated clockwise at $n = 300$ [1/min], in the range of fully turbulent flow ($Re_m \approx 4{,}5 \cdot 10^4$). Distilled water ($\rho = 998$ kg m^3, $\eta = 0{,}001$ Pa·s (at 20°C)) was taken as the tested liquid. The liquid height for all simulations was set at $H = D$. An impeller was located in three different positions inside the tank. Its distance from the tank axis was: $e = 0$ (central position, in accordance with the tank axis) as well as $e = 0.25R$ and $e = 0.5R$, where R is the tank radius. Flow identification in a stirred vessel was carried out based on results of numerical modelling, applying as a mesh generator *GAMBIT 2.4*. For all the mixing vessels tested an un-structural numerical mesh consisting of approximately $7.5 \cdot 10^5$ tetrahedral cells was generated. Model equations were solved using the numerical solver *FLUENT 6.3.26* and the finite volume *(FV)* method. The movement of the impeller was modelled with the multiple reference frames *(MRF)* mode. For a mathematical description of the turbulent liquid flow in a stirred vessel the standard *Navier – Stokes* equations were averaged using the *Reynolds* averaging *(RANS)* approach. Modelling of turbulence was carried out using – recommended for stirred vessels [7] – the *Realizable k-ε* turbulence model with standard wall functions. Detailed information on the mixing vessel design, methodology of simulations and their experimental verification is presented elsewhere [6, 7].

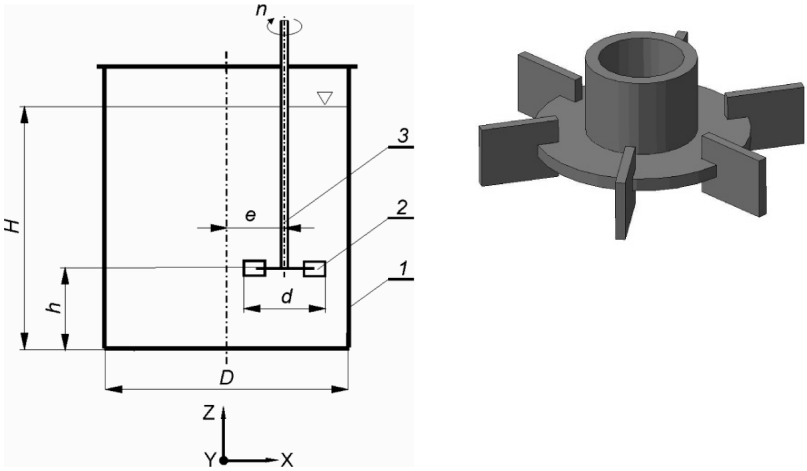

Fig. 1. Stirred vessel with an eccentrically positioned impeller: a) stirred vessel geometry: 1 – cylindrical tank, 2 – impeller, 3 – shaft, b) Rushton turbine

3. Results and discussion

The analysis of the flow generated by an eccentrically positioned *Rushton* turbine was conducted on the basis of qualitative visualisations, created with various flow visualisation criteria (iso-surface graphs, contour and vector maps).

For proper impeller design and structural calculations it is necessary to know the values of the pressure exerted by the liquid on the main elements of the impeller, such as blades, hub and disc. Figure 2 shows contour maps of the total pressure exerted on the *Rushton* turbine, located at positions investigated.

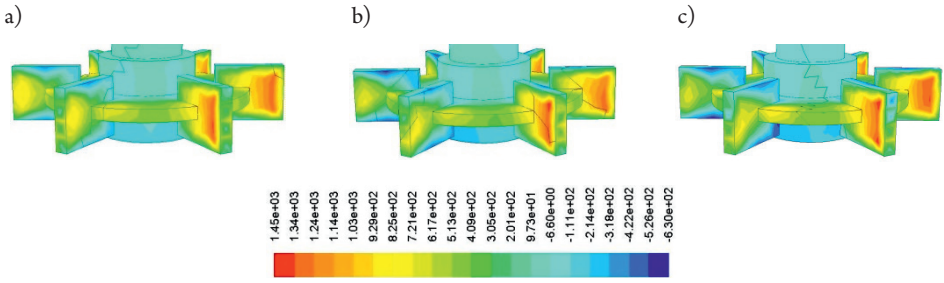

Fig. 2. Contour maps of a total pressure [Pa] exerted on eccentrically positioned Rushton turbine: a) $e = 0$, b) $e = 0.25\ R$, c) $e = 0.5\ R$

The maximum values of the total pressure – independently of impeller eccentricity e – are determined on the front sides of the blades, at the blade's tip. Slightly lower values are observed on the disc between neighbouring blades. On the rear sides of the blades, the pressure distribution is very differential. Close to the blade tip we can see narrow regions of

positive values of pressure, while on the remaining area the total pressure is significantly lower and has negative values (underpressure). Underpressure maximum values were determined close to the top and bottom edge of the blade. The total pressure exerted on the hub and the shaft is low and negligible. Simulations did not show significant differences in the total pressure values with shaft displacement. When the impeller was positioned eccentrically (e = 0.25R or e = 0.5R) the maximum values of the total pressure on the front sides of blades were close (1443 [Pa] and 1448 [Pa] respectively), whereas when the impeller was in a central position (e = 0), the maximum values for the total pressure are slightly (about 5%) lower. Larger differences were observed in the values of underpressure (rear sides of blades). Maximum values of underpressure were determined for the largest shaft eccentricity (e = 0.5R) and differed in comparison with central shaft position (e = 0) by 30%.

During the *Rushton* turbine rotation vortices that differ in shape and scale are generated in the mixing vessel. Some of them have a scale comparable with the apparatus scale [6], the others are smaller and they are inducted in the impeller zone. A location of vortex cores can be visualised in a number of different ways, e.g. Q-criterion, λ – criterion or iso-surfaces of vorticity or helicity. Figure 3 presents example visualisations of trailing vortices generated behind *Rushton* turbine blades, created with the use of the Q-criterion. This criterion is defined as:

$$Q = \frac{1}{2}[|\Omega|^2 - |S|^2] > 0$$

where:

S – the rate-of-strain tensor and Ω is the vorticity tensor.

Each visualisation is prepared at the same scale (Q = 1500 [s^{-2}]). Iso-surfaces are additionally coloured by velocity magnitude.

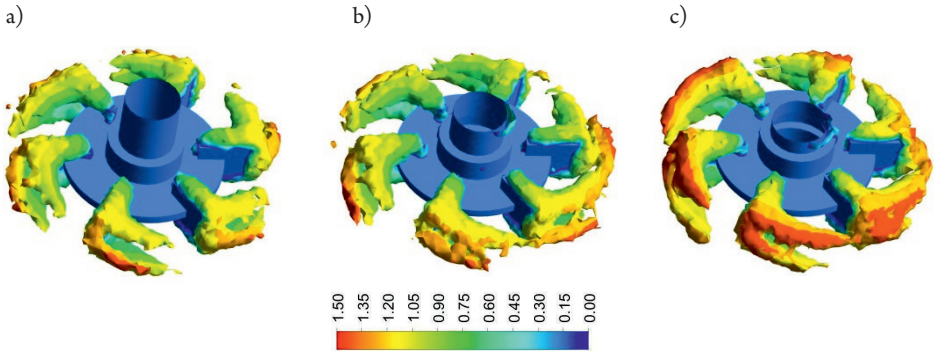

Fig. 3. Trailing vortices behind blades of an eccentrically positioned Rushton turbine (iso-surfaces of Q-criterion (Q = 1500 [s^{-2}] coloured by velocity magnitude [m/s], a) e = 0 , b) e = 0.25 R, c) e = 0.5 R

The movement of the impeller blades induces an intense flow in the blade zone. Firstly, liquid swirls are observed on the front side of the blades and close to the blade edges. Next, two separate, longitudinal trailing vortices above and below the impeller disc are generated. They are elongated in a tangential flow field. The biggest scale trailing vortices are seen for the highest impeller eccentricity e = 0.5R (Fig. 3c). For this case the greatest tangential velocities

were also determined. The above-presented numerical visualisations of trailing vortices formation were confirmed experimentally, e.g. [1, 2, 8].

As a result of an impeller blade movement the main liquid flow is divided into a tangential flow and a radial one. Figure 4 presents velocity vector maps obtained for the vessel's vertical cutting plane (XZ), passing through the vessel axis and collinear with the impeller displacement. These maps show the distribution of velocity vectors for a radial-axial direction.

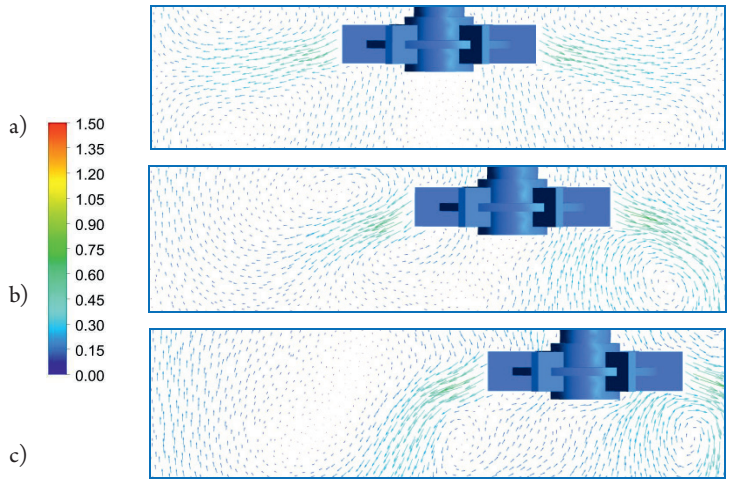

Fig. 4. Vector maps of flow inducted by eccentrically positioned Rushton turbine coloured by velocity magnitude [m/s], a) $e = 0$, b) $e = 0.25\ R$, c) $e = 0.5\ R$

With impeller displacement towards the vessel wall the flow pattern changes. For a central impeller position (Fig. 4a), the generated discharge streams are radial and symmetrical. Displacement of the impeller towards the vessel wall causes a visible deflection of the discharge stream to the bottom and a generation of small-scale vortices in the zone close to the tank wall, under the impeller (Fig. 4b, c). These changes and differences in the flow pattern were caused by the effect of the vessel wall and the generation of unsymmetrical, large-scale vortices, which are initiated in the impeller region [6]. Preliminary comparisons of these maximum values of tangential velocities (Fig. 3) with radial ones showed that tangential components are about 30% greater.

One of the parameters that characterise a turbulence flow in mixing vessels is turbulence kinetic energy k *(TKE)*. This quantity is often used for the estimation of impeller performance efficiency, characterisation of turbulence in an impeller discharge stream and also in dispersion processes. The contour maps presented in Figure 5 show changes of k with impeller eccentricity and confirm earlier described observations and tendencies. When the impeller eccentricity increases, the maximum values of *TKE* increase too (from 0.128 to 0.143 [m^2/s^2], 16%). For $e = 0.5R$ (Fig. 5c), the zones of high turbulence kinetic energy in the vicinity of the impeller are wider and they have greater scope. However, in this location regions of low k values are observed in the opposite part of the vessel. It is noteworthy that this paper mainly presents a qualitative analysis. In second part of this paper a full quantitative analysis of an eccentrically positioned

Rushton turbine performance will be presented, based on CFD modelling as well as Laser Doppler Anemometry (LDA) measurements. Also the advantages and disadvantages of the investigated solution in comparison with conventional, baffled mixing vessels will be discussed.

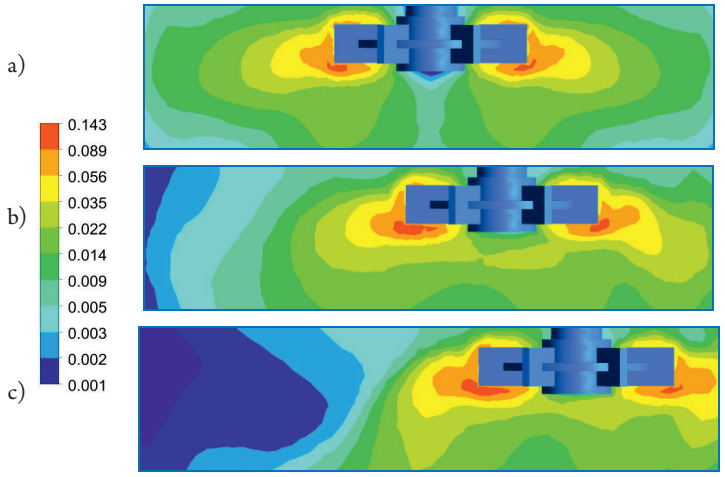

Fig. 5. Contour maps of turbulence kinetic energy k [m^2/s^2] for eccentrically positioned *Rushton* turbine: a) $e = 0$, b) $e = 0.25\ R$, c) $e = 0.5\ R$

References

[1] Paul E.L., Atiemo-Obeng W.A., Kresta S.M., *Handbook of Industrial Mixing,* Wiley & Sons Inc., New Jersey 2004.

[2] Kamieński J., *Mixing of muliphase systems*, WNT, Warszawa 2004 (in Polish).

[3] Taghavi M., Zadghaffari R, Moghaddas J., Moghaddas Y., *Experimental and CFD investigation of power consumption in a dual Rushton turbine stirred tank,* Chemical Engineering Research and Design, 89 (3), 2011, 280–290.

[4] Li Z., Bao Y., Gao Z., *PIV experiments and large eddy simulations of single-loop flow fields in Rushton turbine stirred tanks,* Chemical Engineering Science, 66 (6), 2011, 1219 –1231.

[5] Kamieński J., Talaga J., Wójtowicz R., Duda A., *Parameters of turbulence in a stirred vessel equipped with two impellers,* Chemical and Process Engineering, 28 (3), 2007, 783–793.

[6] Wójtowicz R., Lipin A.A., *The Computational-Fluid-Dynamics study of an unbaffled stirred vessel with eccentrically positioned impeller,* Czasopismo Techniczne, 1-Ch/2015, 2015, 99–108.

[7] Wójtowicz R., Lipin A.A., Talaga J, *On the possibility of using of different turbulence models for modeling flow hydrodynamics and power consumption in mixing vessels with turbine impellers*, Theoretical Foundations of Chemical Engineering, 48 (4), 2014, 360–375.

[8] Bowen R.L. Jr, *Unraveling the mysteries of shear sensitive mixing*, Chemical Engineering, 9, 1986, 55–63.

TECHNICAL TRANSACTIONS 6/2017
CZASOPISMO TECHNICZNE 6/2017
MECHANICS
DOI: 10.4467/2353737XCT.17.101.6577

Krzysztof Wach (krzysztof.wach@mech.pk.edu.pl)
Institute of Automobiles and Internal Combustion Engines, Faculty of Mechanical Engineering, Cracow University of Technology

Robert Kupiec
Laboratory of Coordinate Metrology, Faculty of Mechanical Engineering, Cracow University of Technology

Determination of initial configuration of mechanism of an instrument for measuring the translation and rotation of a steered wheel

Wyznaczanie konfiguracji poczatkowej mechanizmu przyrządu do pomiaru translacji i rotacji koła kierowanego

Abstract

This paper concerns the determination of the initial configuration of a mechanism of a prototypical instrument for measuring the translation and rotation of a steered wheel. It covers the determination of coordinates of characteristic points of the mechanism. They were measured using a ROMER measuring arm. In the paper the methodology of measurements is discussed, and in addition the results obtained are presented and their analysis conducted.

Keywords: car, steered wheel, prototypical measuring instrument, coordinate measurements, ROMER measuring arm

Streszczenie

Praca dotyczy wyznaczania konfiguracji początkowej mechanizmu prototypowego przyrządu do pomiaru translacji i rotacji koła kierowanego. Polegało to na wyznaczeniu współrzędnych charakterystycznych punktów jego mechanizmu. Pomiary przeprowadzono z wykorzystaniem ramienia pomiarowego firmy ROMER. W pracy została omówiona metodologia pomiarów, przedstawiono uzyskane wyniki oraz przeprowadzono ich analizę.

Słowa kluczowe: samochód, koło kierowane, prototypowy przyrząd pomiarowy, pomiary współrzędnościowe, ramię pomiarowe ROMER

1. Introduction

An analysis of car movement parameters is one of the fundamental issues of stability and steerability. Change of the forces generated at the wheel-road contact is dependent on many factors associated with tyre, suspension and steering system construction. Steering wheels are carried out through the spatial mechanisms with flexible constraints [1]. The flexibility is the reason that during a car's movement along the same path, at different speeds, the real kinematic steering ratio changes; a significant difference between the real and theoretical steering angles appears. The measurement of real steering and camber angles in experimental car studies has a significant value. The results of these measurements are used to work outthe relationships between car movement parameters as well as for stability and steerability valuation [2–4]. The measurement of the position and orientation of the wheel relative to the car body is very difficult, only a few studies on this topic can be found in the literature [2, 5–9]. The measurement is complicated and the measured values are not obtained directly but as a result of complex calculations.

The best known devices that allow the measurement of the position and orientation of the steered wheel relative to the car body are the Datron RV-3 and RV-4 instruments [10].

This paper concerns the determination of the initial configuration of the mechanism of a working model of a prototype instrument for linear and angular displacements of steered wheel measurement.

2. Proposed instrument for translation and rotation of steered wheel measurement

The proposed instrument for measuring the translation and rotation of a steered wheel is composed of two plates: external and internal, connected with nine links with linear displacements sensors built in. The external plate (Fig. 1) is fixed to the vehicle body, while the inner plate (Fig. 2) is kinematically connected with the axis of the steered wheel hub. The connection is made using bearing hub. The links of the instrument are attached to the both plates via ball joints, there are 9 joints named H_i, $i = 1–9$ in the case of the external plate and 3 joints named D_j, $j = 1–3$ in the case of the inner plate. A characteristic feature of the joints D_j is that each of them realizes the function of three ball joints with a common centre.

The measurement of angular and linear displacements of a steered wheel of a car, using the prototypical instrument, requires knowledge of the initial configuration of its mechanism. For this purpose it is necessary to know the coordinates of the ball joints D_j, $j = 1–3$ and H_i, $i = 1–9$ in a Cartesian coordinate system $\{x, y, z\}$ attached to the vehicle body. The origin of the system is located at the external plate fixed to the vehicle body (Fig. 1). The coordinates of ball joints centres H_i, $i = 1–9$ were determined using the coordinate measurement method, while the coordinates of the centres of the ball joints D_j, $j = 1–3$ were calculated using mathematical dependences (see Equations (2) and (3)).

An overview of the prototype instrument attached to a car wheel is shown in Fig. 4.

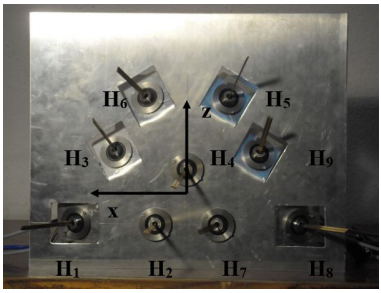

Fig. 1. The external plate of the prototypical instrument for measurement of linear and angular displacements of the steered wheel in overview. The Cartesian coordinate system and the positions of the ball joints H_i, i = 1–9 were marked in the photo

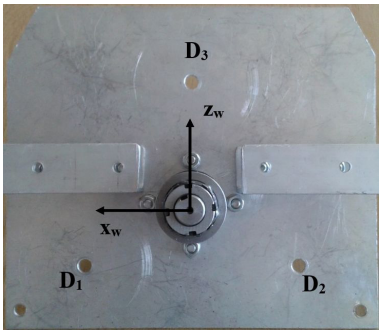

Fig. 2. An overview of the internal plate of the prototypical instrument for measurement of the linear and angular displacements of the steered wheel. Positions of the ball joints D_j, j = 1–3 and the Cartesian coordinate system connected with the plate is shown (The y_w – axis coincides with y – axis of the coordinate system connected with the external plate)

The plain bearings, shown in Fig. 3, were used as the joints D_j, j = 1–3 and H_i, i = 1 (9).

a)

b)

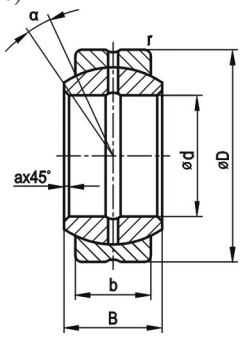

d [mm]	*D* [mm]	*B* [mm]	*b* [mm]	*r* [mm]	*a* [mm]	*α* [°]
16	32	21	15	0.8	0.3	15

Fig. 3. Spherical plain bearings ISKRA PGE 16X [11] used for fixing the links of the instrument to the external and internal plate: a) overview b) dimensions

Fig. 4. An overview of the prototype measuring instrument attached to the car wheel

3. Determination of coordinates of characteristic points of instrument's mechanism

The coordinates of points H_i, i = 1–9 were determined using a ROMER measuring arm [12] shown in Fig. 5.

a) b)

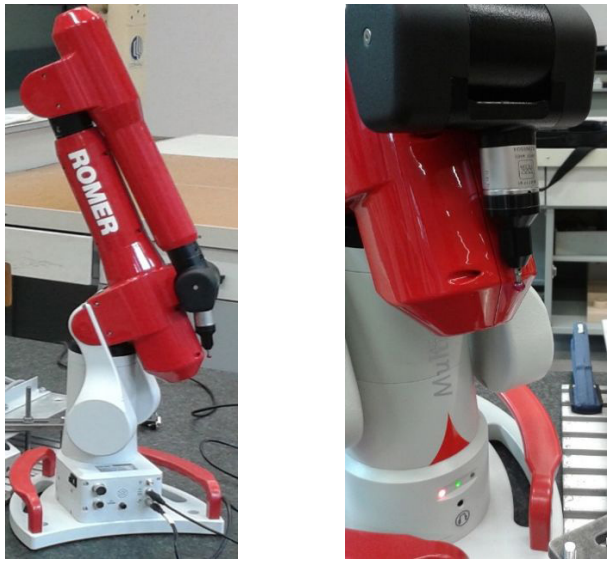

Fig. 5. ROMER measuring arm used to determine the coordinates of points H_i for i = 1–9: a) overview b) close-up of the ruby ball

The basic parameters of the portable measuring arm are given below [12]:

- measuring range: 1.2 m,
- calibrated and certified according to ISO 10360-2,
- accuracy: MPEE = 5 + L/40 ≤ 18 μm; MPEP = 8 μm; where L – length,
- operation temperature: 0–50°C,
- maximum relative humidity: 80% for temp. up to 31°C.

In order to measure, the plate with ball joints has been fixed on a granite measuring plate in such a way as not to cause deformation (Fig. 6).

a)

b)

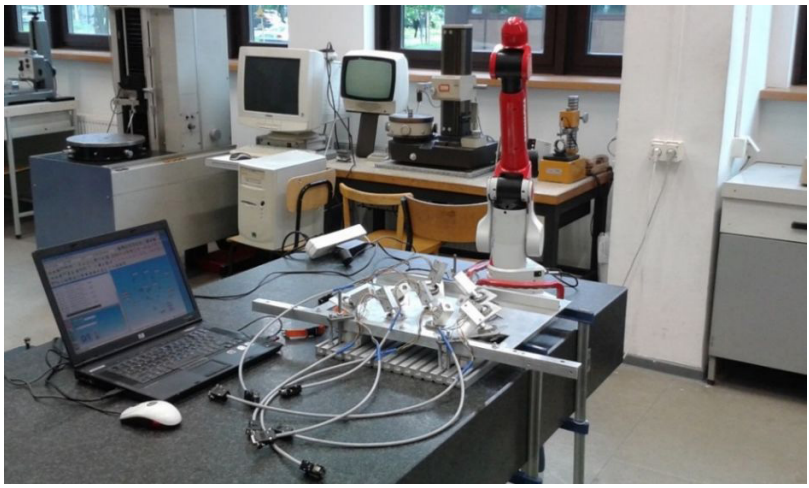

Fig. 6. The external plate of the measuring instrument (with ball joints fixing the optical linear displacements sensors) fixed on a granite measuring plate. The ROMER measuring arm and a computer with the appropriate software, on which disc the results of measurements were recorded are also visible

Before starting the actual measurements, the position of coordinate system, in which the coordinates of points H_i, i =1–9 were determined, should have been unambiguously specified. In order to do this, at first, at the surface of the measured plate the plane PLN1 was determined. Then, on that plane, two circles were defined (CIR1 and CIR2), between the centres of them the length LIN1 was constructed. Axes x and z are on the plane PLN1 and their origin was established at the point PNT3. The y-axis is coincided with a normal vector to the plane PLN1. Its origin was also established at the point PNT3, while its sense was directed in such a way that the coordinate system is right-handed and orthogonal.

Fig. 7 shows a screenshot of the computer program with which the results of the measurements were recorded. The features that were used to construct the coordinate system are visible.

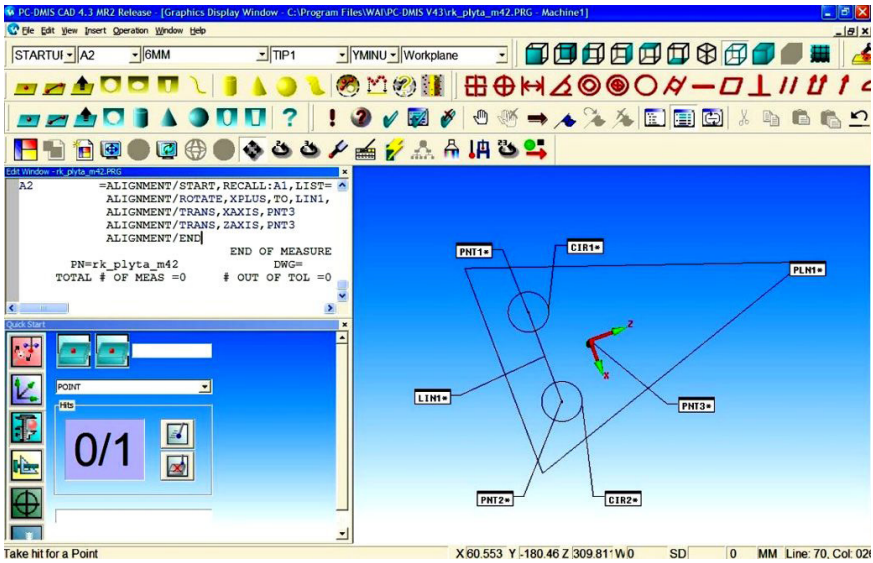

Fig. 7. The screenshot of the computer program with which the results of the measurements carried out using ROMER measuring arm were recorded. The plane PLN1, circles CIR2 and CIR2, length LIN1, the origin of the coordinate system PNT3, the directions and senses of *x* and z axes are shown. The direction and sense of axis *y* were specified in such a way that the coordinate system is right-handed and orthogonal

The coordinates of centres of the ball joints H_i, i =1–9 were determined by measuring the outer surfaces of inner rings of spherical plain bearings (Fig. 3). These surfaces are fragments of the sphere's outline, their measurement consisted in pointing, using the ruby ball of the ROMER measuring arm, eight points, on the basis of which the program determined the diameter, the coordinates x, y, z of the spheres centres, and hence the coordinates of the centres of the ball joints H_i, i = 1–9 in the pre-determined Cartesians coordinate system. To increase the accuracy, the measurement of each surface was conducted three times, then the averages of the results obtained, which were taken as the requested coordinates of ball joints centres H_i, i = 1–9, were determined.

Fig. 8 shows an operator of ROMER measuring arm during the measurements.

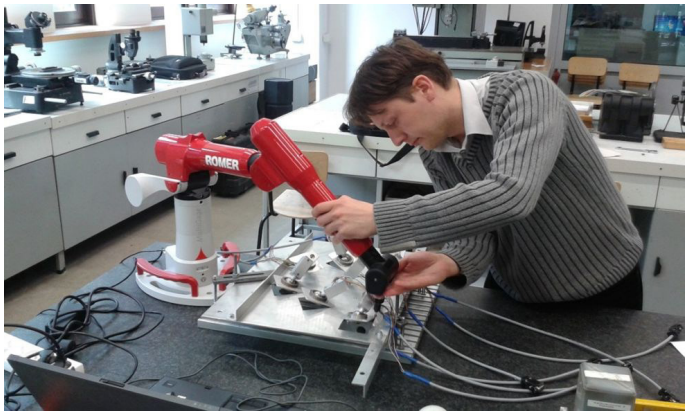

Fig. 8. The measurement of the coordinates of the ball joints H_i, $i = 1(9)$ centres using the ROMER measuring arm

The measurements results are summarized in Tab. 1.

Table 1. The results of the measurements of the coordinates of centres of ball joints H_i, i =1–9 obtained using ROMER measuring arm. The results were measured with an accuracy of three decimal places. In terms of an aim realization, they were rounded to one decimal place

Ball joint	Coordinate	Measurement 1 mm	Measurement 2 mm	Measurement 3 mm	Average mm	Standard deviation mm
1	2	3	4	5	6	7
$\mathbf{H_1}$	x_{H1}	113.4	113.6	113.6	113.5	0.08
	y_{H1}	–11.3	–11.2	–11.2	–11.2	0.05
	z_{H2}	61.5	61.0	61.0	61.2	0.25
$\mathbf{H_2}$	x_{H2}	177.9	177.9	178.0	177.9	0.03
	y_{H2}	–11.9	–11.9	–11.7	–11.8	0.10
	z_{H1}	–49.5	–50.0	–50.0	–49.8	0.28
$\mathbf{H_3}$	x_{H3}	50.1	50.1	50.1	50.1	0.02
	y_{H3}	1.1	1.2	1.1	1.1	0.09
	z_{H3}	–49.8	–50.2	–50.2	–50.1	0.22
$\mathbf{H_4}$	x_{H4}	–0.2	0.0	0.0	–0.1	0.09
	y_{H4}	1.3	1.3	1.3	1.3	0.02
	z_{H4}	36.9	36.5	36.6	36.7	0.22

cd. Tab. 1

1	2	3	4	5	6	7
$\mathbf{H_5}$	x_{H5}	–65.2	–65.0	–64.9	–65.0	0.17
	y_{H5}	–10.9	–11.1	–11.1	–11.0	0.09
	z_{H5}	146.9	146.8	146.8	146.8	0.09
$\mathbf{H_6}$	x_{H6}	63.2	63.6	63.7	63.5	0.24
	y_{H6}	–10.3	–10.3	–10.3	–10.3	0.04
	z_{H6}	147.7	147.3	147.3	147.4	0.22
$\mathbf{H_7}$	x_{H7}	–114.0	–113.9	–113.9	–114.0	0.08
	y_{H7}	–12.9	–12.9	–12.9	–12.9	0.04
	z_{H7}	59.3	59.3	59.3	59.3	0.04
$\mathbf{H_8}$	x_{H8}	–177.6	–177.6	–177.6	–177.6	0.05
	y_{H8}	–12.6	–12.4	–12.5	–12.5	0.09
	z_{H8}	–50.5	–50.6	–50.6	–50.6	0.04
$\mathbf{H_9}$	x_{H9}	–49.8	–49.8	–49.8	–49.8	0.03
	y_{H9}	1.1	1.0	1.1	1.1	0.06
	z_{H9}	–49.9	–50.1	–50.0	–50.1	0.10

The standard deviation, for each measurement, was determined according to the formula:

$$s = \sqrt{\frac{(x_k - \overline{x_k})^2}{n-1}} \tag{1}$$

where:

s – experimental standard deviation,
x – measured value of each coordinate,
$\overline{x}$ – arithmetic mean of all measurements of each coordinate,
k – number of each measurement: $i = 1–3$,
n – number of measurements, $n = 3$.

The determined values of the coordinates of the fixing points of the instrument's links to the external plate are shown below in millimetres:
$H_1(113.6, -11.2, 61.0)$; $H_2(177.9,-11.8,-50.0)$; $H_3(50.1, 1.1, -50.2)$; $H_4(0.0,1.3,36.5)$; $H_5(-64.9, -11.1, 146.8)$; $H_6(63.7, -10.3, 147.3)$; $H_7(-113.9, -12.9, 59,3)$; $H_8(-177.6, -12.4, -50.6)$; $H_9(-49.8, 1.1, -50.0)$.

Shows the window of the computer program which recorded the measurement data, the positions of all ball joints fixing the external plate with the measuring instrument's links are visible. The ball joints were marked as SPH1–SPH9.

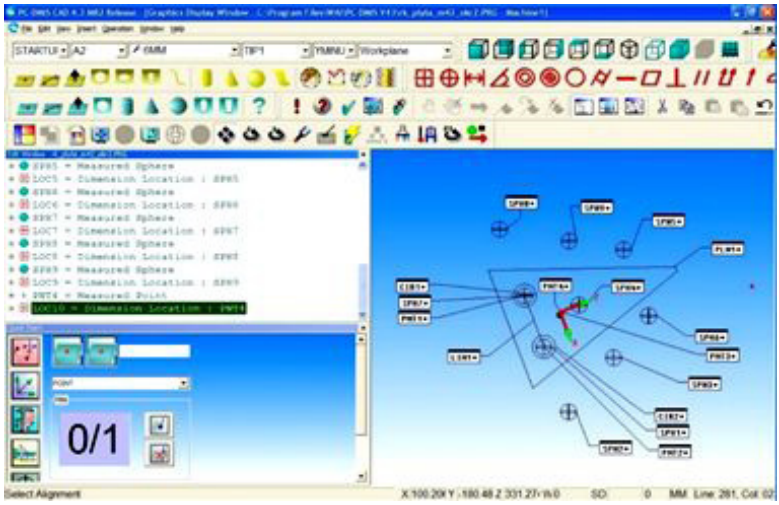

Fig. 9. Window of the computer program which recorded the measurements data. The coordinate system, objects that were used to build it (See Fig. 5) and the positions of ball joints, which coordinates were searched are shown (Symbols SPH1–SPH9)

The coordinates of centres of the ball joints D_j, in coordinate system connected with the external plate, were determined on the basis of known dimensions of the internal plate, the distance between the plates and the coordinates of centres of the ball joints H_i. It was assumed that the plates were parallel and had the same angular orientation. Fig. 10 shows a schematic view of the internal plate with the dimensions needed to calculate the coordinates of ball joints D_j, j = 1–3 centres.

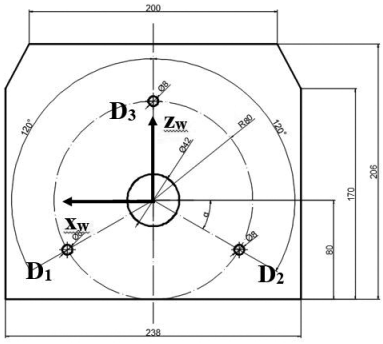

Fig. 10. Schematic view of the internal plate. Dimensions needed to calculate the coordinates of centres of the ball joints D_j, j = 1–3 are shown

The coordinates x_w and z_w were calculated on the basis of basic geometrical relationships (for α = 60°):

$$x_{D1} = -x_{D2} = R \cdot \cos(\alpha) = 80 \cdot 0.5 = 40\,\text{mm} \tag{2}$$

$$z_{D1} = -z_{D2} = R \cdot \sin(\alpha) = 80 \cdot \frac{\sqrt{3}}{2} = 69.3\,\text{mm} \tag{3}$$

The coordinates y_{D1}, y_{D2}, y_{D3} were calculated on the basis of the known distance between internal and external plates and the dimensions of the ball joints D_j.

The determined coordinates of centres of ball joints D_j, j = 1–3 are presented below in millimetres:

$D_1(69.3, -232.2, -40.0)$; $D_2(-69.3, -232.2, -40.0)$; $D_3(0.0, -232.2, 80.0)$.

Knowing the coordinates of ball joints H_i and D_j, the initial lengths of the instrument's links were calculated:

$$\vec{r}^{\,T}_{D_1H_i} \cdot \vec{r}_{D_1H_i} = l^2_{D_1H_i}, \qquad i = 1,2,3 \tag{4}$$

$$\vec{r}^{\,T}_{D_2H_i} \cdot \vec{r}_{D_2H_i} = l^2_{D_2H_i}, \qquad i = 7,8,9 \tag{5}$$

$$\vec{r}^{\,T}_{D_3H_i} \cdot \vec{r}_{D_3H_i} = l^2_{D_3H_i}, \qquad i = 4,5,6 \tag{6}$$

4. Summary

It is necessary to know the coordinates of the ball joints centres H_i, i = 1–9 and D_j, j = 1–3 and the lengths of links of the proposed instrument's mechanism at the beginning of measurements of linear and angular displacements of a steered wheel. The coordinates of nine ball joints H_i were determined using a ROMER measuring arm, an accuracy of three decimal places was obtained, but in terms of aim realization, they were rounded to one decimal place. The measurement of each coordinate x_i, y_i, z_i was repeated three times, than an average and standard deviation were calculated. The average standard deviation obtained a value of 0.1 mm. On the basis of results of these measurements and the known distance between the instrument's plates, the coordinates of the centres of the ball joints D_j and the lengths between plates were calculated.

References

[1] Reimpell J., Betzler W., *Podwozia samochodów. Podstawy konstrukcji*, WKŁ, Warszawa 2002.

[2] Janczur R., *Analityczno-eksperymentalna metoda badań sterowności samochodu*, Politechnika Krakowska, Ph.D. Dissertation, Kraków 2002.

[3] Struski J., *Quasi-statyczne modelowanie sterowności samochodu*, Wydawnictwo PK, Monografia 144, Kraków 1993.

[4] Struski J., *Przyrząd do pomiaru dynamicznego kąta skrętu koła kierowanego* Patent nr P-267693.

[5] Blumenfeld W., Schneider W., *Opto-elektronisches Verfahren zur Spur- und Sturzwinkelmessung am fahrenden Farzeug*, ATZ 87 1, 1985, 17–21.

[6] Struski J,. Kowalski M., *Podstawy teoretyczne uogólnionych zagadnień z zakresu parametryzacji układów prowadzenia kół względem nadwozia*, Technical Transactions, 6-M/2008, 119–129.
[7] Struski J., Wach K., *Analiza mechanizmu przyrządu pomiarowego do wyznaczania translacji i rotacji zwrotnicy z kołem kierowanym*, Technical Transactions, 3-M/2008, 87–100.
[8] Struski J., Wach K., *Teoretyczne podstawy wyznaczania przemieszczeń liniowych oraz kątowych koła kierowanego*, Czasopismo Logistyka-Nauka [Electronic document], – Optic Disc CD, Vol. 4, 2015, 5840–5849.
[9] Wach K., *The theoretical analysis of an instrument for linear and angular displacements of the steered wheel measuring*, IOP Conference Series: Materials Science and Engineering IOP, Vol. 148(1), 2016.
[10] CORSYS- DATRON RV-4 *Wheel Vector Sensor for Simultaneous Measurement of all Wheel Positions and Orientations in 5 Axes*, User manual, Vol. I, Wetzlar, Germany 2008.
[11] Spherical plain bearings ISKRA PGE 16X datasheet: http://www.iskra-zmils.com.plpliki_inne/14.pdf (access: 28.03.2017).
[12] http://apps.hexagon.se/downloads123/hxmt/romer/romer-multi-gage/brochures/ROMER%20Multi%20Gage_brochure_pl.pdf (access: 28.03.2017).
[13] Sładek J., *Dokładność pomiarów współrzędnościowych*, Wydawnictwo PK, Kraków 2012.
[14] Ratajczyk E., *Współrzędnościowa technika pomiarowa*, Oficyna Wydawnicza Politechniki Warszawskiej, Warszawa 2005.

TECHNICAL TRANSACTIONS 6/2017
CZASOPISMO TECHNICZNE 6/2017
MECHANICS
DOI: 10.4467/2353737XCT.17.102.6578

Robert Zarzycki (zarzycki@is.pcz.czest.pl)
Department of Energy Engineering, Częstochowa University of Technology

The use of waste heat from flue gas in the system of regeneration of steam boiler supply water

Wykorzystanie ciepła odpadowego ze spalin w układzie regeneracji wody zasilającej kocioł parowy

Abstract

This study presents an analysis of the process of the use of waste heat from flue gas for the purposes of heating water in the regeneration system of a steam power unit fuelled with brown coal with a power of 900 MW_e. Preparation of flue gas and its initial moistening (increasing the dew point temperature) followed by cooling (condensation of the moisture contained in the flue gas) can ensure intensive heat exchange in the process of heat recovery. Replacing a first regeneration exchanger with the heat recovered from flue gas allows for an increase in steam power unit efficiency by 0.22% and limitation of CO_2 emissions by 22,810 t/year, while reducing the fuel demand by 26,727 tonnes per annum. Depending on the prices of CO_2 emissions permits and prices of brown coal, the proposed heat recovery allows for saving from €500,000 to €1,000,000 per year.

Keywords: waste heat, regeneration system, steam power unit

Streszczenie

W pracy przedstawiono analizę procesu wykorzystania ciepła odpadowego ze spalin na potrzeby podgrzewu wody w układzie regeneracji bloku parowego opalanego węglem brunatnym o mocy 900 MW_e. Poprzez odpowiednie przygotowanie spalin, ich wstępne nawilżenie (podniesienie temperatury punktu rosy), a następnie ochłodzenie (kondesację zawartej w spalinach wilgoci) można uzyskać intensywną wymianę ciepła w procesie odzysku ciepła. Zastąpienie pracy pierwszego wymiennika regeneracyjnego ciepłem pozyskanym ze spalin pozwala na wzrost sprawności bloku parowego o 0.22% oraz ograniczenie emisji CO_2 w ilości 22 810 ton/rok, dodatkowo zmniejsza zapotrzebowanie na paliwo w ilości 26 727 ton/rok. W zależności od ceny uprawnień do emisji CO_2 i ceny węgla brunatnego proponowany odzysk ciepła pozwala na oszczędności od 0.5 do 1 miliona euro/rok.

Słowa kluczowe: ciepło odpadowe, układ regeneracji, blok parowy

1. Introduction

Electricity and heat in Poland is mainly generated through combustion of hard coal and brown coal. These fuels are burnt in power boilers, mainly pulverized coal-fired and fluidized bed furnaces and allow for production of steam with specific parameters and, consequently, electricity. Efficiency of electricity generation in current industrial power boilers reaches a gross value of 50%, resulting mainly from high initial steam parameters and the scale of the energy sector. There are several investments with an installed capacity of 1,000 MW_e class currently being implemented (Opole Power Plant, Jaworzno III Power Plant and Kozienice Power Plant). It can be expected that the next power units in the 1,000 MW_e class are going to be built in the nearest future and replace the obsolete power units built in the 20th century that do not meet the specifications contained in the standards concerning emissions. High efficiency of conversion of chemical energy into electricity helps reduce emissions of CO_2 and other harmful substances to the atmosphere. Therefore, further research is needed to improve the thermodynamic efficiency of the electricity and heat generation process in the nearest future. One of the methods to increase the efficiency of the thermodynamic cycle of a system is to improve the parameters of live steam. However, the material needs and the related costs substantially limit the opportunities for improving these parameters. The increase in the thermodynamic cycle efficiency can be achieved through combined generation of electricity and heat.

This study presents investigations concerning the opportunities for using the heat contained in flue gas that leaves the boiler to heat the condensate in the regeneration system.

2. Steam power unit

Conversion of the chemical energy contained in the fuel into heat in big energy boilers reaches an efficiency of 85% to 95%. This efficiency depends mainly on the type of the fuel (black coal, brown coal) and the water content in the fuel. The highest amounts of energy in power boilers are lost in the form of flue gas waste. Therefore, several technologies of brown coal drying aimed at limitation of the energy loss are being developed [1–4]. The flue gas waste is caused by the high temperature of flue gas that leaves the boiler and the presence of water steam in the flue gas. In the case of boilers fuelled with black coal, the temperature of flue gas ranges from 120–150°C [5–7], and the flue gas humidity is ca. 0.080 kg/kg [5, 6, 8]. In the case of boilers fed with brown coal, the temperature of flue gas ranges from 160–180°C [5–7], and the flue gas humidity is ca. 0.240 kg/kg [5, 6, 8]. The flue gas temperature depends on the content of water and SO_2 in flue gas.

This study presents investigations concerning the opportunities to utilize the heat of flue gas from a power unit with power of 900 MW_e fuelled by brown coal to replace the heat of the first heat exchanger in the water regeneration system. Table 1 presents the basic parameters of the steam power unit fuelled with brown coal.

Table 1. Basic parameters of steam power unit fuelled with brown coal

No.	Parameter		Value
1	Parameters of live steam before the turbine		30 [MPa]; 650 [°C]
2	Electric power of the power unit		900 [MW_e]
3	Boiler efficiency		90 [%]
4	Flue gas temperature		170 [°C]
5	Fuel flow rate		248.35 [kg/s]
6	Wet flue gas flow rate		1090.2 [kg/s]
7	Air-fuel ratio		1.2 [–]
8	Characteristics of fuel in the operational state	Calorific value	7.75 [MJ/kg]
9		Water content	0.5140 [–]
10		Ash content	0.1140 [–]
11		Content of C	0.2320 [–]
12		Content of H	0.0192 [–]
13		Content of O	0.1050 [–]
14		Content of N	0.0032 [–]
15		Content of S	0.0126 [–]
16	Molar fractions of components in wet flue gas	(CO_2)	0.1211 [–]
17		(SO_2)	0.0025 [–]
18		(O_2)	0.0266 [–]
19		(N_2)	0.5943 [–]
20		(H_2O)	0.2484 [–]
21		(Ar)	0.0071 [–]
22	Environment parameters		0.1 [MPa]; 15 [°C]; φ = 0.6 [–]

The diagram of the thermodynamic cycle of the steam power unit is presented in Fig. 1. The system is composed of three turbines: a high-pressure turbine, a medium-pressure turbine and a low-pressure turbine. The supply water regeneration system is composed of four low-pressure heat exchangers and three high-pressure exchangers, and an additional steam attemperator. From the standpoint of heat recovery from the flue gas and using this gas in the regeneration system, one can take into consideration only heat exchangers of the low-pressure section (HE1, HE2, HE3, HE4). The temperature of the condensate that leaves the condenser and feeds the regeneration system is also important from the standpoint of heat recovery. The operational parameters of the low-pressure water regeneration system are presented in Table 2.

The analysis of the operational parameters of heat exchangers presented in the Table 3 can be based on the use of the waste heat from flue gas to replace the operation of the heat exchangers HE1 and HE2. From the standpoint of operation of the steam power unit, the most beneficial solution is to obtain the same parameters in the regeneration system during heat recovery from the flue gas. This will help maintain the operational parameters of other heat exchangers, which has a direct effect on the operation of steam turbine and other regeneration exchangers.

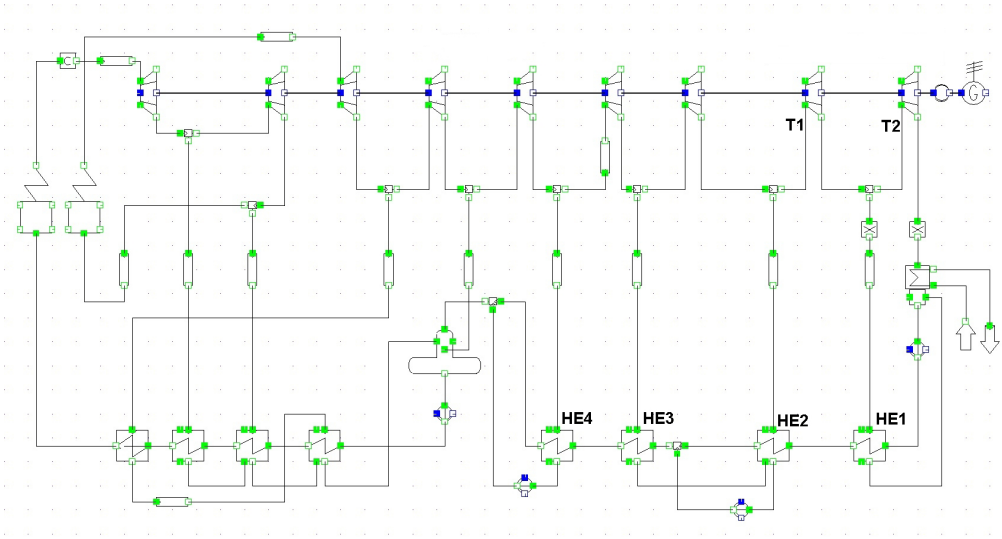

Fig. 1. Diagram of thermodynamic cycle of the steam power unit: case C0

Table 2. Operational parameters of low-pressure heat exchangers

Heat exchanger	Heat power [MW_t]	Condensate temperature [°C]		Steam/condensate temperature [°C]		Mass flow rate [kg/s]	
		Inlet	Outlet	Inlet	Outlet	Condensate	Steam
HE1	51.299	33	64	67	67	394.25	22.24
HE2	49.856	64	94	138.1	97	394.25	19.97
HE3	55.123	94.3	124	228.7	127	437.25	23.03
HE4	56.241	124	154	317.8	157	437.25	23.15

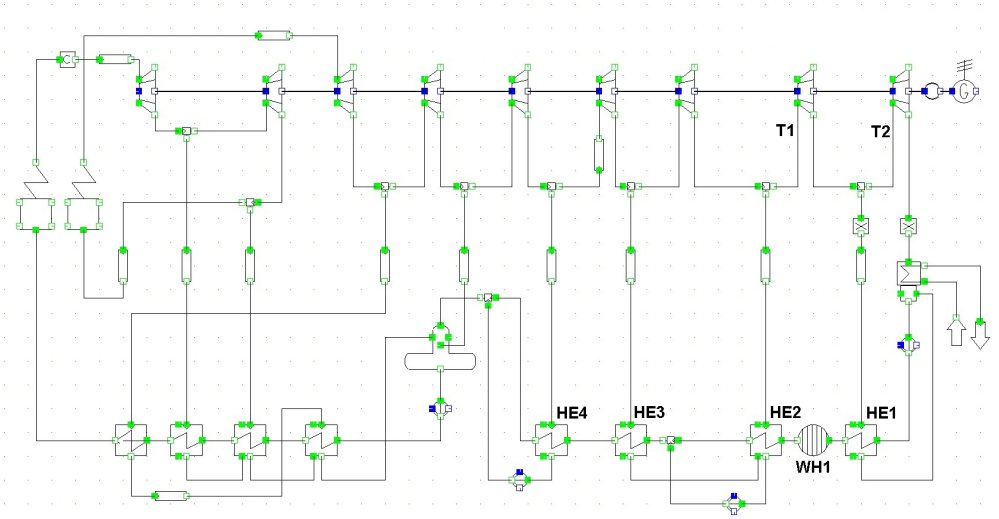

Fig. 2. Diagram of the thermodynamic cycle of the steam power unit with introduction of the waste heat after the heat exchanger HE1 through the exchanger WH1: case C1

Table 3. Comparison of selected parameters of steam power unit before (C0) and after using the heat recovery (C1) by the exchanger WH1

	Case	
	C0	C1
Gross efficiency [%]	46.7029	46.9229
CO_2 emissions [kg/s]	210.21	209.22
Fuel flow rate [kg/s]	248.65	247.49
Boiler heat power [MW_t]	1734.363	1726.245
Power of the power unit [MW_e]	900	900
HE1 power [MW_t]	51.299	0
HE2 power [MW_t]	49.856	49.622
WH1 power [MW_t]	–	51.058
Steam flow rate T1 [kg/s]	396.6	394.7
Steam flow rate T2 [kg/s]	374.3	394.7
Heat collected in the condenser [MW_t]	846.556	889.368

Table 3 presents the results of calculations for the analysed cases of heat recovery from the flue gas for the power unit fuelled with brown coal. Analysis of the data contained in Table 3 reveals that replacement of the operation of the first regeneration exchanger HE1 with the waste heat from flue gas through building the WH1 exchanger (Fig. 2) allows for an improvement in gross electricity generation efficiency by 0.22%. This leads to the reduction of CO_2 emissions by 0.99 kg/s with simultaneous fuel consumption decrease by 1.16 kg/s, which reduces boiler heat power by ca. 8.12 MW_t. These effects were obtained through replacing the HE1 exchanger with a power of 51.299 MW_t with heat exchanger WH1 with a power of 51.058 MW_t. Consequently, the mass flow rate for the stream reaching the turbine T1 declined insignificantly by 1.9 kg/s, which accounts for 0.479% of the nominal flow rate. Due to the exclusion of the exchanger HE1, the flow rate of the steam supplied to the turbine T2 rose by 20.4 kg/s, which is 5.45 % of the nominal flow rate. This led to the increase in flow rate of the heat collected in the condenser by 42.81 MW (5.05% of the nominal heat flow rate to the condenser). After replacement of the heat exchanger HE1 with the waste heat from the exchanger WH1, changes in the operational parameters of the steam power unit reach maximally 5.5% of nominal values, which allows for building this installation without changing the flow in the turbine and condenser.

Due to its high efficiency and fuelling with cheap fuel (brown coal), the power unit of 900 MW_e size should be operated for the longest possible time with nominal power. With variable daily demand for electricity, it can be adopted that the power unit operates for 16 hours a day with a power of 900 MW_e and for 8 hours a day with a load of ca. 40%, which means 360 MW_e. Assuming that the power unit is operated for 8,000 hours a year, the benefits of building the heat recovery installation can easily be calculated. It is possible to reduce CO_2 emissions by 22,810 tonnes per year and the demand for fuel by 26,727 tonnes per year. Based on the above information, the prices of CO_2 emissions permits and prices of brown coal, the economic effect of heat recovery from flue gas can be evaluated. In the scenario "I",

assuming the price for emissions permits as €5 per tonne of CO_2 and €15 per tonne of brown coal, the savings resulting from reduction in CO_2 emissions are €114,050 per year, whereas the savings connected with reduced fuel consumption are €400,900 per year, which in total yields €514,950 per year. With the scenario "II", assuming the price of CO_2 emissions permits per tonne of €15 and price of coal of €25 per tonne, the total savings can reach €1,010,300 per year.

Analysis of the above economic benefits should include the necessity of incurring costs for construction of the heat recovery installation and their operating costs. The detailed economic analyses will justify the profitability of building the heat recovery installation. The study presents only the thermodynamic analysis of heat recovery from the flue gas for the purposes of fuelling of the steam power unit.

3. Utilization of waste heat from flue gas

The use of the heat recovery presented in the previous section to feed the exchanger WH1 (Fig. 2) requires special preparation of the flue gas. The flue gas that leaves the steam boiler fuelled by brown coal has a temperature of 170°C and contains much moisture that is generated from combustion of the wet fuel and the hydrogen contained in the fuel.

The process of heat exchange between hot flue gas and the water inside the pipes of the heat exchanger is limited by the value of the coefficient of heat penetration for the fuel, which, for forced convection, reaches the values of up to 500 W/m^2K [9–11], whereas steam condensation for forced convection allows for achievement of this coefficient at the level ranging from $3 \cdot 10^3$ to $2 \cdot 10^5$ W/m^2K [9–14]. In order to conduct heat recovery from flue gas effectively with the smallest possible size of heat exchanger, it is necessary to utilize the process of steam condensation in the flue gas [15–20]. Condensation of water steam contained in the flue gas also helps clean it from the residue fly ash and other compounds contained in the flue gas e.g. SO_2, Hg.

For the discussed boiler fuelled by brown coal, the outlet temperature of the flue gas is 170°C, and the water content determines the dew point at the temperature of 64.79°C. The present section discusses the calculations for replacing the first regeneration heat exchanger HE1, where the condensate temperature is 64°C, with a heat exchanger WH1 that recovers heat from flue gas and heats the condensate to 64°C. Despite the high temperature of flue gas (170°C), the extension of the surface is needed for the process of heating water in the exchanger WH1. While increasing the dew point temperature, a high coefficient of heat penetration connected with water condensation can be utilized in the flue gas cooling process. In this case, it is possible to ensure intensive heating of the condensate in the regeneration system to 64°C. Currently designed and manufactured condensation heat exchangers [10, 16, 21, 22] can be operated at the temperature difference between the condensing water steam and water in the exchanger pipes of 3°C.

The diagram of the process of flue gas preparation and heat recovery is presented in Fig. 3. It is composed of the system of flue gas moistening and water condensation with condensate

heating. After cleaning from the fly ash, the flue gas that leaves the boiler is separated into two streams *1* and *4*. The stream *1* is supplied to the heat recovery installation, whereas the stream *4*, after mixing with the stream 3, is transported to the chimney *10*. The flue gas supplied to the heat recovery installation with the stream *1* with temperature of 170°C is characterized by the dew point temperature of 64.79°C, which results from the water content in the flue gas. In order to improve the dew point temperature, flue gas is moistened through spraying the water circulating in the closed cycle of *6*, *7*. Moistening leads to the reduction in the flue gas temperature in point *2*, increasing water content and, consequently, increasing the dew point temperature to 67.22°C. It is necessary to reinforce the stream of circulating water with the stream *5*. With the moistening process, flue gas is cleaned of ash, SO_2 and Hg. After this preparation, the flue gas is supplied to the heat exchanger, where it is cooled and the water contained in the flue gas is condensed. The stream *11* is used to remove the condensate. The flue gas is cooled by the water collected after the heat exchange HE1 (*8*) and supplied before the exchanger HE2 (*9*) to the temperature 64°C. Table 4 compares selected process parameters of installation of flue gas preparation and heat recovery.

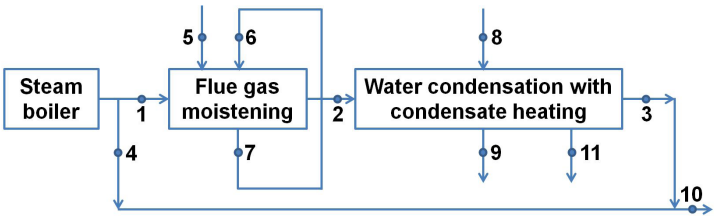

Fig. 3. Flue gas preparation and heat recovery

Table 4. Selected process parameters of installation of flue gas preparation and heat recovery

	Temperature [°C]	Dew point temperature [°C]	Mass flow rate [kg/s]	Water content in flue gas [kg/kg]	Flue gas water content [%]
1	170	64.79	83.51	0.1937	24.84
2	101.9	67.22	85.65	0.2244	27.68
3	36	36	72.55	0.0370	5.95
4	170	64.79	1006.49	0.1937	24.84
5	67	–	2.14	–	–
6	67	–	7.5	–	–
7	67	–	7.5	–	–
8	33	–	394.7	–	–
9	64	–	394.7	–	–
10	160.1	63.95	1079.04	0.1817	23.27
11	36	–	13.1	–	–

For the purposes of the process above, the expected flue gas flow rate that ensures adequate heat flux for condensate heating in the regeneration system amounts to ca. 7.66%

of the nominal flue gas stream. The proposed solution offers more effective utilization of the heat contained in the flue gas for e.g. generation of the system heat for heating purposes or heat for fuelling an absorption cooler used for the production of chilled water.

4. Conclusion

The heat recovery for the purposes of the low-pressure regeneration system allows for improving the gross efficiency of the power unit by 0.22%. This allows for reduction in CO_2 by 0.99 kg/s and demand for the fuel stream by 1.16 kg/s for the nominal power of the power unit. Depending on the prices of CO_2 emissions permits and prices of fuel, it is possible to reach savings ranging from ca. €500,000 to €1,000,000 per year. For the purposes of heat recovery, the use of the flue gas moistening process and cooling with condensation of the water, it is sufficient to collect ca. 7.66% of the total flue gas stream. The use of the process of water condensation helps intensify the process of heat transfer from flue gas to the heated condensate, allowing for a substantial reduction in the size of the heat exchanger. Condensation of water contained in flue gas helps clean the flue gas of fly ash and other water-soluble gaseous components. This also helps recover water from the flue gas.

Apart from the above benefits of the process of heat recovery, one of the drawbacks is high costs of building the condensation heat exchanger as its material has to be resistant to corrosion effect of the condensing flue gas and the gas they contain.

BS/PB-404-301/11

References

[1] Panowski M., Klajny R., *Analiza termodynamiczna wstępnego podsuszania paliwa*, Mat. Konf. XX Jubileuszowy Zjazd Termodynamików, ISBN 978-83-7493-407-7, 2008, 189–193.
[2] Sławiński K., Knaś K., Gandor M., Nowak W., *Suszenie węgla brunatnego w energetyce – możliwości zastosowania młyna elektromagnetycznego*, Zeszyty Naukowe Politechniki Rzeszowskiej – seria Mechanika, Vol. 86 (3/14), 2014, 2300–5211.
[3] Pawlak-Kruczek H., Plutecki Z., *Suszenie węgla niskogatunkowego*, Wydawnictwo „Nowa Energia", 2014.
[4] Lichota J., Plutecki Z., *Suszenie węgla w elektrowniach*, Rynek Energii, 2007, No. 6, 36–41.
[5] B&W, *Steam: Its Generation and Use*, The Babcock & Wilcox Company, New York 2007.
[6] Spliethoff H., *Power Generation from Solid Fuels*, Springer-Verlag Berlin Heidelberg, 2010.
[7] Chmielniak T., Łukowicz H., *Modelowanie i optymalizacja węglowych bloków energetycznych z wychwytem CO_2*, Wydawnictwo Politechniki Śląskiej, Gliwice 2015.

[8] Szulc P., Tietze T., *Odzysk i energetyczne wykorzystanie gazów wylotowych pochodzących z bloków energetycznych elektrowni węglowych*, Materiały VI Konferencji Naukowo-Technicznej „Energetyka gazowa 2016", Vol. II, Wydawnictwo Instytutu Techniki Cieplnej, Gliwice 2016.
[9] Incropera F., DeWitt D., *Fundamentals of heat and mass transfer*, 4th edition. John Wley and Sons, 1996.
[10] Cao E., *Heat transfer in process engineering*, McGraw-Hill, 2009.
[11] Hobler T., *Ruch ciepła i wymienniki*, WNT, Warszawa 1979.
[12] Bohdal T., Matysko R., *Analiza kondensacji pary wodnej na rurze pionowej*, Ciepłownictwo, Ogrzewnictwo, Wentylacja, No. 7–8/2004, 35–41.
[13] Broomley L., *Heat transfer in condensation – effect of heat capacity of condensate*, Ind. Eng. Chem. 44, 1952, 2966–2969.
[14] Siddique M., Golay M., Kazimi M., *Local heat transfer coefficients for forced-convection condensation of steam in a vertical tube in the presence of a noncondensable gas*, Nuclear Technology 102, 1993, 386–402.
[15] Colburn A., Hougen O., *Design of cooler condensers for mixtures of vapors with noncondensing gases*, Industrial and Engineering Chemistry, Vol. 26, 1934, 1178–1182.
[16] Heaphy J.P., Carbonara J., Litzke W., Butcher T.A., *Condensing Economizers For Thermal Efficiency Improvements And Emissions Control*, U.S. Department of Energy No. DE-AC02-76CBOO016, 1993.
[17] Sparrow E., Lin S., *Condensation heat transfer in presence of a noncondensable gas*, Journal of Heat Transfer, 1964, 430–436.
[18] Wójs K., Szulc P., Tietze T., Sitka A., *Concept of a system for waste heat recovery from flue gases in coal-fired power plant*, Journal of Energy Science, Vol. 1, No. 1, Wrocław University of Technology 2010, 191–200.
[19] Chen Q., Finney K., Li H., Zhang X., Zhou J., Sharifi V., Swithenbank J., *Condensing boilers applications in the process industry*, Applied Energy, No. 89, 2012, 22–36.
[20] Wójs K., *Odzysk i zagospodarowanie niskotemperaturowego ciepła odpadowego ze spalin*, Wydawnictwo Naukowe PWN SA, Warszawa 2015.
[21] http://www.radscan.se (access: 03.07.2016).
[22] Shi X., Che D., Agnew B., Gao J., *An investigation of the performance of compact heat exchanger for latent heat recovery from exhaust flue gases*, Int. J. Heat Mass Transfer, 54, 2011, 606–615.

TECHNICAL TRANSACTIONS 6/2017
CZASOPISMO TECHNICZNE 6/2017
PHYSICS
DOI: 10.4467/2353737XCT.17.103.6579

Stanisław Jadach
The Henryk Niewodniczański Institute of Nuclear Physics, Polish Academy of Sciences

Radosław A. Kycia (kycia.radoslaw@gmail.com)
Faculty of Physics, Mathematics and Computer Science,
Cracow University of Technology

Software for calculations of the Higgs boson lineshape in future lepton colliders

Program do obliczeń przekroju czynnego dla bozonu Higgsa w przyszłych zderzaczach leptonowych

Abstract

Simple software for Monte Carlo (MC) calculation of the Higgs boson lineshape and its beam broadening effect due to the beam energy dispersion is described. The software is based on the FOAM [1, 2] adaptive MC integrator from ROOT library [3]. This software enables the reproduction of the results presented in publication [4] and the tests with different parameters for the lineshapes and QED correction factors. A parallel version of the software based on MPI [5] is also described.

Keywords: QCD; the Higgs boson cross section; energy scan; Monte Carlo methods; FOAM; machine energy spread; initial state radiation

Streszczenie

Opisano prosty program do obliczeń Monte Carlo(MC) rozkładu przekroju czynnego dla bozonu Higgsa i poszerzenia tego rozkładu związanego z dyspersją energii wiązki. Program bazuje na adaptacyjnym programie do całkowania metodą MC - FOAM [1, 2] z biblioteki ROOT [3]. Oprogramowanie umożliwia reprodukcję rezultatów z publikacji [4] i testy tych wyników z różnymi parametrami wiązki i czynnikami korekcyjnymi QED. Zrównoleglona wersja oprogramowania bazująca na MPI [5] również została opisana.

Słowa kluczowe: QCD, przekrój czynny dla bozonu Higgsa, skanowanie energią, metody Monte Carlo, FOAM, rozrzut energii wiązki, promieniowanie w stanie końcowym

1. Introduction

One of the main aims of future lepton (electron and muon) colliders is detailed examination of the Higgs boson 's properties, and therefore, examination of effects that can influence this reaction is one of the most important aspect of their design. Initial state radiation (ISR) is one of the key factors – as shown in [4] – it reduces the cross section peak of the Higgs boson by a factor of about 35% for electron and 55% for muon colliders. These derivations use methods from analogous calculations of the same effect for the Z boson made for LEP [4].

Further detailed studies of ISR require specially designed software. The full featured Monte Carlo general generators that incorporate initial and final state radiation are currently developed – see detailed discussion in [12] and [13]. However, as they are multi-purposed software, the number of configuration options is large. In this paper a simplified and specialized software that allows one to simulate the Higgs boson lineshape with ISR effects aimed at use in designing future lepton colliders will be presented. It is useful in performing fast simulations of ISR cross section damping and predicting the cross section dependence on machine parameters.

The software presented here was used to produce results from paper [4] and therefore it is advisable to study this paper before commencing experiments with the programs. In [4] there is also all the theory required to understand the output. The software is available at [6].

This paper is organized as follows. In the next section requirements for running the software are provided followed by a short example. Next, the general idea of the software design is described. Finally a short introduction to the parallel version based on MPI [5] intended for specialists in this field is presented.

2. Requirements

The software requires standard and free software available for most Unix-like systems.
In order to compile and run the programs the following tools are mandatory:

- Unix-like system – POSIX compatible, e.g., Linux;
- Make compatible system, e.g., GNU make [7];
- g++ compiler from GNU Compiler Collection [8] or any other compatible compile
- ROOT library [3][1] .

There is also additional software that is required to perform more advanced operations:

- Doxygen [9] (optional) if one requires generation of the documentation from the code;
- Valgrind [10] (optional) if advanced debugging is required;
- MPI [5], e.g., OpenMPI (optional) if the user wants to use the parallel version of the program located in the MPI directory.

The repository [6] contains three directories:

[1] ROOT 6 or higher is compiled using C++ 2011 standard. Therefore, when GNU`g++` compiler is used then the flag `-std=c++11` should be added during compilation for compatibility, see Makefile.

- Simple – simplified version of software, suitable for learning its structure;
- Full – full version of the software;
- MPI – parallelized version.

In the next two sections the simplified version of the software will be presented.

3. One minute example

A simplified version of the program was constructed to familiarize new users with the philosophy of its design.

In order to run the program, a change directory to Simple is required and then execution of make run in the console. This command triggers the compilation and starts the program. When the program run ends, which should take no more than one minute on current desktop machines, the user will be able to see SimplePlot.eps file containing the example plot show in Fig. 1. These plots demonstrate only some capabilities of the library of functions belonging to the full program. In Fig. 1 the convolution of the Gaussian distribution that describes beam/machine energy spread:

$$G\left(E-E_0,\delta_E\right)=\frac{1}{\delta_E\sqrt{2\pi}}e^{-\frac{\left(E-E_0\right)^2}{2\delta_E^2}},$$

where:

E_0 – the central value of the beam energy,

δ_E – its spread, with a cross section is defined by;

$$\sigma_E^{\text{conv}}\left(E,\sigma_E\right)=\int dE'\sigma\left(E'\right)G\left(E'-E,\sigma_E\right),$$

where:

σ – the cross section – the Born term without or with ISR corrections.

The details are described in [4].

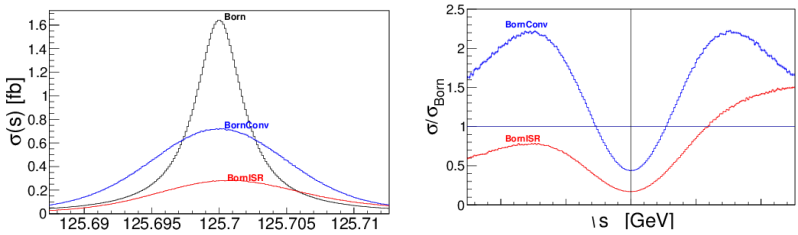

Fig. 1. Upper panel: The Born cross section for e^+e^- à H process – black line, the Born cross section convoluted with the Gaussian distribution for the energy spread (in the centre of mass frame δ_E = 4.2 MeV – blue line, and the Born cross section with ISR corrections included. Lower panel: ratios of the last two plots by the Born term. OX axis is the same for both figures

4. Code analysis – simplified version

We start analysing the code from the main.cxx file from the Simple directory. At the end of the file there is the main() function which is the entry point of the program. The first relevant instruction is:

```
long NevTot = 10000000;
```

which sets up the statistic for the Monte Carlo integrator. The integration error on the ISR corrections or convolution with beam centre energy spread is proportional to $\frac{1}{\sqrt{\text{NevTot}}}$. On the other hand the time of integration is proportional to the statistics.

In the next lines, histograms are created. The line:

```
MakeBorn(string("BornH") );
```

creates the Born term histogram and saves it in BornH.root file. Then in the line

```
MakeConvBorn( string("histo-sig04-born"), 0.0042, NevTot );
```

the histogram for the Born term convoluted with the Gaussian distribution that describes beam energy deviation with the energy spread $\delta_E = 0.0042$ GeV is saved in the file histo-sig04-born.root. Finally, the similar plot including ISR corrections is created in

```
MakeISR( string("histo-sig04-isr2"), 2, 3, 0.0042, NevTot );
```

and it is saved in histo-sig04-isr2.root file. The plots are created in the function

```
plotSimpleFigs();
```

This function can be customized by the user to adjust the plots to her/his requirements. We will analyse the main parts of the function plotSimpleFigs() function. The first part

```
TFile DiskFileBorn(  "./histo-sig04-born.root");
TFile DiskFileISR2(  "./histo-sig04-isr2.root");
TFile DiskFileBornH(  "./BornH.root");

TH1D *h_Born       = (TH1D*)DiskFileBornH.Get("h_SigEne");
TH1D *h_SigEneBorn  = (TH1D*)DiskFileBorn.Get("h_SigEne");
TH1D *h_SigEneISR2  = (TH1D*)DiskFileISR2.Get("h_SigEne");
```

is responsible for retrieving the histograms from the root files. Next, the values of the Higss mass (m_MH) and width (m_GamH) is retrieved from the TDen0sity object:

```
TDensity* Density = new TDensity();
double MH   = Density->m_MH;
double GamH = Density->m_GamH;
```

The class `TDensity` is contained in an appropriate header and class implementation files. This class contains the integrand function and all the relevant physical constants.

In the next part ROOT specific operations are performed in order to format the plots.

The same idea on the large scale is used in the full software – there are more cases for the data generation and more plot functions that prepare customized plots. Fig. 2 describes the general concept of the control flow in the software.

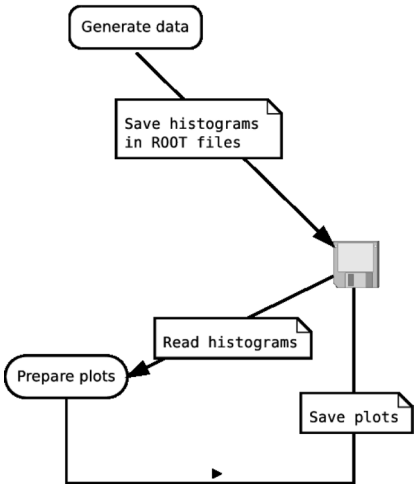

Fig. 2. Flowchart of the software. First, histograms are created and saved in root files on disk. Then they are retrieved, adjusted and saved on disk in PostScript format [14]

5. General overview of the program

In this section the description of general software contained in the Full directory is given. The software contains a few parts:

- `Makefile` compatible with GNU make;
- Class `TDensity` in files `TDensity.h` and `TDensity.cxx` that contains the convolution integrands for the Born term and ISR contributions. It inherits from `TFoamIntegrand class` as it is required by FOAM [1,2];
- Main program and function library in `main.cxx` that contains in addition to the main() the functions described in the previous section.

The following commands are defined in `Makefile`:

- `make run` – compile and run the program;
- `make clean` – clean executables;
- `make cleanests` – clean executables, root, pdf and eps files;

- `make Generate-doc` – generate documentation from the code and display the HTML version in the Firefox web browser;

Makefile is set up for parallel compilation on the maximal number of cores available on the computer. This default setup can be overwritten modifying MAKEFLAGS flag at the top of the file or providing `-j [number of processes]` flag during make call from the line command – for details see [7].

The FOAM [1,2] adaptive integrator requires the density distribution. The class `TDensity` implements the density distribution for the sole Born term, and the Born term convoluted with the Gaussian energy spread and with additional ISR corrections [4]. The class can calculate the cross section for electron and muon Higgs boson production $ll \to H$, where l is electron or muon. The type of reaction can be switched by (un)commenting the appropriate `define` statement in the `TDensity.h` file, e.g., default setup for $ee \to H$ reaction is as follows:

```
#define ELECTRON
//#define MUON
```

The class `TDensity` contains fields which are responsible for selecting appropriate distributions:

- `m_ISROn` – 0 – ISR correction is OFF, only the Born shape; 1 – ISR correction ON;
- `m_keyISR` – selects ISR type defined in details in [4]: 0 for the type (a); 1 for the type (b); 2 for the type (c);
- `m_kDim` – dimension of the distribution to integrate. The following combinations are possible:
  - If `m_ISROn=0` then `m_kDim = 2` – convolution of the Gauss distribution with Born term.
  - If `m_ISROn=1` then `m_kDim = 2` – beam/machine energy spread OFF; 3 – beam/machine energy spread ON;
- `m_sigE` – energy spread in GeV if applicable (`kDim = 3`).

For better understanding, a few examples of correct combinations are provided:

- `m_ISROn = 0, m_kDim = 2, m_sigE = 0.0042` – the Born term convoluted with the beam/machine energy distribution modelled by the Gaussian distribution for the energy spread(the Gaussian standard deviation);
- `m_ISROn = 1, m_kDim = 2, m_keyISR=2` – Born with ISR (c);
- `m_ISROn = 1, m_kDim = 3, m_keyISR=2, m_sigE = 0.0042` – Born with with ISR of type (c) (see [4]) convoluted with the Gaussian distribution for the energy spread.

A set of functions that set up all legitimate combinations is delivered. These were used in the simplified example and are in the details described below – their names start with `Make`, e.g., `MakeBorn(...)`.

The main.cxx file contains two types of functions. The first kind generates the cross section distribution and stores them in a root file. These functions set up appropriately the

TDensity object, and use FOAM to integrate the distributions, to create the histograms and save them into a root file. This root file contains two histograms

- h_Ene – contains the cross section as a function of energy;
- h_NORM – is the two bin histogram: the first one at 0.5 contains the integrated luminosity, and the second one at 1.5 that contains the number of events in h_Ene histogram.

The functions are as follows. The first function creates the Born term histogram and saves it in a root file:

```
void MakeBorn( string filename = "BornH" )
```

The second function calculates the Born term convolution with the Gauss distribution that describes beam energy spread, and saves it into root file:

```
void MakeConvBorn( string filename = "histo1",
Double_t sigE = 0.0041, long NevTot =  1000000 )
```

The last important 'production' function calculates the Born term with ISR contribution convoluted with the Gaussian distribution and saves it into root file

```
void MakeISR( string filename = "histo1", Int_t keyISR = 2,
Int_t kDim = 3, Double_t sigE = 0.0041, long NevTot =  1000000 )
```

The second kind of function retrieves the constructed histograms, does the formatting and stores the results into EPS files. These include

```
void plotISRabc( void )
```

which prepares the plots for the three types of the ISR contributions and saves them in the EPS file ISRabc.eps. The next one

```
void plotISR123( void )
```

prepares the plots with the ISR contribution and its convolution for δ_E = 4.2 MeV and 8MeV. Plots are saved in ISR123.eps. The next two functions

```
void plotBorndelta( void )
void plotISRdelta( void )
```

prepare the plots related to the Born term including the ISR corrections convolution with the Gauss distributions for different machine energy spread values δ_E. The last two functions are responsible for creating and plotting the cross section dependence on the machine energy spread value:

```
int makeISRsigEDistribution( int nbins = 100, long NevTot
=  1000000 )
int plotISRsigEDistribution( int nbins = 100, long NevTot =
1000000 )
```

In particular, the resulting plots can be seen in paper [4], as well as, generated using the software.

6. Parallelization with MPI

In this section the description of the parallel version of the programs is provided. They are located in the MPI directory. The description is brief as it is aimed at specialists on parallelization and is only a technical improvement to the program.

The processes of the generation of histograms are separate, independent and require a large amount of time in order to obtain large statistics. Therefore, they are ideally suitable for parallelization. There are different approaches to the issue. Below, a conceptually simple one is applied. It relies on the MPI (Message Passing Interface) [5] idea, and specifically uses the OpenMP [15] technology for C/C++. The choice is dictated by the fact that standard distribution of FOAM [1, 2] integrator does not work when parallelization is applied on the level of threads, therefore, the most common technology for parallelization on the level of processes was selected, i.e., MPI.

MPI delivers the software infrastructure for the communication between the processes by applying the MPI library calls. It is a popular standard in High Performance Computing. The process management is implemented using the well-known producer-consumer design pattern [11]. The number of processes used in the computations is controlled by NOP variable in Makefile.

There are two programs in the delivered software package [6]. The first one contained in the subdirectory `Basic` generates the plots for all considered types of the cross sections and the second one stored in the subdirectory `sigEPlots` generates the plots for the dependence of the cross section on the centre of mass machine energy spread.

In the first program, the histograms are created according to the data in the array `data` defined at the beginning of `main()` function in `main.cxx` files. Every cell of this array is of the struct type `genData` which contains the generation parameters e.g. the machine energy spread or type of ISR correction. Then every process depending on its unique identification number, assigned by MPI interface, generates the histograms for its range of data in the array, see Fig. 3.

The range of indices of the array for given process is derived using its identification number and is performed by rather standard functions

```
int startIndex( int N, int workers, int rank);
int stopIndex( int N, int workers, int rank);
```

where N is the dimension of the array, workers is the number of all processes and rank is the unique rank of the process. Therefore, every process processes initial data from the array data from the indices range returned by the above functions.

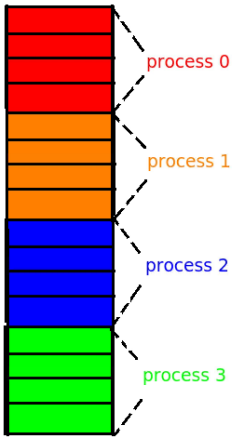

Fig. 3. Data distribution of the array among the processes. Each process, process some range of initial data array, which is determined by unique identification number of the process

A simple check for speeding up the first program is presented in Fig. 4. The calculations were performed using an Intel(R) Core(TM) i7-3610QM CPU @ 2.30GHz processor. Each process worked using a single thread. The maximum number of processes is 8; therefore they allowed 7 processes at maximum to run without disturbance from the operating system and other system tasks. Speedup grows almost linearly when the number of cores is increased, which shows that the plateau of Amdahl's law [11] is not reached in the test.

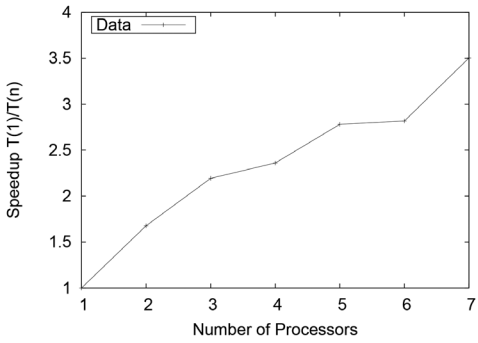

Fig. 4. Speedup for Basic program. The calculations were performed using an Intel(R) Core(TM) i7-3610QM CPU @ 2.30GHz processor. Each process worked on a single core and as there were only 8 cores it is therefore inefficient to run more than 7 processes at the same time. Here $T(i)$ is the time of computation for i processes

In the second program from sigEPlots directory every process generates the values of the cross section for a given range of values of the machine energy spread by calculating convolution integrals for different values of δ_E independently using parallelization. The value of the energy spread for the bin centres are stored in the shared array – every process calculates the cross section for a given range of the energy spread δ_E at given beam energies E.

These computed values are stored by processes in the arrays shared by them. The values are gathered by the main process at the end of the parallel section and then in a single process the plots are generated. In this program it is important that the size of the arrays shared between the processes have to be equal to the multiplicity of the number of processes used in the computation as there is a constraint that jobs are distributed equally among processes. The speedup of the calculations is significant comparing to the single-process program. However, as the number of computations for process have to be a multiplicity of the number of processes there is no precise measure of this speedup in this approach – the size of the job depends on the number of declared processes.

In the implementation, static scheduling of tasks was used, which is the simplest and the most ineffective type of scheduling. Therefore there is much room for improvement.

7. Conclusions

A description of the library and program for calculations of the machine energy spread influence on the cross section lineshape of the Higgs boson production in annihilation of lepton pairs was provided. The program structure can be easily adapted to other similar calculations. Also, a simple approach to program parallelization was described.

References

[1] Jadach S., *Comput. Phys. Commun.*, 152, 2003, 55–100.
[2] Jadach S., *Comput. Phys. Commun.*, 130, 2000, 244–259.
[3] Brun R., Rademakers F., *Proceedings AIHENP'96 Workshop*, Lausanne, Sep. 1996, Nucl. Inst. & Meth. in Phys. Res. A 389, 1997, 81–86.
[4] Jadach S., Kycia R.A., *Phys. Lett. B 755*, 2016, 58.
[5] MPI (Message Passing Interface), http://www.mpi-forum.org/.
[6] https://github.com/rkycia/HiggsLineshapeCalculator, http://fizyk.ifpk.pk.edu.pl/ rkycia/ software.html.
[7] GNU Make, https://www.gnu.org/software/make/.
[8] GNU Compiler Collection, https://gcc.gnu.org/.
[9] Doxygen, http://www.stack.nl/ dimitri/doxygen/.
[10] Valgrind, http://valgrind.org/.
[11] Ben-Ari M., *Principles of Concurrent and Distributed Programming*, Pearson; 2nd edition, 200.
[12] Jadach S., Ward B.F.L., Was Z.A., Yost S.A., *Phys. Rev.*, D 94, 074006, 2016.
[13] Jadach S., Ward B.F.L., Was Z., *Phys. Rev.*, D 63, 2001.
[14] Adobe Systems Inc. Addison-Wesley Educational Publishers Inc., Verlag, 1999.
[15] OpenMPI software, https://www.open-mpi.org/